



Synthesis and Stabilisation of Novel UV Absorbers

By Shuqi Yang

**A thesis submitted in partial fulfilment of the
requirements for the award of Doctor of Philosophy
at Loughborough University**



Acknowledgements

I would like to express my sincere gratitude to my supervisors Dr George Weaver and Dr David Worrall for the continuous support of my PhD study and research, for their patience, motivation, enthusiasm, and immense knowledge. Their guidance helped me in all the time of research and writing of this thesis. I would also like to thank Dr Ken Gargan, my industry supervisor for his assistance and encouragement throughout my research. Especially many thanks for showing us round the British Polythene Limited factory in Scotland and arranging for us to visit the Schulman factory in South Wales.

Besides my supervisors, I would like to thank my report reviewers: Prof. Ray Jones, Prof. Roger Mortimer and Dr Marc Kimber for their insightful comments and encouragement, but also for the hard questions which enabled me to widen my research from various perspectives.

I am grateful to all the support staff at Loughborough University, Dr David Belcher, Jadeen Christie, Callum Crane, Alastair Daley, Andy Kowalski, Claire Lowe and Ed Simpson. Many thanks also to Dr Mark Edgar for NMR spectroscopy, Dr Mark Elsegood for X-ray crystallography, and Dr Ben Buckley for microwave and HPLC assistance.

I would like to thank my friends and colleagues for their help and co-operation in F001, F009 and F102, Alex, Amira, Beatriz, Carlos, Craig, Fatemeh, Maria, Mariam, Matthew, Rebecca, Rob, Rossi, Sam, Shahzad, Vanassa, Vlodya, Yamin and Yubai.

Thanks to Loughborough University and BPI for the financial support and facilities.

I am indebted to Yuqi and his parents for their patience and support throughout these years which enabled me to achieve my goals. I would also like, in particular, to thank my parents for their support and encouragement through my entire life.

Contents

Acknowledgements	i
Abbreviations	1
Abstract.....	3
Chapter 1. Introduction	4
1.1 Photochemical principles	6
1.2 The role of UV-B radiation on terrestrial ecosystems	7
1.3 The role of UV-A radiation on terrestrial ecosystems	12
1.4 Polytunnels.....	16
1.5 Stabilisation and degradation	18
1.6 UV absorbers	22
1.7 Optical brighteners.....	26
1.8 Sunscreens.....	29
1.9 Fries rearrangement	33
1.10 Fluorine-nucleophilic substitution reaction	35
Chapter 2. Uvitex OB degradation and stabilisation.....	40
2.1 Introduction.....	40
2.2 Aims.....	41
2.3 Results and discussion	42
2.3.1 HPLC for Uvitex OB	42
2.3.2 Degradation for Uvitex OB in solution.....	43
2.3.3 Uvitex OB with stabilisers	48
2.3.4 Degradation studies of Uvitex OB in films.....	59
2.4 Conclusions.....	61
Chapter 3. Uvinul A Plus modification	63

3.1 Introduction.....	63
3.2 Aims.....	64
3.3 Results and discussion	65
3.3.1 Organic synthesis	65
3.3.2 UV absorption and degradation	83
3.3.3 Comparison between new hydroxybenzophenone and Uvinul A Plus	103
3.4 Conclusions.....	105
Chapter 4. Synthesis and stabilisation new hydroxybenzophenones and related naphthalene analogues.....	107
4.1 Introduction.....	107
4.2 Aims.....	108
4.3 Results and discussion	109
4.3.1 Organic synthesis	109
4.3.2 UV absorption and degradation	131
4.3.3 Comparison between new hydroxybenzophenones and Uvinul A Plus	146
4.4 Conclusions.....	148
Chapter 5. Overall conclusions.....	149
Chapter 6. Future work.....	151
Chapter 7. Experimental.....	153
Chapter 2. Uvitex OB degradation and stabilisation	153
Chapter 3. Uvinul A plus modification.....	157
Chapter 4. Synthesis and stabilisation new hydroxybenzophenones and related naphthalene analogues	189
References.....	226

Abbreviations

AOX	Alcohol oxidase
b.p.	Boiling point
Comp.	Compound
d	Doublet splitting pattern
DCM	Dichloromethane
1,2-DCE	1,2-Dichloroethane
DMF	Dimethylformamide
DMSO	Dimethylsulfoxide
eq.	Equivalent
EVA	Ethylene vinyl acetate
GC-MS	Gas chromatography–mass spectrometry
HALS	Hindered amine light stabiliser
HPLC	High-performance liquid chromatography
Hz	hertz
IR	Infra-red
<i>J</i>	Coupling constant
LDPE	Low-density polyethylene
m.p.	Melting point
MS	Mass spectrometry
m/z	Mass to charge ratio

NMR	Nuclear magnetic resonance
q	Quartet splitting pattern
r.t.	Room temperature
s	Singlet
SPF	Sun protection factor
t	Triplet splitting pattern
THF	Tetrahydrofuran
TLC	Thin layer chromatography
UV	Ultraviolet

Abstract

Plants can respond differently to different wavelengths in sunlight's spectral range, and crop covers containing additives have a great effect on the growth of crops. This research focuses on synthesising new hydroxybenzophenones bearing long alkyl chains to confer polymer solubility, and to measure their UV absorption and photochemical stability. Compounds substituted with fluorine atoms or different amino groups in particular were under investigated, as these groups may impart stability towards oxidative degradation, or alter the absorption maximum. Related naphthalene analogues were substituted with different amine groups for comparing UV absorption and photostability. Modification of Uvinul A Plus was carried out to improve UV absorption maximum wavelength and light fastness.

The photostability of Uvitex OB was analysed. After irradiating for specific times using a xenon arc lamp, degradation products were separated by HPLC, and analysed by NMR spectroscopy, GC-MS and IR to determine the degradation mechanism. The influence of oxidative and reductive conditions on degradation rates of UV absorbers was tested. The stabiliser Chimmasorb 944 was combined with products synthesised to enhance stability. Outstanding UV absorbers were then added to films to investigate UV properties in the presence of air, nitrogen or oxygen.

This research found hydroxybenzophenones substituted with *N*-methyl-1-butylamino or dihexylamino groups showed excellent UV absorption with an ideal photostability in both the UV-A and UV-B regions. Chimmasorb 944 could improve the stability for most compounds. Irganox 1010 and Irgafos 168 enhanced the stability of Uvitex OB when they were combined with Uvitex OB in a significant concentration.

Chapter 1. Introduction

Sunlight is a key environment factor in almost all ecosystems, especially to humans and plants.^[1] The duration and intensity of sunlight are different in different regions of the world. In the UK, sunshine hours are different between England and Scotland. The average sunshine hours for England are 190-200 h and daily maximum temperatures are 21-22 °C in July over the past 30 years.^[2] In Scotland, daily maximum temperatures are only 16-17 °C with an average of 130-140 h of sunshine in July.^[2] However, the peak in North Africa sees average daily maximum temperatures up to 29 °C with an average of 11 hours of sunshine per day in July.^[3] Sunlight availability for plants and crops is different in these places. In Scotland, much more sunlight is needed for crops than North Africa since it is of lower intensity.

The sunlight which reaches the Earth's surface can be divided into Ultraviolet (220-400 nm), Visible (400-700 nm) and Infrared (700-3000nm) (**Figure 1**).^[4]

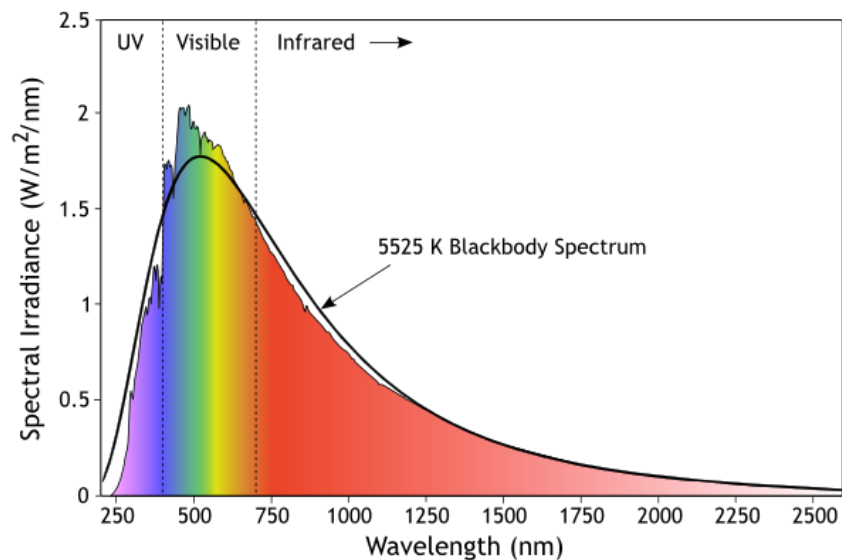


Figure 1. Sunlight spectrum.^[4]

Plants exhibit specific responses to a wide range of radiation wavelengths. Where crops are grown in protected environments such as polytunnels, there is significant scope to exploit these fundamental light responses by manipulating the light environment reaching the crop. Infrared light reaching a crop has been shown to reduce stem extension in several species.^[5] Visible light can control stomatal opening and circadian rhythms.^[6] Additionally, there is a growing understanding of the consequences of changes in the UV environment, and films containing different UV absorbers for greenhouses are needed to provide a suitable sunlight profile for crops in different areas. Understanding the ecological roles of solar ultraviolet (UV) radiation (280–400 nm) has become significantly important.

The UV spectrum is generally divided into three regions: the UV-C region (220-280 nm), the UV-B region (280-315 nm) and the UV-A region (315-400 nm). All of the most damaging UV-C radiation from the sun and most of the UV-B is filtered out by atmospheric ozone before it reaches the earth's surface. UV-C is absorbed in the atmosphere so does not penetrate to the biosphere. Since the early 1970s, ozone layer depletion caused by chlorofluorocarbons and other anthropogenic sources^[7] increased the level of ultraviolet radiation reaching the earth's surface affecting both natural and agricultural ecosystems.^[8] This progressively worsening situation has led to renewed impetus in efforts to understand the effects of UV radiation on plants and other organisms.

In 2003, Paul split the discipline of ultraviolet radiation on terrestrial ecosystems into two broad themes: the effects of increased UV-B radiation resulting from ozone depletion, and the role of UV radiation (largely UV-A) in the vision of many animals.^[1] In the past ten years, thousands of research papers have been published in this field. Both positive and negative effects of increasing UV-B have been demonstrated on plants and crops. The effects of UV-A and UV-B radiation are studied to find new selective UV absorbers as additives for polyethylene films as a means to provide a high yield of crops.

1.1 Photochemical principles

The Beer-Lambert law has been formulated to describe the relationship between the light absorption intensity and concentration of an absorbing species in solution.

$$A = \epsilon cl$$

A is absorbance; ϵ is known as the molar absorptivity or molar absorption coefficient with units of $\text{L mol}^{-1} \text{cm}^{-1}$; c is the concentration of the compound in solution in moles per litre; and l is the path length of the absorbing solution in centimetres.

The Beer-Lambert law can be used to calculate the molar absorptivity (ϵ) of UV-absorbers in this research. ϵ is a measure of the amount of light absorbed per unit concentration. When absorbance $A=1$ and $l=1$ cm, a compound with a very high value of molar absorptivity would need a low concentration, which means a compound with a very high molar absorptivity will be more effective at absorbing light than a compound with a low molar absorptivity. Hence, low concentrations of a compound with a high molar absorptivity can be easily detected.

The ultraviolet spectra of organic compounds are associated with transitions between electronic energy levels. Absorption occurs when the energy contained in a photon is absorbed by a molecule resulting in a transition to an excited state.^[9] Most absorption spectroscopy of organic compounds is based on $n \rightarrow \pi^*$ and $\pi \rightarrow \pi^*$ transitions. Molar absorptivities from $n \rightarrow \pi^*$ transitions are relatively low, and range from 10 to 100 $\text{L mol}^{-1} \text{cm}^{-1}$. $\pi \rightarrow \pi^*$ transitions normally give molar absorptivities more than 1000 $\text{L mol}^{-1} \text{cm}^{-1}$.^[10]

The solvent in which the absorbing species is dissolved also has an effect on the spectrum of the molecule. $\pi \rightarrow \pi^*$ transitions undergo a bathochromic shift with increasing polarity of solvent, since the π^* state is more polar than π in polar molecules. The π^* state is therefore

better stabilised than π in a polar solvent. Hydrogen bonding stabilises n more than π^* in polar solvents, so $n \rightarrow \pi^*$ transitions undergo a hypsochromic shift. Peak absorbance is reduced due to stabilisation of nonbonding electrons.

1.2 The role of UV-B radiation on terrestrial ecosystems

There was only a limited understanding of the influence of solar UV-B radiation on the ecosystem in the early 1970s. Only a few early marine studies had observed that solar UV could reduce phytoplankton production.^{[11][12]} Then this effect was subsequently found to be widespread among aquatic ecosystems.^[13] In the mid-1980s, thinning ozone was discovered over Antarctica and its subsequent link to CFCs, sparked a large research effort on UV-B effects that continues today. By the 1990s, it was widely accepted that UV-B effects on terrestrial ecosystems include decreased primary production, altered plant species composition, and altered secondary chemistry with implications for herbivory, litter decomposition and biogeochemical cycles,^[14] changes in populations of fungi and invertebrates, and morphological changes in the growth patterns of mosses.^[15]

UV-B is potentially detrimental to all living things. Higher UV-B can increase skin cancer, skin ageing and cataracts in the human population,^[16] but is particularly harmful to plants because of their obligatory requirement for sunlight for survival and their inability to move.^[17]

It has been reported that changes in leaves due to UV-B exposure in several species occur where bronze or brown spots appear on the leaf surface and result in chlorosis, necrosis and

desiccation of the leaves,^[18] which also was observed in cotton leaves.^[19] The reason for the appearance of chlorotic and necrotic patches was the decrease in leaf chlorophyll content due to exposure to UV-B.^[20] The damage to chloroplasts and changes in photosynthetic pigments would result in reduction of photosynthesis which gave a chlorophyll reduction.

UV radiation was observed to reduce leaf size, but to increase leaf mass per unit area and leaf thickness.^[21] Many plant species exposed to UV-B increased leaf thickness and concentrated a UV-B absorbing phenol derivative which was formed to protect plants from UV-B damage.^[22] Accumulation of leaf surface waxes which is an important leaf surface character that responds to environmental stresses was noticed after increased UV-B radiation.^[23] Increased wax provided a protective mechanism as it reflects the incident UV-B radiation. Secondary metabolism activity is another key plant response to UV radiation. UV-B induces reduction of carbon assimilate production which then leads to lower efficacy of the biosynthetic system producing secondary metabolites. Finally, the amount of UV-B absorbing compounds might decrease.^[24] Hence, UV-B absorbing compounds might not offer enough protection under increasingly higher levels of UV-B radiation.

The main concern for agricultural scientists is whether or not enhanced UV-B radiation reduces economic yields and product quality of field crops. Not all the effects are negative some researchers found some plants showed positive effects after exposure to UV-B. **Table 1** shows the response of different crops to elevated UV-B radiation.

Table 1. Response of different crops to UV-B radiation.

Species	UV-B (Place)	Response
Big Top fruits	1.69 kJ m ⁻² d ⁻¹ (Italy)	Phenolics decreased. ^[25]
Corn	6.84 kJ m ⁻² d ⁻¹ (Netherlands)	Yield decreased ^[26]
Cotton	0, 4, 8, 12, 16 kJ m ⁻² d ⁻¹ (Mississippi, USA)	Height and size decreased in 16 kJ m ⁻² d ⁻¹ UV-B radiation ^[27]
Forage	Ambient UV-B + 30% UV-B (Finland)	No changes in biomass and yield production ^[28]
Lettuce	0, 5.0, 8 kJ m ⁻² d ⁻¹ (Norway)	UV-B exposed plants showed a stronger red colouration in the leaves but reduction in leaf area and fresh weight. ^[29]
L. sativa	0 kJ m ⁻² d ⁻¹ (Lancaster, UK)	Increased fresh weight, reduced pigment concentration and less green peach aphid ^[30]
Phaseolus vulgaris L.	Ambient + 10.2 kJ m ⁻² d ⁻¹ (Indian)	Yield decreased ^[31]
Soybean	13 kJ m ⁻² d ⁻¹ (Jilin, China)	Decreased plant height, dry weight of individual stem and yield. Seed number per pod was less affected, seed size decreased 12.3%. ^[32]
Sweet basil	0, 2, 4 kJ m ⁻² d ⁻¹ (Lithuania)	Leaf area, biomass increased ^[33]
Tomato	1.2%-1.3% ambient UV-B (Eastern Greece)	Number of insect injured fruit reduced, yield increased ^[34]

Most of these studies showed enhanced UV-B radiation decreased yield. Some showed no UV-B effect on the yield and a few studies showed UV-B radiation increased yields. There are various parameters which are influenced by UV-B radiation, which affect the final yield or biomass. Decreases in chlorophyll concentration, photosynthesis and leaf area result in yield reduction. The stronger red colour of lettuce in **Table 1** shows plants retained more colour and good quality after UV-B radiation. UV-B radiation could result a good approach

to induce antioxidant production in peach fruits.^[35] *Lycopersicon esculentum* respond to UV-B by enhanced synthesis of flavonoid quercetin, a strong antioxidant that helps the plants to acclimatize well to UV-B stress.^[36]

UV-B effect on leaf size has been shown to have both positive and negative changes. This might be because of different crops and areas. Perennial plants and especially long-lived trees may be differently affected by increasing UV-B levels relative to annual plants since they have to face the accumulative effects of UV-B radiation in their life cycle.^[37]

Males and females of sexually dimorphic trees show different growth rates, photosynthesis and phenolic concentrations after UV-B radiation. Enhanced UV-B tended to decrease biomass and leaf thickness in males, and increased the leaf phenolics in females, which suggests females have greater tolerance to UV-B compared to males.^[38]

Researchers also found short- and long-term effects of UV-B radiation showed differences on the leaves of grapevine *Vitis vinifera*. After 20 d at $9.66 \text{ kJ m}^{-2} \text{ d}^{-1}$, significant decreases in net photosynthesis, sub-stomatal CO_2 concentration and total soluble proteins were observed. The activities of several antioxidant enzymes increased significantly. However, after 75 d of exposure to $9.66 \text{ kJ m}^{-2} \text{ d}^{-1}$ UV-B, most photosynthetic and biochemical variables were unaffected and there was no sign of oxidative damage in leaves. The results suggest plants seemed to be tolerant to moderate doses of UV-B after long-term radiation.^[39]

UV-B can also have important effects on herbivorous insects. Solar UV-B significantly reduced insect herbivory and caused a concomitant increase in crop yield.^[40] UV-B effects on agroecosystems are the result of complex interactions involving multiple trophic levels.

UV-B can directly affect herbivorous insects reducing their growth, fecundity and survival behavioural responses.^[41] For example, thrips *Caliothrips phaseoli*, a phytophagous insect, preferred a low UV-B environment and were repelled when exposed to supplementary UV-B.^[42] **Table 2** shows the influence of supplementation UV-B on different insects' behaviour.

Table 2. Response of different insects to UV-B radiation.

Species	Damage	Response
Aphids	Suck sap that leads to wrinkle, curl, dieback, and even death of the whole plant	Reproduction was reduced with higher UV-B conditions ^[43]
Diamondback moth	Eat leaves	Natural herbivory was less severe ^[44]
Frankliniella occidentalis	Transmit spotted wilt virus	Number reduced, less disease and higher yield ^[45]
Geometridae	Eat leaves	Consumed less leave area ^[46]
Grasshoppers	Eat leaves	Fewer leaves were damaged ^[47]
Moth caterpillars	Eat tissue from leaves	Fewer leaves consumed ^[48]

These studies also showed that solar UV-B has a direct influence on phytophagous insects. Insects cannot live under supplementary UV-B radiation and a reduction of the number of insect results in a better yield of crops. However, some insects die for indirect reasons. The indirect responses may be caused by changes in the plant host which are induced by UV-B and other insects whose behaviour is affected by UV-B.^[49]

Ambient levels of UV-B radiation often have beneficial effects, promoting plant immunity against pests and pathogens. Soybean crops grown under attenuated UV-B had higher

numbers of unfilled pods and damaged seeds than crops grown under ambient UV-B radiation.^[50]

All these studies can support the one idea that the effects of UV-B on agro-ecosystems are the result of complex interactions. UV-B can be recommended as a component of an integrated disease management program to reduce secondary spread of plants viruses by decreasing the number of insects. Research on effects of UV-A and UV-B radiation on broccoli also showed that broccoli florets retained more colour after UV-B irradiation than after UV-A.^[51] UV-B can stimulate a good colouration of plants. Therefore, finding a balance between UV-B radiation and agroecosystems will provide crops with good colour and yield, possibly without using chemicals on plants.

Researchers suggested a better understanding of the mechanisms that mediate the anti-herbivore effect of UV-B radiation could be used to design crop varieties with improved adaptation to the cropping systems that are likely to prevail in the coming decades in response to agricultural intensification.^[40]

1.3 The role of UV-A radiation on terrestrial ecosystems

UV-A (315-400 nm) is the less energetic and less hazardous part of UV radiation and is virtually unaffected by changes of ozone concentration. In this respect, UV-A is the major component of the solar UV spectrum to which plants are exposed. Although UV-A is less damaging than UV-B, it can penetrate deeper than UV-B into leaves, produce active oxygen species and increase oxidative stress in mammalian and plant tissue.^[52]

UV-A radiation has positive effects on most plants growth such as increasing leaf weight,^[53] and total plant fresh and dry weights^[54]. UV-A wavelength light can afford plants the ability to cope with environmental stress by inducing the accumulation of phytochemicals with antioxidant properties.^[55] After plants were exposed to UV-A for 2-4 days, the accumulation of anthocyanin as well as polyphenolic compounds, such as phenolic acid, flavonoids and tannins, which have strong antioxidant activity, were significantly increased.^[56]

UV-A radiation changes growth, pigmentation and coenobium formation in plants. Little research has been done on the effects of UV-A on whole plants, but UV-A has been known to play an important role in terrestrial ecosystems, especially on insects. **Table 3** shows responses of different crops to UV-A radiation.

Table 3. Response of different crops to UV-A radiation.

Species	UV-A(Place)	Response
Cucumber	10% transmission at 401nm (Maryland, USA)	Leaf number, height, length of petiole and leaf size increased slight ^[57]
G. lemaneiformis	0.98 MJ m ⁻² d ⁻¹ UV-A (Lianyungang, China)	Significantly enhanced the growth rate compared with non UV-A ^[58]
New red fire lettuce	10% transmission at 390nm (Buffalo, USA)	Leaf number, biomass and dry weight increased ^[59]
Pepper	71.67 kJ m ² d ⁻¹ (Madrid, Spain)	23% shorter than plants grew at near zero UV-A. ^[60]
Tomato seeds	Wavelength 365 nm (South Korea)	Accumulation of anthocyanin in tomato seedlings and tomato fruits. ^[61]

The responses of different crops exposed to UV-A are different as well as to UV-B radiation. Comparing these data, supplementing UV-A at different growth stages may result in differences in plant height or yield. For negative effects, one possible reason is that solar

UV-A may cause reductions in photosynthetic rate.^[59] A second possibility is UV-A radiation may damage the proteins in the photosynthetic reaction centres.^[61] The reason for positive effects may be that UV-A promotes the formation of phytochrome which can induce plants growth; a further possibility is that UV-A radiation has effects on insect population growth. Insects and pests have a significant influence on crop growth and they are sensitive to UV-A radiation.

Research showed *Lactuca sativa* grown under 11% UV-A radiation, and zero UV-B showed increased density of leaf surface phylloplane microbes compared with ambient UV radiation.^[30] Many literature reports showed a clear benefit of low UV environments for insects and fungi control. In 1977, Honda and Yunoki tested a UV-absorbing film with a cut-off of transmission at 390 nm. They found grey mould on cucumber and tomato caused by *B. cinerea*, and sclerotinia disease in eggplant and cucumber caused by *S. sclerotiorum*, were greatly reduced.^[62] After this, in 1982, Nakagaki from Japan provided the first evidence that UV-absorbing films may reduce insect invasion. The population of *A. gossypii*, and *vaporariorum* Westwood were lower on tomatoes grown under exclusion of UV wavelengths than on crops grown in an ordinary UV radiation.^[63]

Table 4 shows the response of insect pests to UV-A radiation. Here insects were placed in a container and exposed to UV-A radiation, except for the test with western flower thrips, which were used in some experiments. In this case, the thrips were released from a black box compartment between two tunnels covered with either UV-transmitting or UV-absorbing materials and their choice of route observed.^[70]

Table 4. Response of different insects to UV-A radiation.

Species	UV-A	Response
Aphids	280-380 nm	Growth slowed ^[64]
Desmodesmus armatus	3.75 mW cm ⁻²	Growth rate was higher than non UV-A ^[65]
Helicoverpa armigera	320-400 nm	Adult longevity decreased ^[66]
Orgyia antiqua	351 nm	Retinal damage ^[67]
Psocoptera	351 nm	Destruction of vision ^[68]
Whiteflies	400 nm, 550 nm	Took off more readily and walked faster towards to 400 nm irradiated area ^[69]
Western flower thrips	95.5% UV-A	82-98% higher proportion than zero UV-A radiation ^[70]

From **Table 4**, it was shown that UV-A radiation can cause eye damage to insects. Also some insects can see UV-A at wavelengths around 400 nm and orientated towards to it. After knowing the influence of UV-A on insects, it is possible to use UV-absorbing films to block insect pests which is also significantly reduces the spread of insect-borne viruses.

Combining all the factors of UV radiation on crops and insects together, the focus turns to the design and production of UV-absorbing films to block part of UV-A and UV-B in order to provide a high quantity and quality of crops, and decrease the number of insect pests without, or with less, pesticide. As mentioned in section 1.2, UV-B radiation can decrease yield of some plants or cause damage to leaf. However, UV-B affords plants with good colour and significantly reduces insect herbivory leading to an increase in yield of crops. Most insects can see 370-390 nm UV-A and **Table 4** shows significant reduction of herbivory of insects after blocking of this part of the UV-A spectrum.

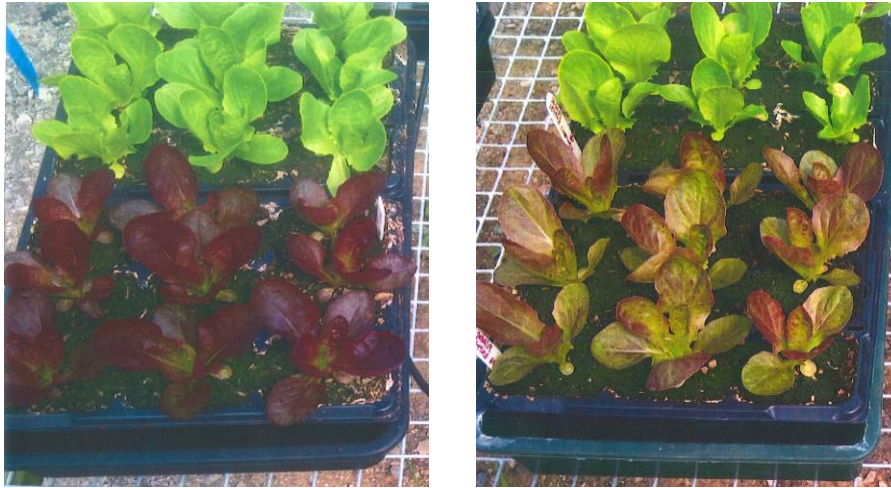
1.4 Polytunnels

Polytunnels are tunnels made of polyethylene film to protect crops and plants from bright sunlight, strong winds, hailstones and pest insects.^[71] They allow fruits, flowers and vegetables to be grown at unseasonal times by providing a suitable temperature and humidity environment. Factors influencing a crop or plant can be controlled in a polytunnel. (**Picture 1**)



Picture 1. Polytunnels for farm^[72]

Researchers in Lancaster university found lettuce in polytunnels containing Uvitex OB (details in Chapter 2) grew better than the one in benzophenone (details in section 1.6) polytunnels (**Picture 2**). Furthermore, insect and pests were fewer in benzotriazole (details in section 1.6) polytunnel compared with the right picture which showed the insect amount in polytunnels without UV additives in **Picture 3**. Therefore, a suitable UV absorber in polytunnels could highly improve plants growth and reduce the number of insect and pests.



Picture 2. Lettuce in different polytunnels
(Left: Uvitex OB polytunnel. Right: benzophenone polytunnel)



Picture 3. Insect and pest amount in different polytunnels
(Left: polytunnel contained benzotriazole. Right: polytunnel without UV absorbers)

Polyethylene, low-density polyethylene (LDPE) and ethylene-vinyl acetate (EVA) copolymers films are currently the most widespread greenhouse covering materials used across the world.^[73] LDPE-based films can offer ultraviolet stabilisation, infrared (IR) opacity, UV-blocking, and near IR (NIR)-blocking by modification with special additives. LDPE films are the most widely used for greenhouse coverings for the relatively good mechanical and optical properties as well as its competitive market price.

A large quantity of plastics is used annually world-wide in the agricultural sector. In 2014, plastics production was around 311 and 59 million tonnes worldwide and in Europe.^[74] Agricultural applications represent 4.3% or 2.5 million tonnes of the plastics in Europe which produced 57 million tonnes of plastic in 2013.^[75]

In 2012, 25.2 million tonnes of post-consumer plastics waste ended up in the waste upstream in Europe.^[75] 62% was recovered through recycling and energy recovery processes while 38% still went to landfill.^[75] Recycling have increased, but landfilling is still the first option in many EU countries.

The degradation of LDPE film is a complicated process. Degradation, in most cases, involves more than one mechanism, and takes place in the harsh conditions met during their use, from ultraviolet irradiation, heat, agrochemicals, as well as due to their limited thickness.^[73] The purpose of this project is to synthesise stable UV absorbers which can be combined with light stabilisers to extend the life time of polytunnel films.

1.5 Stabilisation and degradation

UV-stabilised polyethylene (PE) film is the most widely used plastic in the world for polytunnels. It is easy to handle, has good optical and mechanical properties, low weight and is recyclable. UV absorbers are incorporated in PE films as a means to control the wavelength of UV radiation transmitted. However, polymer films are complex materials, and besides UV absorbers, another important group of additives are stabilisers.

Stabilisers are usually divided into three types: phenolic antioxidants, phosphite-type stabilisers, and hindered amine light stabilisers (HALS).^[76] Typical structures of these stabilisers are shown in **Table 5**.

Table 5. Different stabilisers.

Stabilisers	Structure	Application
Chimassorb 944 (Ciba) ^[77]		A high molecular weight hindered amine light stabiliser (HALS). Imparts excellent light stability to fibres and films.
Irganox 1010 (Ciba) ^[78]		A sterically hindered phenolic antioxidant. Can be applied to polyolefins to protect substrates against thermo-oxidative degradation.
Irgafos 168 (Ciba) ^[79]		A hydrolytically stable phosphite processing stabiliser. Can be combined with other antioxidants comprising polyolefins.
Tinuvin 770 (Ciba) ^[80]		A low molecular weight hindered amine light stabiliser. Provides excellent light stability for thick sections and films.

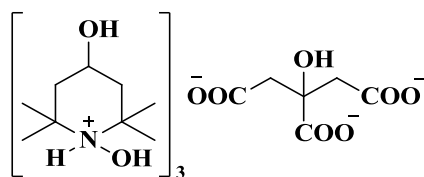
Irganox 1010 and Irgafos 168 are antioxidant stabilisers and the blends of them can provide storage stability and give the polymer long term protection against thermo-oxidative degradation,^[78] such as Irganox B215 with 67 % Irgafos 168 and 33 % Irganox 1010. It can be used in polyolefins such as polyethylene and ethylene-vinylacetate copolymers.^[81] Irganox

B215 and Irgafos 168 as secondary antioxidant can be combined with light stabilisers such as Chimassorb 944 to protect against oxidative degradation.^[79] In this research, focus was on the stability of hindered amine light stabilisers combined with UV absorbers.

Chimassorb 944 is the most widely used stabiliser in the world, with a high-molecular weight and good extraction resistance. Researchers added Chimassorb 944 and Tinuvin 770 to ethylene–octene copolymer (EOC) to test stability and degradation after 1200 h. EOC without stabilisers exhibited a very poor photostability, but the additives both showed an excellent photostabilising effect, which effectively inhibited the gel formation and the chain photooxidation.^[82] In comparison, Chimassorb 944 proved to be more efficient at photostabilising than Tinuvin 770.

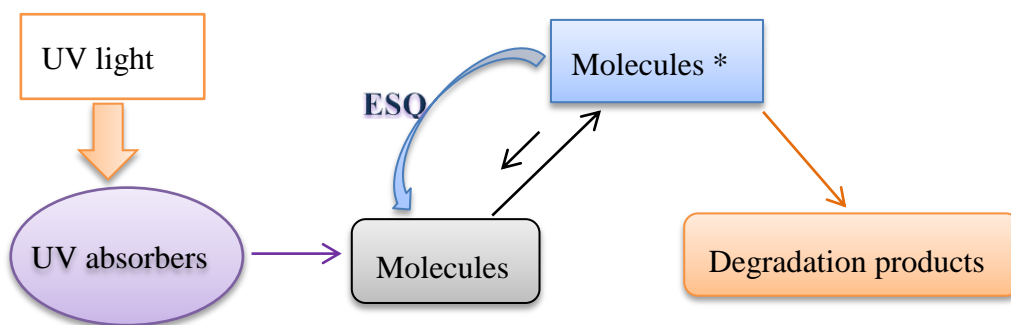
However, this is not the case for every polymer or UV absorbers. When different UV absorbers or other different additives are added in films, which stabiliser is needed is uncertain. For example, Balint *et al.* found that Tinuvin 770 with UV 327 had no additive effect, but the addition with UV 531 had a synergism in resisting photooxidation.^[83] On the photostabilising performance, Tinuvin 770 showed no synergism with UV 531 and antagonism were found when used with UV 327.^[84] Therefore, the choice of stabiliser depends on several factors: the nature of the film, UV absorbers, other additives and applications. Researchers also need to consider the mixing ratio of HALS to UV absorber which will affect photostabilising efficiencies.

Tinogard Q (BASF) is another kind of light stabiliser which is based on excited state quenching technology. It is a liquid formulation containing 10% excited state quencher to stabilise formulations against photolytic degradation.^[85]



Scheme 1. Structure of Tinogard Q

Tinogard Q does not absorb UV light above 200 nm. UV absorbers that absorb light, and then molecules are transferred into an excited state and return to the ground state via energy dissipation, but a certain proportion of molecules may degrade before energy dissipation. Tinogard Q as an excited state quencher (ESQ) could reactive excited states and transfers molecules to stable ground state.^[85] **(Picture 4)**

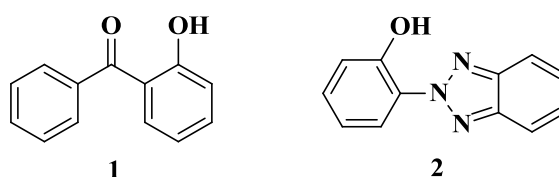


Picture 4. Mode of Tinogard Q action

Tinogard Q is water and alcohol soluble which is suitable for alcoholic and aqueous formulations. Tinogard Q is used by combination with UV absorbers to protect transparent packaged products from light induced degradation.

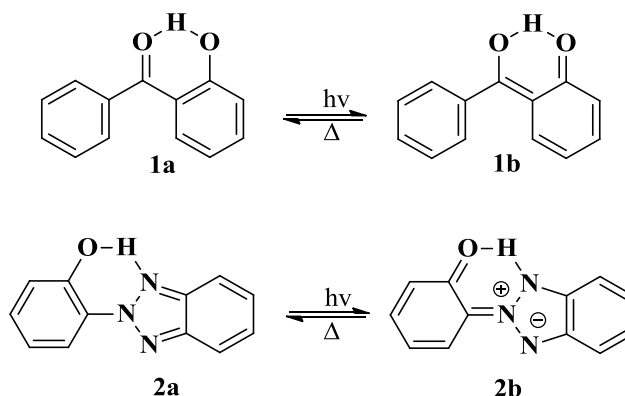
1.6 UV absorbers

The most studied UV-absorbers are benzophenones and benzotriazoles. In 1985, 2-hydroxybenzophenone (**1**) and 2-hydroxyphenylbenzotriazole (**2**) were the most important photostabilisers of polyolefins.^[86]



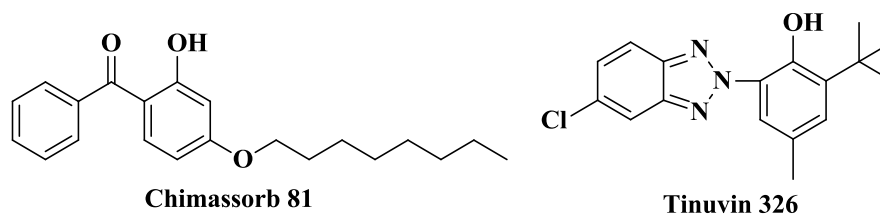
Scheme 2. Structures of two UV-absorbers

Some researchers suggested that their photostability were attributed to excited-state proton transfer and radiationless transitions in the phenol and quinone tautomers to form a reversible six-membered hydrogen-bonded ring system (**Scheme 3**).^[87] The six membered ring imparted stability to the compound.



Scheme 3. Phenol and quinone tautomers.

Chimassorb 81(Ciba) and Tinuvin 326(Ciba) are two important benzophenone and benzotriazole compounds. **Table 6** shows their properties.



Scheme 4. Structures of Chimassorb 81 and Tinuvin 326

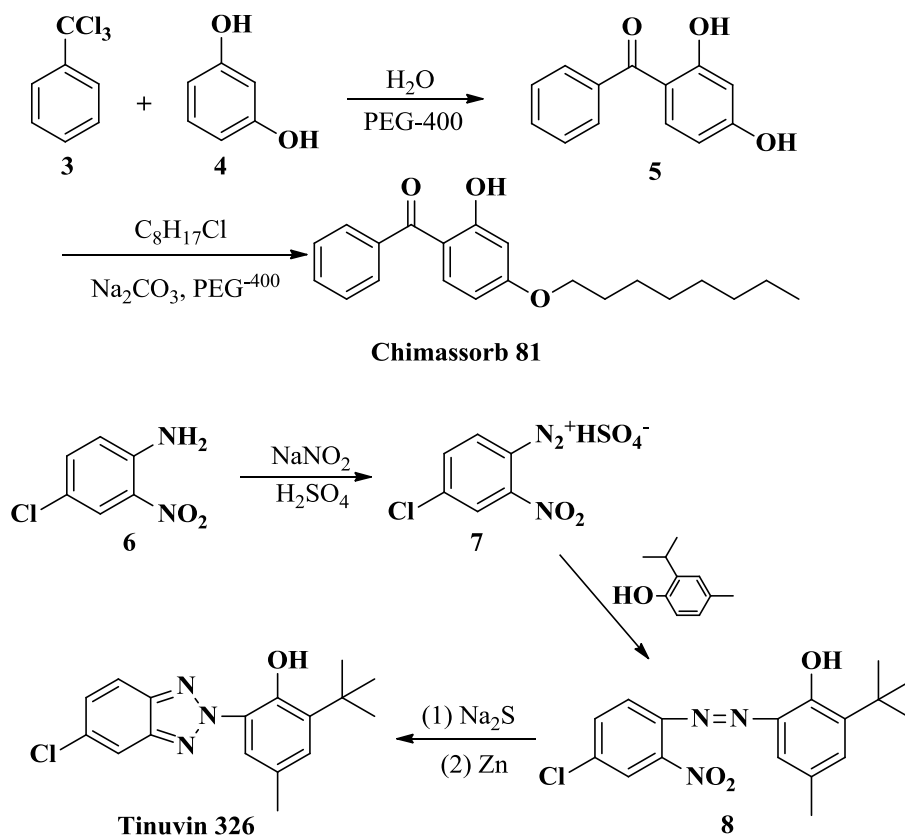
Table 6. Properties of Chimassorb 81 and Tinuvin 326

UV-absorbers	Chimassorb 81 (UV 531) ^[88]	Tinuvin 326 (UV 326) ^[89]
Molecular weight	326.4 g/mol	315.8 g/mol
Appearance	Slightly yellow powder	Slightly yellow powder
Melting range	48-49 °C	138-141 °C
Absorption 10 mg/l, chloroform	Strong absorbance in 280-350 nm, $\lambda_m = 290, 330$ nm	Strong absorbance in 300-400 nm, $\lambda_m = 312, 353$ nm $\epsilon_{(353\text{ nm})} = 16300 \text{ L mol}^{-1}$
Applications	Combine with a HALS for the light stabilisation of low density and linear low density polyethylene as well as ethylene vinyl acetate copolymers for agricultural films. As a UV barrier to protect the contents of packages.	Light stability to plastics and other organic substrates. Suitable for polyolefins and cold cured polyesters. Can be used without significant loss or decomposition in the polyolefin compounding and molding processes.

The main absorption of Chimassorb 81 is in the UV-B range, but it has a broad absorption between 260 nm and 370 nm. Chimassorb 81 is usually used in combination with light stabilisers to protect polymers against light exposure degradation. It also can be combined with antioxidants and phosphites. ^[88] Tinuvin 326 with a high melting point has low volatility

at high temperatures and high resistance to thermal degradation, which provide good stability.^[89]

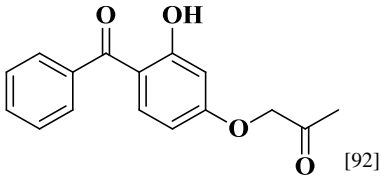
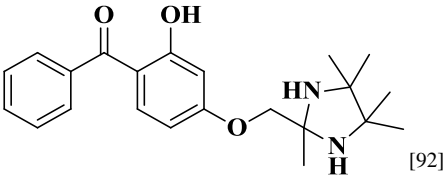
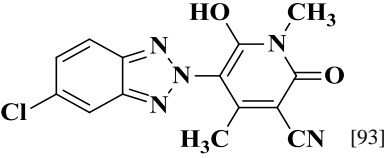
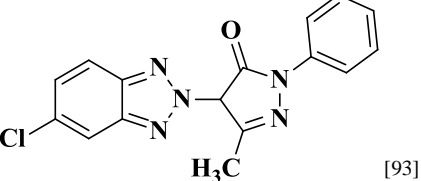
There are several different methods to synthesise Chimassorb 81. The traditional way was to use benzotrichloride (**3**) and resorcinol (**4**) together with PEG-400 as catalyst to form (2,4-dihydroxyphenyl)phenyl-methanone (**5**) which was alkylated with 1-chlorooctane to provide the target product (**Scheme 5**).^[90] For synthesising Tinuvin 326, 4-chloro-2-nitroaniline (**6**) was diazotized with sodium nitrite in sulfuric acid, and was then reacted with 2-isopropyl-4-methylphenol to afford 2-(tert-butyl)-6-((4-chloro-2-nitrophenyl) diazenyl)-4-methylphenol (**8**) which was reduced with sodium sulphide and zinc powder to provide the final product.^[91] (**Scheme 5**)



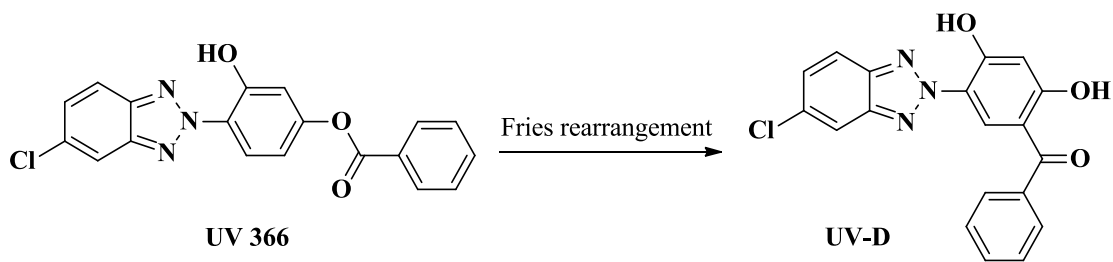
Scheme 5. Synthesis of Chimassorb 81 and Tinuvin 326

After this, researchers synthesised several new UV absorbers based on Chimassorb 81 and Tinuvin 326. **Table 7** shows their structure, UV absorption maxima and the molar absorptivity (ϵ).

Table 7. UV absorption maxima and the molar absorptivity of UV absorbers

Compound	λ_m (nm)	ϵ (L mol ⁻¹ cm ⁻¹)
	286 327 (methanol)	5300 3200
	286 322 (methanol)	19000 12000
	327 (ethanol)	27000
	340 (chloroform)	28500

From **Table 7** the benzophenone compounds show a strong absorption around 280 nm and the benzotriazole compounds have a relative strong absorption band in the UV-A region. Then researchers suggested combining these two parts together to form the adduct UV absorber which has two strong absorption bands in both the UV-A and UV-B regions. Therefore, UV 366 was used to synthesise the adduct UV absorber, UV-D.^[94] (**Scheme 6**)



Scheme 6. Synthesis of UV-D

UV-D was synthesised from UV 366 through Fries rearrangement and showed a strong absorption between 250 and 450 nm and the maximum molar absorption coefficients were about $25000 \text{ L mol}^{-1} \text{ cm}^{-1}$ at 355 nm and $16000 \text{ L mol}^{-1} \text{ cm}^{-1}$ at 285 nm in DMF.

1.7 Optical brighteners

Optical brighteners with a broad UV absorption in UV-A radiation could be applied as UV absorbers in polytunnels. Optical brighteners have been used for many years to improve the colour of various plastics and have been applied for biopesticide formulations, ultraviolet protectors, enhancers in pathogenicity of viruses, ink jet recording media, cosmetics and increasing the visibility of fabrics and in night vision devices.^[95] The paper industry uses brighteners to increase the whiteness and brightness stability of paper products.^[96] Brighteners are also added to laundry soaps, detergents, or cleaning agents, where they adsorb to fabrics or materials during the washing or cleaning process and when illuminated by ultraviolet light they fluoresce in the blue region making and fabrics appear brighter.^[97]

Optical brighteners, also known as fluorescent whitening agents, are additives that alter the visual properties of polymers. Optical brighteners are often used in combination with other

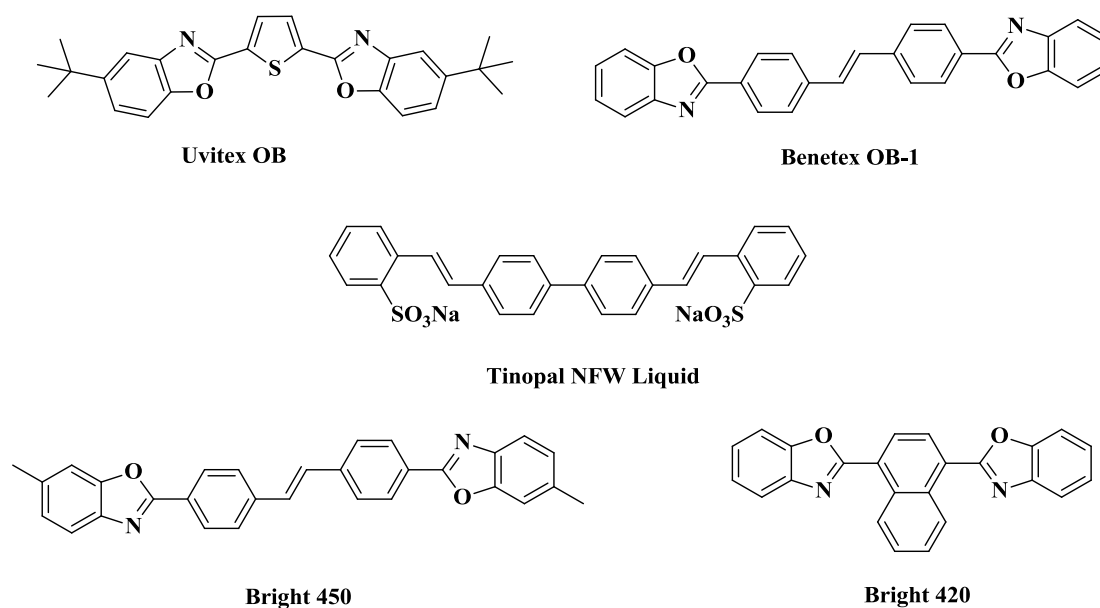
dyes or with pigments to produce specific shades.^[98] There are several optical brighteners commonly used in plastics (**Table 8**), which show strong absorption in the UV-A region.

Table 8. Optical brighteners

Brighteners	λ_m (nm)	Absorption range (nm)
Uvitex OB (Ciba)	372 (ethyl acetate)	300-400
Uvitex OB-1(Mayzo)^[99]	~365 (methyl chloroform) ^[98]	320-400
Tinopal NFW Liquid (BASF)^[100]	350(DMF/H ₂ O)	300-400
Bright 450 (MPI)^[101]	371(MeOH)	~280-400
Bright 420 (MPI)^[101]	366(MeOH)	~300-400

As shown in **Table 8**, optical brighteners have characteristic absorptions in the range of 300–400 nm. Uvitex OB is a heat resistant, solvent soluble, chemically stable fluorescent whitener that provides brighter looking colours. It can be used as a tracer in various applications and as an optical brightener in thermoplastics, coatings, printing inks, dyes, man-made fibres, waxes, fats, and oils.^[102] Uvitex OB is a good UV-A absorber and the wavelength of maximum absorption is 372 nm. In addition, Uvitex OB shows good compatibility in polyethylene, flexible polyvinyl chloride (PVC) and other thermoplastics. However, it shows a low photostability and absorption decreased significantly after UV radiation.^[103] Therefore, much research has been done to test stability in this study.

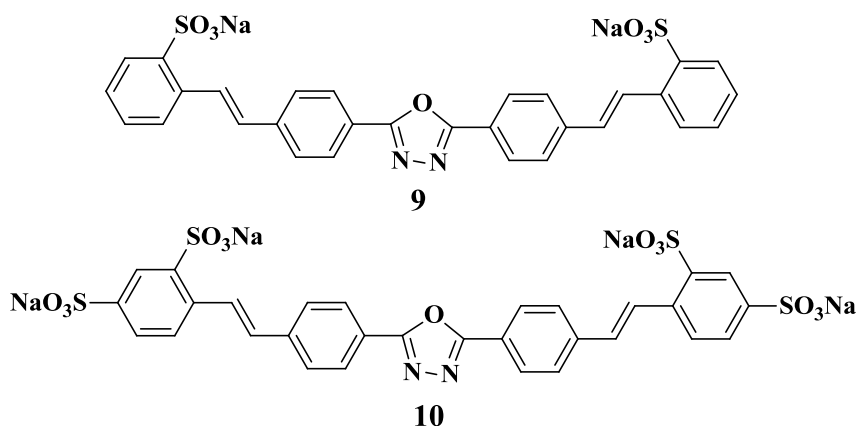
Benetex OB-1 has a similar structure and absorption range with Uvitex OB but lower solubility in chloroform, acetone and methanol, and shows subtle migration in polyethylene.^[103] Therefore, it is rarely the additive of choice. Benetex OB-1 has, however, a higher decomposition temperature.^[101]



Scheme 7. Chemical structures of the optical brighteners in **Table 8**

Tinopal NFW Liquid is a sodium salt which results in good water solubility suitable for paints. Bright 450 has the best whitening effect, the highest quantum yield, and exhibits better lightfastness than the other optical brighteners in **Table 8**.^[101] Bright 450 is more often used in polypropylene, polystyrene and polyester fibre.^[104] Bright 420 is recommended for the use in a wide variety of plastics, especially EVA-foamed plastics, and has a maximum UV absorption at 366 nm.^[104]

Optical brighteners are not only used for coating or printing; they can exhibit biological activity as well. For examples stilbene optical brighteners are known to enhance the activity of viruses in a number of *Lepidoptera*.^[105] 1,3,4-Oxadiazoles are an important class of heterocyclic compounds which have been reported to be biologically versatile compounds displaying a variety of biological effects.^[106] Researchers synthesised two novel symmetrical stilbene optical brighteners (**Scheme 8**) based on 1,3,4-oxadiazole-bearing sodium sulfonate units. The maximum absorption wavelengths of compounds **9** and **10** were 348 nm and 364 nm in DMF, respectively, which enhanced the insecticidal effect of *Spodoptera litura* nuclear polyhedrosis virus (SINPV) against 2nd-instar *S. litura* larvae.^[107]



Scheme 8. Chemical structures of novel optical brighteners.

Optical brighteners have shown good absorbance of UV radiation, but with low photostability, poor solubility in polyethylene and good solubility in water. All these properties could result in a fast degradation of polyethylene films.

1.8 Sunscreens

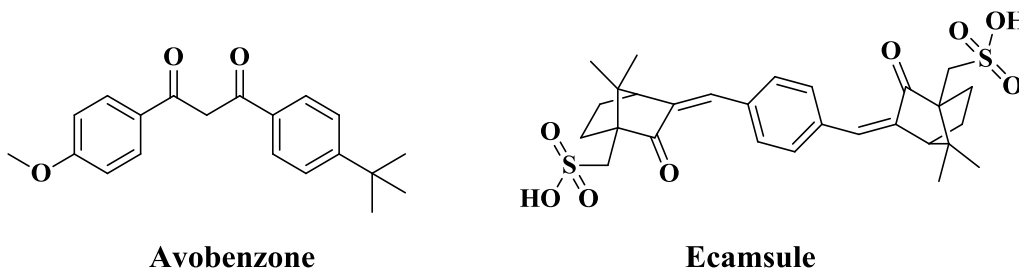
Sunscreens have been available since 1928. They play a major role in skin cancer prevention and sun protection,^[108] and could be modified for UV absorbing additives in polytunnels. Sunscreens are available in the form of topical lotions, creams, ointments, gels or sprays that can be applied to the skin. Sunscreen ingredients are found in many types of skin care products to absorb UV light. While UV-B protection and high SPF are imperative, UV-A protection is now recognized to be equally essential and has become a target for enhanced sunscreen efficacy.^[109] Sunscreen ingredients which absorb UV-A radiation are useful for this study. Several relevant sunscreen ingredients are listed in **Table 9**.

Table 9. Sunscreen ingredients ^[108]

Sunscreen ingredients	λ_m (nm)	Range of absorption (nm)
Avobenzene	360	310-400
Dioxybenzone	352	206-380
Ecamsule	345	295-390
Meradimate	336	200-380
Oxybenzone	290, 325	270-350
Zinc oxide (inorganic)	Varies	290-400

However, Avobenzene is highly photolabile. Its photoprotective properties can decrease around 60% after exposure to the sun for 1 hour.^[108] Avobenzene can also affect the stability of other active sunscreen ingredients.^[110] Dioxybenzone is mainly used as a UV absorber for coating and polymer.^[108] Oxybenzone is most commonly used, but has the highest incidence of photoallergic contact dermatitis and its oxidation can interrupt the antioxidant system.^[111] Meradimate is a weaker filter used to enhance longer UV-A wavelength protection.^[108]

Ecamsule (terephthalydene dicamphor sulfonic acid) is a molecule developed by L'Oréal® Paris and first patented in Europe in 1982^[111] with a broad spectrum and water resistance which reduces UV radiation effectively, and can prevent or reduce UV-induced pigmentation, pyrimidine dimer formation and photodermatoses.^[112] Ecamsule absorbs wavelengths from 295 to 390 nm, with a peak absorption at 345 nm. Marketed as Anthélios SX™ (La Roche Posay, division of L'Oréal, New York, NY), Ecamsule (2%) is combined with avobenzene (2%) and octocrylene (10%).^[111] Octocrylene functions boost photostability.



Scheme 9. Chemical structures of Avobenzone and Ecamsule

Zinc oxide is typically used as powder in combination with organic filters to enhance protection in the longer UV-A range, but is not as efficacious as organic UV-A filters.^[113] Skin penetration of ZnO nanoparticles has been investigated in a large set of *in vitro* and *in vivo* studies, but studies showed that ZnO nanoparticles were toxic to zebrafish embryos to different extents.^[114]

A broad-spectrum sunscreen with the same SPF, but providing a high protection in the UV-A range, significantly reduced local UV-induced immunosuppression.^[112] Broad-spectrum (UV-B/UV-A) products are produced by combining filters with varying UV absorption spectra. For example, octocrylene is often combined with benzophenones and avobenzone to improve sunscreen photostability.^[108] The combination of organic and inorganic filters can increase the SPF because inorganic filters scatter UV light, increasing the photons' optical pathways and enhancing subsequent absorption by organic agents.^[115]

Recently, a number of researchers tried to find effective UV absorber additives from plants and fruits. Due to limitation of the organic UV-filters which are characterized by their narrow spectrum of protection and low photostability, polyphenols appear particularly promising as cosmetic sunscreens because they can absorb a broad spectrum of UV radiation including the UV-B and UV-A regions.^[116] In addition they have immunomodulatory and antioxidant

properties as they can react with free radicals and reactive oxygen species produced by UV radiation (singlet oxygen and hydroxyl radicals) and inhibit or delay their harmful effects.^[117]

Helichrysum arenarium, *Sambucus nigra*, and *Crataegus monogyna* extracts are rich in phenolic compounds, including phenolic acids, flavonoids, catechins, and proanthocyanidins.^[118] For *C. monogyna*, the ethyl acetate fraction had wavelengths of maximum absorption at 320 and 360 nm, and for *H. arenarium* and *S. nigra*, λ_{\max} =341 and 319 nm.^[119] The individual polyphenolic fractions isolated from them provide good protection against ultraviolet radiation and show strong antioxidant activity and high photostability.^[119] Therefore *H. arenarium*, *S. nigra*, *C. monogyna* extracts represent useful additives for cosmetic formulation.

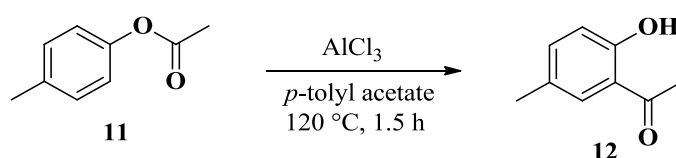
Furthermore, several natural polyphenols belonging to the classes of stilbenes (piceid), flavonoids (apigenin, chrysin) and hydroxycinnamic acid derivatives (caffeic acid, coumaric acid) show both antioxidant activity and photoprotective characteristics. They can be found in fruits, vegetables, red wine and tea, and protect plants from solar UV radiation.^[120] As a consequence, they could be interesting components for pharmaphotoprotective formulations.

Some sunscreens show ideal UV absorption in the UV-A/B region which could be a good reference point for selecting new UV absorbers as targets for synthesis. Additionally, another advantage reported by Ronald is sunscreen agents are capable of undergoing intramolecular photo-rearrangement to form a second sunscreen which could absorb more UV radiation than the first agents.^[121] This is similar with UV366 which was mentioned in section 1.6. The rearrangement product UV-D showed much stronger UV absorption than UV366, which also represented Fries rearrangement was an effect method for hydroxybenzophenones synthesis.

1.9 Fries rearrangement

The Fries rearrangement is a rearrangement reaction of a phenyl ester to a hydroxy aryl ketone catalysed by Lewis acids.^[122] This research focus is on synthesising new hydroxybenzophenones, and the Fries rearrangement is a well-known and reliable method to make benzophenones easily.

Aluminium chloride (AlCl_3) is the most common catalyst in the Fries rearrangement but usually requires prolonged heating times. For example, dry nitrobenzene (boiling point is $210.9\text{ }^\circ\text{C}$) has been used as a solvent.^[123] However, it was not easy to remove the nitrobenzene after reaction. Some researchers have performed the Fries rearrangement without solvent. In **Scheme 10**, a mixture of *p*-tolyl acetate (b.p. $104\text{-}105\text{ }^\circ\text{C}/25\text{ mm Hg}$) and AlCl_3 was heated at $120\text{ }^\circ\text{C}$ for 1.5 h and then 2 M HCl was added at $0\text{ }^\circ\text{C}$ to liberate the target product (yield 80-90%).^[124]



Scheme 10. Fries rearrangement

Thermally conducted Fries reactions give rise to mixtures of *ortho*- and *para*- substituted products, the proportion of each being strongly influenced by the temperature. Generally, high temperature favours *ortho*-shifts while low temperatures lead to *para*-shifts.^[125] Moreover, during the rearrangement, most Lewis acids are deactivated by the free hydroxyl groups of the products. The photo-Fries rearrangement could overcome the disadvantages of

the Lewis acid-promoted reactions. However, it is often a problem to carry out for large scale synthesis.^[126]

Therefore, some new catalysts such as hafnium trifluoromethanesulfonate (Hf(OTf)₄) and scandium trifluoromethanesulfonate (Sc(OTf)₃) have been developed more recently for Fries rearrangement.(**Table 10**)

Table 10. Catalysts and conditions for Fries rearrangement

Catalysts	Conditions	Yield range
Hf(OTf) ₄ (20% mmol) ^[127]	Toluene-MeNO ₂ (6.7:1), 100 °C, 6 h	60-70%
Sc(OTf) ₃ (5% mmol) ^[126]	Toluene , 100 °C, 6 h	70-90%
ZrCl ₄ (4 eq) ^[128]	Dichloromethane, r.t.	80-90%
SnCl ₄ (0.41 eq) ^[129]	Neat, microwave, 700 W, 2 min	80-90%
TfOH (100 eq) ^[130]	Neat, 100 °C, 2-16 h	60-80%

Hf(OTf)₄ and Sc(OTf)₃ are stable Lewis acids in water, and they are not trapped by the carbonyl oxygens of aromatic ketones as occurs with AlCl₃. Also the free hydroxyl and carboxylic groups do not decrease the Lewis acidity.^{[126][127]} A catalytic amount of these two catalysts could afford the rearranged product in good yields.

Tin(IV) chloride (SnCl₄) and trifluoromethanesulfonic acid (TfOH) could be used as catalyst of Friedel-Crafts acylation and Fries rearrangement. These two new methods are easy, and clean reactions for the preparation of *ortho*-hydroxyaryl ketones occur in excellent yields.^{[129][130]} As shown in **Table 10** rearrangement with SnCl₄ was carried out under microwave, which could be a problem for a large scale preparation. Trifluoromethanesulfonic

acid (TfOH), which can be considered a super-acid, forms water-stable salts,^[131] and can act as a protic catalyst. Fries rearrangement proceeded effectively in neat TfOH.

Zirconium tetrachloride ($ZrCl_4$) has been found to be an excellent mediator with rearrangement occurring at ambient temperature. Four equivalents of $ZrCl_4$ were used with dichloromethane as solvent with simple stirring at room temperature, or reaction in an ultrasound cleaning bath, leading to substantial improvements in reaction rate and efficiency.^[128]

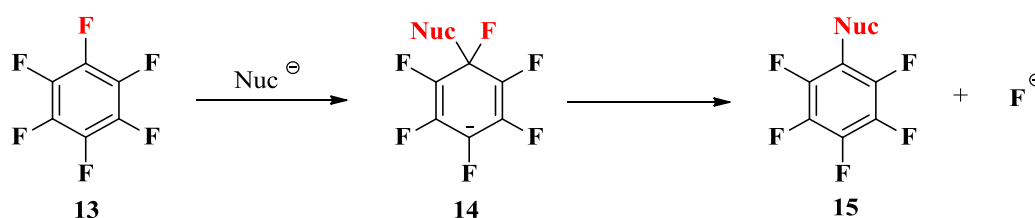
Moghaddaman found that an $AlCl_3$ - $ZnCl_2$ mixture supported on silica gel is an efficient medium for promotion of the Fries rearrangement without solvent under microwave dielectric heating. The support was made by evaporation of an aqueous suspension of a mixture of SiO_2 : $AlCl_3 \cdot 6H_2O$: $ZnCl_2$ (5:4:1 w/w/w). Three equivalents of support were used, and after microwave irradiation for 7 min, work-up gave a 95% yield of the *ortho*-substituted products.^[125]

Comparing all these methods, the use of $ZrCl_4$ as catalyst was the easiest and highest yielding. In this project, this method was thus used to prepare benzophenones from the corresponding esters.

1.10 Fluorine-nucleophilic substitution reaction

Nucleophilic aromatic substitution is a substitution reaction in which the nucleophile replaces a leaving group on an aromatic ring.^[132] Fluorinated aromatic rings are different from their

hydrogen analogues in terms of substitution. Fluorine allows nucleophilic attack on the aromatic ring, (**Scheme 11**) which is difficult to effect on hydrogen-based aromatic rings. Since the great breakthrough in the study of organofluorine chemistry was achieved in 1930's, the first publications dealing with issue of nucleophilic substitution of fluorine originated in the year 1968 which focused on nucleophilic substitution of *o*-fluorine and *p*-fluorine by dimethylamine followed by sodium hydrogen sulphide, sodium thiophenoxide, and sodium methoxide *para*-substitution on pentafluorobenzaldehyde.^[133] Other research was published later and dealt with nucleophilic substitution of *p*-fluorine by sulphur, oxygen, nitrogen and azide anion nucleophiles.^[134]



Scheme 11. Mechanism of fluorine-nucleophilic substitution reaction^[135]

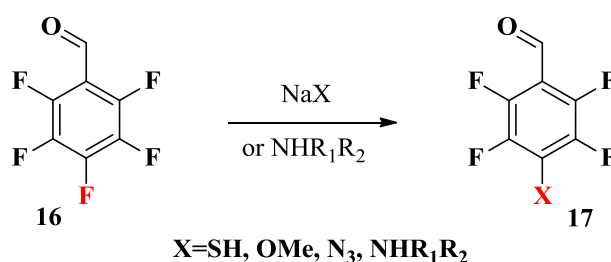
In **Scheme 11**, a nucleophilic reagent attacks the carbon of the highly fluorinated aromatic ring, and forms an intermediate complex (**14**) which is a resonance-stabilised carbanion with a new carbon–nucleophile bond known as a Meisenheimer complex. Then aromatisation takes place by elimination as a fluoride ion from the ring in the next step.^{[136][137]}

It is well known that the C–F bond in fluorinated aromatic compounds towards nucleophilic substitution. The presence of halogen on aromatic ring and the number and strength of the electron withdrawing/donating group on the ring have an influence on the rate of whole S_NAr reaction.^[138] Fluorine is the smallest halide with the least steric hindrance to the reaction which increases the rate of the nucleophilic aromatic substitution reaction on fluorinated

aromatic systems. Electron-withdrawing groups on the aromatic ring help to stabilise the intermediate complex in the state of the negative charge and activate nucleophile to attack the ring at the *para*-site. Electron-donating groups on the ring increase the proportion of *meta*-substitution.^[136]

The presence of a fluorine atom can benefit the properties of a compound, and perfluorinated substituents are often incorporated to affect the oxidation and reduction potential and to increase the stability of the macrocyclic compound.^[139] *ortho*-, *meta*- and *para*- Substitution of fluorine by nucleophiles in the nucleus of poly-fluoroaromatic compounds are all possible.

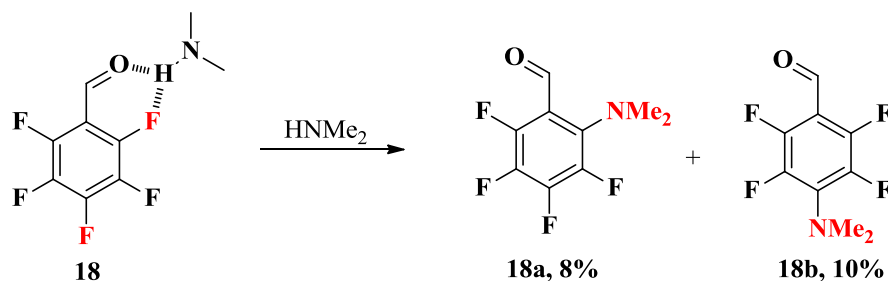
Most fluorine substitution reactions take place at the *para*-position due to reaction usually occurring at the most electrophilic site in the compound which allows for the most effective stabilisation of the negatively charged primary addition product. (**Scheme 12**)



Scheme 12. Fluorine-nucleophilic substitution on *para*-position ^[134]

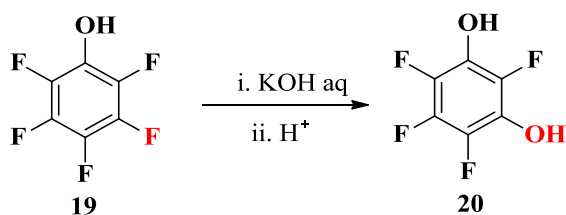
In a few special cases, *ortho*-substitution predominates in reactions caused by specific interaction between the substituent in poly-fluoroaromatic compounds and the attacking nucleophile. Researchers have explained the substitution of *o*-fluorine with dimethylamine by this mechanism. (**Scheme 13**) A hydrogen bond between the aldehydic hydrogen and amine,

or by association between the nucleophile and the substrate, involves the positively polarized aldehydic carbon and lone-pair electrons of nitrogen in amino group.



Scheme 13. *ortho*-Fluorine-substitution reaction ^[134]

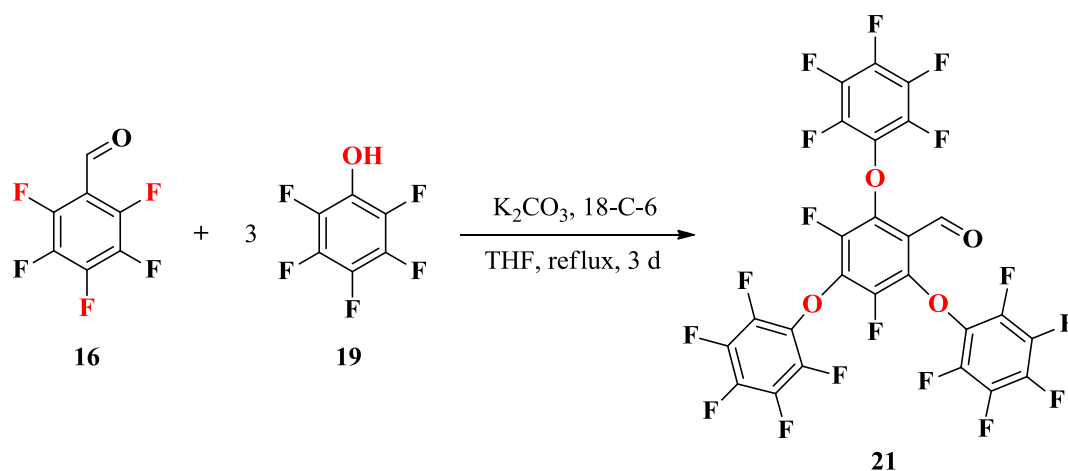
meta-Position substitution on fluorinated arenes is the least common site of attack and requires vigorous conditions such as powerful electron-donating group upon the aromatic ring. The reaction of pentafluorophenol (**19**) with potassium hydroxide only takes place with *meta*-substitution. ^[140] (**Scheme 14**)



Scheme 14. *meta*- Fluorine-substitution reaction ^[140]

More than one fluorine atom can be replaced by nucleophilic groups on perfluorinated compound. Pentafluorobenzaldehyde (**16**) can be substituted by 3 eq. of pentafluorophenol (**19**) to afford the trisubstituted derivative (**21**) with both *para*- and *ortho*- positions replaced. ^[141] Poly-substitution nucleophiles usually attack the *ortho*-site after the *para*-

position has been substituted. *ortho*-Position is considered to be more susceptible to attack compared with the *meta*-position.



Scheme 15. Fluorine-substitution reaction

The second and third nucleophilic groups attack is more difficult compared with the first one. Because first substituent added to the fluorinated aromatic ring usually deactivates further attack towards the ring.^[136] The reaction in **Scheme 15** which used 18-crown-6 with potassium acetate as a more powerful nucleophile under required refluxing THF for 3 days, which confirmed the next nucleophilic attack is more difficult than the first one.

As fluorine substituents contribute to a subtle change in the molecular conformation or reactivity, fluorinated aromatic compounds have gained great interest by the scientific community. In this project, fluorine-nucleophilic substitution reaction played a significant role in synthesising the desired UV absorbers.

Chapter 2. Uvitex OB degradation and stabilisation

2.1 Introduction

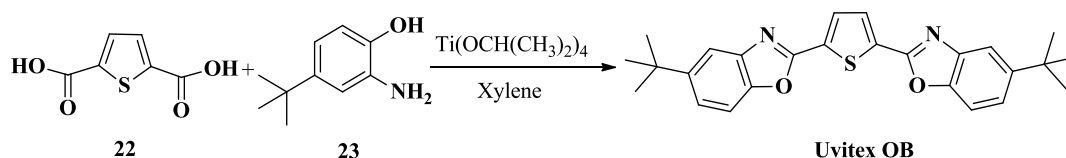
Uvitex OB (Tinopal OB, 2,5-thiophenediylbis(5-tert-butyl-1,3-benzoxazole), as mentioned earlier (section 1.7) is a high molecular weight optical brightener (fluorescent whitening agent). Uvitex OB is an ideal UV-A absorber which can be used as UV-A filter to absorb UV-A radiation and has a wavelength of maximum absorption at $\lambda_{\max} = 372$ nm. Furthermore, it is easily added to ethylene vinyl acetate (EVA). **Table 11** shows the solubility of Uvitex OB in different solvents.

Table 11. Uvitex OB solubility ^[102]

Solubility (20 °C)	% w/w
Chloroform	14
Ethyl acetate	1
n-Hexane	0.2
Methanol	< 0.1
Water	< 0.01

The poor solubility in water of Uvitex OB is an advantage when for incorporation into polyethylene films for polytunnels and the high melting range gives it excellent resistance to heat. Uvitex OB as an optical brightener could give a bright appearance to polyethylene films.

Uvitex OB can be synthesised from thiophene-2,5-dicarboxylic acid (**22**) and 2-amino-4-*tert*-butylphenol (**23**) with a catalyst such as isopropyl orthotitanate or boric acid in xylene or toluene (**Scheme 16**).^[142]



Scheme 16. Synthesis of Uvitex OB

A Dean-Stark water separator is needed during this reaction because it is a condensation reaction and 4 equivalents of water are formed. Therefore, a secondary solvent *N*-methylpyrrolidone is helpful to remove water from the reaction mixture.

Researchers found polytunnel polymer films containing Uvitex OB stopped insects and pests and led to a good colour for plants growth (section 1.4). However, Uvitex OB showed a low photostability. Therefore, it is worth to find a good light stabiliser to enhance the stability.

2.2 Aims

The aim of the project outlined in this chapter was to test the photostability of Uvitex OB using a Xenon arc lamp and to determine the degradation mechanism, which might be achieved by using HPLC, NMR, IR and GC-MS to separate and analyse degraded products.

Based on the results, the target core was to find the best light stabilisers for combining with Uvitex OB in an ideal concentration to enhance the photostability in polytunnels.

2.3 Results and discussion

2.3.1 HPLC for Uvitex OB

Uvitex OB was irradiated in solution for a prolonged time under oxygen. HPLC was used to separate degraded products from starting material. An HPLC instrument equipped with a diode array detector, which records the whole UV spectrum to provide a UV absorption spectrum for each component eluted, was used initially to analyse products. Uvitex OB and the irradiated compounds were dissolved in THF.

Originally, a MAX-RP column was employed with different mobile phase (methanol, methanol: water (50:50) and hexane). Unfortunately, only the solvent (THF) peak was detected. Then Zorbax Columns (ZORBAX CN 4.6 mm x 25 cm) was tested with different mobile phase (acetonitrile, methanol, MeCN: MeOH (50:50), MeCN: H₂O (50:50) and hexane). Acetonitrile (100%) was the best solvent for this column but could not separate the product peaks even with a lower flow rate. UV spectra for each fraction showed several mixed lines because of poor separation.

Therefore, an HPLC instrument with a fixed wavelength UV detector was used which did not give the UV spectrum for each compound eluted. The solubility of Uvitex OB in some organic solvents is low. Separation was first investigated with hexane: 2-propanol (95:5) which did not allow separation of the products. However, 98% hexane with 2% propanol as mobile phase was effective for analysis. The detector wavelength was set up at 282 nm because the UV-Vis

spectrum showed the maximum absorption of degraded product was at 282 nm. And at this wavelength, the differences between irradiated product and starting material could be observed clearly.

2.3.2 Degradation for Uvitex OB in solution

Uvitex OB was dissolved in ethyl acetate ($c=0.19 \times 10^{-4}$ mol/L) for irradiation under an arc lamp in air for 8 h (**Figure 2**). **Figure 3** shows the effect of irradiation after oxygen, or nitrogen respectively was passed through the solution for 10 min before irradiating for 3 h, and 8 h respectively.

Comparing **Figures 2** and **3** shows Uvitex OB degraded faster under oxygen than air. Degradation under nitrogen in **Figure 3** was the slowest. Passing nitrogen through the solution enhanced stability. Therefore, the irradiation of Uvitex OB was carried out under oxygen for studying degradation.

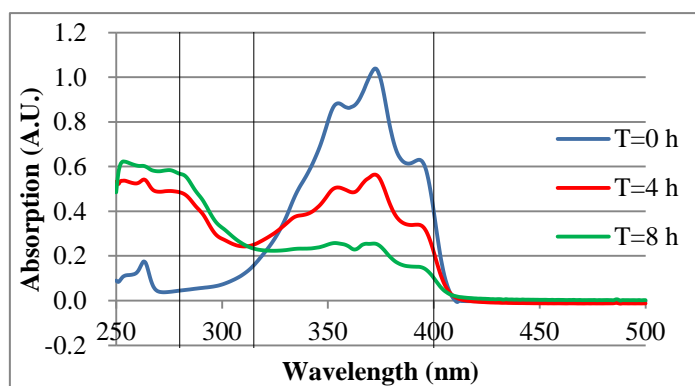


Figure 2. Degradation for Uvitex OB under air

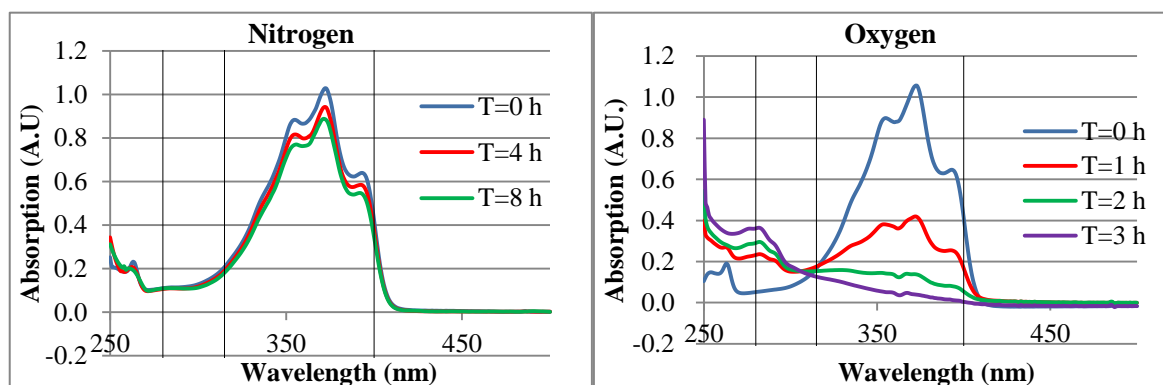


Figure 3. Degradation for Uvitex OB under air or oxygen

Uvitex OB was dissolved in ethyl acetate at a higher concentration ($c=0.58 \times 10^{-4}$ mol/L). Oxygen was passed through the solution before irradiating for 7 h. However, HPLC did not show any difference from the starting material despite the changes originally observed in the UV absorption spectra.

As no difference was observed in the HPLC trace, the concentration of the solution was reduced ($c=0.37 \times 10^{-4}$ mol/L). During the irradiation, UV absorption was monitored, and absorption decreased from 2.02 A.U. to 0.06 A.U. after 6 h. Then the solvent was evaporated and the solid was dissolved in THF for HPLC (**Figure 4**). **Figure 5** is the HPLC trace for Uvitex OB.

The peak intensities are different in **Figures 4** and **5** because the concentration of the degraded product was lower than starting material ($c=0.58 \times 10^{-4}$ mol/L). Peak 2 in **Figure 4** shows that some Uvitex OB remained. The percentage of starting material in degraded product also reduced, and different several new products formed.

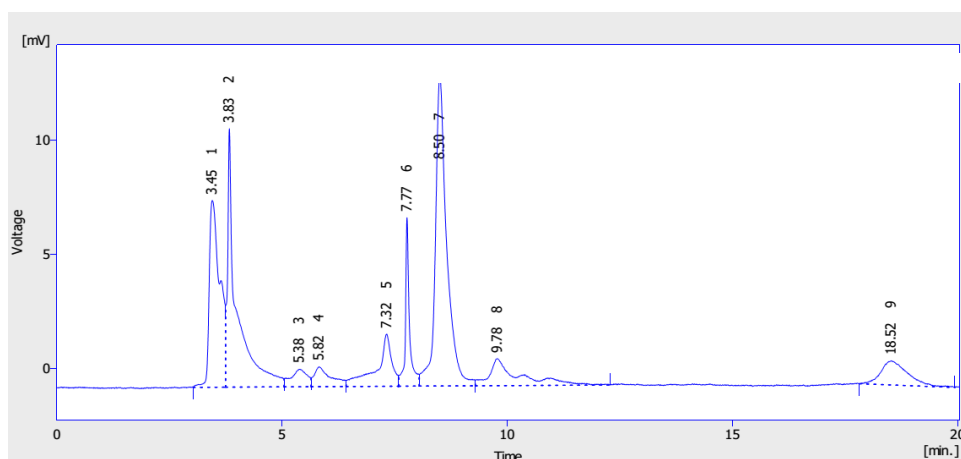


Figure 4. HPLC trace for degraded product

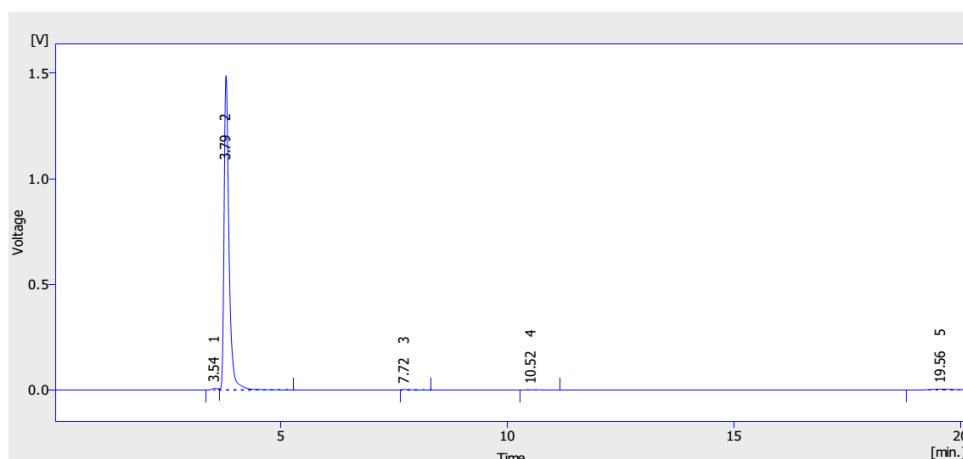


Figure 5. HPLC trace for Uvitex OB

Since HPLC showed several different compounds forming from the starting material (Uvitex OB), GC-MS was used to try to identify the products. GC-MS showed two major peaks. One signal was due to starting material which gave m/z 430 corresponding to $C_{26}H_{26}N_2O_2S$. Another signal was at m/z 321 indicating a lower molecular mass compound, which does not correspond to a fragment of Uvitex OB and has not yet been identified.

In order to get more material for analysis, a higher concentration of Uvitex OB in ethyl acetate ($c=0.23 \times 10^{-1}$ mol/L) was used. The solution was treated with oxygen for 10 min and irradiated

for 64 h under a balloon of oxygen to provide a constant supply of O₂. The same conditions were used as previous for HPLC analysis, but peaks were not separated perfectly. Mobile phase were changed to 98.7% hexane with 1.3% 2-propanol, and flow rate was changed to 0.8 ml/min in order to achieve separation.

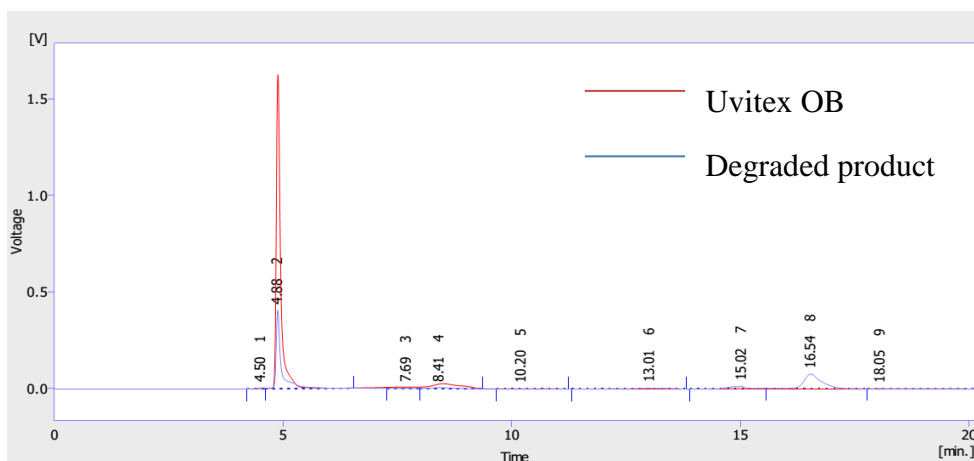


Figure 6. HPLC trace for irradiated product (flow rate: 0.8 ml/min)

The red line in **Figure 6** was Uvitex OB and the blue line was degraded product. Peaks 1 and 2 were starting material. Peak 8 was the major product after irradiation. The eluate of each peak was collected for measuring the UV absorption with ethyl acetate as solvent. The UV spectrum showed the eluate between 4 min and 6 min was starting material Uvitex OB. But no absorption was observed for the eluate between 16 min and 20 min because the sample was too weak to be detected.

Therefore, the solution of Uvitex OB ($c=0.47 \times 10^{-1}$ mol/L) in ethyl acetate was irradiated for 137 h under oxygen. Because of larger scale preparation, preparative TLC was carried out instead of collecting the eluate from HPLC for the irradiated product.

Three main fractions were collected from the prep TLC, and UV absorptions were measured for each fraction in ethyl acetate. As shown in **Figure 7**, fraction Uvitex OB-1-1 showed a similar UV absorption spectrum to the starting material Uvitex OB. Fraction Uvitex OB-1-2 exhibited a similar spectrum in the UV-A region with $\lambda_{\max}=355$ nm, but a different absorption between 250 nm and 320 nm, while fraction Uvitex OB-1-3 showed strong absorption around 279 nm and 332 nm.

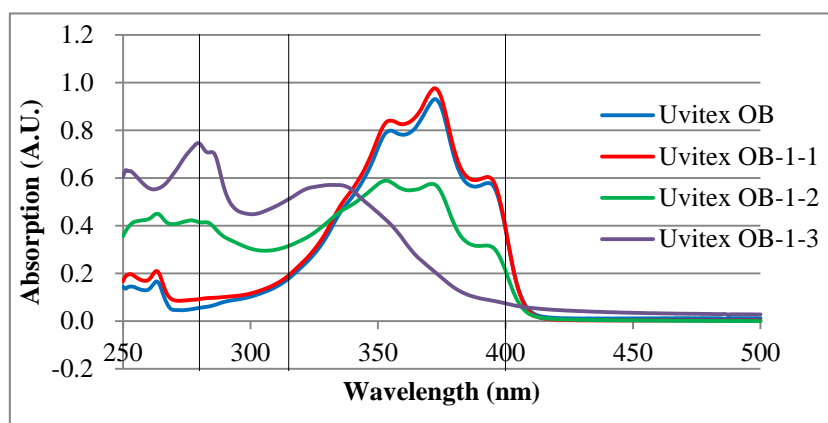


Figure 7. UV absorption for Uvitex OB after preparative TLC

The weight of material from fraction Uvitex OB-1-1 was 9 mg which showed most of the starting material remained after 137 h degradation time. Only 1 mg of fraction Uvitex OB-1-2 was obtained and showed similar absorption with in UV-A region, and 4 mg of material was afforded from fraction Uvitex OB-1-3. The ^1H NMR spectra showed complicated and weak signals which did not clarify what kind of compounds formed. GC-MS gave peaks at m/z 430 and 415 of Uvitex OB-1-1 which confirmed it was starting material. For Uvitex OB-1-2 and Uvitex OB-1-3, GC-MS did not give any detectable signals.

The total weight of the three parts was 14 mg which was greater than the starting amount of 10 mg. We considered that oxygen or ethyl acetate might have added to Uvitex OB and broken the

ring system thus reducing the conjugation. Hence the maximum absorption in the UV-A region shifted to a lower wavelength.

2.3.3 Uvitex OB with stabilisers

Uvitex OB with Chimassorb 944

Chimassorb 944 as mentioned in section 1.5 is a high molecular weight hindered amine light stabiliser that shows excellent light stability to fibres and films. Uvitex OB was combined with Chimassorb 944 (C944) by weight ratio (1:1) in all the following experiments.

Uvitex OB ($C=0.17 \times 10^{-4}$ mol/L) and C944 were dissolved in ethyl acetate for irradiation under an Xenon arc lamp in air for 8 h, and the spectra was recorded when oxygen was passed through the solution for 10 min before irradiating for 3 h. **Figure 8** shows degradation for Uvitex OB in the presence of C944 in oxygen was faster than in air, and the degradation under air did not show C944 enhanced the photostability significantly compared with **Figure 2**.

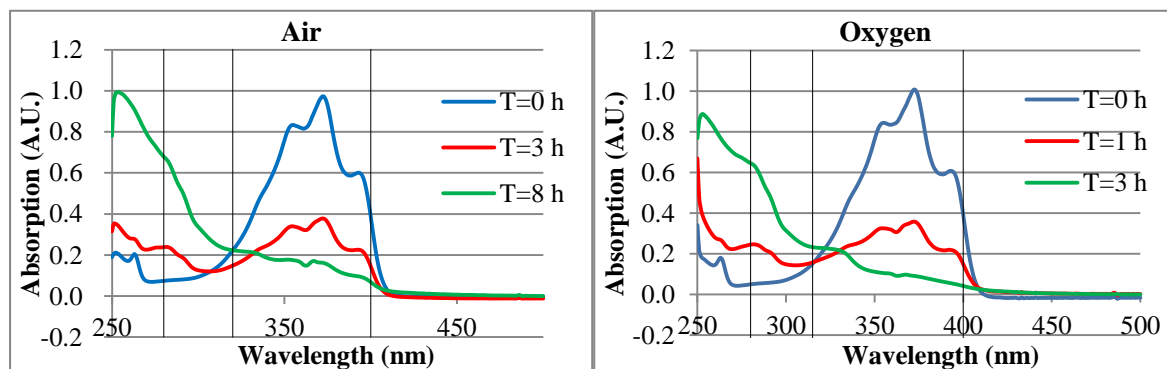


Figure 8. Degradation for Uvitex OB with C944 under air or oxygen

Uvitex OB ($c=0.19 \times 10^{-4}$ mol/L) and C944 were irradiated under oxygen for 8 h, and the degraded products was dissolved in THF for HPLC separation (**Figure 9**).

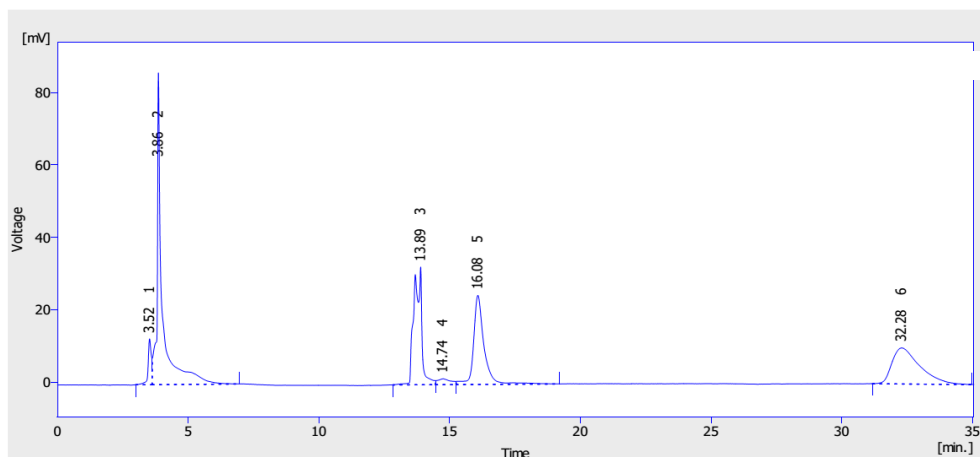


Figure 9. HPLC trace for degraded product

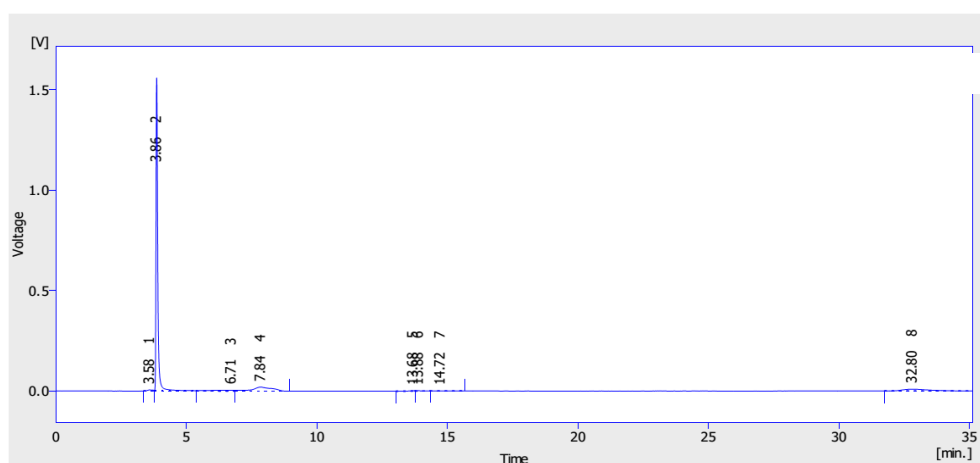


Figure 10. HPLC trace for Uvitex OB with C944

Figure 10 shows Uvitex OB with C944 as starting material for comparison with **Figure 9**. Peak 2 in both figures was starting material. Peaks 3-6 in **Figure 9** were new products. Different degraded products formed after irradiating for 8 h under the arc lamp.

In order to get more material for analysis, the solution of Uvitex OB and C944 in 5 ml ethyl acetate ($c=0.47 \times 10^{-2}$ mol/L) was irradiated under oxygen. After 6 h degradation, white solid precipitated out, the irradiation was stopped. The product was analysed by HPLC which showed the starting material only. Therefore, this experiment was conducted under same conditions. After 6 h, white solid precipitated out as in the previous experiment. The white solid was filtered after 86 h irradiation, and the soluble material from the supernatant was separated by preparative TLC.

Four main fractions were collected. UV absorption was measured in ethyl acetate for each fraction (Uvitex OB-2-2 → Uvitex OB-2-4) (**Figure 11**).

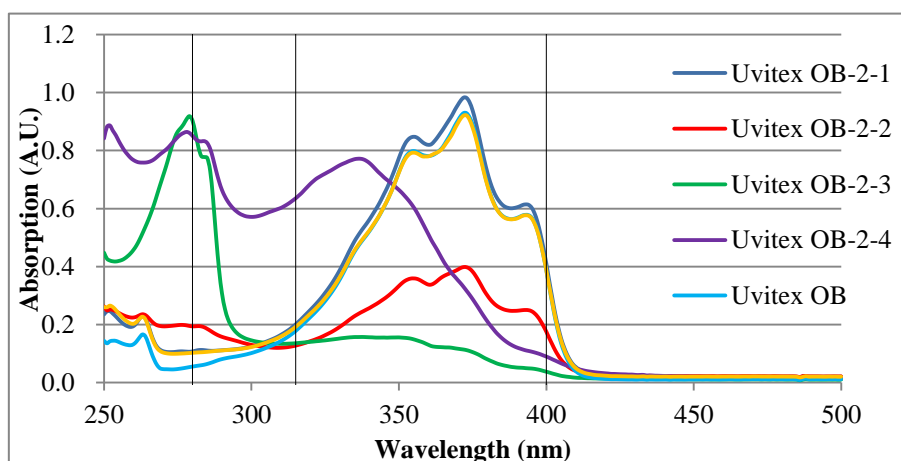
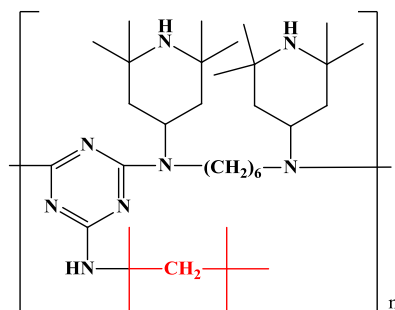


Figure 11. UV absorption for Uvitex OB with C944 after preparative TLC

From **Figure 11**, the absorption of Uvitex OB-2-1 and Uvitex OB-2-2 in UV-A region was similar to starting material. Uvitex OB-2-3 and Uvitex OB-2-4 exhibited absorptions between 250 nm and 400 nm wavelength which were different from the starting material.

The NMR spectrum and GC-MS confirmed that Uvitex OB-2-1 was starting material which weighed 3 mg (30% recovery). NMR spectra for the other fractions were complicated and weak, and were not ideal for identification. For Uvitex OB-2-2 (4 mg obtained), GC-MS gave peaks at m/z 415, 430, 503 and 535 which suggested the material contained starting material and other unidentified products. Mechanistically the C-O bond in Uvitex OB might break. The oxygen could possibly attack the carbonyl group in ethyl acetate to form an ester and the carbon could potentially form a C=O bond, which would give a mass of 550 and meet the GC-MS value found (m/z 535) if a methyl group was also lost.

The solid which precipitated out during irradiation weighed 6 mg did not dissolve in chloroform, methanol or acetone. The IR spectrum was similar to C944, which suggested the white solid might be related to Chimassorb 944.



Scheme 17. Structure of Chimassorb 944

However, Chimassorb 944 is soluble in ethyl acetate and methanol. It suggested the $(\text{CH}_3)_2\text{CCH}_2\text{C}(\text{CH}_3)_3$ groups may have been lost from the amine backbone resulting in higher polarity for rest of the molecule. Additionally, GC-MS showed peaks at m/z 647 and 662 for both Uvitex OB-2-3 (1 mg) and Uvitex OB-2-4 (3 mg), which might suggest the two C-O bonds were broken and the alkyl group (molecular weight 113) was added twice on oxygen in Uvitex OB by giving a mass around 662 (647 assuming loss of a methyl group).

For comparison, 10 mg C944 were dissolved in 5 ml ethyl acetate which was irradiated under oxygen. After 8 h, white solid did not precipitate out which suggested Uvitex OB reacted with C944 resulting in faster degradation. This may be the reason that C944 cannot enhance the stability of Uvitex OB.

Degradation for both Uvitex OB and Uvitex OB with C944 was faster in oxygen than in air. Oxidation may have happened during irradiation and reduced the stability of Uvitex OB. Therefore, antioxidants could be studied in combination with Uvitex OB which might enhance the stability.

Uvitex OB with Irganox 1010 and Irgafos 168

Irganox 1010 is a sterically hindered phenolic antioxidant which can be added to polyolefins to protect substrates against thermo-oxidative degradation. In order to find out the best ratio for enhancing the stability of Uvitex OB, Uvitex OB was combined with Irganox 1010 in weight ratio from 1:1 to 1:200 in ethyl acetate. Degradations were carried out under air, nitrogen and oxygen. Results are compared by plots with absorption at 372 nm wavelength against degradation time. (**Figures 12, 13 and 14**)

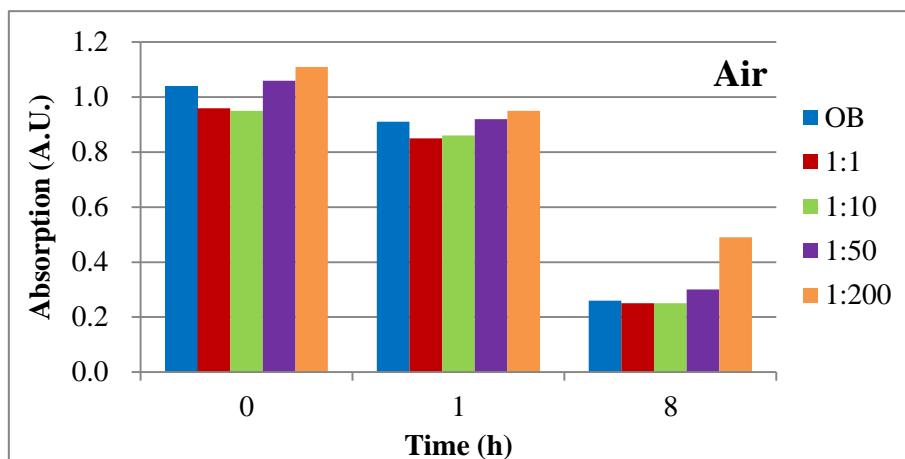


Figure 12. Degradation of Uvitex OB with I1010 in different ratio under air

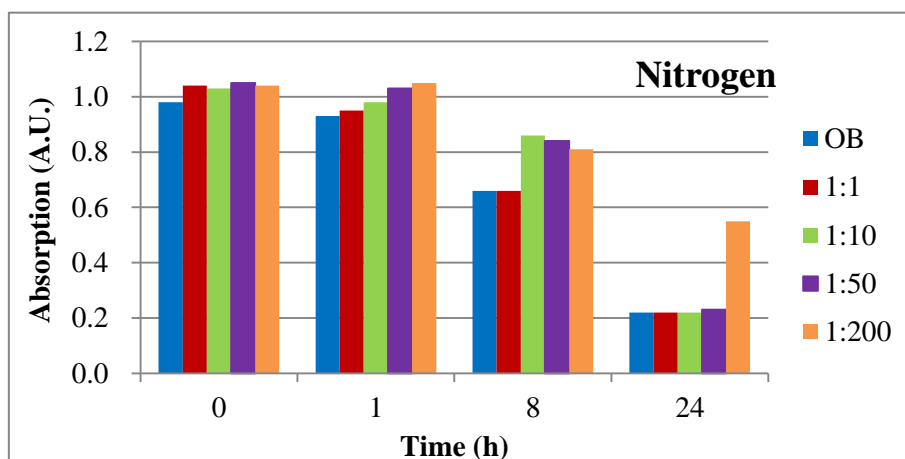


Figure 13. Degradation of Uvitex OB with I1010 in different ratio under nitrogen

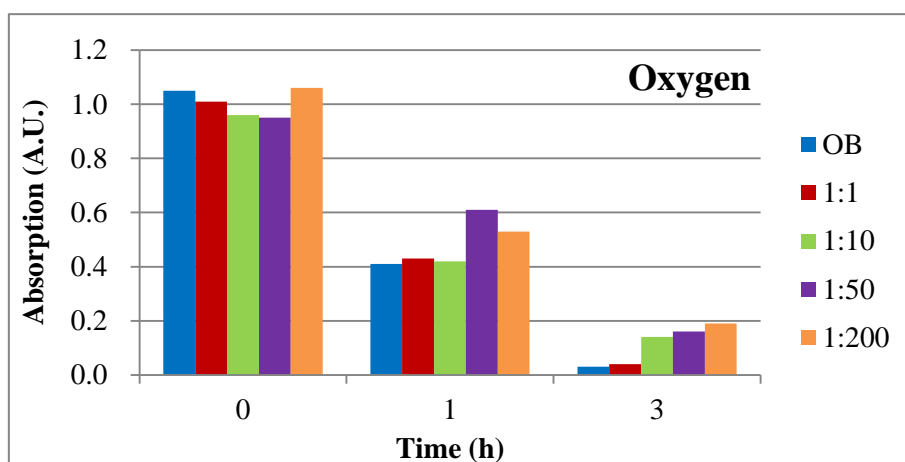


Figure 14. Degradation of Uvitex OB with I1010 in different ratio under oxygen

Figures 12, 13 and 14 show Irganox 1010 did not enhance the photostability of Uvitex OB when they were combined in ratio 1:1 by weight. However, stability was enhanced when the ratio of I1010 was increased which is showed clearly in **Figure 12** and **Figure 13**. After 8 h degradation under air, absorbance of Uvitex OB at 372 nm was decreased from 1.04 to 0.26. When combined with I1010 in 1:200 ratio, absorbance only reduced from 1.11 to 0.49 under air, and Uvitex OB degraded only 47% after 24 h under nitrogen, which was lower than 78% without I1010.

Therefore, Irganox 1010 could enhance the stability of Uvitex OB when it was combined with Uvitex OB in a high concentration. However, the combined compounds showed major and significant absorption in both the UV-C and UV-B regions due to the absorption of Irganox 1010 (**Figure 15**). And the absorption moved towards longer wavelength after 8 h degradation under air, which is different with the target to block part of UV-B radiation. Therefore, a high concentration of Irganox 1010 cannot be used to enhance Uvitex OB stability in polytunnels.

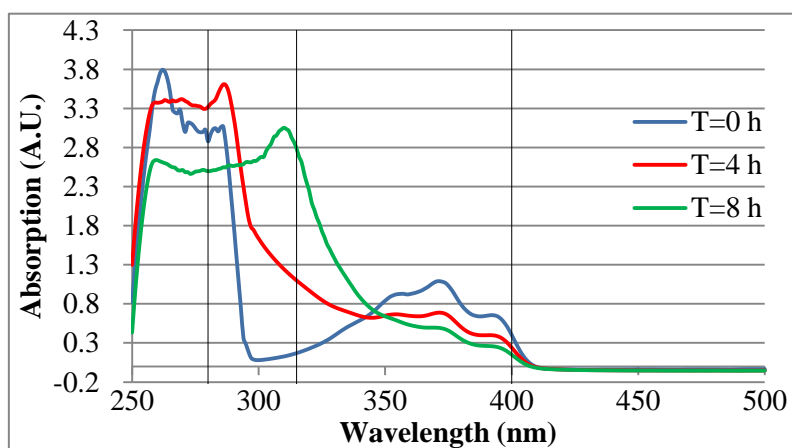


Figure 15. Degradation of Uvitex OB with Irganox 1010 in 1:200 ratio

Irgafos 168 as mentioned in section 1.5 is a hydrolytically stable phosphite processing stabiliser, which was combined with Uvitex OB in different weight ratios. (**Figure 16**)

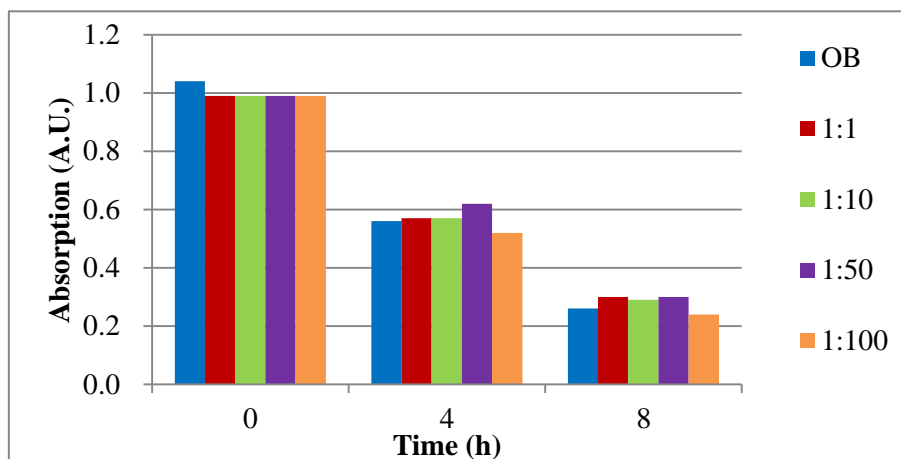


Figure 16. Degradation of Uvitex OB with Irgafos 168 in air

Figure 16 shows that when Uvitex OB was combined with Irgafos 168 in 1:1, 1:10 and 1:50 ratios, the stability was improved slightly. The differences were not significant. Although the ratio at 1:50 was the best in **Figure 16**, the results were not ideal. Uvitex OB degraded 70% after 8 h irradiation, only a little bit lower than without Irgafos 168 (75%).

As mentioned in the general introduction (section 1.5), Irgafos 168 can be combined with Irganox 1010 named as Irganox B215 to protect against oxidative degradation. Uvitex OB was combined with Irganox B215 (67 % Irgafos 168 and 33 % Irganox 1010) in different weight ratios in ethyl acetate for irradiation in air. (**Figure 17**)

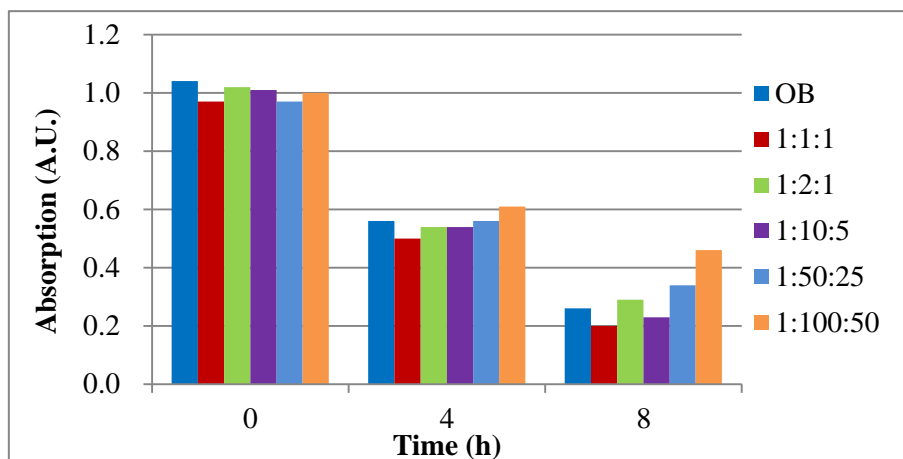


Figure 17. Degradation of Uvitex OB with Irgafos 168 and I1010 in air

The photostability was enhanced when Uvitex OB was combined with Irganox B215 which is shown clearly by the blue and orange bars. Irganox B215 could enhance the stability of Uvitex OB in high concentration. Compared with the previous results, the stability of Uvitex OB was improved significantly when Irgafos 168 was combined with Irganox 1010, especially when they combined in 1:100:50 ratio.

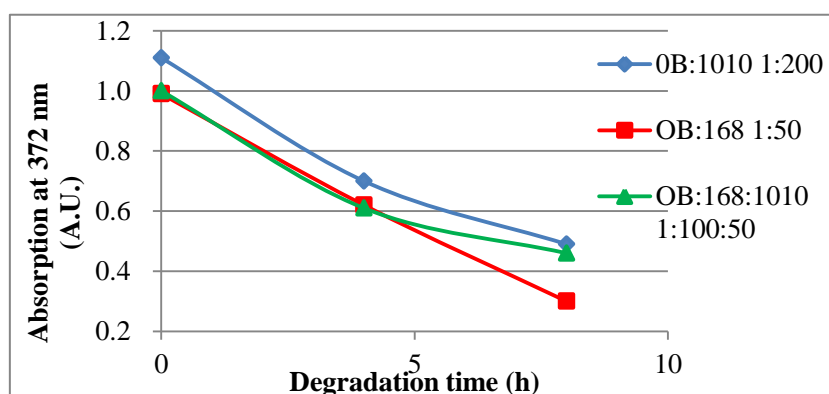


Figure 18. Comparison for degradation of Uvitex OB with Irgafos 168 and I1010

Shown in **Figure 18** is the comparison of degradation among Uvitex OB combined with Irgafos 168, I1010 and Irganox B215. When Irgafos 168 and I1010 were used separately, the degradation rates of Uvitex OB were similar. When Irgafos 168 and I1010 were combined in

a 1:2 ratio, the stability of Uvitex OB was enhanced, and there was not a significant increasing absorption in the UV-B region. (**Figure 19**)

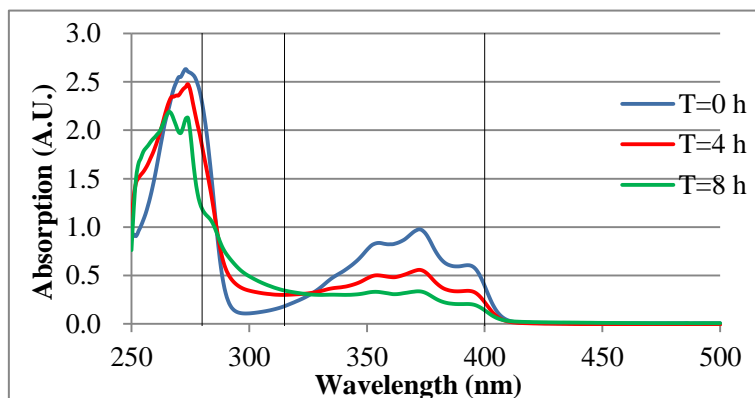


Figure 19. Degradation of Uvitex OB with I168 and I1010 in 1:100:50 ratio

Uvitex OB with Tinogard Q

Tinogard Q, an excited state quencher (section 1.5), was combined with Uvitex OB in different weight ratios to study enhancement of photostability. (**Figure 20**)

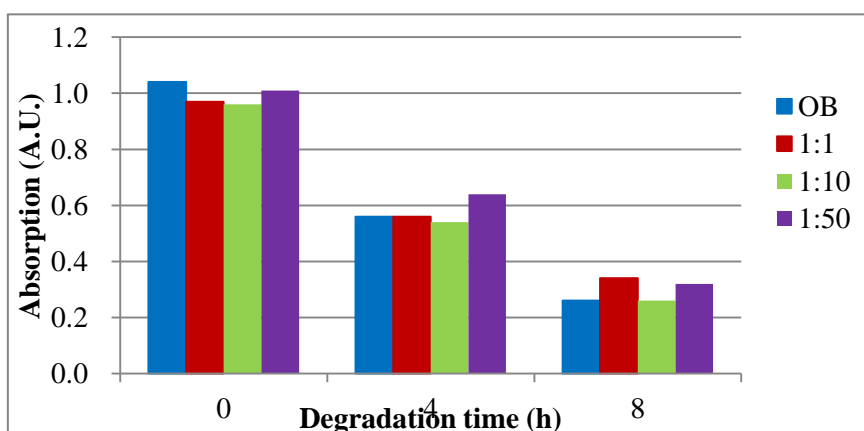


Figure 20. Degradation of Uvitex OB with Tinogard Q

Uvitex OB was combined with Tinogard Q in 1:1, 1:10 and 1:50 ratios. **Figure 20** shows a 1:1 ratio was the best, which enhanced the stability. Uvitex OB degraded 65% lower than without Tinogard Q (75%). A higher concentration of Tinogard Q (1:50) enhanced the stability in the first 4 h, but Uvitex OB degraded 68% after 8 h irradiation.

Fluorescence quantum yield and excitation lifetime

The fluorescent properties of Uvitex OB were measured to help understand the behaviour of this molecule. As shown in previous discussion, Uvitex OB has characteristic UV absorption in the range of 300–400 nm. The wavelength with maximum absorption (372 nm) was chosen as the excitation wavelength to explore its fluorescent properties. The fluorescence emission of Uvitex OB is located in the range 380–600 nm as shown in **Figure 21** and the maximum emitting wavelength was 429 nm. The quantum yield was found to be 71% in ethyl acetate relative to 1,4-bis(5-phenyloxazol-2-yl) benzene (POPOP) as a standard.

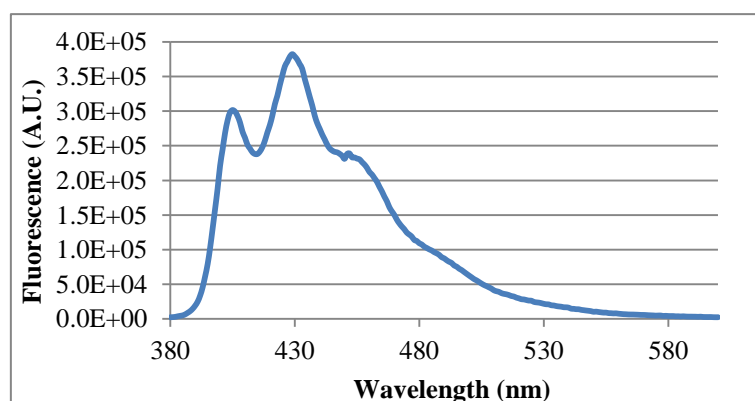


Figure 21. Fluorescence spectrum for Uvitex OB

The fluorescence lifetimes were measured for Uvitex OB and Uvitex OB combined with stabilisers, which is shown in **Table 12**. Uvitex OB ($C=0.86 \times 10^{-6}$ mol/L) and Tinogard Q ($C=1.42 \times 10^{-6}$ mol/L) were dissolved in ethyl acetate. The lifetime of Uvitex OB in air was only 1.21 ns but increased slightly to 1.26 ns under nitrogen.

Table 12. Life time for Uvitex OB

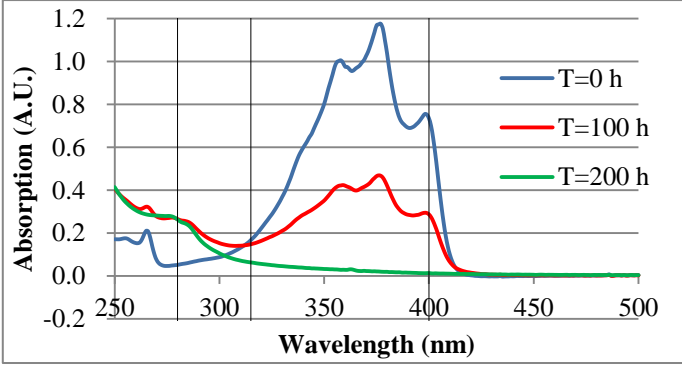
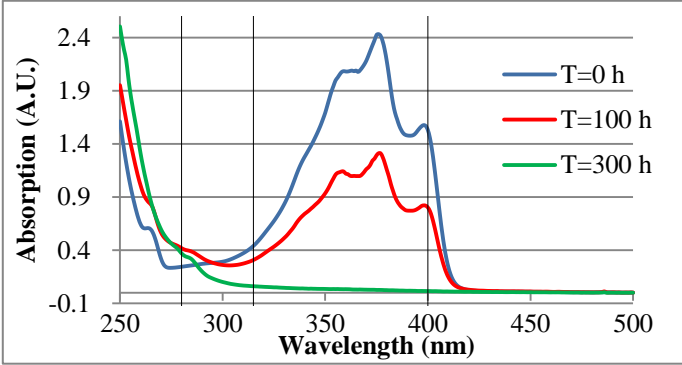
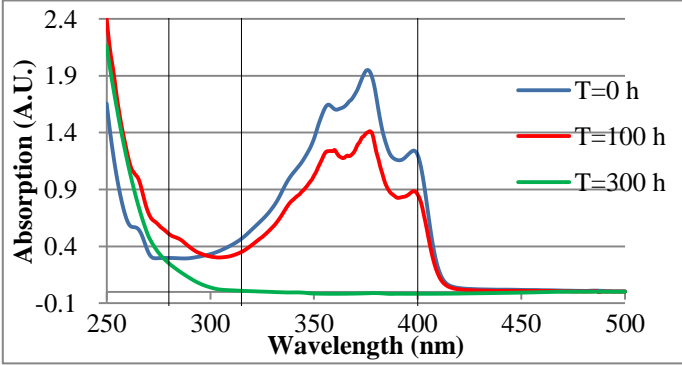
Material	Life time (ns) air	Life time (ns) nitrogen
Uvitex OB	1.21	1.26
OB:I168:I1010 (1:2:1)	1.22	1.26
OB:Tinogard Q (1:1)	1.20	1.29

The combination Tinogard Q did not decrease the lifetime of Uvitex OB significantly which may be expected if there were an excited singlet state interaction.

2.3.4 Degradation studies of Uvitex OB in films

Uvitex OB incorporated into films was degraded for 100 h and 300 h in QUV, an accelerated weathering tester by industry (details in Chapter 7). A reference film consisting of Sabic 2102TX00 80% and EXXON FL00218 20% was used as blank film, and the absorption spectrum of each film was measured to compare with the data from irradiation of Uvitex OB in ethyl acetate. The composition of the films is shown in **Table 13**.

Table 13. UV degradation in QUV spectrums for Uvitex OB films

Films	Spectra
<p>Film 1 SABIC 2102TX00 79.4% EXXON FL00218 20% Uvitex OB 0.20%</p>	
<p>Film 2 SABIC 2102TX00 79.0% EXXON FL00218 20% Uvitex OB 0.2% Chimassorb 944 0.8%</p>	
<p>Film 3 SABIC 2102TX00 78.9% EXXON FL00218 20% Uvitex OB 0.20% Chimassorb 944 0.8% Irganox B215 0.1%</p>	

*The film was irradiated in QUV, and measured UV absorption with UV-Vis spectrophotometer.

Film 1 formed a different product from **Films 2** and **3**. Absorption at 280 nm wavelength in **Film 1** increased during degradation. **Film 1** and **Film 2** degraded 61% and 44% after 100 h respectively, which means C994 enhanced the stability of Uvitex OB. This is in contrast to with the degradation in solution. **Film 3** shows Irganox B215 enhanced the stability of Uvitex OB before 100 h. However, **Film 3** degraded fast after 100 h.

The degradation of Uvitex OB in film (Film 1 SABIC 2102TX00 79.4%, EXXON FL00218 20%, Uvitex OB 0.2%) was measured using Xenon arc lamp irradiation (experiment details in chapter 7). (**Figure 22**)

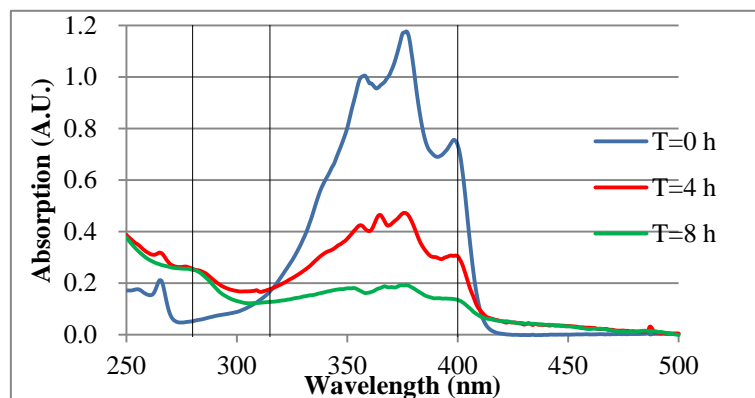


Figure 22. Degradation of Film 1 under Xenon arc lamp

Film 1 degraded faster under the arc lamp at the specified point than under QUV. Compared with **Figure 2** (Uvitex OB degradation in ethyl acetate), film degradation formed a different product. After 8 h, spectrum did not show any absorption in the UV-B region which is different from the degradation of Uvitex OB in ethyl acetate.

2.4 Conclusions

Uvitex OB degraded 96% after 3 h irradiation under oxygen in ethyl acetate, which was faster than under air, where Uvitex OB degraded 76% after 8 h irradiation under the Xenon arc lamp. A nitrogen environment resulted in a significant slower degradation (14% after 8 h). This result suggests that it may be worth incorporating Uvitex OB into an oxygen impermeable material to slow down oxidation.

Chimassorb 944 did not enhance the photostability for Uvitex OB. The white solid formed during the degradation in ethyl acetate solution suggested Uvitex OB could react with C944 under oxygen resulting in faster degradation. This is in contrast to with the degradation in films, where C944 enhanced the stability in QUV after 100 h irradiation.

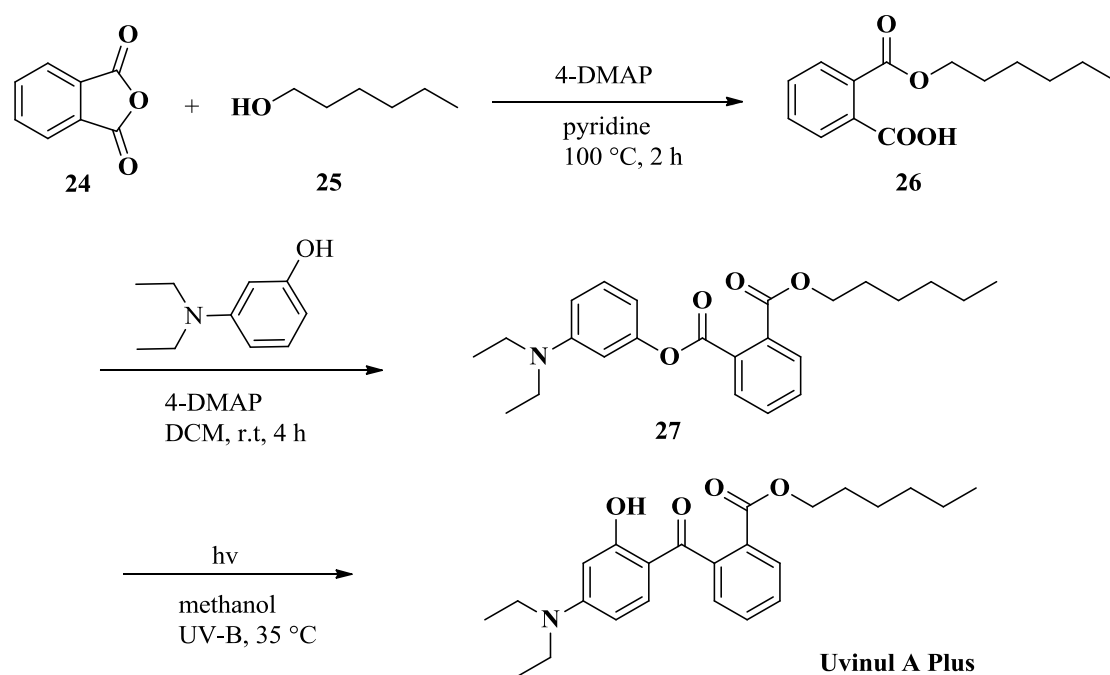
Irganox 1010 and Irgafos 168 enhanced the stability of Uvitex OB when they were combined with Uvitex OB in a significant concentration. However, the combined compounds showed major and significant absorption in the UV-B region which was not optimal for this project. Tinogard Q slowed down the degradation rate of Uvitex OB when combined in 1:1 and 1:50 ratio, but the differences were not obvious.

Chapter 3. Uvinul A Plus modification

3.1 Introduction

Uvinul A Plus (BASF) (diethylamino hydroxybenzoyl hexyl benzoate) is a well-known UV absorber which shows an absorption peak at 350 nm, $\epsilon=4.1 \times 10^4 \text{ L}\cdot\text{mol}^{-1}\text{cm}^{-1}$ in ethyl acetate. It is widely used in skin and sun care products. Uvinul A Plus offers reliable protection against UV-A radiation that can penetrate deeper into the skin over long periods without the need for additional stabilisation, and can be combined easily with other organic and inorganic UV filters to produce sunscreens and other cosmetic products.^[143]

Uvinul A Plus can be synthesised from phthalic anhydride (**24**) and hexanol (**25**) in pyridine with 4-dimethylaminopyridine as catalyst to afford 2-hexanoxycarbonylbenzoic acid (**26**) which is then reacted with 3-diethylaminophenol in DCM to provide 3-diethylamino-phenyl-2-hexanoxycarbonylbenzoate (**27**). Then Uvinul A Plus is formed after a rearrangement by phototransformation in methanol under UV-B radiation.^[144] (**Scheme 18**)

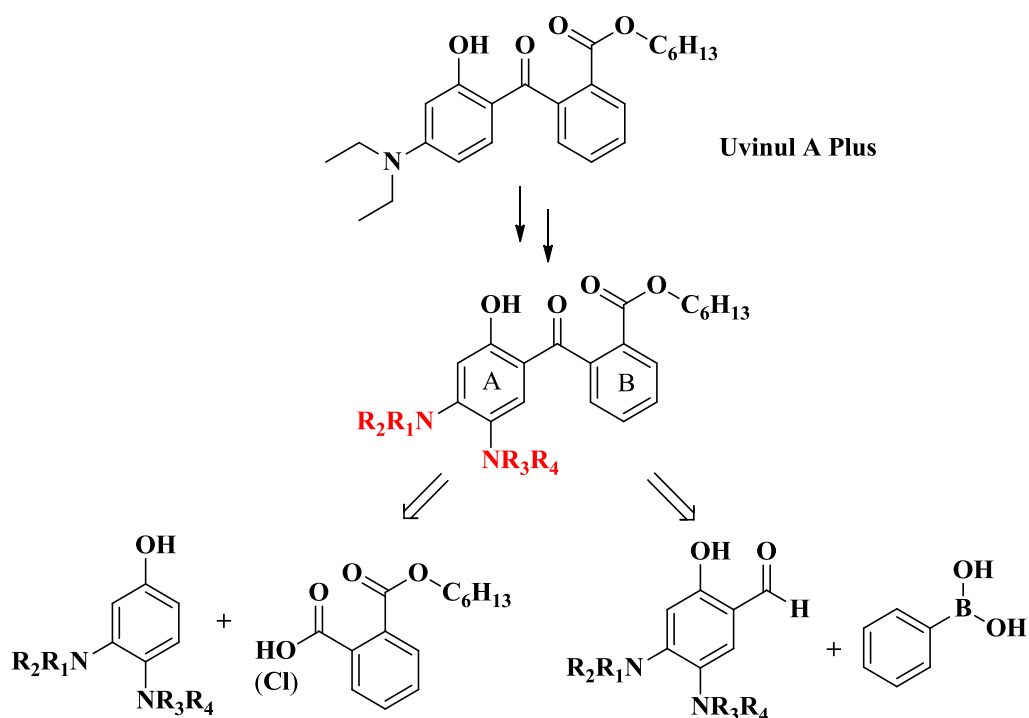


Scheme 18. Synthesis of Uvinul A Plus

Uvinul A is reliable and has long-lasting action due to its outstanding photostability.^[145] Photostability is potentially a problem with all UV filters. Therefore, Uvinul A Plus is an ideal UV absorber for incorporation into polymer films, in addition to its good solubility in a wide range of solvents.

3.2 Aims

The aim of the research outlined in this chapter was to synthesise a novel UV absorber with UV absorption around 372 nm with a good photostability, which might be achieved by the modification of Uvinul A plus due to its outstanding light fastness. (**Scheme 19**)



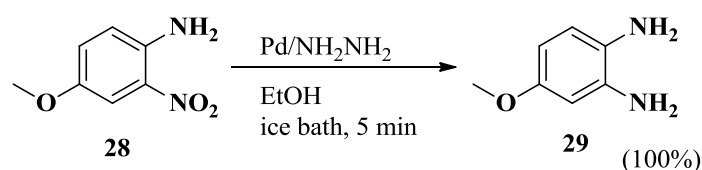
Scheme 19. Propose route for Uvinul A plus modification

It was planned to introduce a second amine group onto ring A at the *para* position of hydroxyl group which should help to increase the maximum UV absorption wavelength due to its auxochromic effect.

3.3 Results and discussion

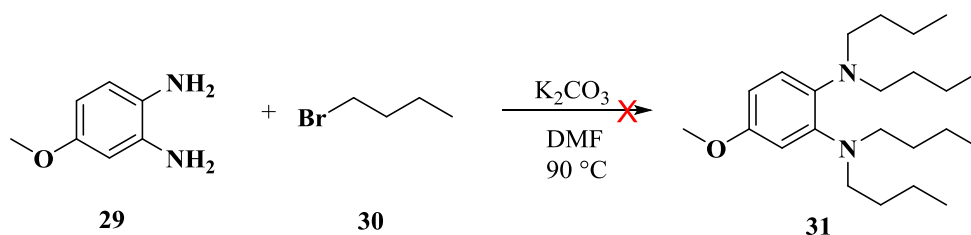
3.3.1 Organic synthesis

Research firstly aimed towards the formation of 4-methoxy-1,2-phenylenediamine (**29**) based on conditions reported by Tian *et al.*,^[146] but reaction in ethanol at 0 °C, instead of reflux in methanol for 6 h, was found to be effective. Nitro reduction was complete in just 5 min at ice bath temperature, and resulted in 100% yield of the diamine (**Scheme 20**).



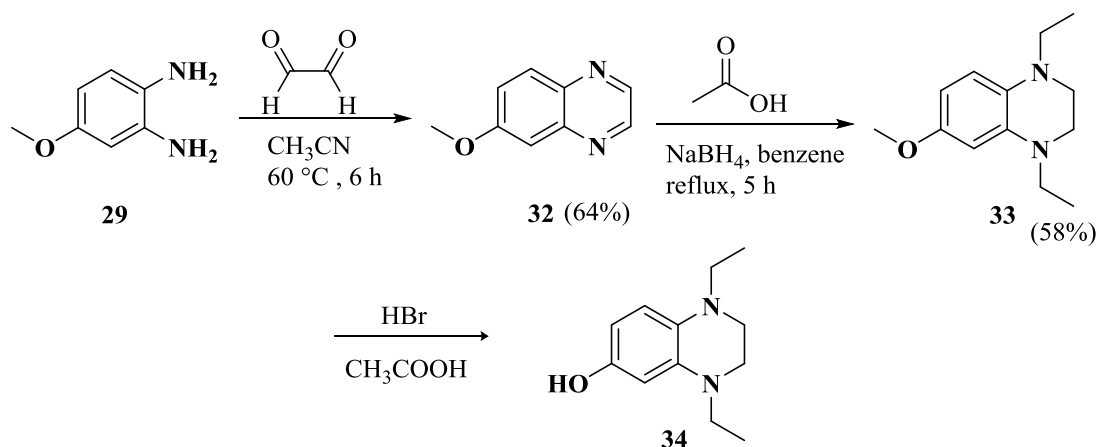
Scheme 20. Optimal conditions for nitro compounds reduction

4-Methoxy-1,2-phenylenediamine (**29**) was then treated with 1-bromobutane (**30**) in DMF with K₂CO₃ as base to form the *N*-alkylated **31** (Scheme 21).^[147] However, after investigation of a number of reaction conditions including increasing the reaction temperature, changing solvent to DMSO, ethanol or THF, there was no evidence that the target product was being formed, but giving product mixture.



Scheme 21. Proposed formation route for **31**

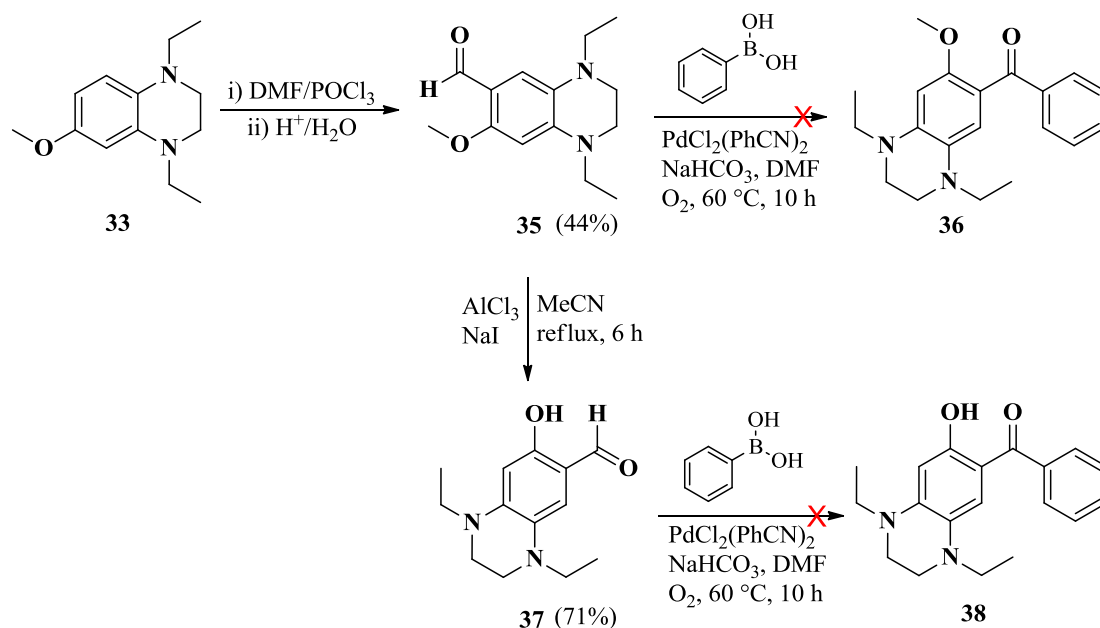
Therefore, in an alternative method, diamine **29** was reacted with glyoxal to prepare 6-methoxyquinoxaline (**32**), obtained as a white solid^[148]. In ¹H NMR spectrum, a broad singlet signal around 3.28 ppm for two NH₂ groups disappeared, and signals at 8.75 (1H, d, *J*=2.4 Hz) and 8.69 (1H, d, *J*=2.4 Hz) for two protons on the new ring were observed. Then sodium borohydride and acetic acid were used in a reductive amination step to reduce the ring and add two ethyl substituents, forming intermediate **33**.^[148] (Scheme 22)



Scheme 22. Proposed formation route for **34**

Demethylation was then studied, however, 1,2,3,4-tetrahydroquinoline **33** could not be converted to **34**^[146] because of its instability. **34** is very electron rich, and changed from yellow to black quickly in the air, suggesting rapid aerial oxidation occurs.

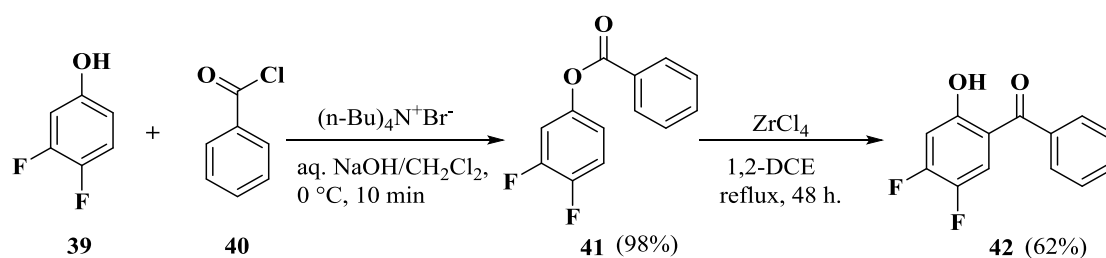
Formylation was investigated and carboxaldehyde **35** was obtained through a Vilsmeier–Haack reaction adding an electron withdrawing CHO group to improve the stability.^[148] ¹H NMR signal at 10.12 ppm stands for CHO group. An attempt to arylate the aldehyde group was made by treatment with phenylboronic acid via the conditions in **Scheme 23** using palladium catalysis to ketone **36**.^[149] However, only starting material **35** was observed.



Scheme 23. Possible synthetic method for **36** and **38**

Then **35** was subjected to demethylation with AlCl_3 and NaI in acetonitrile under reflux for 6 hours giving the hydroxy aldehyde **37**,^[150] which showed a broad singlet peak at 6.56 for OH group in ^1H NMR. Phenol **37** was then treated with phenylboronic acid with a palladium catalyst. After 10 h heating, TLC indicated a complicated mixture had formed, and no signals corresponding to product **38** were seen in the NMR spectrum.

Due to the multi-step reaction routes and difficulty in forming the expected benzophenone product from the previous two methods for Uvinul A modification, an alternative route was chosen to start, using a Fries rearrangement. The method in **Scheme 24** was conducted and provided a good yield of difluorohydroxybenzophenone **42**. The first step to form an ester used phase-transfer catalysis conditions.^[151] Treatment of 3,4-difluorophenol (**39**) with benzoyl chloride (**40**) under phase-transfer catalysis conditions, using tetra-butylammonium bromide in a mixture of aqueous NaOH and dichloromethane, afforded ester **41** in nearly 100% yield without further purification.



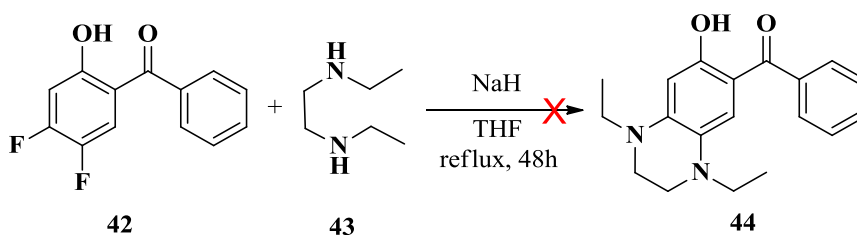
Scheme 24. Synthesis route of **42**

Fries rearrangement of benzoate ester **41** to **42**, was studied using conditions reported by David Harrowven with zirconium chloride as catalyst.^[128] The method in the paper utilizing DCM as a solvent under ultrasound irradiation for 8 h was investigated, but was unsuccessful. The reaction mixture was found to reflux due to the low boiling point (40 °C) of DCM showing this solvent to be unsuitable. Then 1,2-dichloroethane (b.p. 84 °C) was used instead and the mixture was stirred under reflux for 17 h, which was successful, but in a low yield. Additionally, as the product (**42**) and starting material ester have similar polarities, it was difficult to separate them. The best way was to rearrange ester **41** to hydroxybenzophenone **42** completely to avoid the separation issue. Different amounts of zirconium(IV) chloride and variation of the reaction time in 1,2-dichloroethane were studied to find the best conditions for the Fries rearrangement (**Table 14**).

Table 14. Different conditions for Fries-rearrangement with ZrCl_4 in 1,2-DCE

Equivalent	Conditions	Isolated yield
4 eq.	reflux, 17 h	5%
4 eq.	reflux, 40 h	50%
3 eq.	reflux, 40 h	52%
2 eq.	reflux, 48 h	62%
2 eq.	reflux, 36 h	50%
1 eq.	reflux, 48 h	36%

From **Table 14**, it can be seen that 2 eq. ZrCl_4 with 1,2-dichloroethane as solvent under reflux for 48 h provided the highest yield. In ^1H NMR spectrum, signals at 12.17 (1H, d, $J=1.2$ Hz) for OH group was observed, and ^{19}F NMR spectrum showed two fluorine peaks at 39.0 and 14.3 confirmed the target product. After the success of synthesising difluoro **42**, it was expected that *N,N'*-dimethyl-ethylenediamine could be added to replace the fluorines using sodium hydride as base in THF. However, after heating under reflux for 48 h only starting material was observed. Then this reaction was also investigated neat. The reagent, *N,N'*-dimethylethylenediamine, was used as the solvent, but there was no evidence that the target product was being formed. (**Scheme 25**)

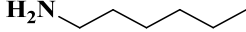
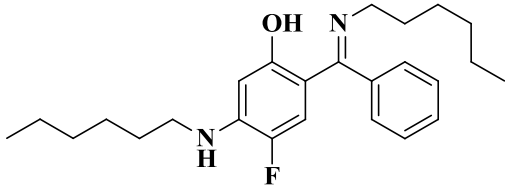
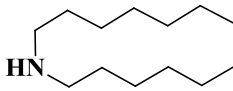
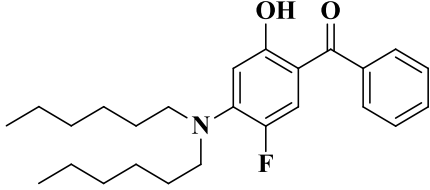
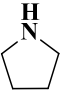
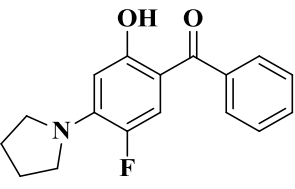
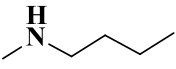
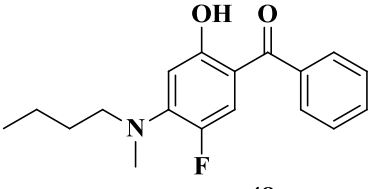


Scheme 25. Proposed formation route for **44**

Many other different amine nucleophiles could be attempted to substitute fluorine (**Table 15**). Hydroxybenzophenone **42** was treated with 1-hexylamine in an attempt to replace the fluorine at 4-position, but it was found that another equivalent 1-hexylamine attacked the carbonyl group and formed a new carbon-nitrogen double bond giving imine **45** in 97% yield.

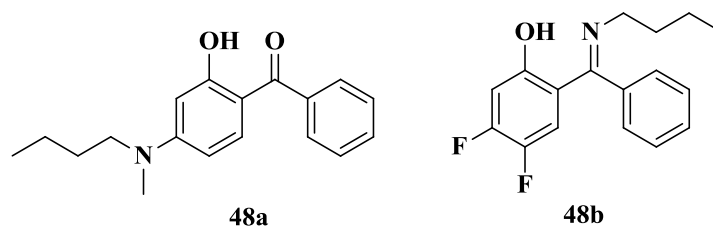
The 4-fluorine in **42** could be substituted by another two nucleophiles dihexylamine and pyrrolidine, and formed 4-amino-5-fluoro substituted hydroxybenzophenone **46** and **47** on reaction in THF under reflux. The reaction for **46** was conducted neat at 90 °C for 24 h, and gave 82% target product but with a dark yellow colour instead of yellow. Reactions with THF as solvent afforded the highest yield 93%. However, it needed a longer reaction time.

Table 15. Hydroxybenzophenone **42** reacted with different nucleophiles

Nucleophiles	Conditions	Products	Yields
	Neat 80 °C 18 h	 45	97%
	THF Reflux 3 d	 46	93%
	THF Reflux 17 h	 47	90%
	Neat r.t. 24 h	 48	84%

Hydroxybenzophenone **42** reacted successfully with *N*-methyl-1-butylamine giving amino derivative **48** as only one fluorine signal around 27.6 ppm was observed in ^{19}F NMR spectrum. When **42** was treated with *N*-methyl-1-butylamine at room temperature instead of 80 °C, the yield of *N*-methylbutylamine **48** improved from 46% to 84%. However, two side products **48a** and **48b** were observed in the reaction mixture at room temperature (**Scheme 26**). The formation of **48a** showed hydrodefluorination occurred in this reaction. The fluorine at the 5-position was replaced by a proton. This reaction usually constitutes a great challenge in catalysis, because carbon–fluorine bonds are of high thermodynamic stability and kinetic

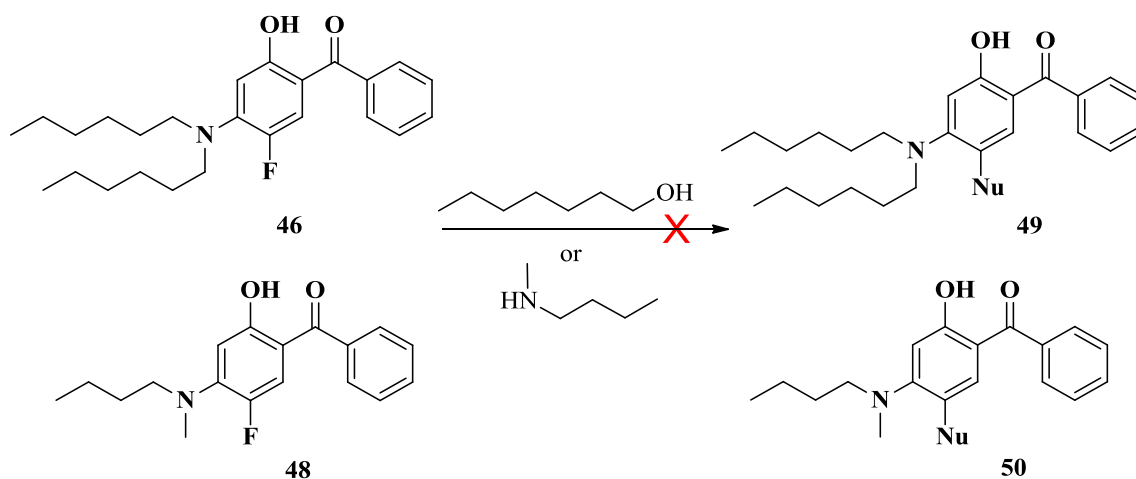
inertness as the consequence of the small size ($r_w = 1.47 \text{ \AA}$) and high electronegativity ($\chi = 4$) of the fluorine atom.^[152] In this reaction, extra *N*-methyl-1-butylamine provided proton to added on carbon, and electron transfer from the hydroxyl and amino group could lead to the reductive defluorination. MS peaks at m/z 282.1492 ($M+H^+$) confirmed the formation of **48a**.



Scheme 26. Two side products from formation for **48**

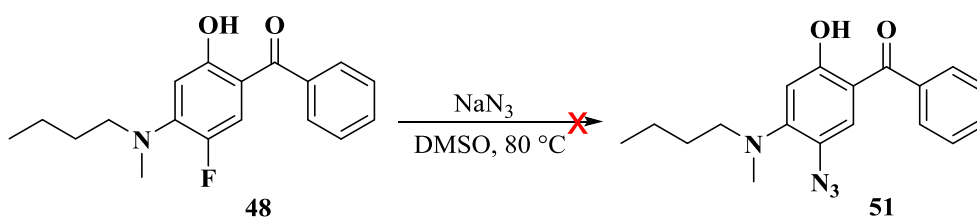
N-Methylbutylamine also attacked the carbonyl group instead of displacing a fluorine atom with loss of the methyl group forming a carbon-nitrogen double bond resulting in imine **48b**, which could be proved by two fluorine signals around 33.0 and 9.9 ppm in ^{19}F NMR spectrum and MS peak at m/z 290.1351 ($M+H^+$). This reaction was similar with 1-hexylamine substitution. This could suggest carbon-nitrogen double bond formed before amine replaced fluorine in formation of imine **45** (Table 15).

An attempt was made to introduce another molecule of nucleophile to replace the second fluorine in amino derivatives **46** and **48**. Each starting material was treated with neat *N*-methylbutylamine under reflux for 4 days, but only starting material was observed. Reactions with 1-heptanol were also carried out with NaH as base in THF under reflux for 3 days to generate the alkoxide. However, both of them were unsuccessful, and showed same results with above. (Scheme 27)



Scheme 27. Proposed disubstitution formation route for **49** and **50**

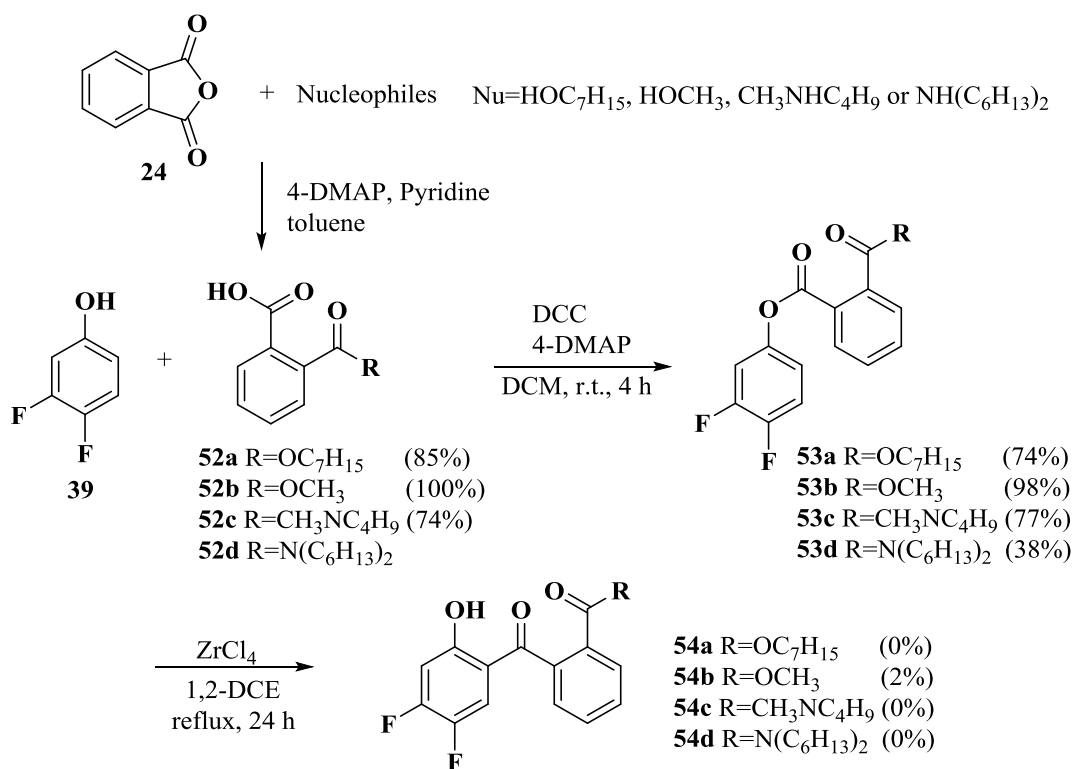
Aminobenzophenone **48** was next treated with the highly nucleophilic azide ion in an attempt to replace the remaining fluorine atom under the conditions in **Scheme 28**, but again only starting material was recovered. The hydroxyl group is an electron-donating group which directs nucleophilic attack at the *meta*-site, whereas the carbonyl group is an electron-withdrawing group which increases the proportion of *para*-substitution. Therefore, the fluorine at 4-position is easy to be replaced, but the second fluorine is more resistant to substitution.



Scheme 28. Proposed formation route for **51**

Due to the successful synthesis of dihexylamine **46** with a maximum absorption around 367 nm wavelength, the next step was to add an ester group on the benzene ring (ring B, **Scheme 19**) to find out how it affects absorption wavelength and photostability.

Benzoic acid **52a** was successfully synthesised from phthalic anhydride (**24**) and 1-heptanol.^[144] A singlet ¹H NMR signal around 11.35 for COOH group confirmed the product. Then **52a** was treated with difluorophenol by using propylphosphonic anhydride (T₃P) as activating agent to afford ester **53a**, but in a low yield with some starting material remaining. Then DCC and 4-DMAP were used as dehydrating agent and catalyst instead of T₃P with DCM as solvent which resulted in a higher yield of 75% instead of 40%.^[144] In attempts to make the ester substituted hydroxybenzophenone **54a** (**Scheme 29**), problems arose when ester **53a** was rearranged to form benzophenone **54a**. Many spots were observed by TLC and the target product signals could not be observed in the NMR spectrum after attempted purification by chromatography on silica gel.



Scheme 29. Proposed formation route for Uvinul A modification

A mixture of ester **53b** with ZrCl₄ in 1,2-dichloroethane was refluxed for 60 h. However, only 6 mg **54b** was formed, and mostly starting material remained. Then 1,2-dibromoethane with higher boiling point was used as solvent, but there was no evidence product was formed as expected. As **54b** was provided 2% in 1,2-dichloroethane, there should most likely be a method to improve the yield. However, none of the conditions in **Table 16** were successful in promoting the rearrangement. Starting materials phenol and acid were observed in the reaction with AlCl₃ and TiCl₄ as catalyst which showed the carbon-oxygen bond was broken, but a new carbon-carbon bond on the *meta*- position did not form.

Since the rearrangement of ester **53a** was difficult, a compound with a shorter alkyl chain on the ester was considered worthy of synthesis to check how an ester group on the benzene ring affects photostability. The anhydride was stirred in methanol instead of 1-heptanol under reflux for 24 h which afforded 2-(methoxycarbonyl)benzoic acid **52b** in 100% yield instead of 78% found using 4-DMAP and pyridine as catalyst in toluene.^[153] (**Scheme 29**)

Table 16. Different conditions for Fries-rearrangement for **54b**

Catalyst	Conditions	Results
AlCl ₃	DCE, reflux, 20 h	Ester hydrolysed to phenol and acid
TiCl ₄	DCE, reflux, 20 h	Ester hydrolysed to phenol and acid
TfOH	Neat, 100 °C, 17 h	Unknown white solid formed
Sc(OTf) ₃ ^[154]	Toluene, 100 °C, 24 h	Unknown compounds formed

Phthalic anhydride was treated with *N*-methyl-1-butylamine in toluene under reflux for 18 h which provided 74% of **52c**. Ester **53c** was synthesised as a colourless oil through the method in **Scheme 29** resulting in 77% yield. Then 1,4-dichlorobutane with a high boiling point was used as solvent for Fries rearrangement to speed up the reaction to produce *N*-methylbutylamine **54c**. However, many side products formed in the reaction and after

numerous changes to reaction conditions including changing catalyst to TfOH or TiCl₄ and solvent to 1,2-DCE, there was no evidence that the target product was being formed.

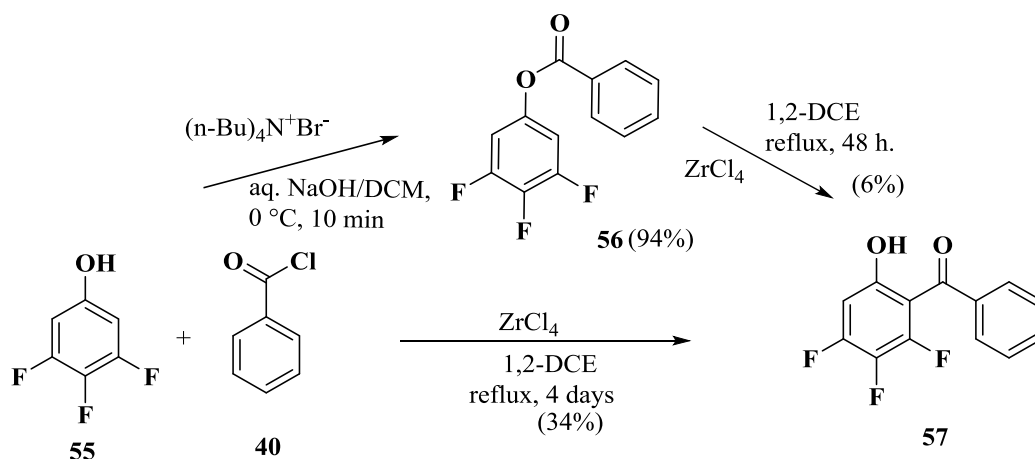
Phthalic anhydride was treated with dihexylamine under different methods as shown in **Table 17** to try to synthesise benzoic acid **52d**. However, none of them provided a good yield of product. Most of the starting material remained after reaction. Since the high polarity of acid **52d** made chromatography difficult, crude product was used in the next step without purification.

Table 17. Different methods for **52d** preparation

Entry	Catalyst	Conditions
1	None	Toluene, reflux, 4 h
2	None	Neat, r.t. 24 h
3	None	Neat, 80 °C, 24 h
4	4-DMAP, pyridine	Toluene, reflux, 24 h

Acid **52d** was treated with 3,4-difluorophenol using the conditions shown in **Scheme 29** but formed ester **53d** in only 38% yield. The compound showed a complicated NMR spectrum due to the hindered rotation of the molecule. Only starting material, ester **53d** was observed instead of rearranged product **54d** after reflux in 1,2-DCE with ZrCl₄ as catalyst. Therefore, an ester group on the benzene ring made the Fries rearrangement difficult to complete. A different methods need to be developed to synthesise this kind of compounds.

Due to the difficulty replacing both the fluorine atoms in difluorohydroxybenzophenone **42** with amine groups to increase UV absorbance, it was necessary to add a third fluorine atom to the ring to increase the absorption wavelength or to be replaced by nucleophiles.



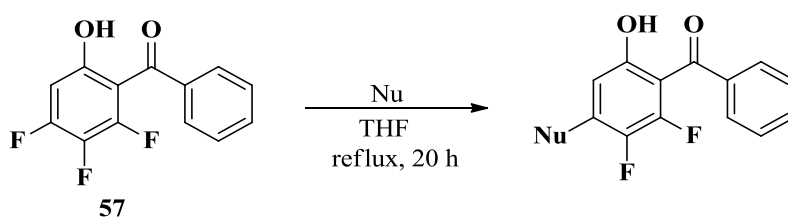
Scheme 30. Synthesis route of **57**

Three fluorine atoms substituted compound **57** could be synthesised under phase-transfer conditions followed by Fries rearrangement (**Scheme 30**), but the ester (**56**) which was prepared from 3,4,5-trifluorophenol (**55**) and benzoyl chloride (**40**) provided target rearrangement product in only 6% yield. A new method was thus developed to synthesise trifluorohydroxybenzophenone **57**. Treatment of 3,4,5-trifluorophenol (**55**) with benzoyl chloride (**40**) in 1,2-dichloroethane with ZrCl_4 as catalyst under reflux for 4 days gave a 34% yield of the rearrangement product **57** directly (**Scheme 30**). Three fluorine signals 39.9, 39.0 and -8.2 ppm were observed in ^{19}F NMR spectrum, and a singlet peak in ^1H NMR around 11.26 for OH group could also confirm the target product. Different solvents such as 1,4-dichlorobutane with a higher boiling point were tested. When the mixture was stirred at 120 $^\circ\text{C}$, many spots were observed from TLC, but none of them was the desired target product. The temperature then was reduced to 60 $^\circ\text{C}$. TLC showed similar results as before. To sum the results above, it was concluded that 1,2-dichloroethane with ZrCl_4 as catalyst was the best condition for synthesising trifluorohydroxybenzophenone **57**.

The replacement of fluorine in **57** with three different amine nucleophiles is shown in **Table 18**. The reactions were carried out in THF under reflux for 20 h and afforded high yields of amine substitution products **59** and **60**, apart from dihexylamine which only provided a 22%

yield of difluoro-dihexylamine **58**. Starting material **57** was a mixture with ester **56**. Dihexylamine could react with ester compound and the product showed similar polarity to **57**. Therefore, the reaction was stopped before starting material transferred to product completely which led to a low yield of dihexylaminohydroxybenzophenone **58** with starting material remaining.

Table 18. Different amines used for nucleophilic substitution

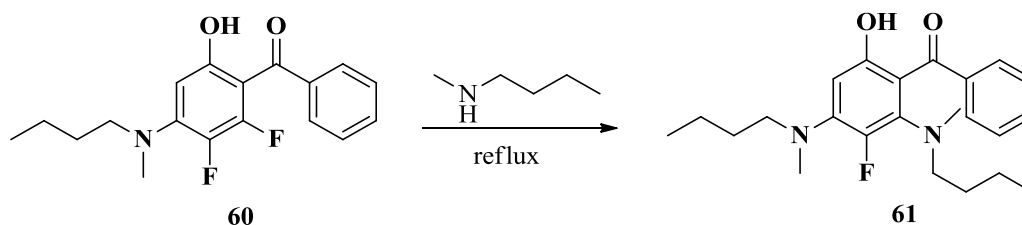


Nucleophiles	Products	Yields
	<p style="text-align: center;">58</p>	22%
	<p style="text-align: center;">59</p>	99%
	<p style="text-align: center;">60</p>	95%

In ^{19}F NMR spectra, only two fluorine signals were detected for these three compounds. ^1H NMR spectra showed the signals for long alkyl groups which successfully proved one of the

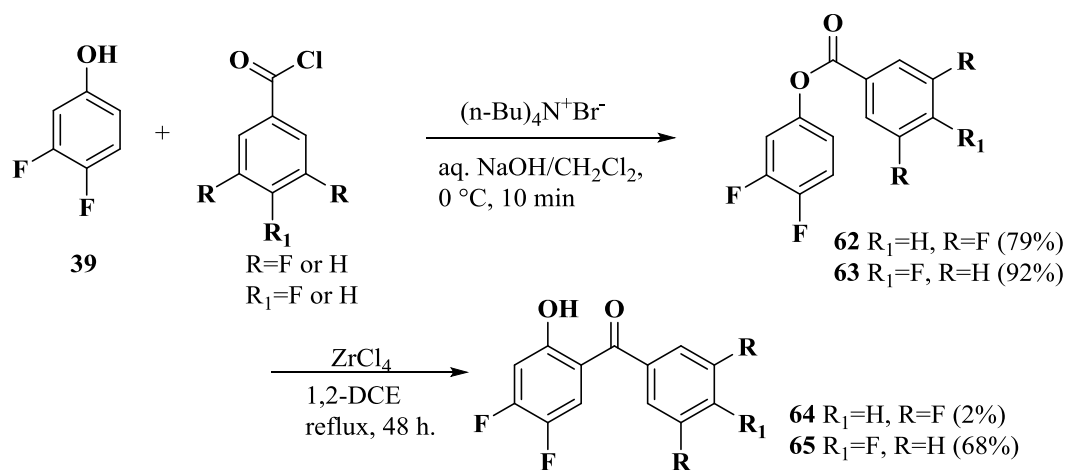
fluorines was replaced by amine. And the big coupling between carbon at 4 position and fluorine disappeared in ^{13}C NMR. Peak at 155.6 (ddd, $J=256.0, 10.0, 5.0$ Hz, C-4) was observed for **57**. Peaks around 151 (t) with coupling constant around 5 Hz were noticed for amino hydroxybenzophenones **58-60**.

Amine substituted benzophenone **60** with one fluorine *meta* to the hydroxyl group could be replaced by another molecule amine. Therefore, **60** was treated with *N*-methyl-1-butylamine under reflux to synthesise diaminobenzophenone **61** (**Scheme 31**). However, starting material remained after 2 days and showed similar polarity to the target product **61** which made it difficult to purify the product. Diaminohydroxybenzophenone **61** showed lower stability and turned from yellow to black quickly on a silica gel TLC plate, suggesting easy oxidation due to the three electron donating groups on the same benzene ring, and **61** was thus not ideal as a UV absorber.



Scheme 31. Proposed formation route for **61**

Therefore, it was determined to study the effect of having the third or fourth fluorine on the other benzene ring instead of having all the fluorine atoms on the same ring. 3,4-Difluorophenol (**39**) could be treated with 4-fluorobenzoyl chloride or 3,5-difluorobenzoyl chloride through the conditions in **Scheme 32** to provide esters **62** and **63** which could be rearranged by ZrCl_4 in 1,2-dichloroethane to form hydroxybenzophenones.



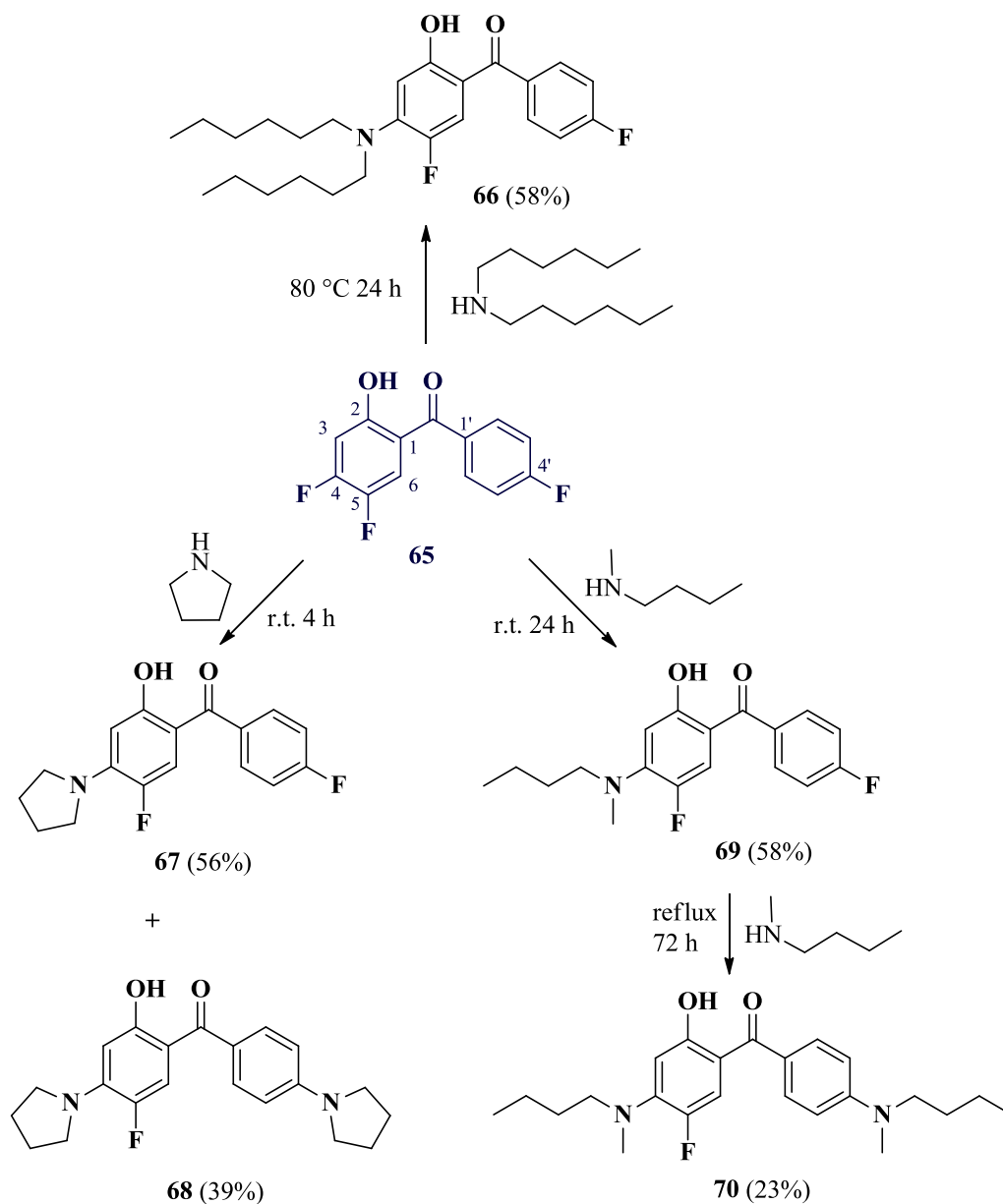
Scheme 32. Synthesis route of **64** and **65**

However, rearranged product tetrafluoro ketone **64** was not successfully formed. The NMR spectrum showed only a small amount product was provided and most starting material was recovered after 2 days with 2 eq. ZrCl₄ as catalyst. After numerous changes to reaction conditions including increasing the amount of catalyst, or the reaction time to 4 days, and changing the solvent to methanol, starting material mostly still remained in all cases.

Trifluorohydroxybenzophenone **65** was successfully prepared in 68% yield through the method in **Scheme 32**. Three fluorine signals 56.9, 39.3 and 14.6 ppm in ¹⁹F NMR spectrum confirmed the target product, which was then reacted with dihexylamine, pyrrolidine or *N*-methyl-1-butylamine (**Scheme 33**). Trifluoro **65** was treated with dihexylamine neat at 80 °C for 24 h affording difluoro-dihexylaminohydroxybenzophenone **66** in 58% yield.

Another 4-amino-5-fluoro substituted hydroxybenzophenone **67** (55% yield) was successfully synthesised from **65** and pyrrolidine at room temperature after 4 h, but a second product dipyrrolidine **68** was provided in 36% yield in this reaction as well. Pyrrolidine replaced the second fluorine after forming difluoro-amino ketone **67**.

Amino substituted hydroxybenzophenone **69** was synthesised by treating **65** with *N*-methyl-1-butylamine for 24 h at room temperature in 68% yield. Diamino substituted compound **70** was successfully prepared after refluxing for 60 h but with a lot of starting material **69** remaining even after reacting for 72 h. Only 20% pure product was obtained.



Scheme 33. Substitution of **65**

Table 19. ^1H NMR and ^{13}C NMR signals for compounds **65-70**

Comp.	NMR signals (ppm)				
	OH	H-3	H-6	C-4	C-4'
65	12.03 (d)	6.86 (dd)	7.39 (dd)	155.7 (dd)	165.3 (d)
	$J=0.8$ Hz	$J=10.8, 6.4$ Hz	$J=10.4, 9.2$ Hz	$J=259.4, 14.3$ Hz	$J=252.7$ Hz
66	12.57 (s)	6.18 (d)	7.06 (d)	145.3 (d)	164.5 (d)
		$J=8.0$ Hz	$J=16.0$ Hz	$J=8.6$ Hz	$J=250.8$ Hz
67	12.71 (s)	6.07 (d)	7.05 (d)	144.2 (d)	164.5 (d)
		$J=8.0$ Hz	$J=15.2$ Hz	$J=11.4$ Hz	$J=250.7$ Hz
68	12.97 (s)	6.09 (d)	7.26 (d)	143.2 (d)	150.2 (s)
		$J=8.4$ Hz	$J=15.6$ Hz	$J=11.5$ Hz	
69	12.55 (s)	6.21 (d)	7.07 (d)	146.3 (d)	164.6 (d)
		$J=8.4$ Hz	$J=15.6$ Hz	$J=21.9$ Hz	$J=250.7$ Hz
70	12.80 (s)	6.28 (d)	7.32 (d)	145.5 (d)	151.8 (s)
		$J=8.0$ Hz	$J=15.6$ Hz	$J=9.5$ Hz	

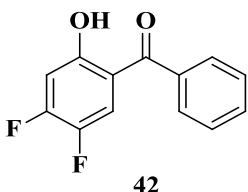
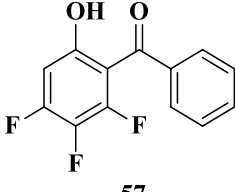
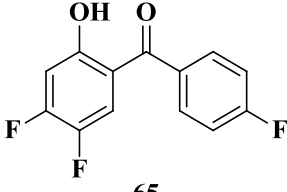
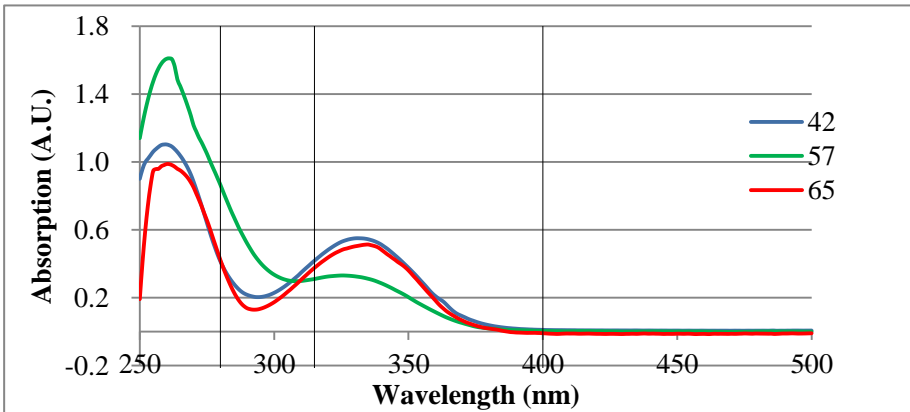
Table 19 shows the ^1H NMR peak for the OH group in **65** changed from a singlet to doublet splitting pattern after F-4 was replaced by an amine group. Similarly with H-3 and H-6, two couplings between proton and fluorine were observed in **65**. However, in compounds **66-70**, only one coupling was seen, which showed one of the fluorines on the phenol ring was substituted. Additionally, the signal for C-4 in **65** was a double-doublet, with $J=259.4, 14.3$ Hz. In compounds **66-70** the peak changed to doublet, and $J=8.6$ Hz which could confirm the fluorine at 4 position was replaced. For hydroxybenzophenones **68** and **70**, ^{13}C NMR showed a single peak at 165 ppm for C-4', and no coupling between carbon and fluorine was observed which proved F-4' was replaced by the second amine. All these data could confirm the amine first attacked carbon at the 4 position, and then the second amine replaced the fluorine at 4' position.

3.3.2 UV absorption and degradation

Synthesised compounds in solution

Pure compounds from the synthesis were then measured for their UV absorption spectra and stability towards prolonged irradiation in ethyl acetate. There are three hydroxybenzophenones **42**, **57** and **65** only substituted with fluorines which showed maximum UV absorption in the UV-C region and a small absorption around 331 nm wavelength. (Table 20)

Table 20. UV absorption for **42**, **57** and **65**

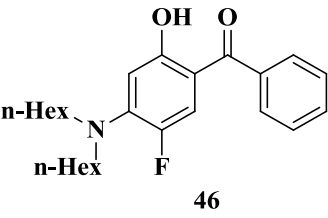
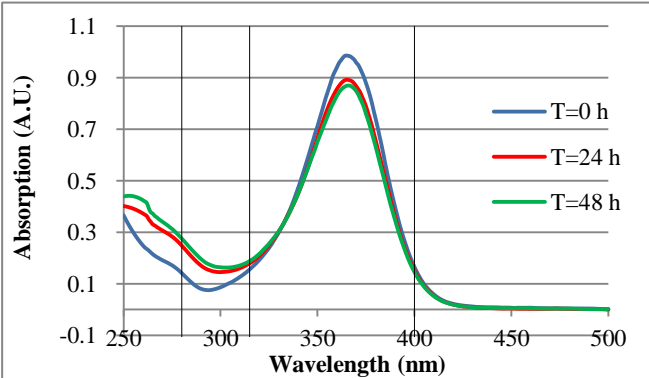
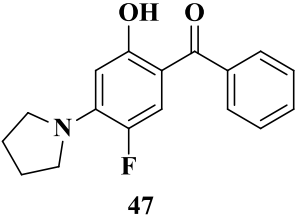
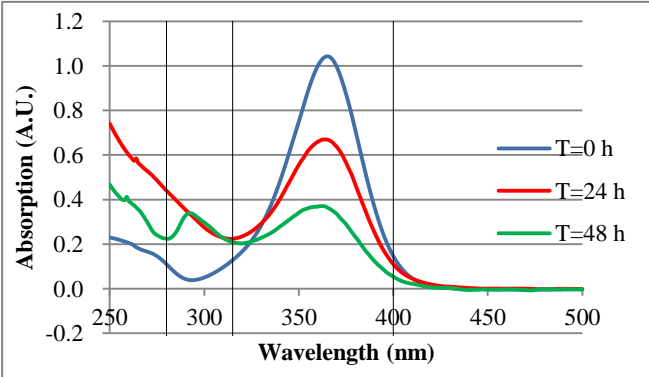
Structure	 42	 57	 65
λ_{max} and ϵ (L·mol ⁻¹ cm ⁻¹)	331 nm, $\epsilon=0.56 \times 10^4$	331 nm, $\epsilon=0.26 \times 10^4$	332 nm, $\epsilon=0.60 \times 10^4$
Spectra			

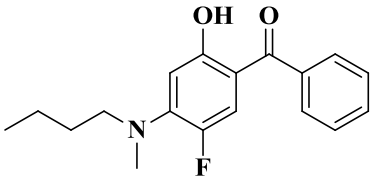
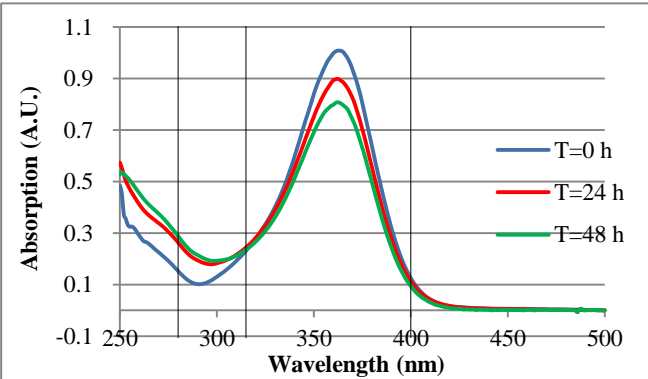
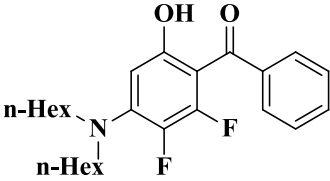
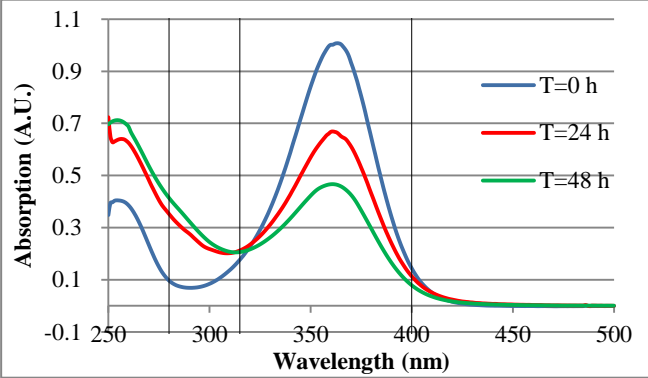
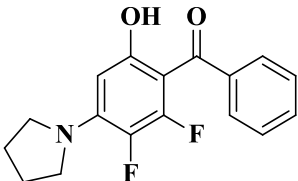
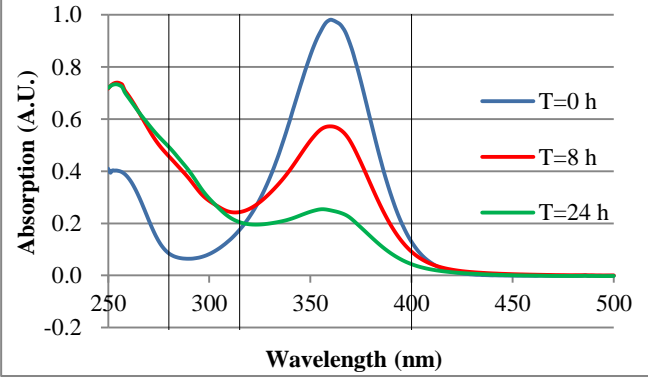
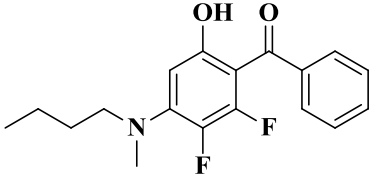
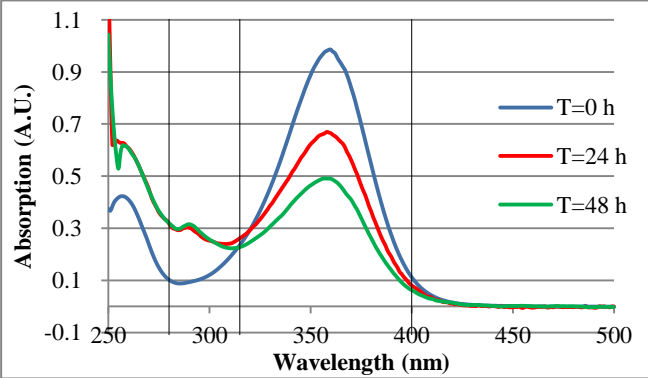
Trifluorohydroxybenzophenone **65** with one fluorine atom on the other benzene ring showed a 1 nm wavelength higher in the UV-A region than other two compounds. **57** containing three

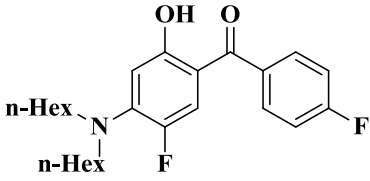
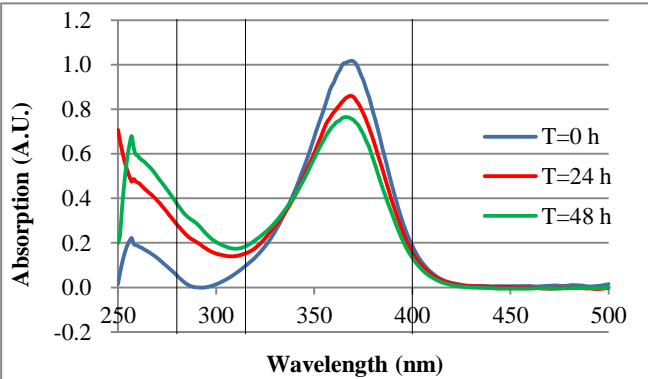
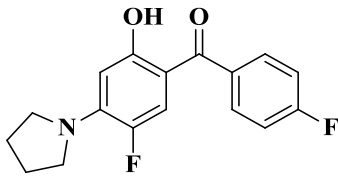
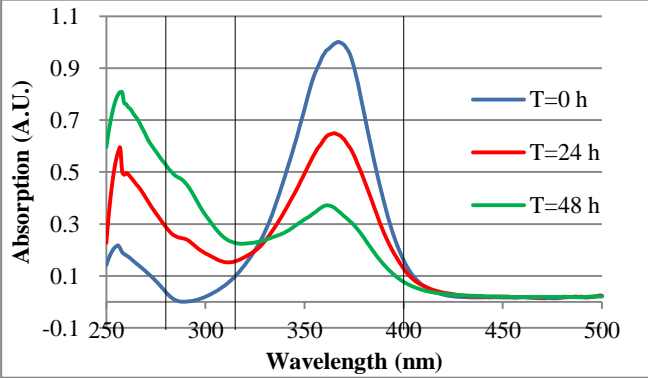
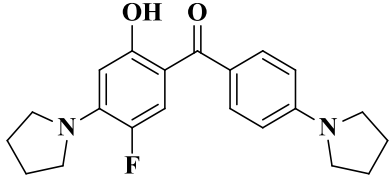
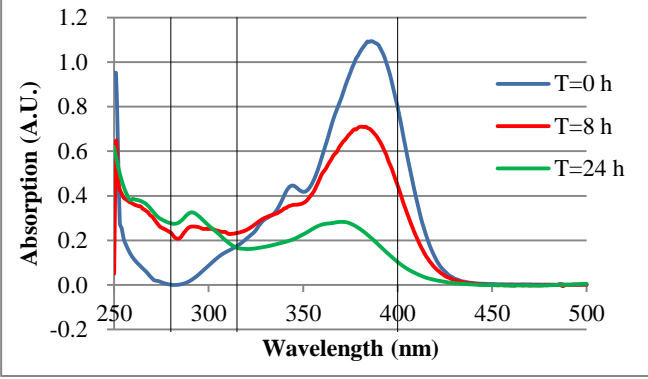
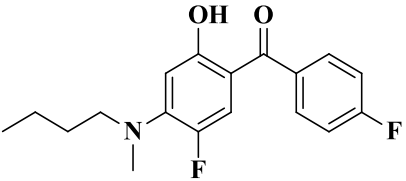
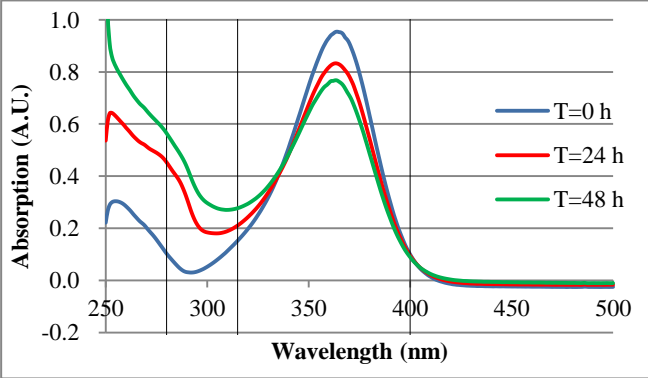
fluorines on the same ring showed UV absorption at 331 nm wavelength with a lower molar absorptivity in the UV-A region compared to difluorohydroxybenzophenone **42**.

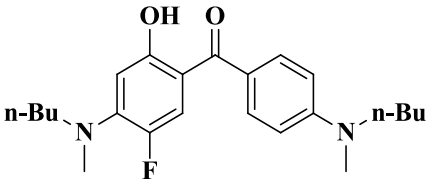
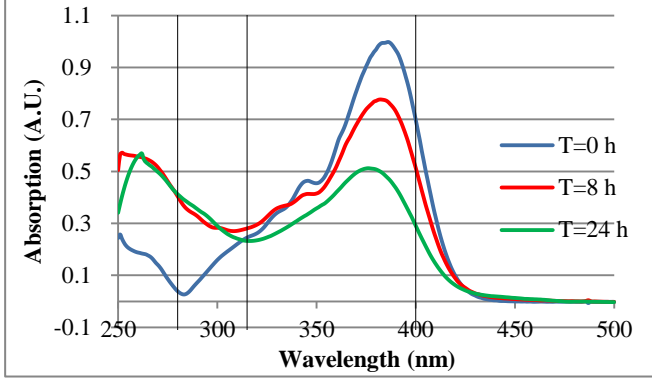
Table 21 shows UV absorption and degradation spectra for all the amine substituted hydroxybenzophenones. Imine **45** containing a carbon-nitrogen double bond instead of a carbonyl group showed maximum UV absorption at 337 nm wavelength with molar absorptivity $2.30 \times 10^4 \text{ L}\cdot\text{mol}^{-1}\text{cm}^{-1}$. Compared with other compounds in **Table 21**, a carbon-nitrogen double bond cannot afford the target absorption in the UV-A region.

Table 21. UV absorption and degradation for amine substituted benzophenones

Compounds	λ_{max} & ϵ Degradation spectra
 <p style="text-align: center;">46</p>	<p style="text-align: center;">$\lambda_{\text{max}}=367 \text{ nm}, \epsilon=2.94 \times 10^4 \text{ L}\cdot\text{mol}^{-1}\text{cm}^{-1}$</p> 
 <p style="text-align: center;">47</p>	<p style="text-align: center;">$\lambda_{\text{max}}=365 \text{ nm}, \epsilon=3.53 \times 10^4 \text{ L}\cdot\text{mol}^{-1}\text{cm}^{-1}$</p> 

Compounds	λ_{\max} & ϵ Degradation spectra
<div style="text-align: center;">  <p>48</p> </div>	<p style="text-align: center;">$\lambda_{\max}=363 \text{ nm}, \epsilon=2.25 \times 10^4 \text{ L}\cdot\text{mol}^{-1}\text{cm}^{-1}$</p> 
<div style="text-align: center;">  <p>58</p> </div>	<p style="text-align: center;">$\lambda_{\max}=363 \text{ nm}, \epsilon=2.27 \times 10^4 \text{ L}\cdot\text{mol}^{-1}\text{cm}^{-1}$</p> 
<div style="text-align: center;">  <p>59</p> </div>	<p style="text-align: center;">$\lambda_{\max}=360 \text{ nm}, \epsilon=3.07 \times 10^4 \text{ L}\cdot\text{mol}^{-1}\text{cm}^{-1}$</p> 
<div style="text-align: center;">  <p>60</p> </div>	<p style="text-align: center;">$\lambda_{\max}=359 \text{ nm}, \epsilon=1.77 \times 10^4 \text{ L}\cdot\text{mol}^{-1}\text{cm}^{-1}$</p> 

Compounds	λ_{\max} & ϵ Degradation spectra
<p data-bbox="341 203 512 237">Compounds</p>  <p data-bbox="432 546 459 568">66</p>	<p data-bbox="791 253 1294 286">$\lambda_{\max}=369 \text{ nm}, \epsilon=2.94 \times 10^4 \text{ L}\cdot\text{mol}^{-1}\text{cm}^{-1}$</p> 
 <p data-bbox="421 987 448 1010">67</p>	<p data-bbox="791 696 1294 730">$\lambda_{\max}=367 \text{ nm}, \epsilon=4.30 \times 10^4 \text{ L}\cdot\text{mol}^{-1}\text{cm}^{-1}$</p> 
 <p data-bbox="405 1435 432 1458">68</p>	<p data-bbox="791 1140 1294 1173">$\lambda_{\max}=385 \text{ nm}, \epsilon=4.26 \times 10^4 \text{ L}\cdot\text{mol}^{-1}\text{cm}^{-1}$</p> 
 <p data-bbox="440 1872 467 1895">69</p>	<p data-bbox="791 1583 1294 1617">$\lambda_{\max}=365 \text{ nm}, \epsilon=1.78 \times 10^4 \text{ L}\cdot\text{mol}^{-1}\text{cm}^{-1}$</p> 

Compounds	λ_{\max} & ϵ Degradation spectra
 <p style="text-align: center;">70</p>	<p style="text-align: center;">$\lambda_{\max}=384 \text{ nm}, \epsilon=3.34 \times 10^4 \text{ L}\cdot\text{mol}^{-1}\text{cm}^{-1}$</p> 

*Compounds were irradiated under the Xenon arc lamp for 24-48 h in ethyl acetate in air. The UV absorption was measured with UV-Vis spectrophotometer.

Comparing all the degradation spectra in **Tables 20** and **21**, amine substituted compounds exhibited higher UV wavelength than fluoro hydroxybenzophenones. There is a pronounced red shift after fluorine was replaced with amine due to the extension of the chromophore from the electron donating group to the electron withdrawing donating group through the benzene ring.

Table 21 clearly shows pyrrolidine substituted compounds showed less photostability, but with a higher molar absorptivity, and a bigger UV absorption wavelength than *N*-methyl-1-butylamino substituted compounds, but lower than dihexylamine. This is because the long alkyl chain on amine could help push the electrons of the nitrogen through the benzene ring, which could lead to a higher UV absorption wavelength. The conjugation of the lone pair of electrons on the nitrogen atom of hydroxybenzophenone with the π bond system of benzene ring is removed on protonation. A C=N bond could form, which will make the angle between the two alkyl chain on nitrogen around 120° . For pyrrolidine, the angle in five member ring is 108° . Therefore, the ring strain might result in a faster degradation.

Diamino hydroxybenzophenones **68** and **70** with two amine groups in the structure showed much higher UV absorption around 385 nm, but degraded 50% and 80% respectively after 24 h irradiation under the arc lamp. Amino hydroxybenzophenones **46**, **47** and **48** with one fluorine atom showed similar absorbance and photostability with difluoro

hydroxybenzophenones **66**, **67** and **69** containing one fluorine atom on each ring, which is confirmed in **Figure 23**.

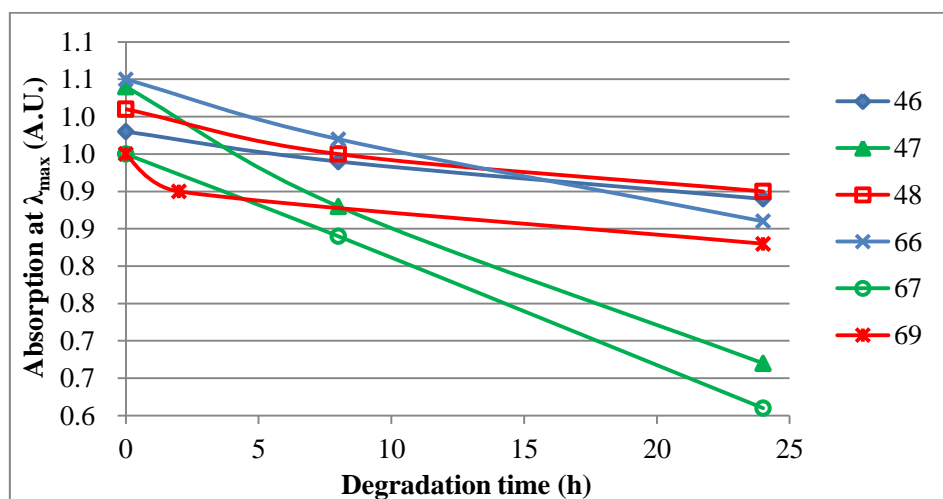


Figure 23. Absorption at λ_{\max} against degradation time

Table 21 and **Figure 23** show dihexylamino substituted fluorinated hydroxybenzophenones such as **46** and **66** provided better photostability than *N*-methyl-1-butylamine and pyrrolidine. Dihexylamine **46** with one fluorine on the ring degraded 9% after 24 h irradiation provided better stability than hexylamine **66** (18%) with two fluorines in the structure. Pyrrolidine substituted hydroxybenzophenones **47** and **67** degraded 35% and 36% respectively, and *N*-methylbutylamino hydroxybenzophenones **48** and **69** degraded 10% and 13%. It suggested one more fluorine atom on the ring did not have a significant effect on photostability.

Aminohydroxybenzophenones **58**, **59** and **60** with two fluorine atoms on the same ring showed lower absorbance and less photostability than one fluorine substituted aminohydroxybenzophenones. In **Figure 24**, difluoro-amine **59** degraded faster than fluoro-amine **47**, especially in first four hours which can be clearly seen for **58** as well.

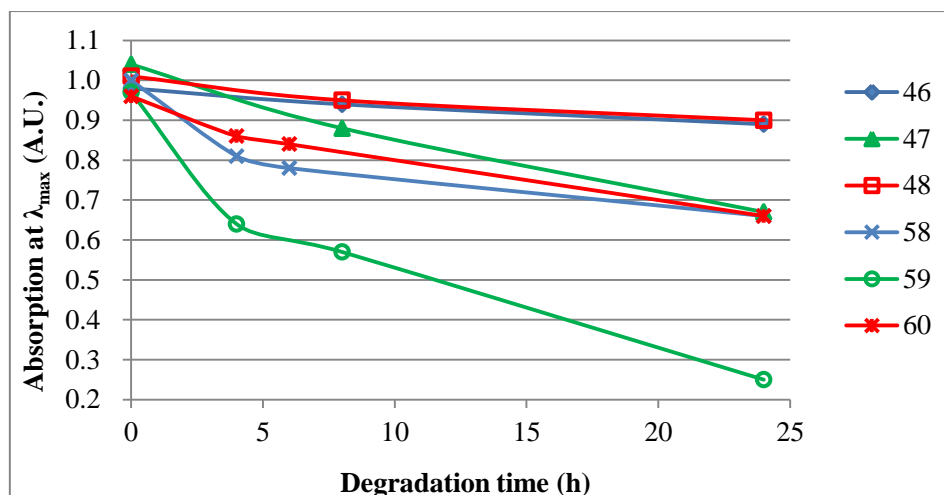


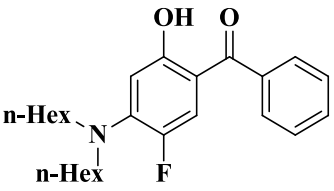
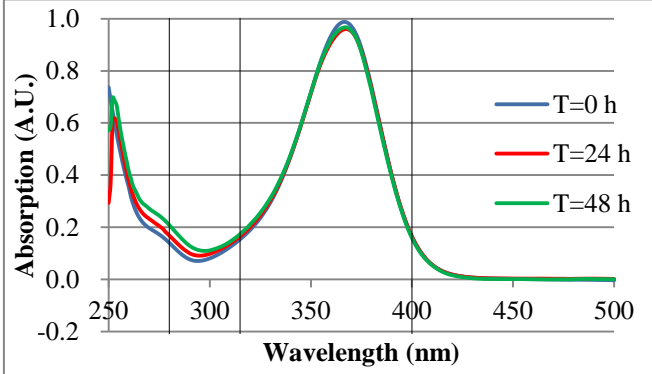
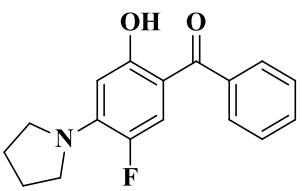
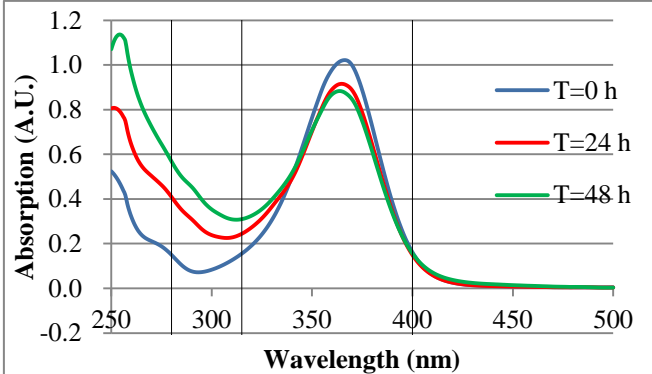
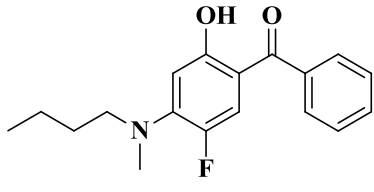
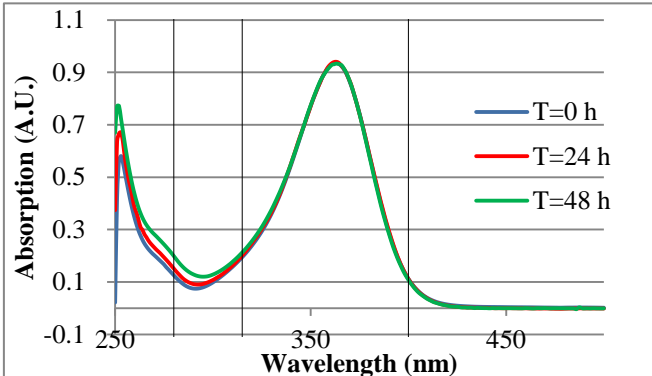
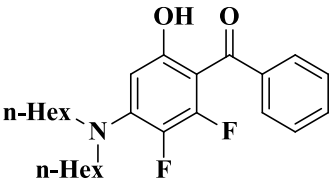
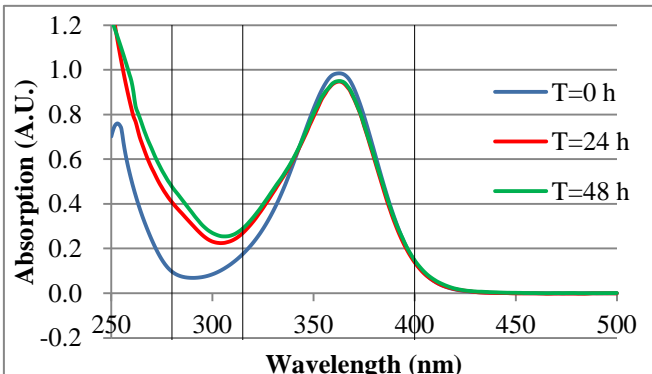
Figure 24. Absorption at λ_{\max} against degradation time

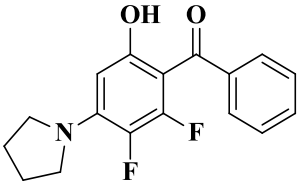
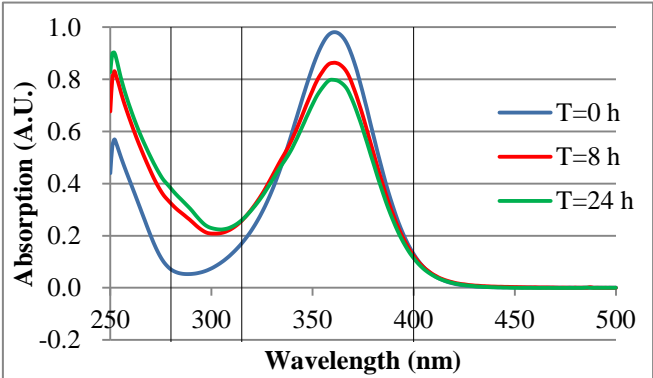
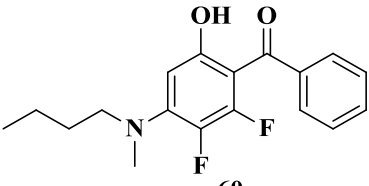
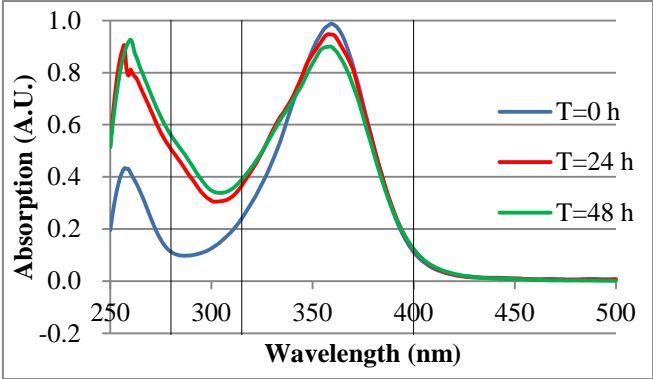
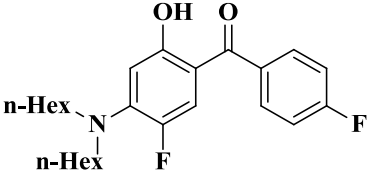
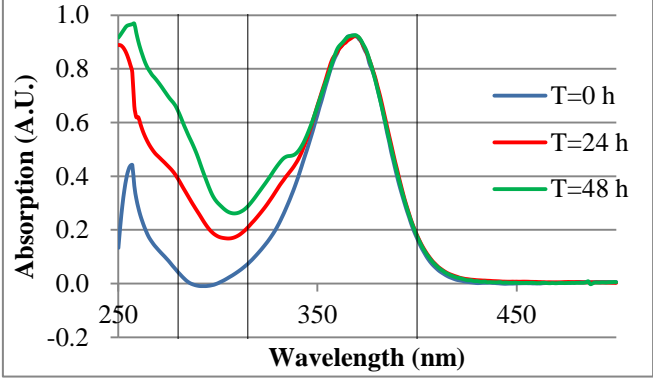
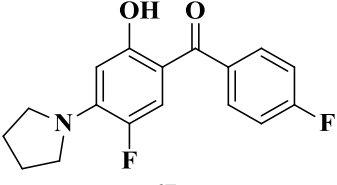
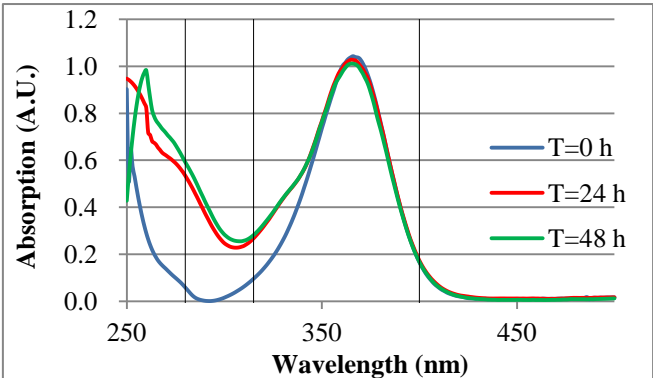
Therefore, amine substituted hydroxybenzophenones displayed good UV absorption characteristics, and dihexylamine provided better photostability than *N*-methyl-1-butylamine and pyrrolidine. Compounds containing one fluorine or two fluorine atoms on a different ring showed better absorbance and stability than hydroxybenzophenones with two fluorine atoms on the same phenol ring.

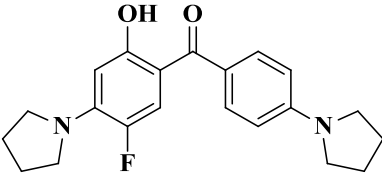
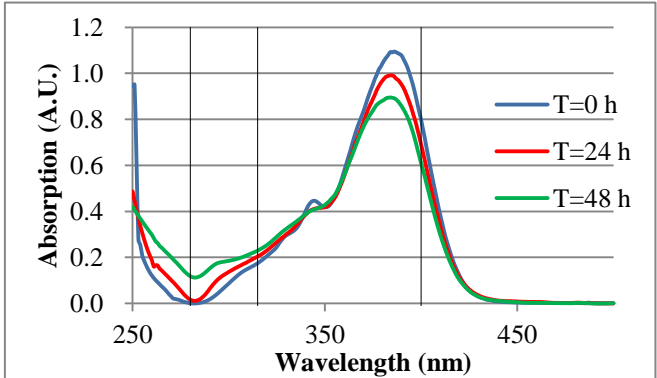
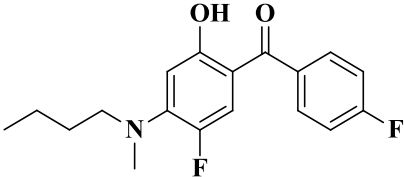
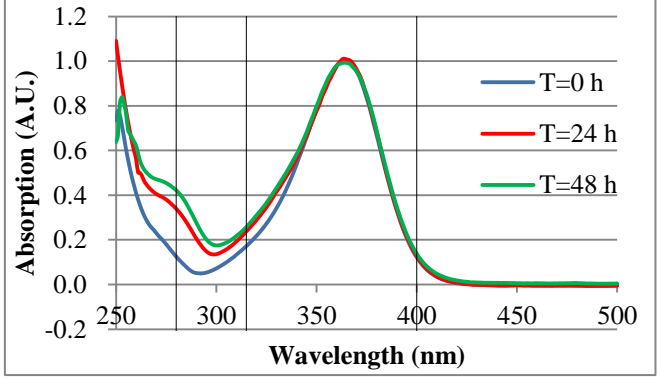
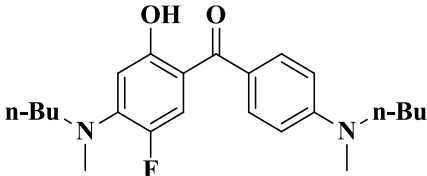
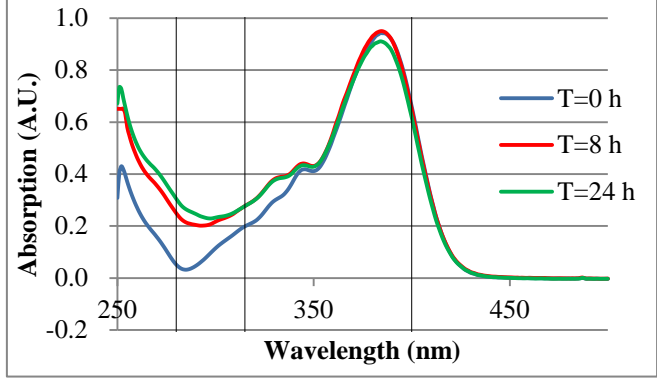
Synthesised compounds combined with Chimassorb 944 in solution

In order to enhance photostability and find how Chimassorb 944 (C944) affects the stability of each compound, C944 was combined with hydroxybenzophenones in a 1:4 ratio by weight for irradiation. (**Table 22**)

Table 22. Degradation for compounds combined with C944

Compounds	Degradation spectra
<div style="text-align: center;">  <p>46</p> <p>$\lambda_{\text{max}}=367 \text{ nm,}$ $\epsilon=2.94 \times 10^4 \text{ L}\cdot\text{mol}^{-1}\text{cm}^{-1}$</p> </div>	
<div style="text-align: center;">  <p>47</p> <p>$\lambda_{\text{max}}=365 \text{ nm,}$ $\epsilon=3.53 \times 10^4 \text{ L}\cdot\text{mol}^{-1}\text{cm}^{-1}$</p> </div>	
<div style="text-align: center;">  <p>48</p> <p>$\lambda_{\text{max}}=363 \text{ nm,}$ $\epsilon=2.25 \times 10^4 \text{ L}\cdot\text{mol}^{-1}\text{cm}^{-1}$</p> </div>	
<div style="text-align: center;">  <p>58</p> <p>$\lambda_{\text{max}}=363 \text{ nm,}$ $\epsilon=2.27 \times 10^4 \text{ L}\cdot\text{mol}^{-1}\text{cm}^{-1}$</p> </div>	

Compounds	Degradation spectra
<div style="text-align: center;">  <p>59</p> <p>$\lambda_{\max}=360$ nm, $\epsilon=3.07 \times 10^4$ L·mol⁻¹cm⁻¹</p> </div>	
<div style="text-align: center;">  <p>60</p> <p>$\lambda_{\max}=359$ nm, $\epsilon=1.77 \times 10^4$ L·mol⁻¹cm⁻¹</p> </div>	
<div style="text-align: center;">  <p>66</p> <p>$\lambda_{\max}=369$ nm, $\epsilon=2.94 \times 10^4$ L·mol⁻¹cm⁻¹</p> </div>	
<div style="text-align: center;">  <p>67</p> <p>$\lambda_{\max}=367$ nm, $\epsilon=4.30 \times 10^4$ L·mol⁻¹cm⁻¹</p> </div>	

Compounds	Degradation spectra
<div style="text-align: center;">  <p>68</p> <p>$\lambda_{\text{max}}=385 \text{ nm}$, $\epsilon=4.26 \times 10^4 \text{ L}\cdot\text{mol}^{-1}\text{cm}^{-1}$</p> </div>	
<div style="text-align: center;">  <p>69</p> <p>$\lambda_{\text{max}}=365 \text{ nm}$, $\epsilon=1.78 \times 10^4 \text{ L}\cdot\text{mol}^{-1}\text{cm}^{-1}$</p> </div>	
<div style="text-align: center;">  <p>70</p> <p>$\lambda_{\text{max}}=384 \text{ nm}$, $\epsilon=3.34 \times 10^4 \text{ L}\cdot\text{mol}^{-1}\text{cm}^{-1}$</p> </div>	

*Compounds combined with C944 were irradiated under the Xenon arc lamp for 24-48 h in ethyl acetate in air. The UV absorption was measured with UV-Vis spectrophotometer.

Table 22 shows C944 enhanced photostability for all the compounds in the UV-A region, especially for dihexylamino and *N*-methyl-1-butylamino substituted benzophenones. However, C944 did not show a significant influence in the UV-B region, but it improved photostability in the UV-B region for some compounds (**46**, **59**, **68**, **69** and **70**), and especially for pyrrolidine substituted compounds **59** and **68** which can be clearly seen from **Figure 25** which shows the relation between absorption at 290 nm and degradation time. The absorbance of hydroxybenzophenones **46**, **59** and **68** in the UV-B region was increasing during irradiation. C944 significantly slow down their increasing rate in the UV-B region.

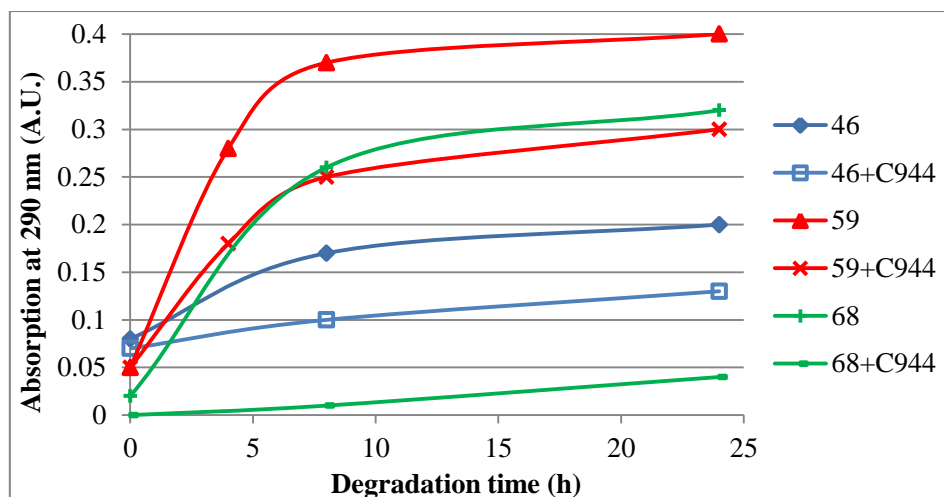


Figure 25. C944 improved stability in the UV-B region

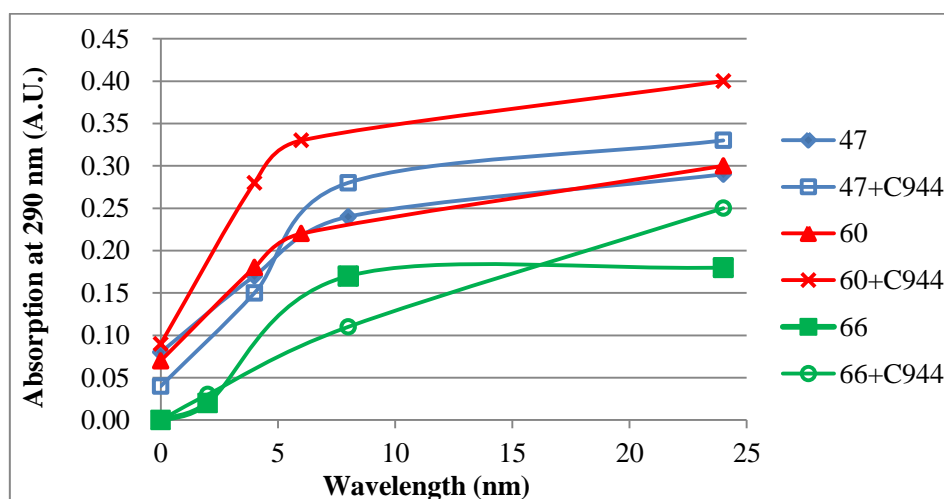


Figure 26. C944 showed less improvement in the UV-B region

Some compounds, in contrast, the absorbance in the UV-B region increased even faster compared to the degradation experiment without C944, such as **47**, **60** and **66**. **Figure 26** shows absorbance of compounds combined with C944 at 290 nm increased faster than without C944 after irradiating for 24 h.

C944 could enhance the photostability in the UV-A region for all the compounds, but not in the UV-B region. The relationship between compound structure and the effect of C944 has not been fully elucidated. Comparing the spectra in **Tables 21** and **22**, compounds with or without C944 showed a similar degraded spectrum, which could suggest the irradiation under

the Xenon arc lamp produced similar degraded products. The presence of C944 could slow down the degradation product formation which provided an absorption in the UV-B region and a similar absorbance with starting material in the UV-A region.

Reductive and oxidative degradation of synthesised compounds

Reductive and oxidative processes were observed for **46** and **48** by studying degradation rates in the UV-A and UV-B region in deoxygenated and oxygen saturated solutions.

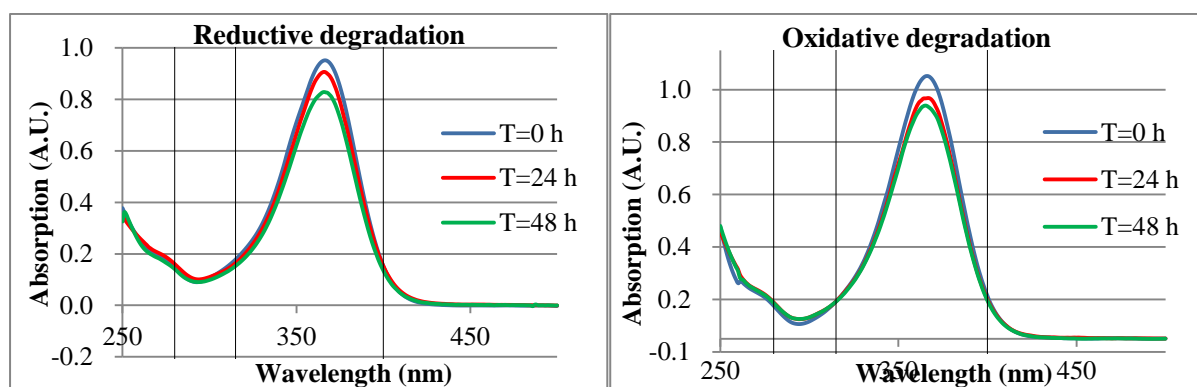


Figure 27. Reductive and oxidative degradation of **46**

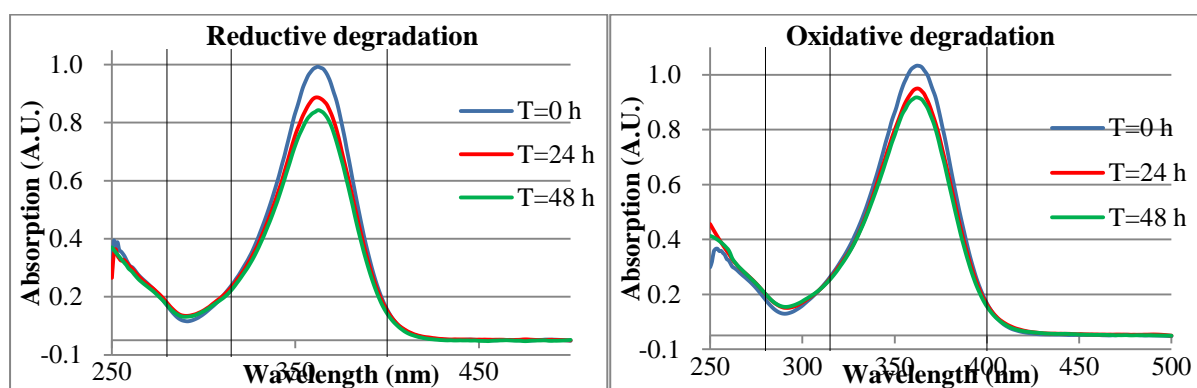


Figure 28. Reductive and oxidative degradation of **48**

Degradation spectra of reductive and oxidative reactions showed in **Figure 27** and **28** were similar in both the UV-A and UV-B regions, and demonstrated even better photostability than

in the air after 48 h irradiation, such as *N*-methylbutylamine **48** which degraded 15% in nitrogen, 12% in oxygen, and 20% under air in the UV-A region. Dihexylamine **46** degraded similarly under air, nitrogen and oxygen in the UV-A region around 12% after 48 h. Absorption in the UV-B region did not increase in a nitrogen or oxygen environment for both compounds.

A nitrogen environment removed oxygen diffusion, and oxygen saturated solution reduced reductive reaction. This could result in slower degradation in these two environments than in the air where both reductive and oxidative reaction processes could produce simultaneously.

Synthesised compounds in films

Films made in lab

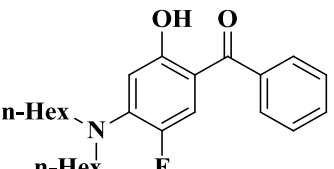
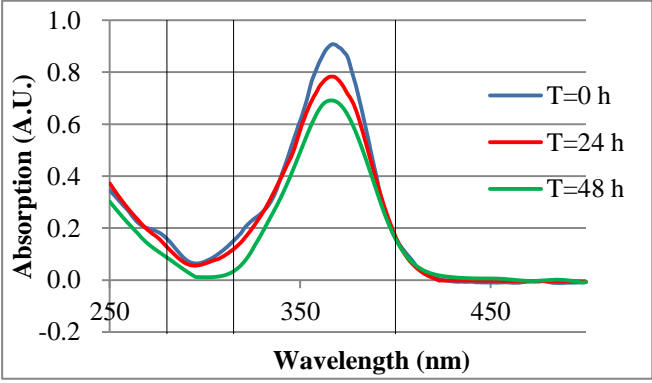
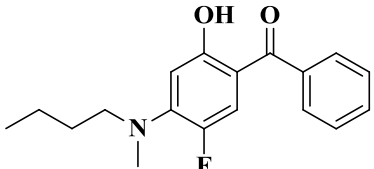
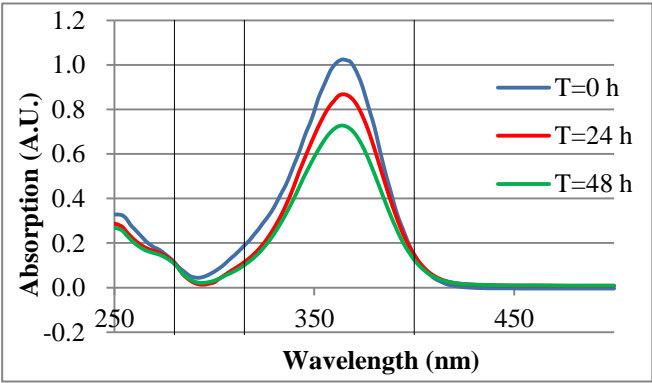
UV absorbers will eventually be put in films for their final application. A small film could be made in lab with Elvax 460 to check UV properties of the compounds in film before producing a large amount of compound for film.

Elvax® 460 is an ethylene-vinyl acetate copolymer which contains 18 % by weight vinyl acetate comonomer content and thermal stabiliser: BHT antioxidant.^[155] ELVAX 460 was combined with sample compounds in 100:1 ratio with hot THF as solvent, and cast as thin films on glass. At first, attempts were made to keep the absorption and molar absorptivity of UV absorbers in film the same as in ethyl acetate solution, but the resulting film proved too thin to remove from the glass. Therefore, it was found better to make the film thicker to facilitate peeling off from the glass. But crystallization was observed after evaporation of THF, and films were not even. It was hard to keep the blank film the same thickness as the films containing sample, which led to a messy UV absorption spectrum.

On the basis of these results, toluene was used as solvent. ELVAX 460 dissolved better in hot toluene than THF, and films which were made by evaporation from toluene were more

evenly formed. Films with 1% compound by weight were made, but a small degree of crystallization could be seen on the film. Therefore, films which contained 0.5% of compounds **46** and **48** were used for degradation studies.

Table 23. Lab films degradation

Compound	Films degradation spectra
<div style="text-align: center;">  <p>46</p> <p>$\lambda_{\text{max}}=367 \text{ nm,}$ $\epsilon=2.94 \times 10^4 \text{ L}\cdot\text{mol}^{-1}\text{cm}^{-1}$</p> </div>	
<div style="text-align: center;">  <p>48</p> <p>$\lambda_{\text{max}}=363 \text{ nm,}$ $\epsilon=2.25 \times 10^4 \text{ L}\cdot\text{mol}^{-1}\text{cm}^{-1}$</p> </div>	

*Films were irradiated under the Xenon arc lamp for 48 h in air. The UV absorption was measured with UV-Vis spectrophotometer.

From **Table 23**, absorption in the UV-B region of both compounds decreased during the degradation. In the UV-A region, **46** and **48** degraded 14% and 28% after 24 h which were faster than in solution (8% and 19%). The thickness of films changed under arc lamp irradiation which could be a reason for a faster degradation. However, the stability in the UV-B region was highly improved in films without showing a significant absorption. It suggested a different degradation product was formed in films. These two compounds were also combined with C944 in films for degradation studies, but the results showed C944 did not make any difference during the films irradiation. It was supposed that the films were not

even, and C944 was possibly not located physically close to the absorber molecules and so could not help to enhance the stability.

Films prepared by BPI

Dihexylaminohydroxybenzophenone **46** was put in film due to its easy preparation, high yield, good UV absorption and photostability for checking the UV properties in film by the collaborating company, BPI. The film consisted EVA COPO1003 89%, LDPWD 10%, C944 0.8% and 0.2% hydroxybenzophenone **46**.

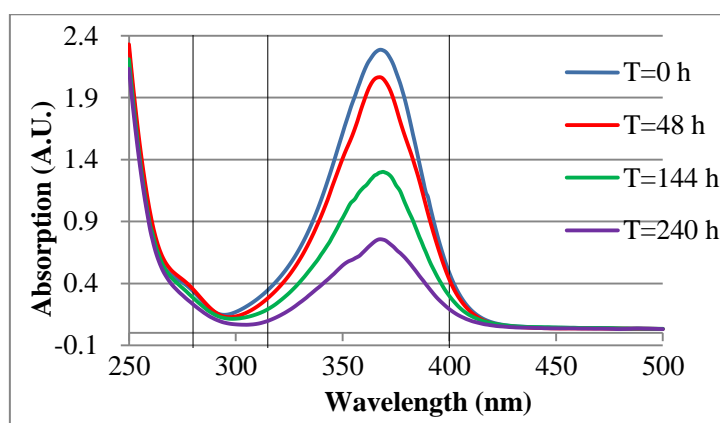


Figure 29. **46** film degradation under air

Figure 29 shows the degradation of the **46** film under the arc lamp, which showed good photostability after 10 days degradation. Although it degraded 66%, the transmission of UV-A was below 0.17. The absorbance in the UV-B region did not increase during the irradiation the same as the films made in lab. After 48 h irradiation, **46** degraded 9% in film which was lower than 12% in solution.

The film of **46** was irradiated in nitrogen or oxygen environments to investigate how reductive and oxidative processes affect the films. (Figure 30)

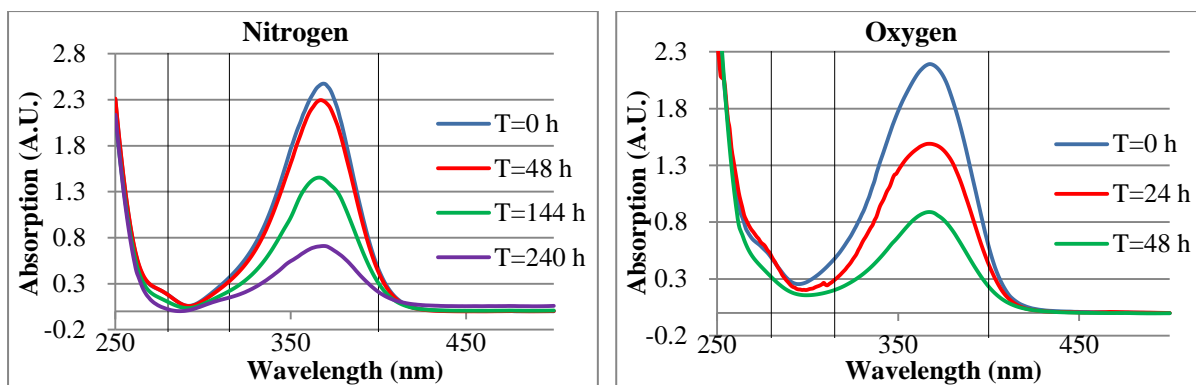


Figure 30. 46 film degradation under nitrogen or oxygen

A nitrogen environment enhanced the stability in first 96 h of irradiation, but it did not show a significant difference in both the UV-A and UV-B region from air after 10 days under the Xenon arc lamp as is clearly shown in **Figure 31**.

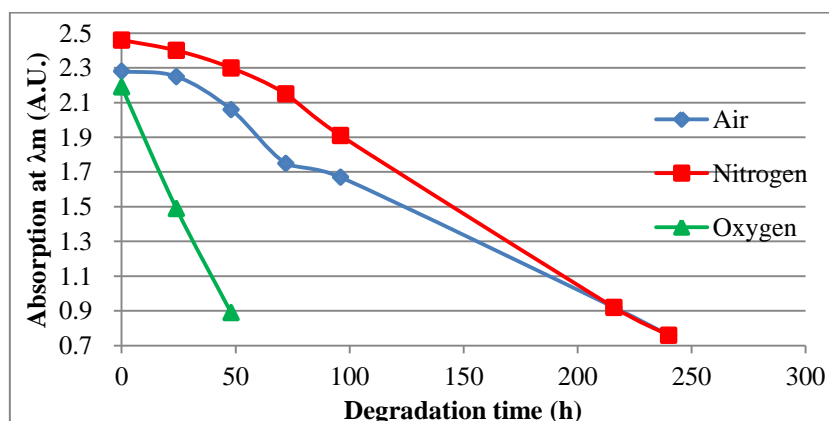


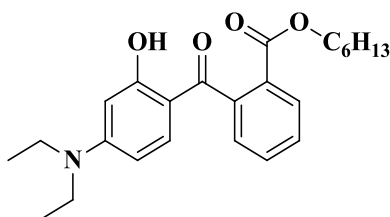
Figure 31. 46 film degradation in air, nitrogen and oxygen

When 46 film was irradiated under oxygen, absorption in the UV-A and UV-B region decreased much faster than under air or nitrogen after 48 h, which was different from the degradation in oxygen saturated solution where the oxygen environment enhanced photostability. Oxidation resulted in a faster degradation on films than in solution, which could suggest excited state lifetime was longer in films. It was easy for films to react with oxygen resulting in a fast degradation.

Uvinul A plus in solution and films

Uvinul A Plus in solution

In order to compare with the newly synthesised hydroxybenzophenones, UV absorption and degradation of Uvinul A Plus were measured.



Scheme 34. Structure of Uvinul A Plus

Uvinul A Plus showed maximum UV absorption at 350 nm wavelength with molar absorptivity around $4.1 \times 10^4 \text{ L} \cdot \text{mol}^{-1} \text{cm}^{-1}$ in ethyl acetate. **Figure 32** shows Uvinul A Plus afforded a good photostability under arc lamp which degraded 8% after 48 h.

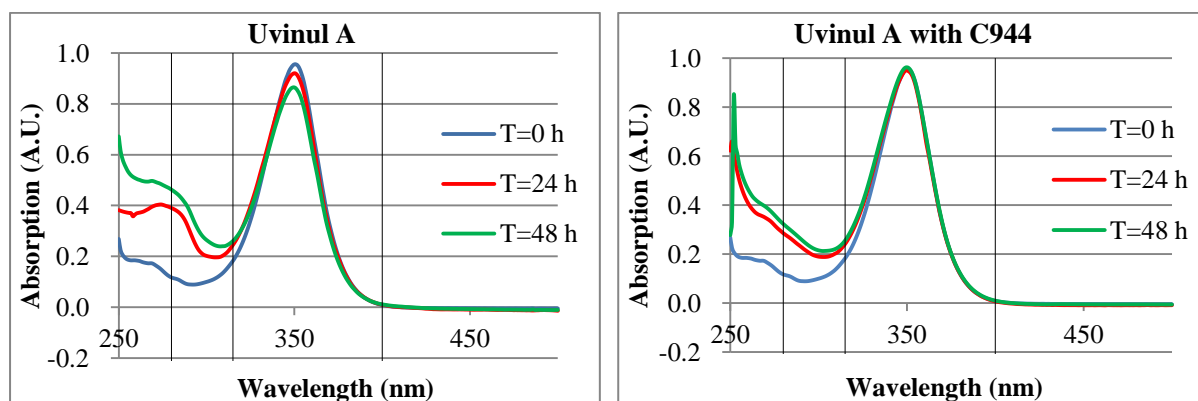


Figure 32. Uvinul A Plus degradation

Then Uvinul A Plus was combined with 4 times its weight of C944 for irradiation as shown in **Figure 32**. C944 enhanced stability significantly over 48 h irradiation in the UV-A region, and improved the stability in the UV-B region. The absorption in the UV-B region showed C944 resulted in a different degradation product from the irradiation without C944.

Uvinul A Plus in film

For comparison, Uvinul A was put in film with Elvax® 460 in lab. **Figure 33** shows the compound in film degraded faster (56%) than in solution after 48 h which was similar to **46**, and absorbance in the UV-B region did not increase during the degradation. C944 was combined in film for irradiation as well, but as found for **46** it did not improve the stability.

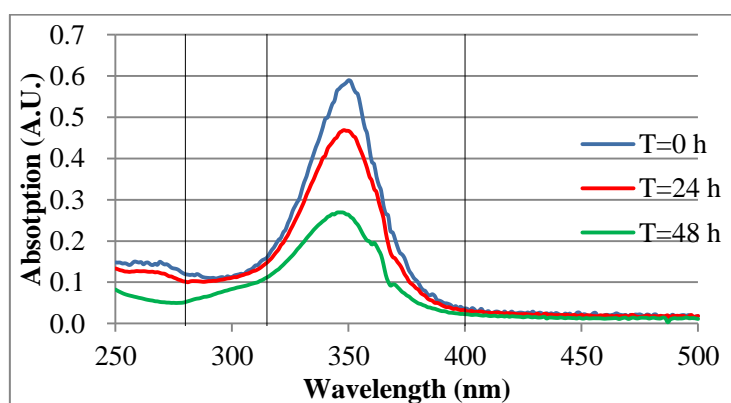
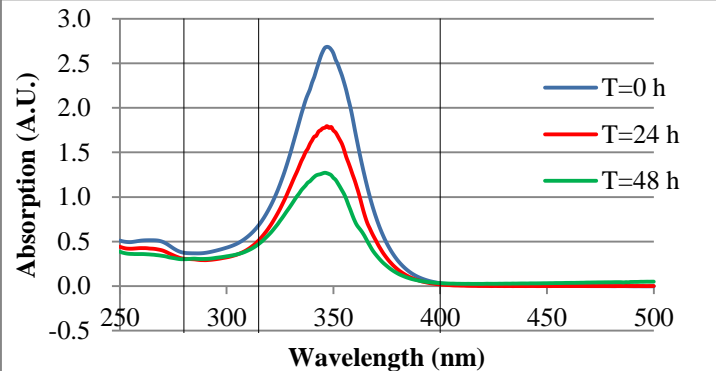
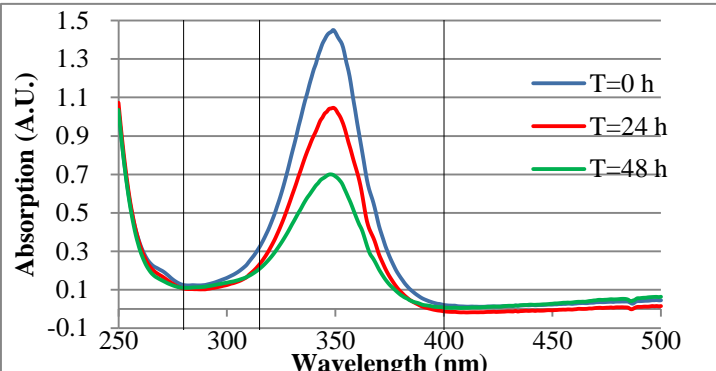


Figure 33. Degradation of Uvinul A Plus film made in the lab

Then Uvinul A Plus films made at the company were irradiated under the arc lamp. **Table 24** shows films with and without C944 were degraded 32% and 28% respectively after 24 h which suggested C944 enhanced photostability in 24 h. However, after 48 h irradiation, both of them degraded to 55%, and C944 did not show a significant influence on photostability in film. This is similar to the results from films made in lab.

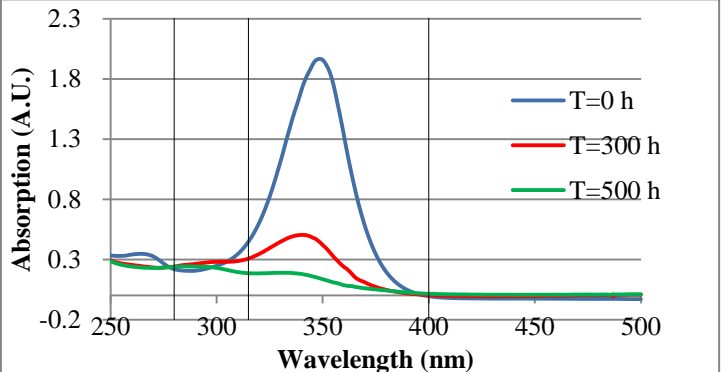
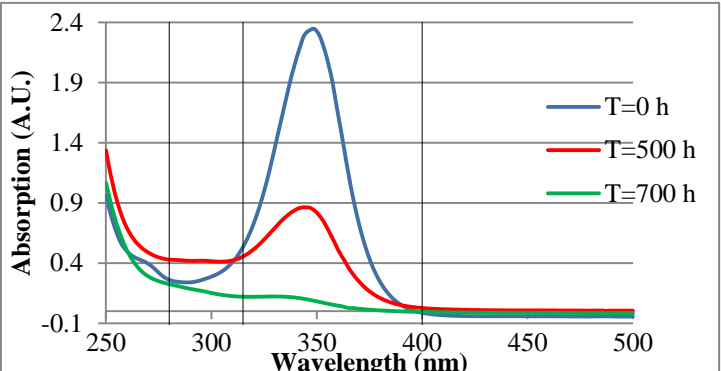
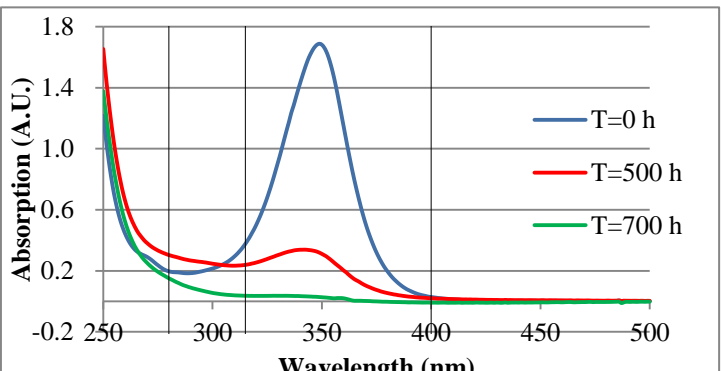
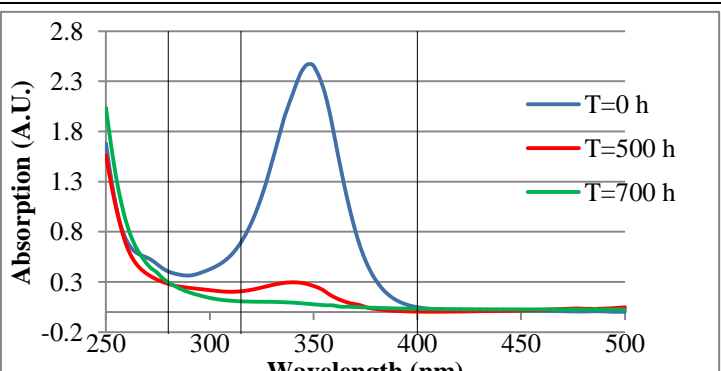
Table 24. UV degradation under xenon arc lamp for Uvinul A Plus films

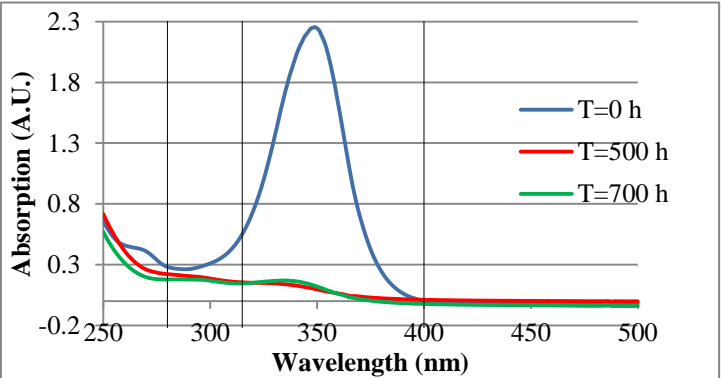
Films	Spectra
<p>Film 1 Sabic 2102TX00 79.8% Exxon FL00218 20% Uvinul A Plus 0.20%</p>	
<p>Film 3 Sabic 2102TX00 79.0% Exxon FL00218 20% Uvinul A Plus 0.20% Chimassorb 944 0.8%</p>	

*The film was irradiated under the Xenon arc lamp in air for 48 h, and measured UV absorption with UV-Vis spectrophotometer.

For comparison, the absorption of films was measured which contained Uvinul A Plus with different stabilisers after degradation in QUV for 500 h and 700 h in industry (experimental details in chapter 7) (**Table 25**). Film with Sabic 2102TX00 (80%), Exxon FL00218 (20%) was used as a blank film.

Table 25. UV degradation in QUV for Uvinul A Plus films

Films	Spectra
<p>Film 1 Sabic 2102TX00 79.8% Exxon FL00218 20% Uvinul A Plus 0.20</p>	
<p>Film 2 Sabic 2102TX00 79.4% Exxon FL00218 20% Uvinul A Plus 0.2% Chimassorb 944 0.4%</p>	
<p>Film 3 Sabic 2102TX00 79.0% Exxon FL00218 20% Uvinul A Plus 0.20% Chimassorb 944 0.8%</p>	
<p>Film 4 Sabic 2102TX00 78.9% Exxon FL00218 20% Uvinul A Plus 0.20% Chimassorb 944 0.8% AOX 0.1%</p>	

Films	Spectra
Film 5 Sabic 2102TX00 78.2% Exxon FL00218 20% Uvinul A Plus 0.20% Chimassorb 944 1.6%	

*The film was irradiated in QUV and measured UV absorption with UV-Vis spectrophotometer.

From **Table 25**, Chimassorb 944 enhanced the photostability of Uvinul A Plus during the degradation in QUV which is same as the result for Uvinul A Plus in ethyl acetate. **Films 2, 3** and **5** showed Chimassorb 944 could enhance the stability and 0.4% C944 was the best concentration for adding in the film. **Film 4** contained 0.1% alcohol oxidase (AOX) which is flavoenzyme that catalyzes the oxidation of alcohols to the corresponding carbonyl compounds with a concomitant release of hydrogen peroxide^[156] did not show any difference on the stability.

Film degradation rates under QUV were slower than using the xenon arc lamp. That is because the spectral distribution for arc lamp was 185 nm to 1800 nm, and it was from 295 nm to 365 nm in QUV. Additionally, the Xenon arc lamp concentrated all its power at one spot which is much higher than QUV.

3.3.3 Comparison between new hydroxybenzophenone and Uvinul A Plus

Dihexylamino substituted hydroxybenzophenone **46** was the most stable compound with an ideal absorption (367 nm) in the UV-A region which was compared with Uvinul A Plus in solution and film.

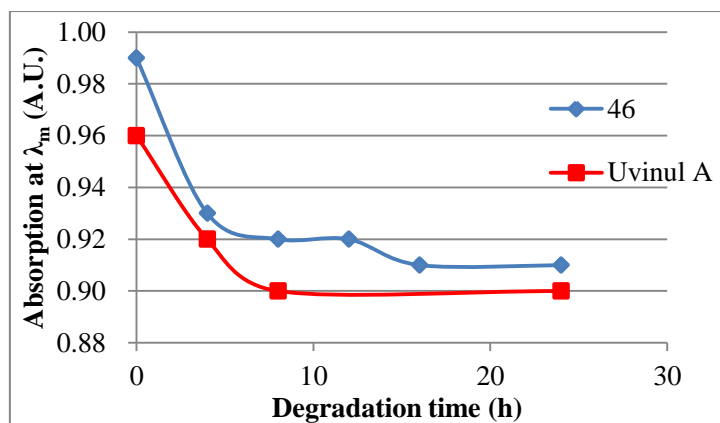


Figure 34. Comparison between **46** and Uvinul A in solution

Figure 34 shows the comparison of absorption between **46** and Uvinul A in ethyl acetate during 24 h irradiation. The two compounds showed similar photo stability and both of them degraded faster in the first 8 h than for the period 8-24 h. This could suggest degradation products formed which showed similar UV absorption with starting material in the UV-A region. Otherwise **Table 21** and **Figure 32** confirmed the absorbance in the UV-B region demonstrated formation of degraded products under air.

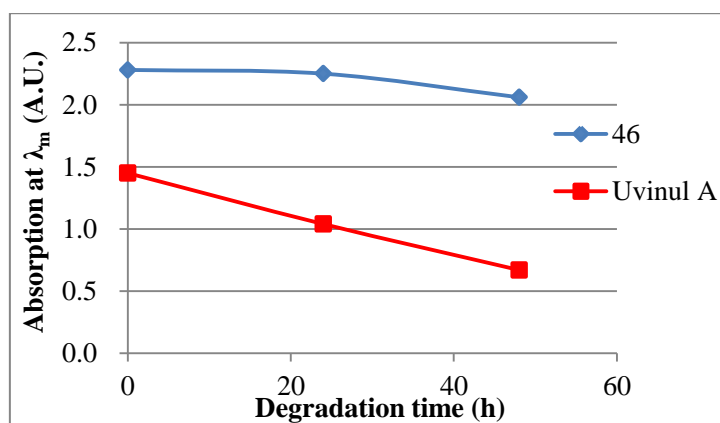


Figure 35. Comparison between **48** and Uvinul A in film

UV absorber **46** with 4 times its weight of C944 in film was compared with Uvinul A with 0.8% C944 in film. **Figure 35** shows after 48 h degradation, **46** degraded 11% provided better stability than Uvinul A which degraded 54% in film.

3.4 Conclusions

Phase transfer catalyst condition followed by Fries rearrangement was found to be a good method for synthesis of hydroxybenzophenones, and 2 eq. $ZrCl_4$ in 1,2-DCE was the best condition for the Fries rearrangement as described in this chapter. Ring substituents, such as an ester group or several fluorine atoms in different positions, had an effect on the rearrangement results. Nucleophilic substitution of fluorine was the easiest way to make amino substituted hydroxybenzophenones. The fluorine at *para* to the hydroxyl group was more difficult to replace by nucleophiles than that at the *meta*-position. Pyrrolidine was more reactive in substitution of fluorine on the hydroxybenzophenones than *N*-methyl-1-butylamine or dihexylamine.

Hydroxybenzophenones **46**, **48**, **66**, and **69** showed ideal UV absorption range and good photostability in ethyl acetate under the Xenon arc lamp. Amino-hydroxybenzophenones substituted with two fluorine atoms on the same ring such as **58**, **59** and **60**, provided less stability than compounds **66**, **67**, and **69** with one fluorine atom on each ring.

Chimassorb 944 enhanced the stability for all the compounds in the UV-A region and improved the stability in the UV-B region for some compounds in ethyl acetate. However, experiments did not show that Chimassorb 944 enhanced the stability of some compounds in the lab made films such as **46** and **48**.

The absorbance increase in the UV-B region in solution was not be seen when degradation was carried out in a pure nitrogen or oxygen environment. An oxygen environment resulted in a faster degradation of films, as measured by absorption in both the UV-A and UV-B region than air or nitrogen environments.

5-Fluoro-4-dihexylamino-2-hydroxybenzophenone **46** was easy to prepare, which could be synthesised in only two steps with 77% high yield in total. It showed an ideal UV absorption around 367 nm and fantastic photostability in both solution and film under the Xenon arc

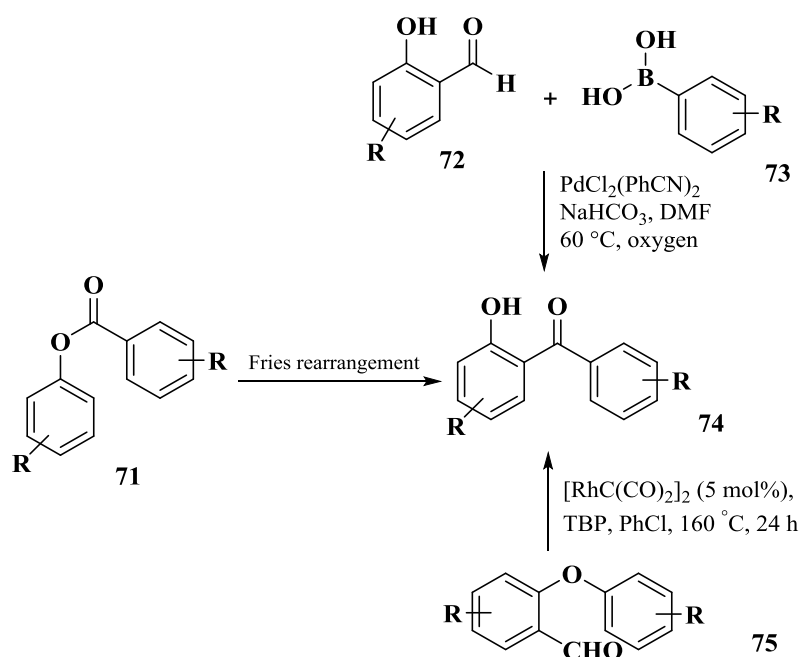
lamp. Especially in films, after 48 h irradiation, **46** degraded only 11%, which is much lower than Uvinul A Plus (54%). In this project, dihexylamino hydroxybenzophenone **46** exhibited better UV absorption and photostability than the current UV absorber, Uvinul A Plus.

Chapter 4. Synthesis and stabilisation new hydroxybenzophenones and related naphthalene analogues

4.1 Introduction

The requirements on the properties and environmental behaviour of polymeric materials are increasing together with their production and application.^[75] It is well known that all commonly used plastics degrade under the influence of sunlight. That is why the problem of their stabilisation is of eminent importance. As mentioned in the general introduction (section 1.6), hydroxybenzophenones are a well-known class of UV absorbers with simple structure. They are photostable because their excited states can dissipate the absorbed energy as heat by a rapid internal hydrogen transfer ^[157] with formation of a reversible six-membered hydrogen-bonded ring system. Therefore, hydroxybenzophenones could be also used as UV stabilisers such as Chimassorb 81.

There are many methods reported towards the construction of 2-hydroxybenzophenone derivatives due to their prevalence in materials science and medicine. The classical approach relies on the Fries rearrangement of a phenyl ester derived from a phenol. There also are transition-metal-catalyzed transformations for access to these compounds. For example, a Pd-catalyzed oxidation coupling has been developed by Weng ^[158] while use of $[\text{Cp}^*\text{RhCl}_2]_2$ as catalyst together with $\text{Cu}(\text{OAc})_2$ in DMF was reported by Wang ^[159] for coupling of salicylaldehyde with arylboronic acids. Recently, Li reported a Rh-catalyzed rearrangement of 2-aryloxybenzaldehydes to 2-hydroxybenzophenones.^[160] (**Scheme 35**)

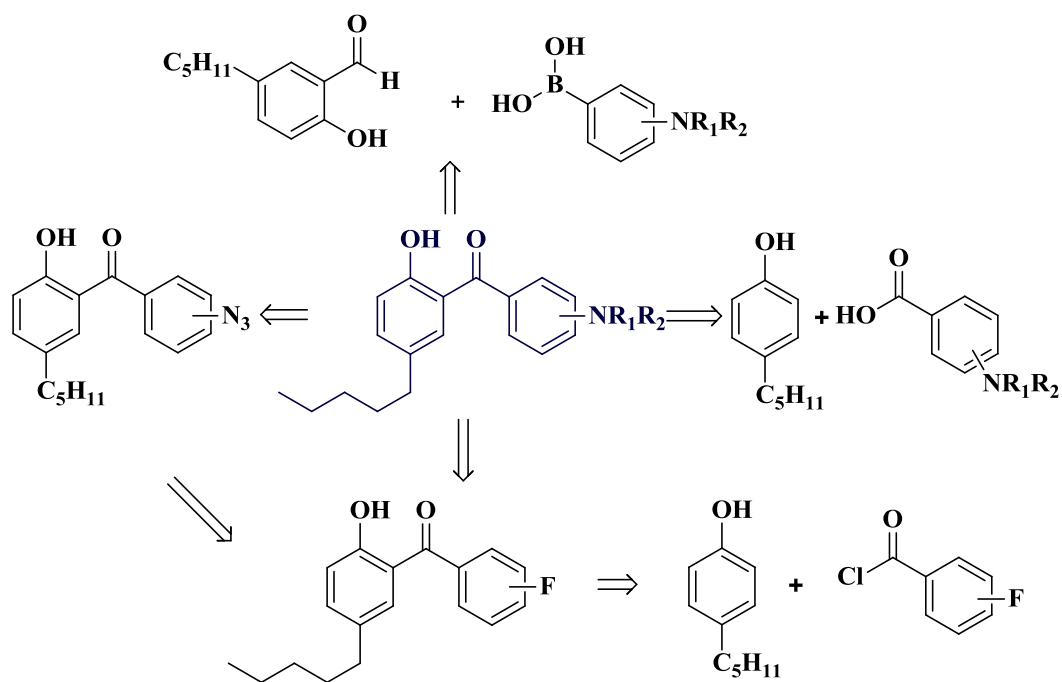


Scheme 35. Formation of 2-hydroxybenzophenone derivatives

2-Hydroxybenzophenone derivatives have found wide applications due to their efficiency as UV absorbers, light stabilisers and photo-antioxidants for polymeric materials. Different substituents affect the UV absorption characteristics and photoantioxidant activities of 2-hydroxybenzophenone compounds. This project aimed to study the synthesis and stabilisation of fluorine or amine substituted 2-hydroxybenzophenone derivatives.

4.2 Aims

The aim of the research outlined in this chapter was to prepare new hydroxybenzophenones bearing long alkyl chains to confer polymer solubility. Three different methods (**Scheme 36**) for the synthesis were envisaged. The synthesis of some related naphthalene analogues was also planned to understand their UV absorption properties and photostability. Compounds substituted with fluorine atoms or dialkylamino groups were needed to determine their potential for use in polytunnels.



Scheme 36. Proposed synthesis routes to alkyl substituted hydroxybenzophenones

All the compounds synthesised would then have their UV absorption spectra, molar absorptivity (ϵ) and photochemical stability measured. The compounds which were targeted should block most of UV-A especially in the range of 370-390 nm.

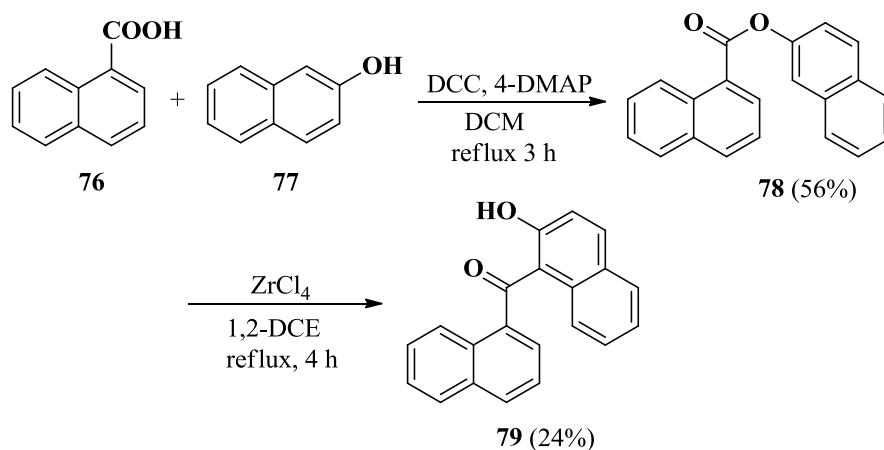
4.3 Results and discussion

4.3.1 Organic synthesis

Naphthalene analogues

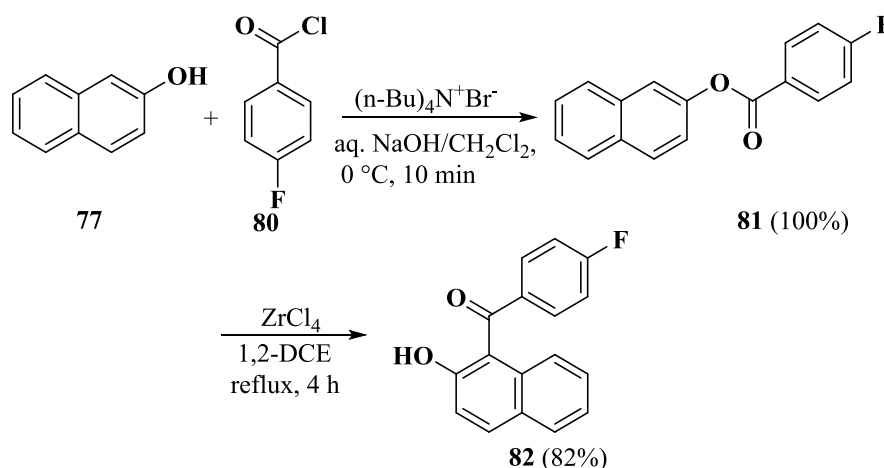
Naphthalene based hydroxyketones were studied in this project in order to determine their UV absorption and photostability and if they could be good UV absorbers for polytunnel films. Research firstly started by studying the synthetic route outlined in **Scheme 37** using naphthalene-1-carboxylic acid (**76**) and 2-naphthol (**77**) in the presence of DCC/4-DMAP in

dry dichloromethane under reflux to give ester **78** in 57%.^[161] This was then subjected to Fries rearrangement using $ZrCl_4$ in 1,2-dichloroethane under reflux affording ketone **79**.



Scheme 37. Synthesis of 1-naphthoyl-2-naphthol

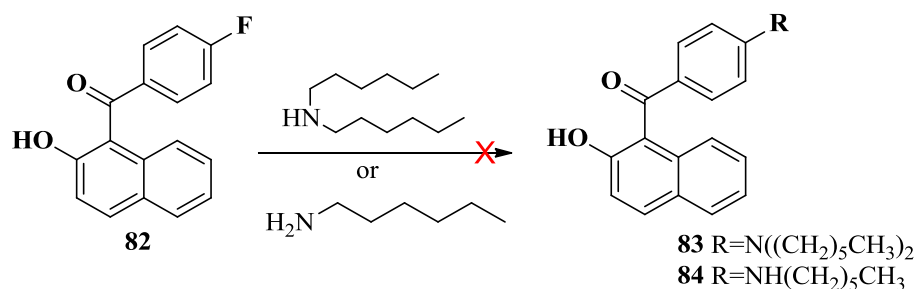
Then 4-fluorobenzoyl chloride was then used instead to react with 2-naphthol under phase transfer conditions as shown in **Scheme 38** affording ester **81**, which after Fries rearrangement formed ketone **82** in a yield of 82%. A singlet signal around 10.96 in 1H NMR spectrum stands for OH group confirmed the target product.



Scheme 38. Synthesis of 1-(4-fluorobenzoyl)-2-naphthol

In Chapter 3, dihexylamino substituted hydroxybenzophenones were reported which showed good UV absorption and photostability. Therefore, 1-(4-fluorobenzoyl)-2-naphthol (**82**) was

treated with dihexylamine in an attempt to synthesise aminonaphthol **83** by displacement of the fluorine as shown in **Scheme 39** with the different methods tested listed in **Table 26**. Conditions shown in entries **1**, **3** and **4** led to complicated mixture of compounds. The reaction mixtures showed many different spots on TLC. Also, no reaction was observed at room temperature as in entry **2**. A significant amount of starting material was recovered.



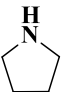
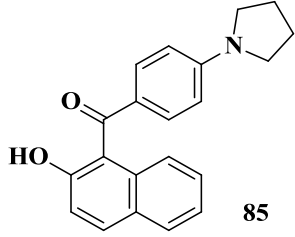
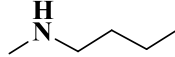
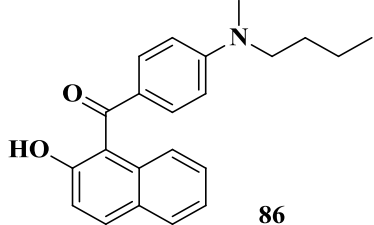
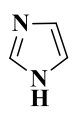
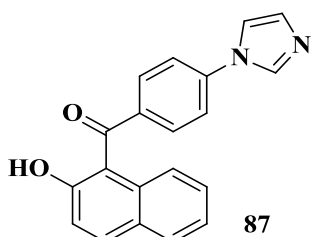
Scheme 39. Proposed formation route for **83** and **84**

Table 26. Different methods tried for synthesising naphthalene derivatives **83**

Entry	Catalyst	Conditions	Results
1	None	80 °C, 2 d	82 and by-products
2	None	r.t., 2 d	82
3	None	1,2-DCE, reflux, 2 d	82 and by-products
4	K ₂ CO ₃ , TBAB	DMSO, 80 °C, 2 d	82 and by-products

1-(4-Fluorobenzoyl)-2-naphthol (**82**) was stirred in neat 1-hexylamine (**Scheme 39**) at r.t. for 2 days, but only starting material was observed even after increasing the temperature to 50 and then 80 °C. Dihexylaminonaphthol **84** could not be synthesised by these methods. However other amine nucleophiles including pyrrolidine and *N*-methyl-1-butylamine substituted fluoronaphthol **82** successfully (**Table 27**).

Table 27. Naphthalene **82** reacted with different nucleophiles

Nucleophiles	Conditions	Products	Yields
	1,4-Dioxane reflux 48 h	 85	52%
	Neat reflux 24 h	 86	60%
	Neat 150 °C 2 d	 87	32%

Because of the difficulty in effecting nucleophilic aromatic substitution of fluorine in **82**, 1,4-dioxane (b.p. 101 °C) was used instead of THF in order to increase the reaction rate. After reflux for 48 h, 52% of the target product **85** was provided. However, this condition was found not ideal for formation of **86** and **87**.

Table 28. Different methods for synthesising naphthalene derivatives **86**

Entry	Conditions	Results
1	r.t., 24 h	Starting material (82) and by-products
2	50 °C, 24 h	Starting material (82) and by-products
3	Reflux, 24 h	Starting material (82), 60% 86

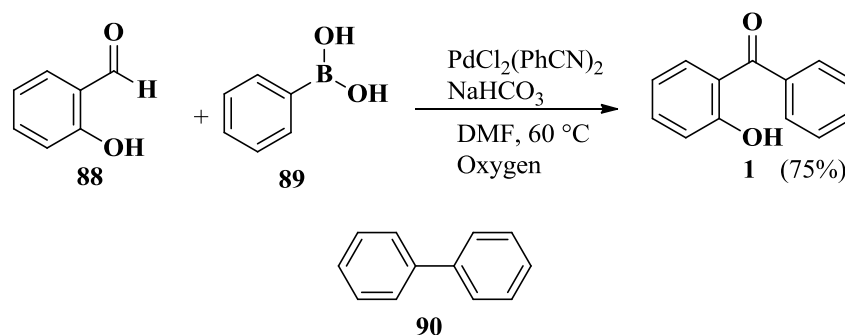
Naphthalene derivative **86** was firstly attempted to be synthesised at room temperature, as many impurities were formed at high temperature in **Table 26**. However, this condition still generated side products with most starting material remaining. Therefore, the reaction was conducted at 50 °C or under reflux (**Table 28**). Heating directly under reflux turned out to

give a better yield for target product **86**. The nitrogen heterocycle imidazole (m.p. 89-91 °C) is an effective nucleophile, and was heated with **82** at 150 °C for 2 days, affording target product **87** in 32% yield. No fluorine signals in ^{19}F NMR spectrum were observed for the three compounds which proved the successful fluorine substitution.

Hydroxybenzophenones

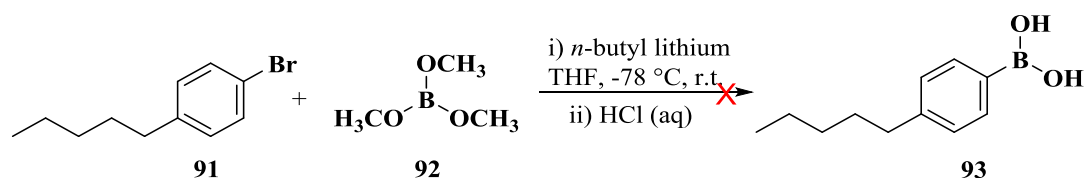
Oxidation coupling

Hydroxybenzophenones can be synthesised by many methods from different starting materials. Research firstly was aimed towards synthesising 2-hydroxybenzophenones (**1**) from salicylaldehyde (**88**) and phenylboronic acid (**89**) to find a good method for preparing other hydroxybenzophenones with different substitution patterns. Using the same method reported by Wang ^[158] (Pd and Cu both present as catalysts) afforded biphenyl (**90**), instead of the expected benzophenone product **1**. Applying the method in **Scheme 40** without CuCl_2 afforded product **1** in a 75% yield. However, the starting salicylaldehyde still remained even after a long reaction time (40 h).



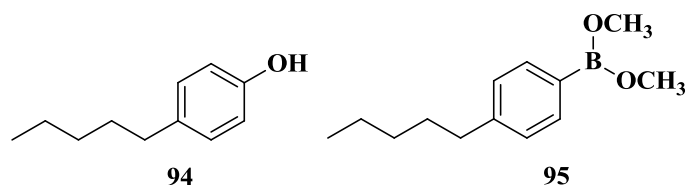
Scheme 40. Proposed synthetic route for 2-hydroxybenzophenone

4-Pentylbromobenzene (**91**) and trimethyl borate (**92**) were next used to form benzeneboronic acid **93** with a long alkyl chain to confer solubility as shown in **Scheme 41**.



Scheme 41. Proposed synthetic route for 4-pentylbenzeneboronic acid

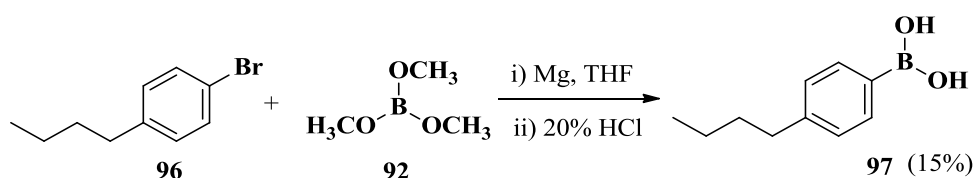
Butyllithium was used to affect bromine-lithium exchange with THF as solvent at $-78\text{ }^\circ\text{C}$ with subsequent warming to room temperature.^[162] After 20 h, hydrochloric acid was added and the mixture was stirred for 1 h to hydrolyse the boronate ester. After extraction, TLC showed starting material still remained with many other spots. GC-MS did not show signal for boronic acid **93**, but displayed signals at m/z 164.1 for 4-pentylphenol (**94**), and m/z 219.3, 204.2 and 188.1 for dimethyl (4-pentylphenyl) boronate (**95**) indicating hydrolysis had not been complete.



Scheme 42. Side products of reactions for 4-pentylbenzeneboronic acid

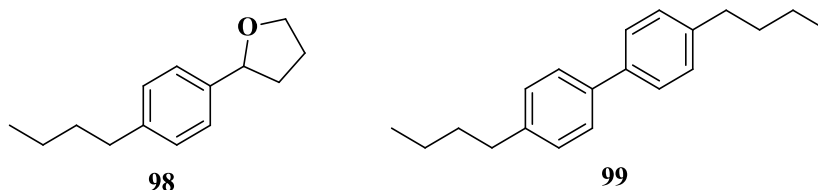
After further purification by column chromatography dimethyl boronate **95** was obtained, an attempt to hydrolyse it to be boronic acid was made, dissolution in diethyl ether, and addition of 20% HCl. The mixture was stirred at room temperature for 4 h to afford a white solid (**93**) in a yield of 14%. However, the melting point range was $60.5\text{--}70.8\text{ }^\circ\text{C}$ and the NMR spectrum indicated there were other side products.

Because of the low yield of the previous method, another approach to synthesise an alkyl substituted benzeneboronic acid (**92**) was undertaken (**Scheme 43**). Magnesium turnings were employed to react with 4-bromobenzene (**96**) to form a Grignard reagent, then trimethyl borate was added at $-78\text{ }^\circ\text{C}$.^[163] After purification, only 15% of the target product (**97**) was afforded.



Scheme 43. Synthesis of 4-butylbenzeneboronic acid

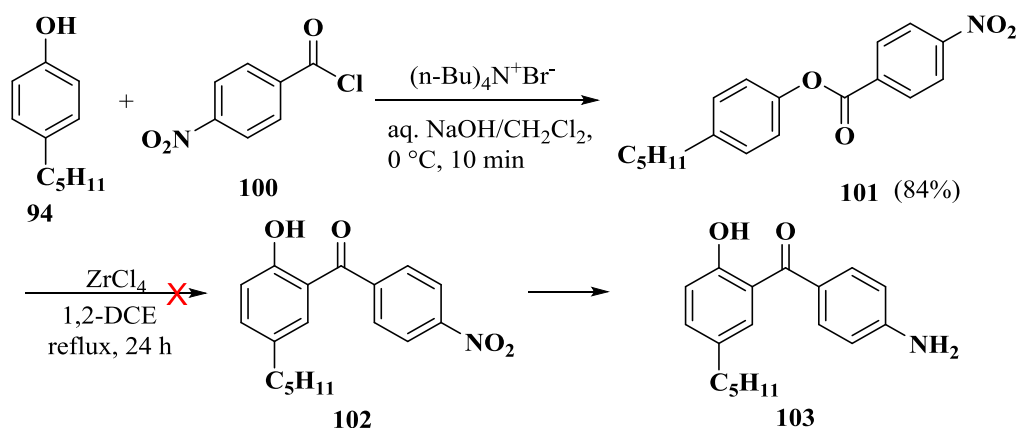
Both NMR spectroscopy and GC-MS were used to analysis the other by-products. As with the previous method, the presence of 4-butylphenol was shown which exhibited a signal at 5.24 (1H, bs). Another two side products, **98** and **99** were observed. For compound **98** ^1H NMR showed signals at 4.85 (1H, t, $J=6.4$ Hz), 4.08 (1H, q, $J=7.6$ Hz), 3.92 (1H, q, $J=7.2$ Hz), and GC-MS gave peaks at m/z 204.2, 161.0 and 147.1. 4-Butylbromobenzene reacted with magnesium turnings under reflux to afford a Grignard reagent which then reacted with solvent THF to provide **98**, or reacted with 4-butylbromobenzene to afford biphenyl **99** with major peaks at m/z 266.2, 223.1, 179.9 and 151.8 in the GC-MS spectrum.



Scheme 44. Side products of reactions for 4-butylbenzeneboronic acid

Reactions with amine substituted benzoic acid and benzoyl chloride

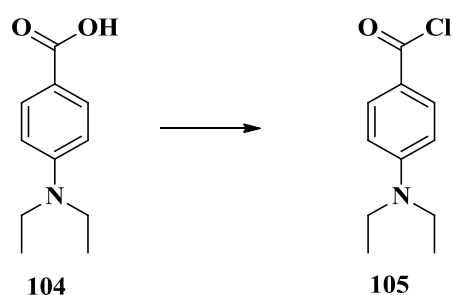
Because of the low yields and many side products forming from the previous two approaches for boronic acid synthesis, methods outlined in Chapter 3, using phase transfer conditions and Fries rearrangement were next attempted to synthesise amino substituted hydroxybenzophenones. 4-Aminobenzoylphenol (**103**) was chosen as a good target compound which could be substituted with different groups. The same method for synthesising hydroxybenzoylphenones as described in Chapter 2 was used to form product **103** as shown in **Scheme 45**. The first step afforded ester **101** in 84%. However, in the second step involving rearrangement only 3% yield of ketone **102** was obtained. Ketone **102** showed a similar polarity to ester **101**, which led to a difficult separation.



Scheme 45. Synthesis of hydroxybenzophenone **102**

Therefore, another attempt was made to form an alternative substrate for Fries rearrangement, and to make 4-(diethylamino)benzoyl chloride (**105**) from 4-(diethylamino)- benzoic acid (**104**). The methods listed in **Table 29** were investigated, but it proved difficult to obtain.

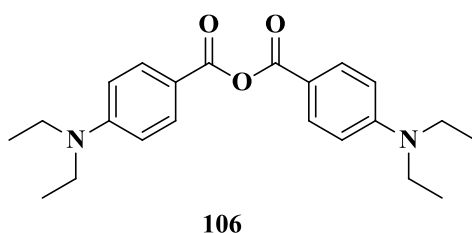
Table 29. Different methods for synthesis 4-(diethylamino)benzoyl chloride



Entry	Reagents	Conditions	Yield
1	SOCl ₂	reflux, 2 h	0%
2	SOCl ₂	DCM, 0 °C, 7 h	30%
3	SOCl ₂ ^[164]	DCM, r.t.	0%
4	SOCl ₂	DCM, reflux, 24 h	0%
5	SOCl ₂	DCM, DMF, r.t., 16 h	0%
6	Oxalyl chloride ^[165]	DCM, DMF, r.t., 16 h	0%

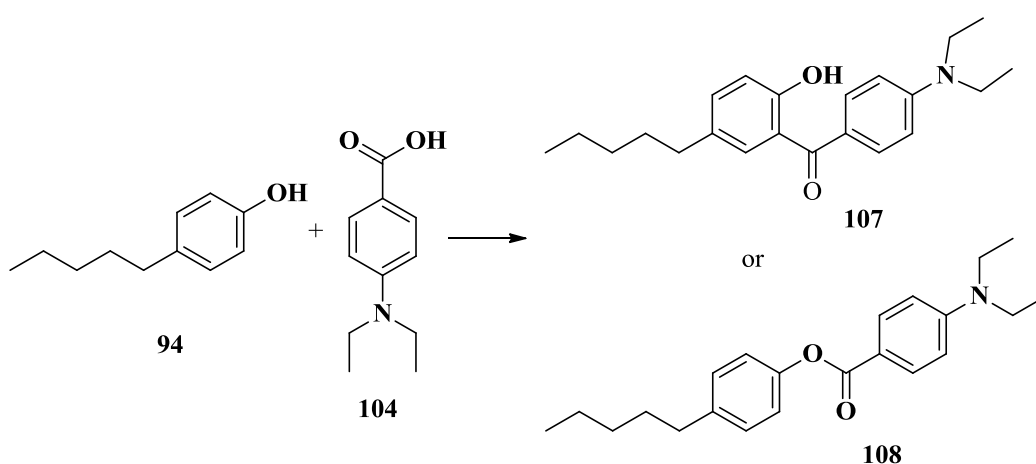
Thionyl chloride was used as solvent under reflux in entry **1**, led to the solution turning black after 2 hour, and afforded a black oil. It showed a complicated NMR spectrum. Method **2** only resulted in 30% target product, and starting material remained. For entries **3** and **4**, NMR

spectroscopy showed just 4-(diethylamino)benzoic acid (**104**) to be present. In contrast, methods for entries **5** and **6** afforded 4-(diethylamino)benzoic anhydride (**106**) which gave ^1H NMR signals at 8.13 (4H, d, $J=8.4$ Hz) and 7.37 (4H, d, $J=8.4$ Hz). They were different from the starting material signals 8.27 (2H, d, $J=8.4$ Hz) and 7.89 (2H, d, $J=8.4$ Hz). The IR spectrum showed two double peaks at 1749, 1715 for two carbonyl groups and at 1177, 1155 cm^{-1} for the two C-O bond, characteristic of the symmetric and asymmetric vibrations of an anhydride, which confirmed the compound.



Scheme 46. Side product of acid chloride formation

Other methods were then investigated to synthesise ester **108** or benzophenone **107** directly from 4-pentylphenol and 4-(diethylamino) benzoic acid, as shown in **Table 30**. 4-(Diethylamino)benzoic acid was found to be insoluble in 1,2-dichloroethane, so DMF was used instead in entry **2**. Unfortunately, after stirring under reflux for 18 h, only the two starting materials were observed. The same was found for entry **5** by using trifluoroacetic acid as a catalyst to synthesise ester **108**. Entries **3** and **4** provided many side products. After purification by column chromatography, only 5% product was afforded



Scheme 47. Proposed formation route for **107** and **108**

Table 30. Different methods attempted for synthesising **107** and **108**

Entry	Reagents	Conditions	Product	Yields
1	SnCl ₄ ^[166]	Dichloroethane, reflux, 16 h	107	0
2	SnCl ₄	DMF, reflux, 18 h	107	0
3	Graphite, MeSO ₃ H ^[167]	120 °C, 15 h	107	5%
4	BF ₃ ·Et ₂ O ^[168]	100 °C, 18 h	107	5%
5	CF ₃ COOH ^[169]	Acetonitrile, 60 °C, 38 h	108	0
6	TFAA/H ₃ PO ₄ ^[170]	r.t. 3 h	108	28%
7	TFAA/H ₃ PO ₄	50 °C, overnight	108	10%
8	T ₃ P	Ethyl acetate, reflux, 16 h	108	80%

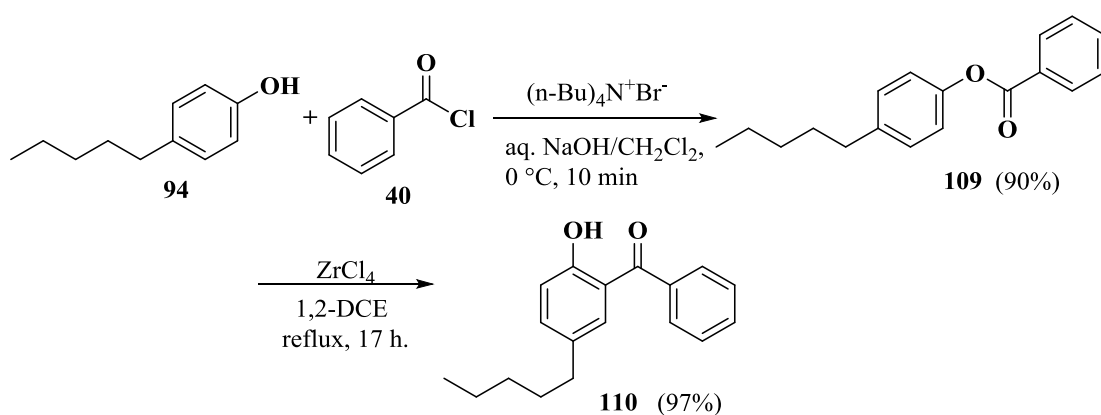
Entries **6** and **7** in **Table 30** employed trifluoroacetic anhydride and 85% phosphoric acid to prepare ester **108**. When conducted at room temperature or at 50 °C, the reactions only provided target product in a low yield, and most of the starting materials were recovered. Excess 4-diethylaminobenzoic acid was not helpful, and 4-pentylphenol still remained. This method thus was not ideal. Finally, propylphosphonic anhydride solution (T₃P), as shown in entry **8**, afforded 80% yield of target compound.

Disappointingly, after the effort spent in making ester **108** the method for Fries rearrangement with ZrCl₄ in 1,2-dichloroethane failed to afford **107**. When ester **108** (0.21 g) and 2 equivalents of ZrCl₄ was stirred under reflux in 1,2-dichloroethane for 24 h, only a small amount of yellow oil (0.02 g) was collected after chromatography purification, which proved to be a complicated mixture by NMR spectroscopy. Another attempted was carried out with DMF instead of 1,2-dichloroethane, but only starting material was recovered from this attempt. Therefore, as unlikely preparation of **107** from **108**, an alternative was designed to synthesise the desired hydroxybenzophenone compounds.

Fluorine-nucleophilic substitution reaction

The aromatic nucleophilic substitution (S_NAr) of fluorine resulted in an ideal method for preparing amino substituted benzophenones as reported in Chapter 3. Due to long Fries rearrangement reaction time and low yield, the initial intention for the formation of fluorinated hydroxybenzophenones in this chapter was to carry forward the optimised

conditions for synthesis of known compound **110**. Treatment of 4-pentylphenol with benzoyl chloride under phase-transfer catalysis conditions, using tetra-butylammonium bromide in a mixture of aqueous NaOH and dichloromethane, afforded **109** in nearly 100% yield without the need for further purification.



Scheme 48. Synthesis route for **111**

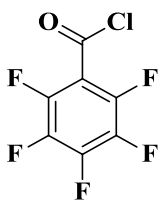
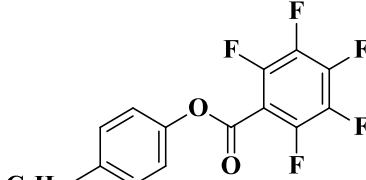
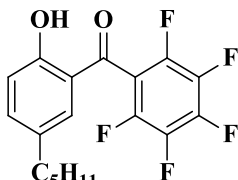
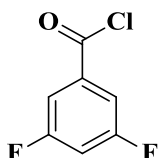
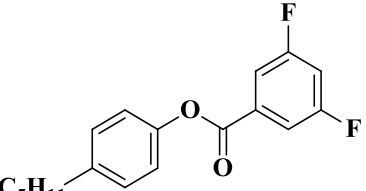
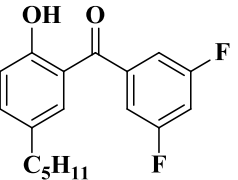
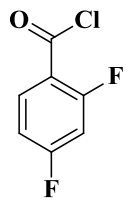
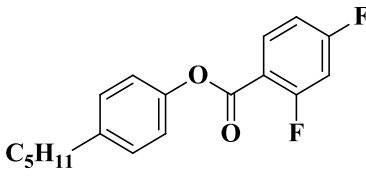
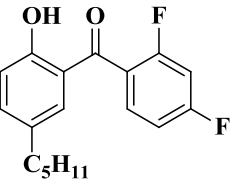
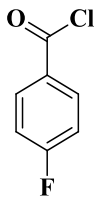
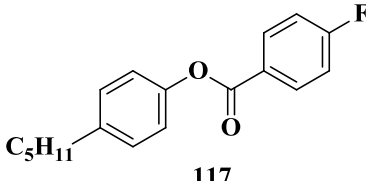
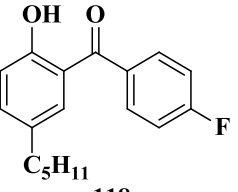
Fries rearrangement of benzoate ester **109** to **110** was studied with different catalysts and conditions (**Table 31**), but due to the two compounds having similar polarity, it was difficult to separate them. The best approach was to ensure complete rearrangement of **109** to **110**, so no ester remained needing removal.

Table 31. Different methods for Fries-rearrangement

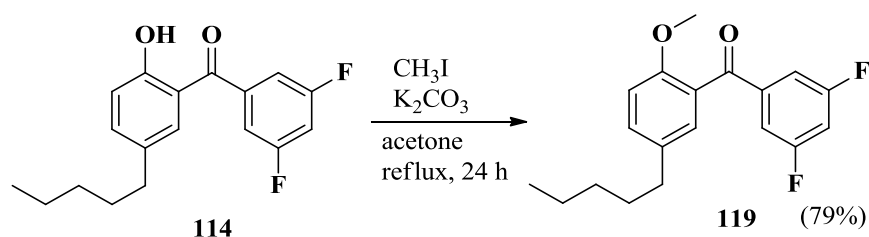
Catalysts	Solvent	Conditions	Yield
ZrCl ₄ (4 eq.) ^[128]	DCM	ultrasound, r.t., 8 h	0%
ZrCl ₄ (4 eq.)	DCE	reflux, 15 h	55%
ZrCl ₄ (2 eq.)	DCE	reflux, 15 h	97%
ZrCl ₄ (2 eq.)	DCE	reflux, 7 h	80%
ZrCl ₄ (1 eq.)	DCE	reflux, 15 h	62%
AlCl ₃ ^[124]	None	130 °C, 2 h	75%
AlCl ₃	DCE	reflux, 23 h	2%
AlCl ₃ -ZnCl ₂ (4:1) ^[121]	None	130 °C, 17 h	74%
AlCl ₃ -ZnCl ₂ (4:1)	DCE	reflux, 19 h	3%
AlCl ₃ -ZrCl ₄ (2:1)	None	130 °C, 5 h	0%
AlCl ₃ -ZrCl ₄ (2:1)	DCE	reflux, 25 h	84%

From **Table 31**, it demonstrated that 2 eq. $ZrCl_4$ with 1,2-dichloroethane as solvent still provided the highest yield which was the same as reported in Chapter 2, but with a shorter reaction time. A singlet peak at 11.85 ppm for OH group in 1H NMR proved the rearranged product. After the successful synthesis of hydroxybenzophenone **110**, several different benzophenone compounds (**Table 32**) were prepared from 4-pentylphenol with the same method and different aroyl chlorides (**Scheme 48**). However, different substituent groups on the benzoyl chloride affected the yield of reaction. Pentafluorobenzoyl chloride only provided **112** in a 4% yield whereas **114**, **116** and **118** were formed in very high yields, which were used for further research.

Table 32. Different hydroxybenzophenone compounds prepared

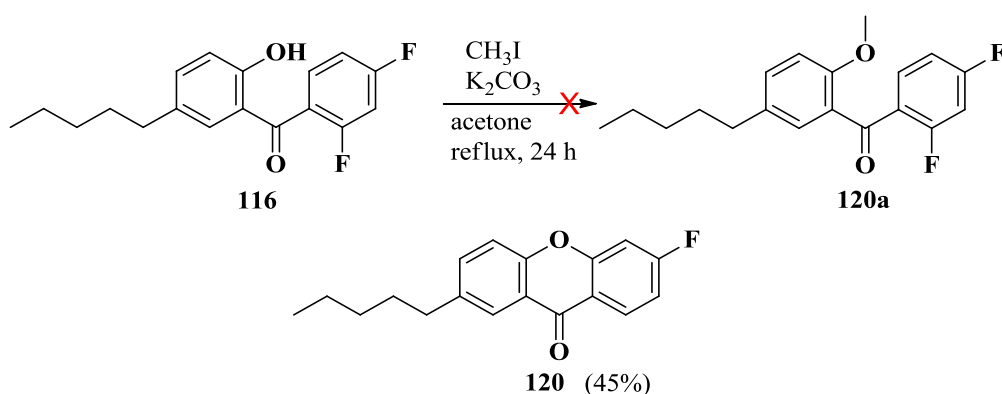
Reactants	Intermediates/yields	Products/yields
	 111 90%	 112 4%
	 113 100%	 114 97%
	 115 99%	 116 97%
	 117 98%	 118 90%

As a further study on **114** and **116**, methylation of the phenolic OH group was investigated to convert it to methoxy in order to compare UV absorption and photostability. The methoxy substituted benzophenones were synthesised by the reaction of difluorohydroxybenzophenones **114** and **116** with methyl iodide in the presence of anhydrous potassium carbonate (Scheme 49).^[171] 3,5-Difluorobenzophenone **114** afforded methoxy derivative **119** in a 79% yield. Signal at 11.53 ppm for OH group disappeared in ¹H NMR, and a singlet peak at 3.68 for methyl group in **119** was observed.



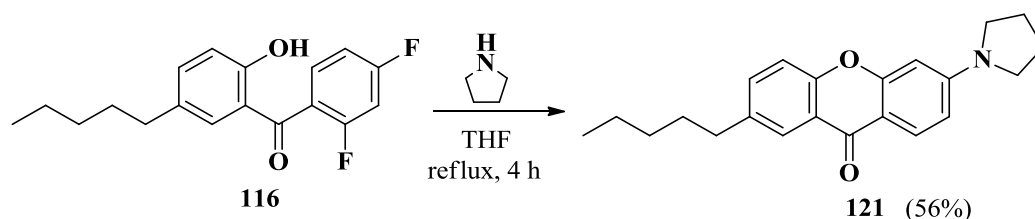
Scheme 49. Methylation of the phenolic OH group

However, 2,4-difluorobenzophenone **116** afforded a different product, and underwent cyclisation to xanthone **120** (Scheme 50). The phenolate anion must have displaced fluorine on the second position in a S_NAr reaction. In the ¹⁹F NMR spectrum there was only one fluorine signal 60.24 (1F, q, *J*=7.52 Hz). The GC-MS spectrum showed peaks at *m/z* 284.3, 241.2 and 227.1. All these data matched with xanthone **120**.



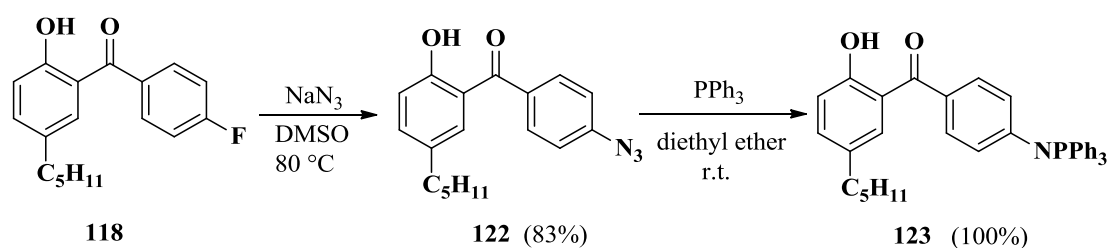
Scheme 50. Proposed methylation route for **120a**

Similar cyclisation occurred again when treating 2,4-difluorobenzophenone **116** with pyrrolidine (**Scheme 51**), which afforded xanthone derivative **121** under the basic conditions, and the 4-fluoro substituent was also replaced.



Scheme 51. Proposed formation of **121**

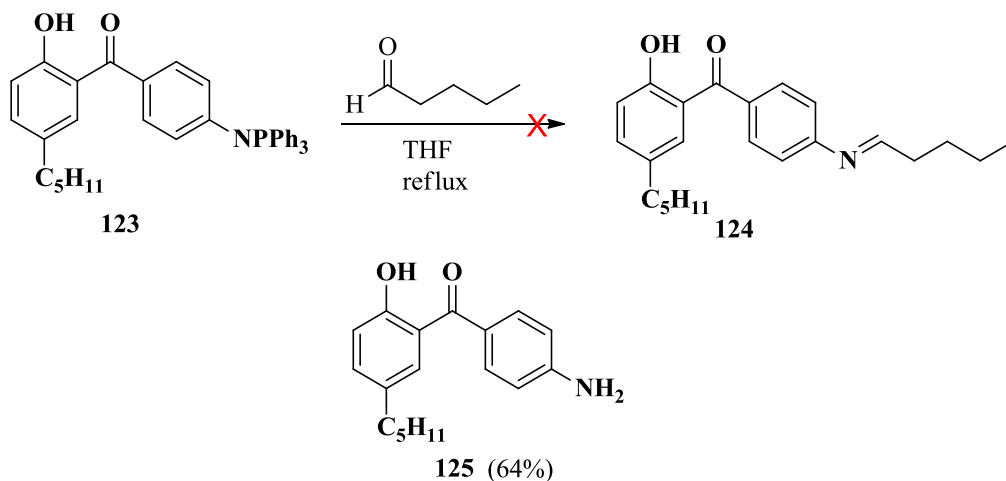
Sodium azide is a good reagent to introduce the azide functional group which can thereafter be converted to different amines. Therefore, sodium azide was used to replace fluorine in **118**, and then the azido substituted compound could be reacted with triphenylphosphine to afford different amines with aldehydes or halogen compounds by an aza-Wittig reaction.



Scheme 52. Synthesis route for **123**

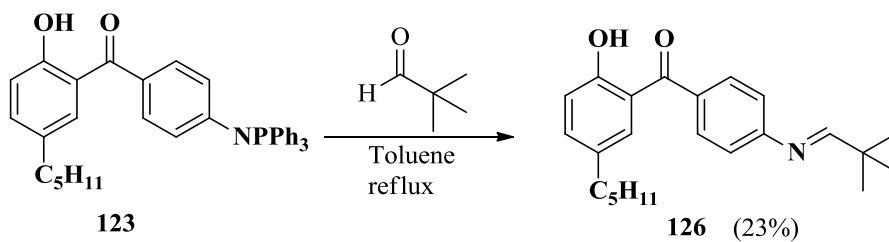
Treatment of 4-fluorobenzoylphenol (**118**) with sodium azide in DMSO at 80 °C afforded **122** in 80% yield (**Scheme 52**). No fluorine signal was observed in ^{19}F NMR. The ^{13}C NMR peak for carbon at 4 position changed from doublet to singlet. Coupling between carbonyl and fluorine disappeared and mass m/z at 287.1443 for $(\text{M}+\text{H}^+)$ confirmed the azido **122**. Another method using acetone and water as solvents ^[172] under reflux was proved unsuccessful, with all starting material being recovered. Azido-hydroxybenzophenone **122** was then reacted with triphenylphosphine in diethyl ether at room temperature for 2 h providing product **123** in 91% yield, which was then treated with valeraldehyde in THF under reflux in an attempt to form **124** (**Scheme 53**). However 4-aminobenzoylphenol (**125**) was formed by hydrolysis of the iminophosphorane **123** instead of imine formation. A single peak

at 4.2 ppm contained 2 protons for NH₂, and mass signal m/z at 284.1642 for (M+H⁺) proved the primary amino hydroxybenzophenone **125**.



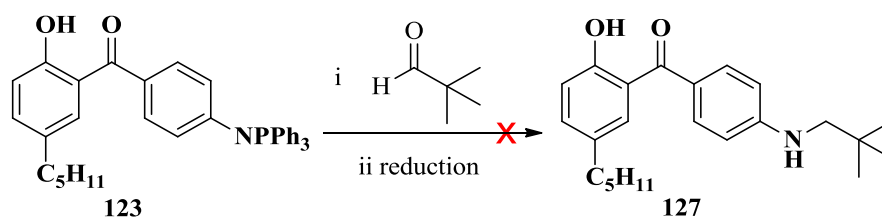
Scheme 53. Proposed formation for **124** and side product

As shown in **Scheme 54**, toluene was then used as solvent instead of THF to synthesise **126** using trimethylacetaldehyde as the carbonyl component, so that the imine product was expected to be reduced to afford an amino substituted benzophenone^[173]. However, after stirring under reflux for 24 h, only 23% of target product was obtained together with amine **125**. ¹H NMR signals at 7.58 (1H, s) for N=CH and 1.38 (9H, s) for 3 methyl groups confirmed the target product.



Scheme 54. Proposed formation route for **126**

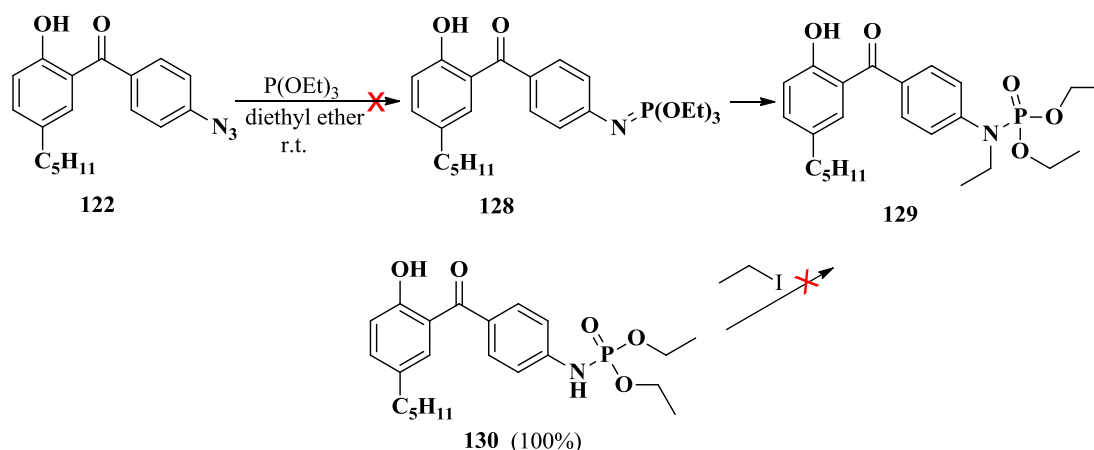
Imine **126** was easily hydrolysed via an intermediate hemiaminal which would result in 4-aminobenzoylphenol (**125**). Therefore, reduction of the imine was undertaken and the hydroxybenzophenone **126** was treated with NaBH₄ in a one-pot process (**Scheme 55**).



Scheme 55. Proposed formation route for **127**

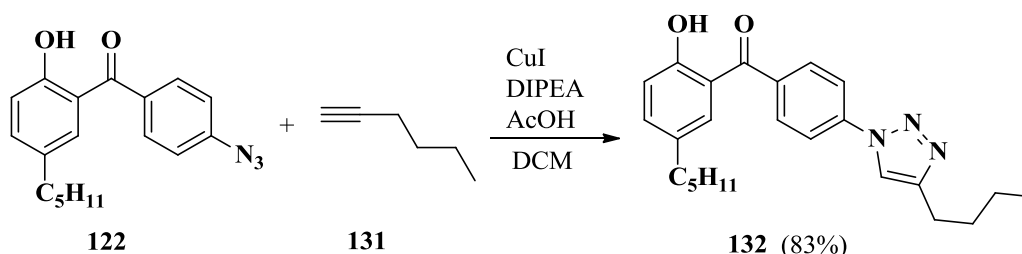
Sodium borohydride was used as a reducing agent in ethanol, however it reduced the ketone C=O to CH-OH, which was confirmed by the two OH signals in NMR spectrum. Therefore, sodium cyanborohydride was chosen to selectively reduce the imine only. After 3 days, the NMR spectrum showed 4-aminobenzoylphenol (**125**) was formed again and **126** was not reduced to target product **127**.

Azide **122** was investigated to form **129** as shown in **Scheme 56**. 4-Azido benzoylphenol (**122**) was treated with triethyl phosphite in diethyl ether in order to afford **128** which was hoped could be rearranged to form the phosphoramidate **129** containing an *N*-alkyl group. However, after 2 h in diethyl ether, the reaction provided phosphoramidate **130** with loss of one ethyl substituent. In NMR spectra, signals for only two ethoxy groups were observed, and mass m/z at 420.1926 for $(M+H^+)$ proved the formation of **130**.



Scheme 56. Proposed formation route for **129**

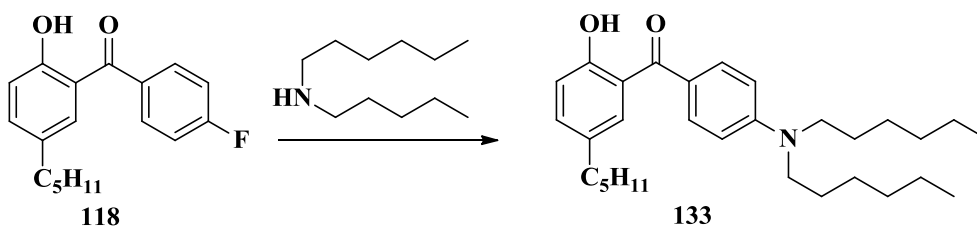
Two different methods were attempted to synthesise **129** from **130**. Firstly, iodoethane was used to add an ethyl group to form phosphoramidate **129** in toluene under reflux. In the second method, potassium carbonate was employed as a base in acetone with starting material **130** for the reaction. However, only starting material was observed in both cases.



Scheme 57. Synthesis of hydroxybenzophenone **132**

Another reaction of azide **122** involved treatment with 1-hexyne (**131**) to attempt to form a cycloaddition product, 1,2,3-triazole **132**^[174] (**Scheme 57**). In this reaction, a combination of CuI/DIPEA/AcOH (1:2:2) was developed as a highly efficient catalytic system. After 24 h, 85% of **132** was successfully formed as a yellow solid with maximum UV absorption around 285 nm wavelength. These three new compounds prepared from the versatile azide functional group however did not show ideal UV absorption in the UV-A region. Therefore, replacing fluorine in hydroxybenzophenones with amine groups directly still showed significant advantage.

In Chapter 3, it was reported that dihexylamine substituted compounds showed higher UV absorption and better photostability, compared to compounds with pyrrolidine and *N*-methyl-1-butylamino substituted compounds. Dihexylamine was then used to replace the fluorine in 4-fluorobenzophenone **118**.



Scheme 58. Proposed amination of for **133**

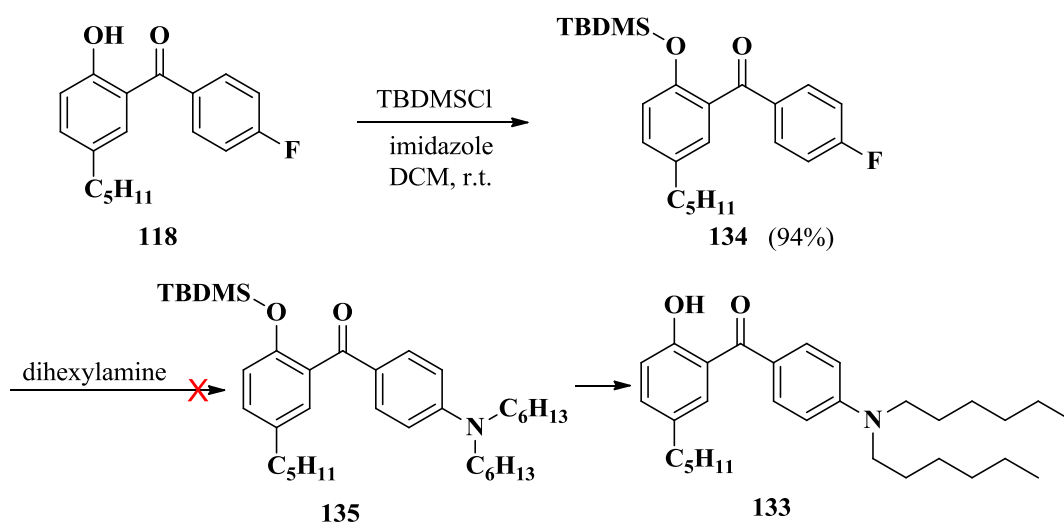
As the two long hexyl chains in dihexylamine make it less active as a nucleophile towards 4-fluorobenzoylphenol, seventeen different methods were attempted to synthesise dihexylamino **133** as shown in **Table 33**. Most of these methods did not work and gave starting material back. Some of them conducted at a high temperature such as entries **2**, **3** and **4** formed of mixtures decomposition products with a strong amine smell. Only starting material was recovered, and the dihexylamine most likely degraded. Only routes **14** and **16** provided target product in a low yield. In these two reactions, sodium hydride or *n*-butyllithium was used as a base and deprotonated the hydroxyl group which made the 4-fluorobenzoyl group less electrophilic, and so a large amount of starting material remained.

Table 33. Different conditions for synthesising **133**

Entry	Reagents	Conditions	Results
1	None	80 °C, 2 d	Starting material
2	None	Reflux (195 °C), 2 d	Starting material with strong amine smell
3	None	Reflux (195 °C), 24 h	Same as Entry 2
4	None	110 °C, 2 days	Same as Entry 2
5	None	THF, reflux, 2 days	Starting material
6	None	DCE, reflux, 2 d	Starting material
7	None	Dioxane, reflux, 24 h	Starting material
8	None	DMSO, reflux, 24 h	Starting material and by products
9	K ₂ CO ₃ , TBAB ^[175]	DMSO, 90 °C, 2 d	Starting material and by products
10	K ₂ CO ₃ , TBAB ^[175]	DMSO, 90 °C, 24 h	Starting material and by products
11	K ₂ CO ₃	DMSO, THF, reflux, 6 h	Starting material
12	Cesium carbonate	DMSO, 100 °C, 20 h	Starting material
13	Sodium acetate	DMSO, THF, reflux, 24 h	Starting material
14	NaH	THF, reflux, 24 h	Starting material, 8% 133
15	DBU	THF, reflux, 24 h	Starting material
16	<i>n</i> -BuLi	THF, r.t., 24 h	Starting material, 7% 133
17	<i>n</i> -BuLi	THF, reflux, 24 h	Starting material and by products

Dihexylamine substituted hydroxybenzophenone **133** showed a maximum UV absorption at 378 nm with an ideal photostability which met the target requirements (**Table 38**). Therefore, different methods should be developed to improve the yield.

The hydroxyl group in 4-fluorobenzoylphenol (**118**) was easily deprotonated with base which made the 4-fluorobenzoyl group less electrophilic. Therefore, trimethylsilyl chloride (TMSCl) was used to protect the hydroxyl to afford a protected compound, which it was expected, could then react with dihexylamine. However, TMS was found to be lost easily during the second step. The more stable protecting group agent *tert*-butyldimethylsilyl chloride (TBDMSCl) was treated with 4-fluorobenzoylphenol (**118**) in DCM with imidazole as catalyst to afford 94% product **134**, which showed signals in ¹H NMR at 0.68 ppm for three methyl groups (CCH₃), and 0.58 ppm for two methyl groups on silicon. Peak at 11.69 ppm for OH group was disappeared. Then **134** could react with dihexylamine to form dihexylamine **135**. Then target product **133** can be synthesised by removing the protect group from **135**. (**Scheme 59**)



Scheme 59. Proposed formation route for **133**

Nine different methods were attempted to synthesise **135** as shown in **Table 34**. However none of them afforded target product **135** successfully. Most of reactions did not work, and starting material was recovered. The protecting group TBDMS came off in reactions reported

in entries **2**, **4**, **6** and **8**. Entry **7** and **9** showed loss of the protecting group under basic conditions.

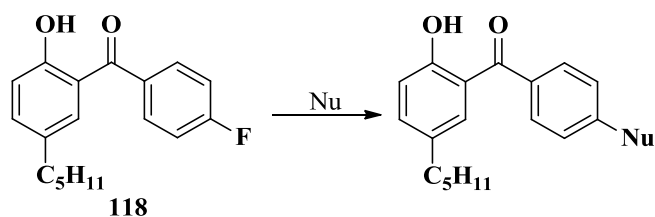
Table 34. Different methods for synthesising **135**

Entry	Reagents	Conditions	Products (ratio W:W)
1	Neat	r.t. 24 h	134
2	Neat	reflux, 24 h	133 and 134 (2:1)
3	None	THF, reflux, 48 h	134
4	NaH	THF, reflux, 48 h	133 and 134 (1:0.1)
5	n-BuLi	THF, 0 °C to r.t., 20 h	complicated results
6	None	DMSO, 90 °C, 24 h	133 and 134 (2:1)
7	K ₂ CO ₃ , TBAB ^[175]	DMSO, 90 °C, 24 h	133
8	None	Dioxane, reflux, 48 h	133 and 134 (1:0.1)
9	NaH	Dioxane, reflux, 48 h	133

The results in **Table 34** showed that use of a silyl protecting group for the hydroxyl group was not an effective strategy to synthesise 4-dihexylaminobenzoylphenol (**133**) and it was not easy to replace fluorine by dihexylamine directly. Therefore, instead of dihexylamine, pyrrolidine, *N*-methyl-1-butylamine, imidazole and 1-hexylamine were used as nucleophiles by reacting with 4-fluorobenzoylphenol (**118**) to afford hydroxybenzophenones using the methods outlined in **Table 35**.

4-Fluorobenzoylphenol **118** afforded pyrrolidine **136** in a 92% yield which occurred via an S_NAr (addition–elimination) mechanism. In most cases of such nucleophilic substitution reactions, sodium or potassium carbonate was utilized as bases, but in this reaction (**Table 35**), 4 equivalents pyrrolidine were used, and the excess pyrrolidine acted as base to neutralize hydrogen fluoride. However, reaction with *N*-methyl-1-butylamine substitution in THF did not provide product. Only starting material and other by products were observed which was same with the reaction by using NaH as base. Using *N*-methyl-1-butylamine neat as both reagent and solvent and heating at its boiling point (90.5-91.5 °C) for 2 d was found to be the best way to afford *N*-methylbutylamine **137** in a good yield (58%) (**Table 35**).

Table 35. Hydroxybenzophenone **118** reacted with different nucleophiles

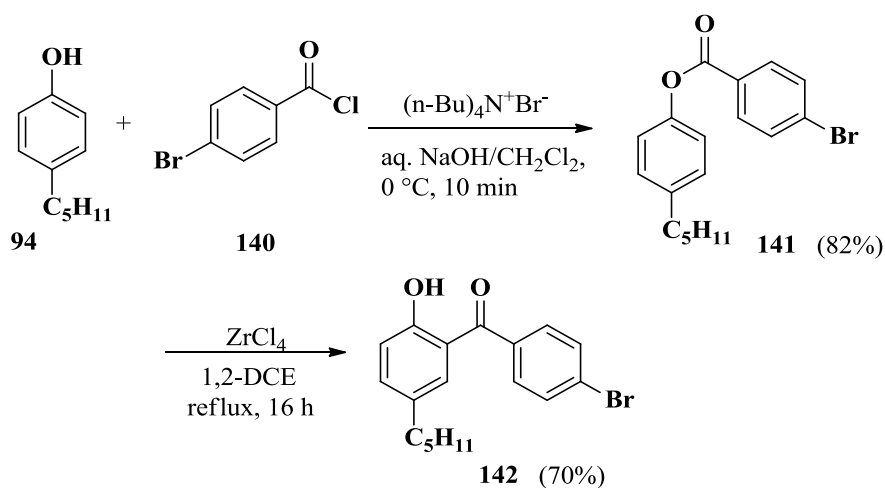


Products	Conditions	Results
<p style="text-align: center;">136</p>	4 eq pyrrolidine, THF, reflux, 24 h	92% product
<p style="text-align: center;">137</p>	THF, reflux, 2 d	118 and by products
	NaH, THF, reflux, 2 d	Starting material 118
	Reflux, 2 d	118 and 58% product
<p style="text-align: center;">138</p>	THF, reflux, 2 d	Starting material 118
	NaH, THF, reflux, 2 d	Starting material 118
	Neat, 150 °C, 2 d	118 and 72% product
<p style="text-align: center;">139</p>	THF, reflux, 2 d	118 and 79% product
	80 °C, 24 h	118 and 89% product

Imidazole (m.p. 89-91 °C) was heated with hydroxybenzophenone at 150 °C for 2 days to afford target product **138** in 72%. 1-Hexylamine attacked the carbonyl group first instead of substituting fluorine with loss of water and formed imine **139** which was similar to the reaction reported earlier with 1-hexylamine substitution which afforded imine **45** in Chapter 3.

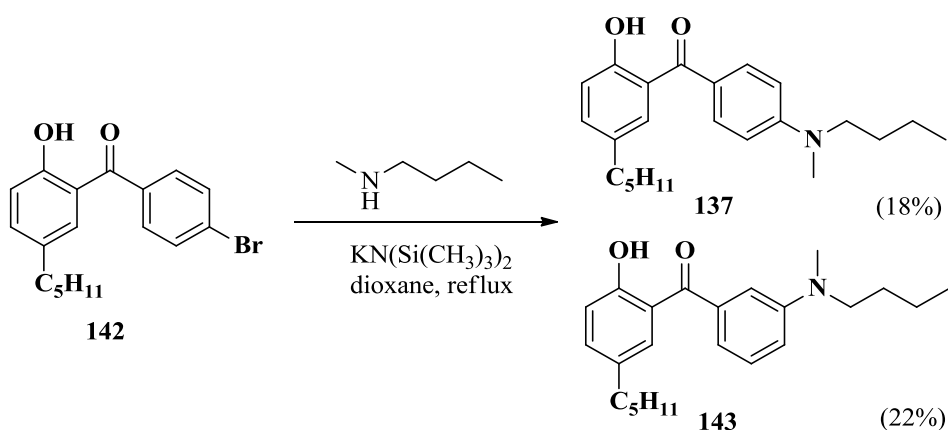
In order to study the UV absorption of amine substituents at different positions of hydroxybenzophenones, 4-bromobenzoylphenol (**142**) was successfully synthesised by the

route in **Scheme 60** by using 4-bromobenzoyl chloride, which can be used to afford hydroxybenzophenones with amine group substituted. Mass spectrum signals m/z at 347.0642 for $C_{18}H_{20}^{79}BrO_2$, and 349.0621 $C_{18}H_{20}^{81}BrO_2$ ($M+H^+$) confirmed the target product.



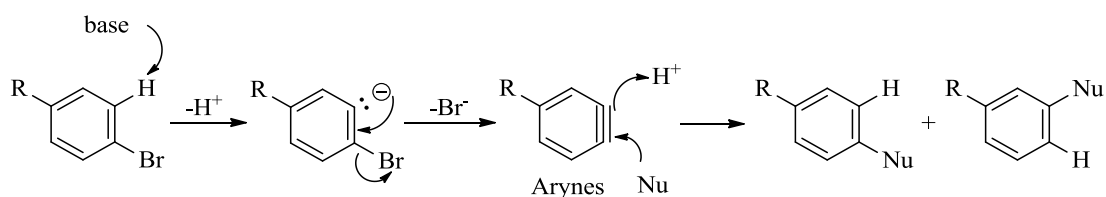
Scheme 60. Synthesis route for **142**

By using 4-bromobenzoylphenol (**142**) to react with *N*-methyl-1-butylamine, the route in **Scheme 61**^[176] used $\text{KN}(\text{Si}(\text{CH}_3)_3)_2$ as a base which provided a mixture of compounds **143** and **137** presumably due to an aryne mechanisms.



Scheme 61. Synthesis route for **137**

The aryne-type mechanism of reaction is a stepwise process which proceeds first by base-catalyzed elimination of hydrogen halide from the aryl halide. The product of the elimination reaction is a highly reactive intermediate called an aryne (or benzyne) which reacts rapidly with any available nucleophile. The mixtures in these reactions result from the attack of the nucleophile at one or the other of the aryne carbons in the intermediate. (Scheme 62)



Scheme 62. Mechanism of nucleophilic addition to an aryne

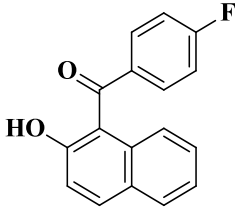
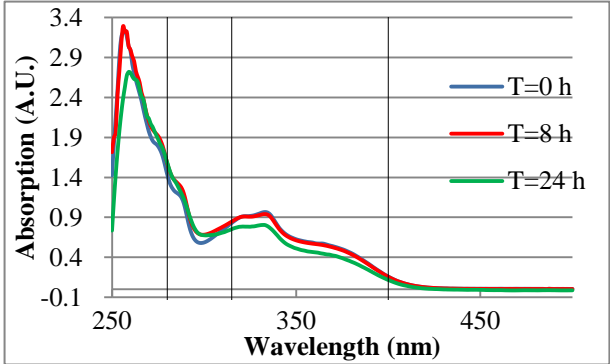
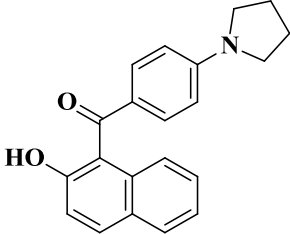
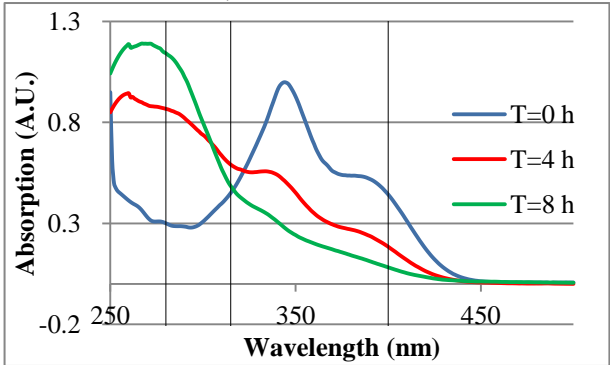
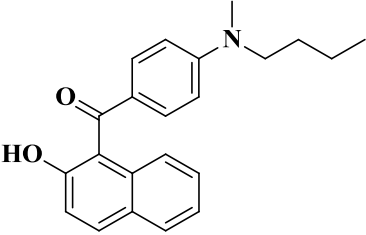
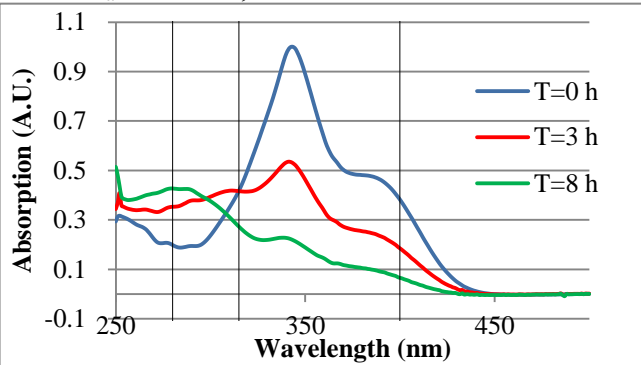
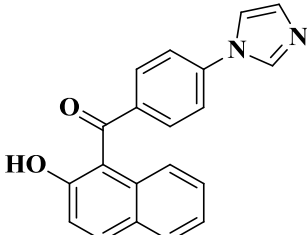
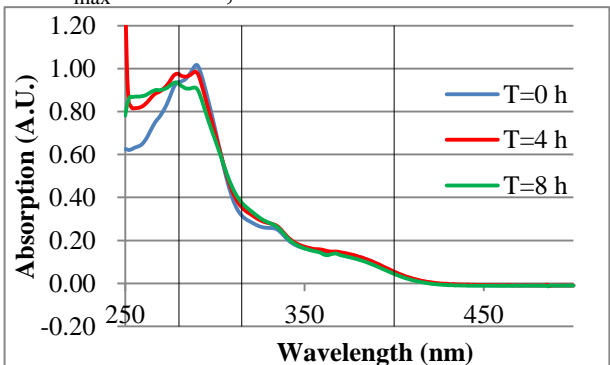
Three main different synthesis routes confirmed that the fluorine-nucleophilic substitution reaction provided good yields and easy substituted with different amine groups.

4.3.2 UV absorption and degradation

In solution

Pure compounds from the synthesis were then measured for their UV absorption spectra and stability towards prolonged irradiation in ethyl acetate. **Table 36** shows UV absorption and degradation spectra for all the naphthalene analogues synthesised.

Table 36. UV absorption and degradation for naphthalene analogues

Compound	λ_{\max} & ϵ Degradation spectra
<div style="text-align: center;">  <p>82</p> </div>	<p style="text-align: center;">$\lambda_{\max}=333 \text{ nm}, \epsilon=0.35 \times 10^4 \text{ L}\cdot\text{mol}^{-1}\text{cm}^{-1}$</p> 
<div style="text-align: center;">  <p>85</p> </div>	<p style="text-align: center;">$\lambda_{\max}=344 \text{ nm}, \epsilon=2.24 \times 10^4 \text{ L}\cdot\text{mol}^{-1}\text{cm}^{-1}$</p> 
<div style="text-align: center;">  <p>86</p> </div>	<p style="text-align: center;">$\lambda_{\max}=343 \text{ nm}, \epsilon=2.21 \times 10^4 \text{ L}\cdot\text{mol}^{-1}\text{cm}^{-1}$</p> 
<div style="text-align: center;">  <p>87</p> </div>	<p style="text-align: center;">$\lambda_{\max}=343 \text{ nm}, \epsilon=2.21 \times 10^4 \text{ L}\cdot\text{mol}^{-1}\text{cm}^{-1}$</p> 

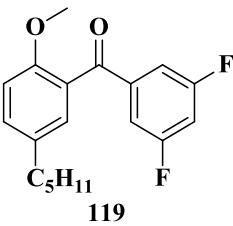
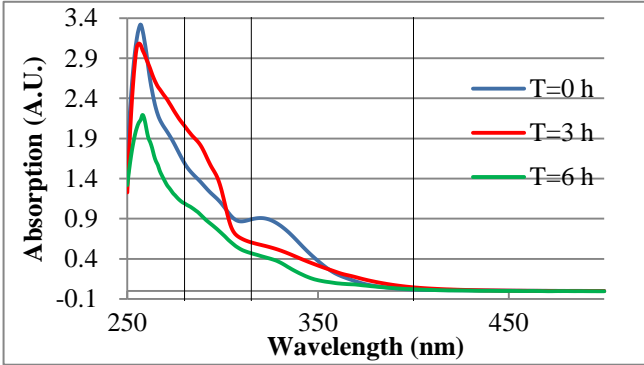
*Compounds were irradiated under the Xenon arc lamp for 8-24 h in ethyl acetate in air. The UV absorption was measured with UV-Vis spectrophotometer.

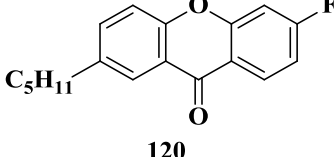
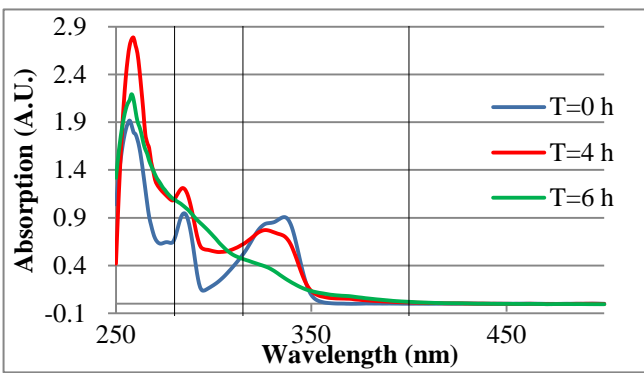
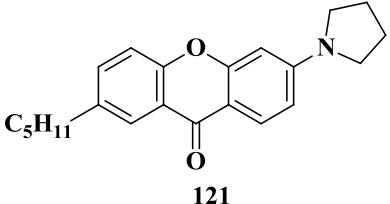
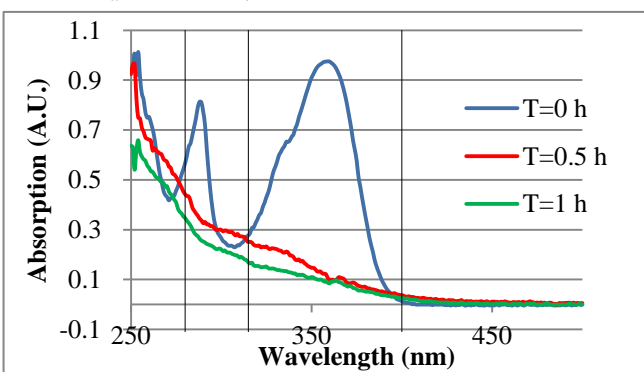
Table 36 shows fluoronaphthol **82** and imidazole naphthol **87** provided maximum UV absorption in the UV-B and UV-C region, and both of them showed a small absorption in the UV-A region, but with a good photostability under Xenon arc lamp irradiation. Aminonaphthol **85** and **86** exhibited a broad UV absorption in the UV-A region with λ_{\max} at 344 nm, but they showed poor photo stability after 8 h irradiation.

There are three compounds without an OH group which were assessed for UV absorption and degradation (**Table 37**). Difluoro ketone **119** with a methoxy group showed strong UV absorption around 260 nm and less stability which confirmed proton transfer from the OH to the excited carbonyl group oxygen forming a six-membered ring system contributed to photo stability as described in the general introduction (section 1.6).

Xanthone derivatives **120** and **121** exhibited UV absorbance around 353 nm and 359 nm, but degraded to other unidentified compounds after a few hours irradiation. Pyrrolidino xanthone **121** was particularly unstable and showed a totally different UV spectrum after 0.5 h.

Table 37. UV absorption and degradation for compounds without OH group

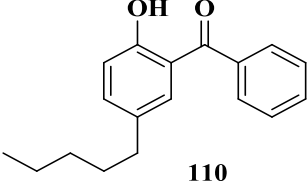
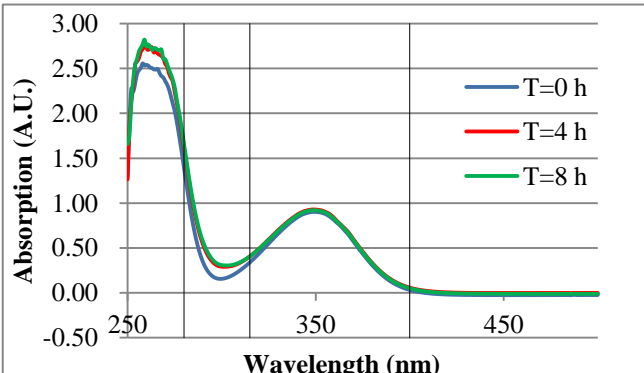
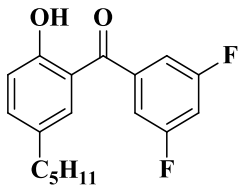
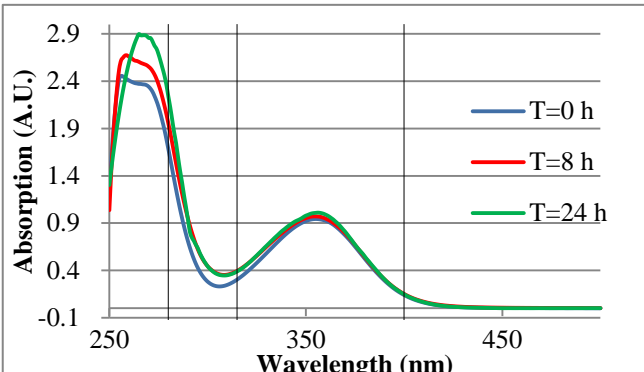
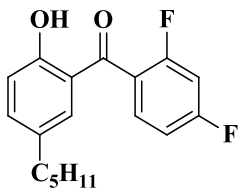
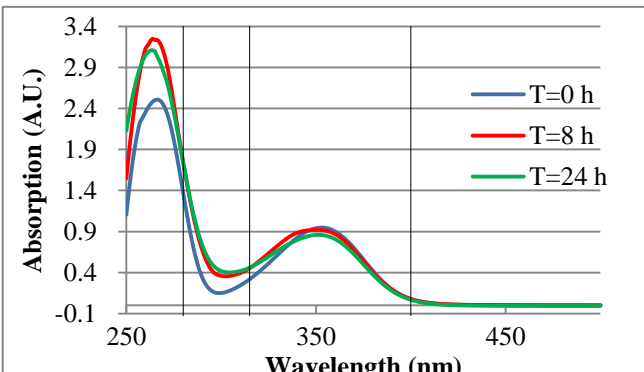
Compound	λ_{\max} & ϵ Degradation spectra
 <p style="text-align: center;">119</p>	<p style="text-align: center;">$\lambda_{\max}=321 \text{ nm}, \epsilon=0.17 \times 10^4 \text{ L}\cdot\text{mol}^{-1}\text{cm}^{-1}$</p> 

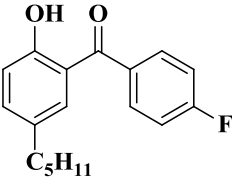
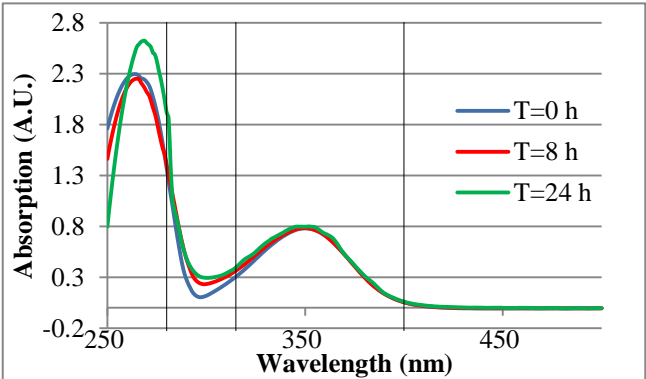
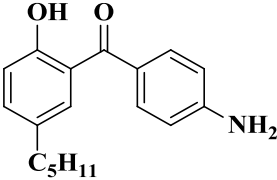
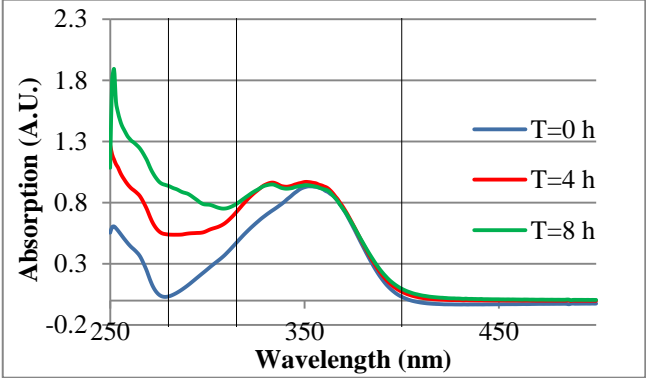
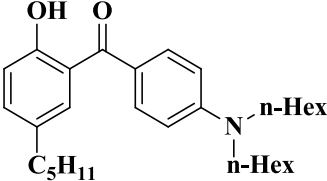
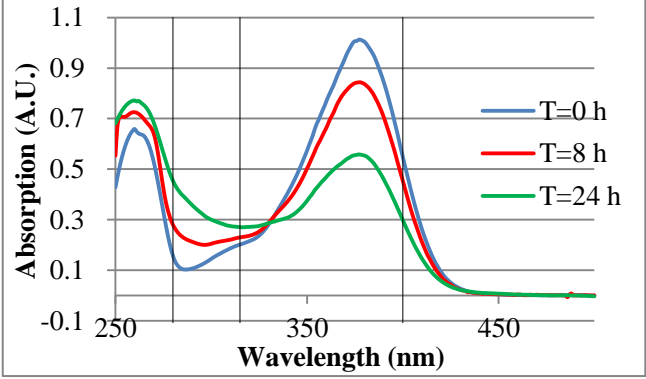
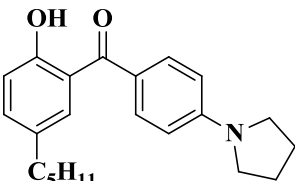
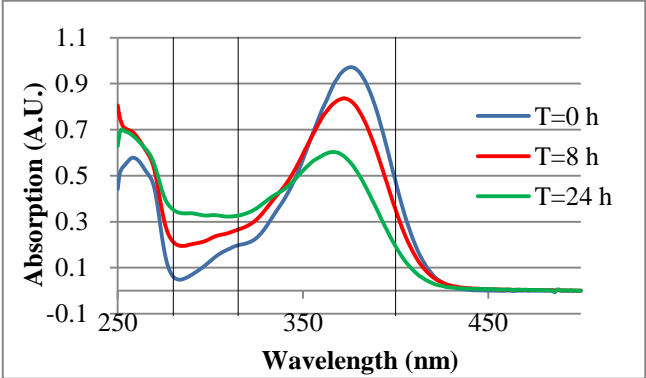
Compound	λ_{\max} & ϵ Degradation spectra
<div style="text-align: center;">  <p>120</p> </div>	<p style="text-align: center;">$\lambda_{\max}=353 \text{ nm}, \epsilon=0.78 \times 10^4 \text{ L}\cdot\text{mol}^{-1}\text{cm}^{-1}$</p> 
<div style="text-align: center;">  <p>121</p> </div>	<p style="text-align: center;">$\lambda_{\max}=359 \text{ nm}, \epsilon=0.17 \times 10^4 \text{ L}\cdot\text{mol}^{-1}\text{cm}^{-1}$</p> 

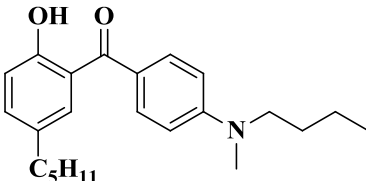
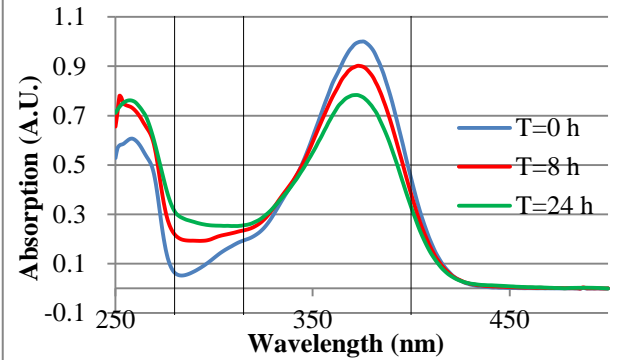
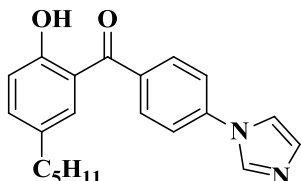
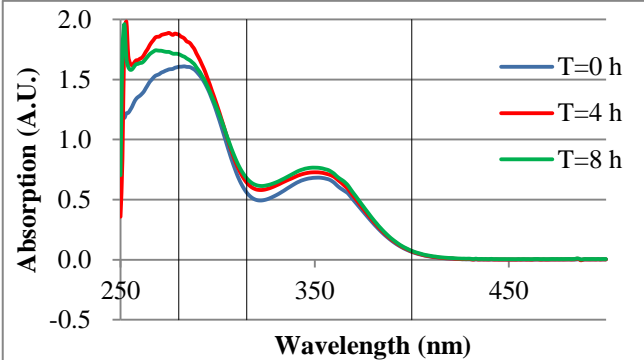
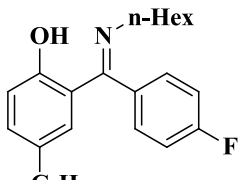
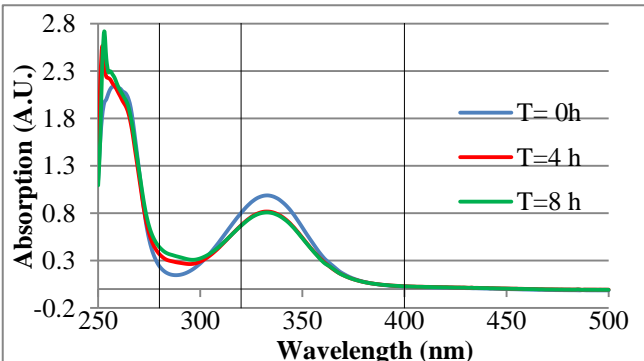
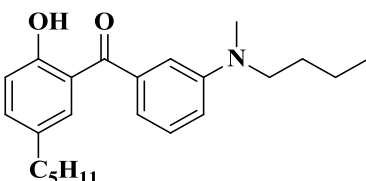
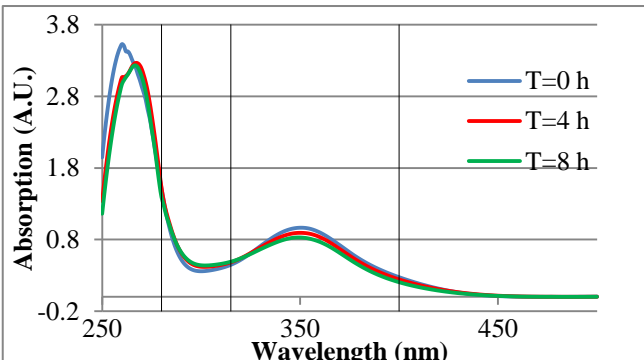
*Compounds were irradiated under the Xenon arc lamp for 1-6 h in ethyl acetate in air. The UV absorption was measured with UV-Vis spectrophotometer.

The UV absorption and degradation results of other hydroxybenzophenones synthesised are listed in **Table 38**.

Table 38. UV absorption and degradation for hydroxybenzophenones

Compound	λ_{\max} & ϵ Degradation spectra
<div style="text-align: center;">  <p>110</p> </div>	<p style="text-align: center;">$\lambda_{\max}=349 \text{ nm}$, $\epsilon=0.44 \times 10^4 \text{ L}\cdot\text{mol}^{-1}\text{cm}^{-1}$</p> 
<div style="text-align: center;">  <p>114</p> </div>	<p style="text-align: center;">$\lambda_{\max}=355 \text{ nm}$, $\epsilon=0.41 \times 10^4 \text{ L}\cdot\text{mol}^{-1}\text{cm}^{-1}$</p> 
<div style="text-align: center;">  <p>116</p> </div>	<p style="text-align: center;">$\lambda_{\max}=353 \text{ nm}$, $\epsilon=0.42 \times 10^4 \text{ L}\cdot\text{mol}^{-1}\text{cm}^{-1}$</p> 

Compound	λ_{\max} & ϵ Degradation spectra
<div style="text-align: center;">  <p>118</p> </div>	<p style="text-align: center;">$\lambda_{\max}=352 \text{ nm}, \epsilon=0.41 \times 10^4 \text{ L}\cdot\text{mol}^{-1}\text{cm}^{-1}$</p> 
<div style="text-align: center;">  <p>125</p> </div>	<p style="text-align: center;">$\lambda_{\max}=351 \text{ nm}, \epsilon=0.42 \times 10^4 \text{ L}\cdot\text{mol}^{-1}\text{cm}^{-1}$</p> 
<div style="text-align: center;">  <p>133</p> </div>	<p style="text-align: center;">$\lambda_{\max}=378 \text{ nm}, \epsilon=2.69 \times 10^4 \text{ L}\cdot\text{mol}^{-1}\text{cm}^{-1}$</p> 
<div style="text-align: center;">  <p>136</p> </div>	<p style="text-align: center;">$\lambda_{\max}=376 \text{ nm}, \epsilon=2.66 \times 10^4 \text{ L}\cdot\text{mol}^{-1}\text{cm}^{-1}$</p> 

Compound	λ_{\max} & ϵ Degradation spectra
<div style="text-align: center;">  <p>137</p> </div>	<p style="text-align: center;">$\lambda_{\max}=374 \text{ nm}, \epsilon=1.89 \times 10^4 \text{ L}\cdot\text{mol}^{-1}\text{cm}^{-1}$</p> 
<div style="text-align: center;">  <p>138</p> </div>	<p style="text-align: center;">$\lambda_{\max}=352 \text{ nm}, \epsilon=0.57 \times 10^4 \text{ L}\cdot\text{mol}^{-1}\text{cm}^{-1}$</p> 
<div style="text-align: center;">  <p>139</p> </div>	<p style="text-align: center;">$\lambda_{\max}=333 \text{ nm}, \epsilon=0.46 \times 10^4 \text{ L}\cdot\text{mol}^{-1}\text{cm}^{-1}$</p> 
<div style="text-align: center;">  <p>143</p> </div>	<p style="text-align: center;">$\lambda_{\max}=350 \text{ nm}, \epsilon=0.47 \times 10^4 \text{ L}\cdot\text{mol}^{-1}\text{cm}^{-1}$</p> 

*Compounds were irradiated under the Xenon arc lamp for 8-24 h in ethyl acetate in air. The UV absorption was measured with UV-Vis spectrophotometer.

As shown in **Table 38**, fluorine and imidazole substituted hydroxybenzophenones (**110**, **114**, **116**, **118** and **138**) showed strong absorption in the UV-C and UV-B regions, and good photostability after 8 h or 24 h degradation under the Xenon arc lamp. The absorption in the UV-A region did not decrease significantly during irradiation. Amine **125** provided a maximum absorption at 351 nm, but with a low molar absorptivity. Imine **139** containing a carbon nitrogen double bond instead of carbonyl group showed maximum UV absorption at 333 nm wavelength with molar absorptivity $0.46 \times 10^4 \text{ L}\cdot\text{mol}^{-1}\text{cm}^{-1}$ which is similar to imine **45** as described in Chapter 3. Hydroxybenzophenone **130** showed maximum UV absorption in the UV-B region around 306 nm. The diethyl phosphoryl group in **130** on the amino substituent prevents electron donation into the benzophenone chromophore giving a smaller λ_{max} value. This confirmed that extension of the chromophore from the electron donating group to the benzene ring could result in a pronounced red shift, as mentioned in section 3.3.2.

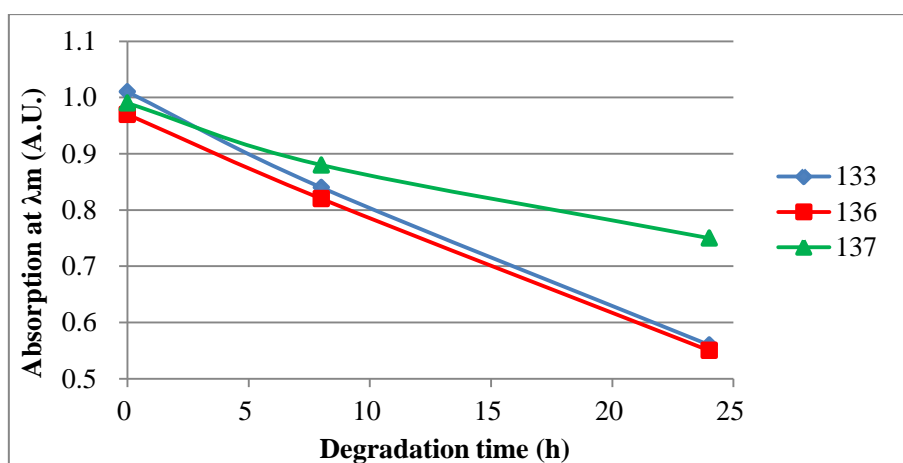


Figure 36. Absorption at λ_{max} against degradation time

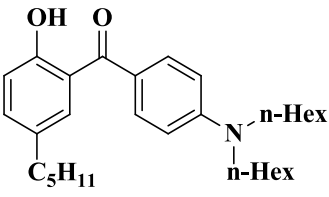
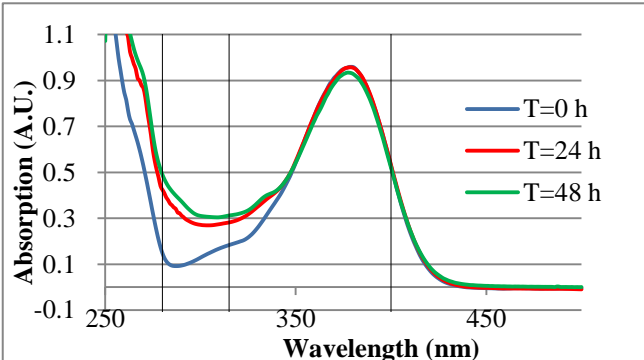
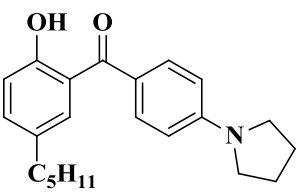
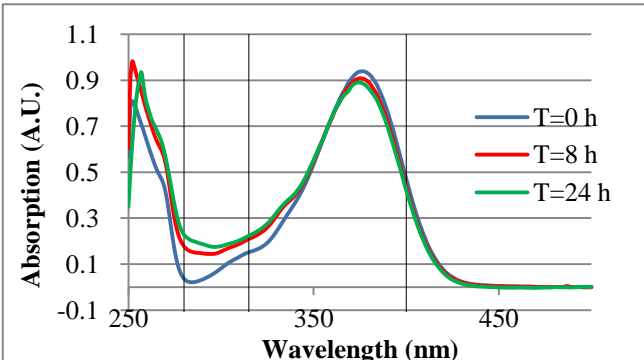
Dihexylamine **133**, pyrrolidine **136** and *N*-methylbutylamine **137** were shown to be the best three UV absorbers in **Table 38** with a good and strong absorption around 375 nm. **Figure 36** shows the change of absorbance at λ_{max} during irradiation. Dihexylamine **133** and pyrrolidine **136** provided similar photostability after 24 h, but were less stable than *N*-methylbutylamine **137**, which degraded 24% after 24 h. The maximum absorption of pyrrolidine **136** moved to shorter wavelength, changing to 366 nm.

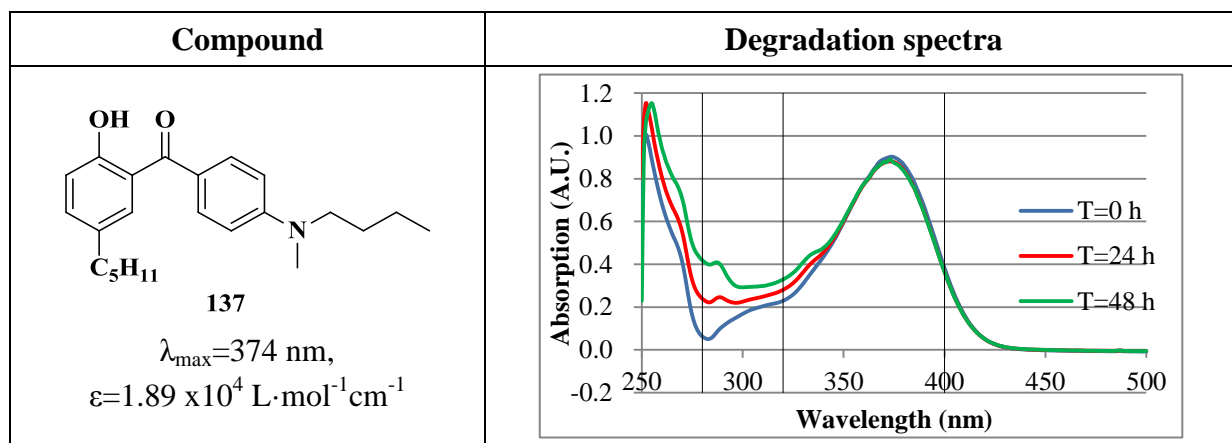
Hydroxybenzophenone **143** with *N*-methyl-1-butylamine substituted at the *meta*-position to the carbonyl group showed maximum absorption in the UV-C region and a small absorbance at 350 nm. Compared with **137**, it suggested the UV absorption wavelength is better improved by introducing a substituent into the *para*-position rather than *meta*- to the carbonyl group.

Combined with Chimassorb 944 in solution

In order to enhance photostability and find how Chimassorb 944 (C944) affects the stability of each compound, C944 was combined with different hydroxybenzophenones which showed good absorption in UV-A region in a 1:4 ratio by weight for irradiation.

Table 39. Degradation for compounds combined with C944

Compound	Degradation spectra
 <p style="text-align: center;">133</p> <p style="text-align: center;">$\lambda_{\max}=378 \text{ nm,}$ $\epsilon=2.69 \times 10^4 \text{ L}\cdot\text{mol}^{-1}\text{cm}^{-1}$</p>	
 <p style="text-align: center;">136</p> <p style="text-align: center;">$\lambda_{\max}=376 \text{ nm,}$ $\epsilon=2.66 \times 10^4 \text{ L}\cdot\text{mol}^{-1}\text{cm}^{-1}$</p>	



*Compounds combined with C944 were irradiated under the Xenon arc lamp for 24-48 h in ethyl acetate in air. The UV absorption was measured with UV-Vis spectrophotometer.

Table 39 shows C944 enhanced the stability of these three compounds significantly after 24 or 48 h in the UV-A region compared with the results in **Table 38**, and improved the stability in the UV-B region which is shown clearly in **Figure 37**.

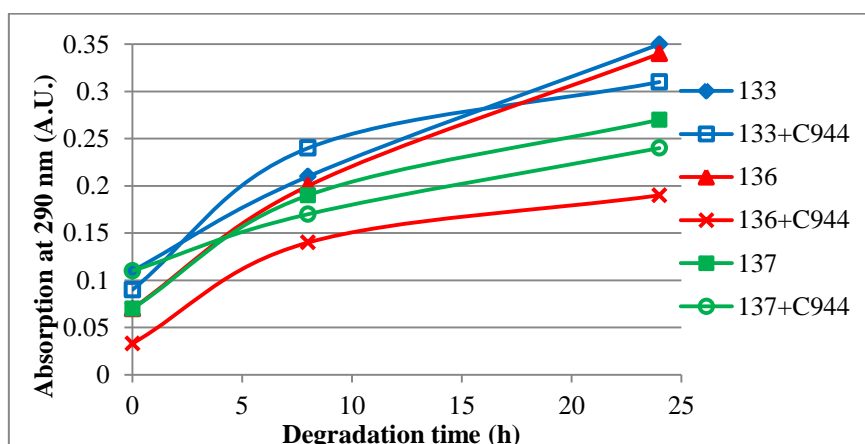


Figure 37. Degradation of compounds with C944 in the UV-B region

The absorbance of dihexylamine **133** with C944 at 290 nm wavelength increased rapidly in the first 8 h, and then the increase was slower than observed for irradiation without C944. During the irradiation under the Xenon arc lamp, the degraded product exhibited UV absorption in the UV-B region. C944 enhanced the stability of starting material, and slow down the formation of degraded products, which resulted in a slower increasing absorption in the UV-B region.

Reductive and oxidative processes

Reductive and oxidative processes were observed for pyrrolidine **136** and *N*-methylbutylamine **137** by observing degradation rates in deoxygenated or oxygen saturated solutions. (Figures 38 and 39)

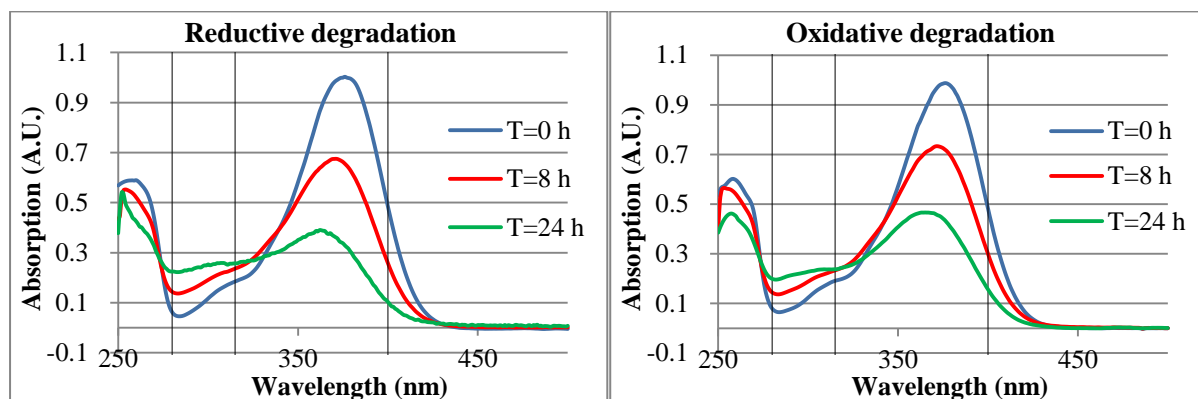


Figure 38. Reductive and oxidative degradation of **136**

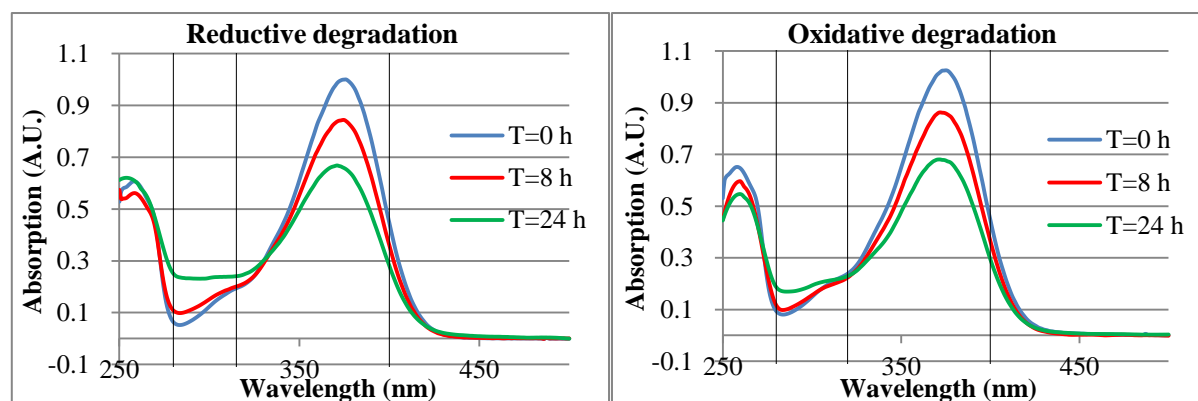


Figure 39. Reductive and oxidative degradation of **137**

136 and **137** degraded faster under nitrogen or oxygen than under air as shown by change in the UV-A region. Figure 40 shows the degradation time against absorption at λ_{\max} for these two compounds under air, nitrogen or oxygen. It indicates both compounds degraded faster under nitrogen or oxygen than air. **136** degraded 67% under nitrogen and 56% under oxygen after 24 h. More than half of starting materials were degraded, which might suggest irradiation could occur on degraded product as well. However, nitrogen and oxygen

environments improved the stability in the UV-B region especially in the first 8 h, as is shown in **Figure 41**. These results could suggest different degraded products formed under air, nitrogen and oxygen.

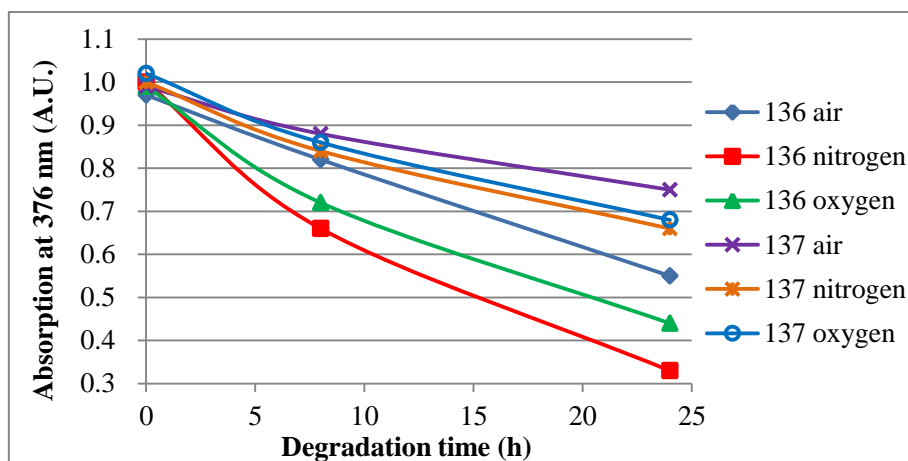


Figure 40. Degradation of **136** and **137** at λ_{\max} under air, nitrogen or oxygen

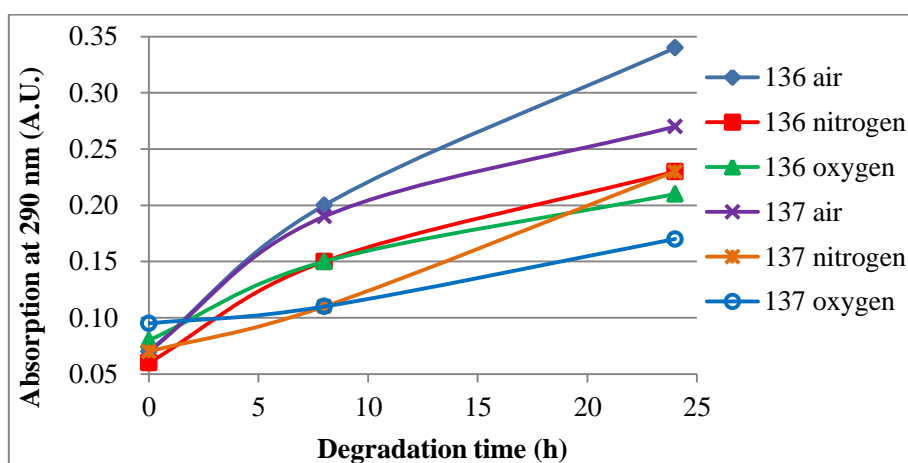


Figure 41. Degradation of **136** and **137** at 290 nm under air, nitrogen or oxygen

High nitrogen or oxygen content resulted in a fast degradation in the UV-A region, but not in the UV-B region, which is different to the observation reported in Chapter 3 where the photostability of fluoro hydroxybenzophenone **48** with *N*-methyl-1-butylamino group substituted on the phenol ring, was enhanced in both UV-A and UV-B region. This could confirm amino groups substituted on a different ring would have an effect on the photostability of the compounds.

Absorption studies in films

Hydroxybenzophenones **136** and **137** each with 4 times their weight of Chimassorb 944 were added to polyethylene film by the collaborating company to allow study of the UV properties. The films contained 89% EVA COPO 1003, 10% LD PWD, 0.8% C944 and 0.2% UV absorbers. **Figure 42** shows the degradation of **136** film under air for 96 h which degraded faster than in solution, but still showed good stability. The absorption at 376 nm decreased from 2.70 to 0.52 after 96 h, and the transmission of UV-A radiation increased to 0.3. The spectrum shows the maximum absorption move to 360 nm, which is similar to the results from solution phase degradation.

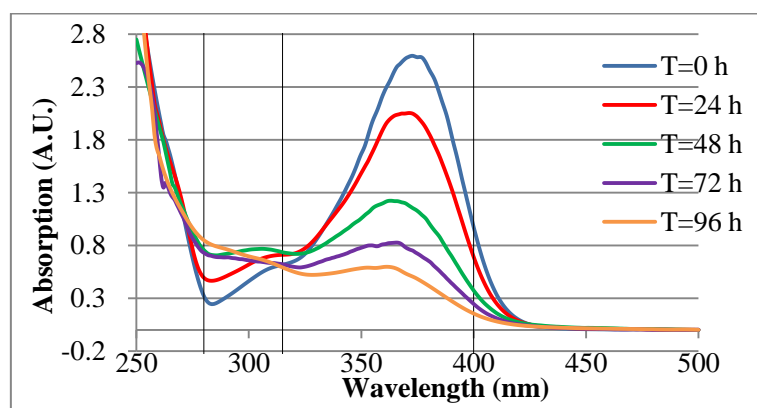


Figure 42. 136 film degradation in air

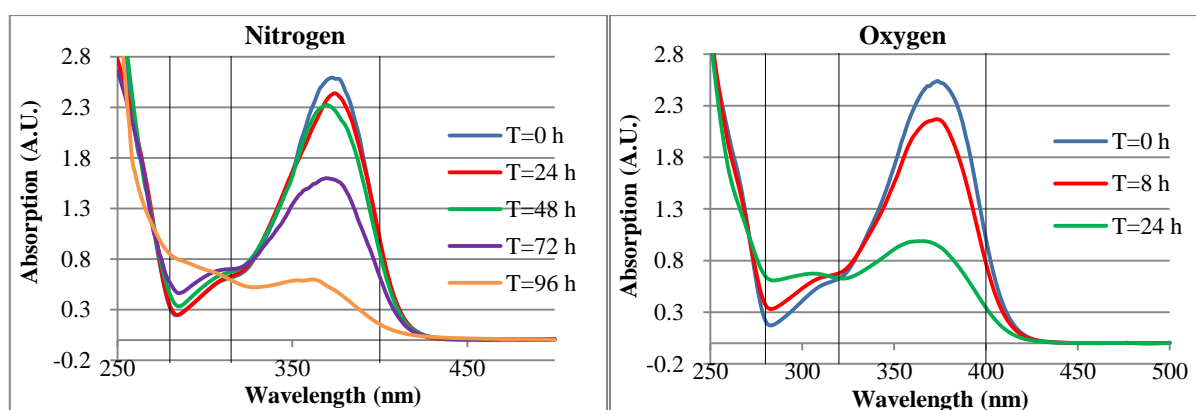


Figure 43. 136 film degradation under nitrogen and oxygen

The **136** film was then irradiated under nitrogen environment for 96 h (**Figure 43**), and showed a similar degradation rate with the film under air. An oxygen environment however resulted in a much faster degradation. Films degraded 63% after only 24 h, and the maximum absorbance moved from 376 nm to 360 nm wavelength.

Figure 44 shows the film absorption at 290 and 376 nm wavelength against degradation time under air, nitrogen or oxygen. A nitrogen environment enhanced the stability at 376 nm and 290 nm wavelength in first 48 h. Then film degraded 80% after 96 h irradiation, providing similar results with the film under air (81%).

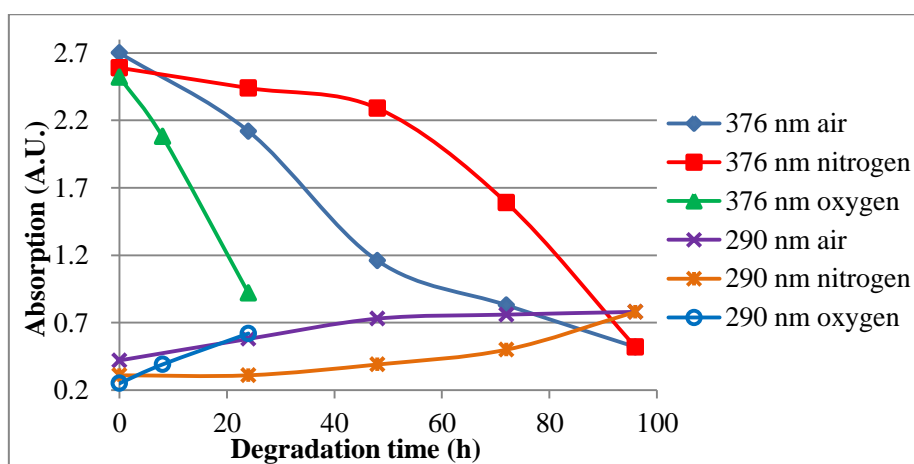


Figure 44. 136 film degradation at 290 and 376 nm under air, nitrogen or oxygen

Figure 45 represents the degradation of *N*-methylbutylamine **137** film under the arc lamp in the air, which demonstrated a good photostability after 96 h degradation. Although it degraded 54%, the transmission of UV A was below 0.08. The absorbance in the UV-B region did not increase as high as in solution during the irradiation.

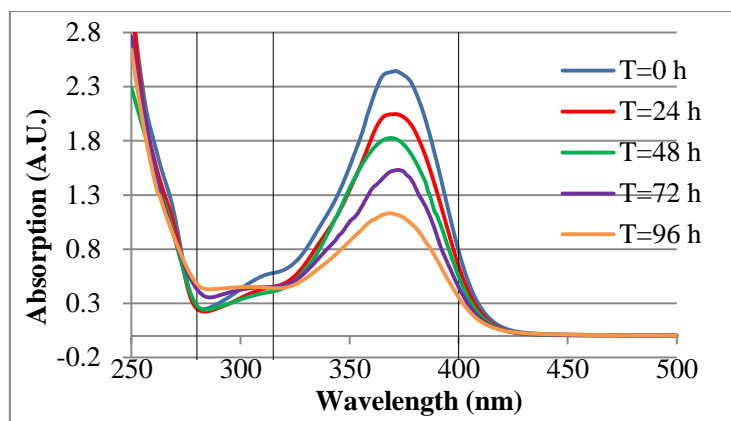


Figure 45. 137 film degradation in air

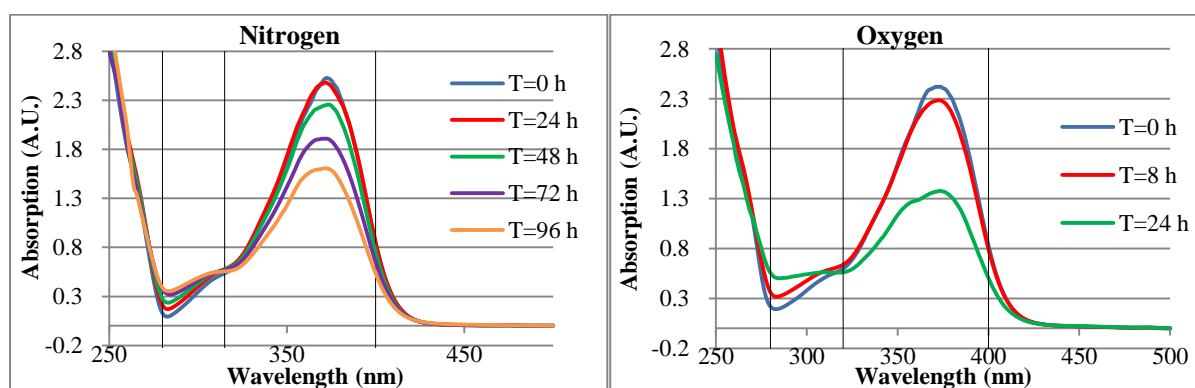


Figure 46. 137 film degradation under nitrogen

Figure 46 shows spectra of *N*-methylbutylamine **137** films when irradiated under nitrogen or oxygen. Same with pyrrolidine **136**, films degraded faster under oxygen. However, a nitrogen environment enhanced the photostability of **137** films (Figure 47), which degraded 36.4% after 96 h irradiation.

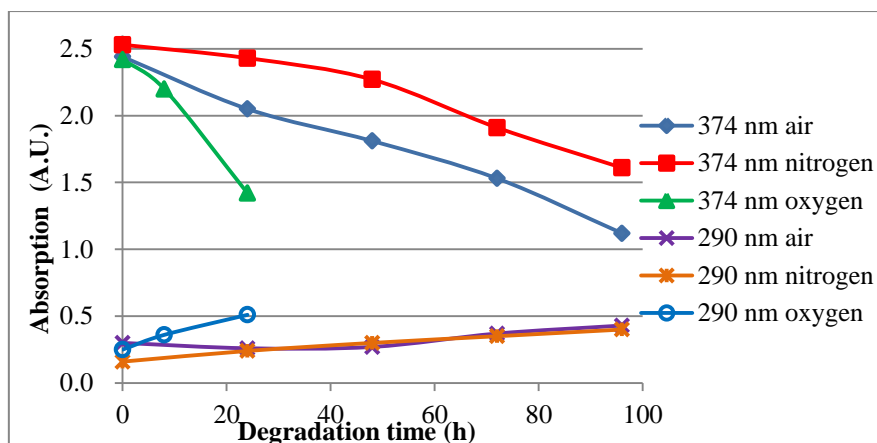


Figure 47. 137 film degradation at 290 and 376 nm in air, nitrogen or oxygen

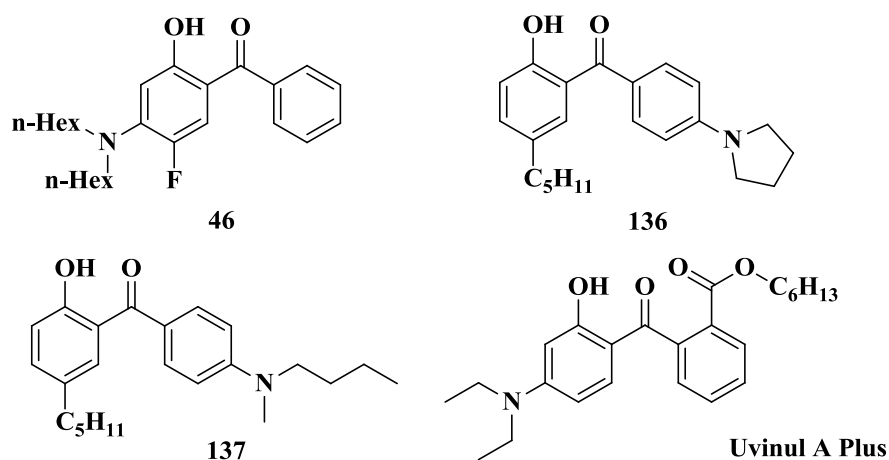
Both films showed good photostability under the arc lamp under air after 96 h. The difference of absorption in the UV-B region between solution and films suggested that different degraded products formed. Degraded products in films demonstrated a small absorption in the UV-B region, and similar absorption with starting material in the UV-A region. A nitrogen environment enhanced the stability, but the presence of oxygen resulted in a faster degradation which might suggest oxidation has a greater effect on the compound in films than solution.

4.3.3 Comparison between new hydroxybenzophenones and Uvinul A Plus

Pyrrolidine **136** and *N*-methylbutylamine **137** were compared with 5-fluoro-dihexylamine **46** and Uvinul A Plus as described in Chapter 3 in both solution and film. **Figure 48** shows that **136** and **137** degraded faster than **46** and Uvinul A Plus in solution after 24 h irradiation, but **136** and **137** exhibited higher UV absorption wavelength than **46**, which shows conformance to the target.

Pyrrolidine **136** film degraded 57% after 48 h irradiation, more than the Uvinul A film which degraded 53%. However, the **137** film degraded 25%, which showed better photostability and UV absorption wavelength compared with Uvinul A. 5-Fluoro-dihexylamine **46**, degraded

10%, is the most stable compound among the three new amino hydroxybenzophenones. Compounds **46** and **137** both exhibited better photostability than Uvinul A Plus.



Scheme 63. Structures for new hydroxybenzophenones and Uvinul A

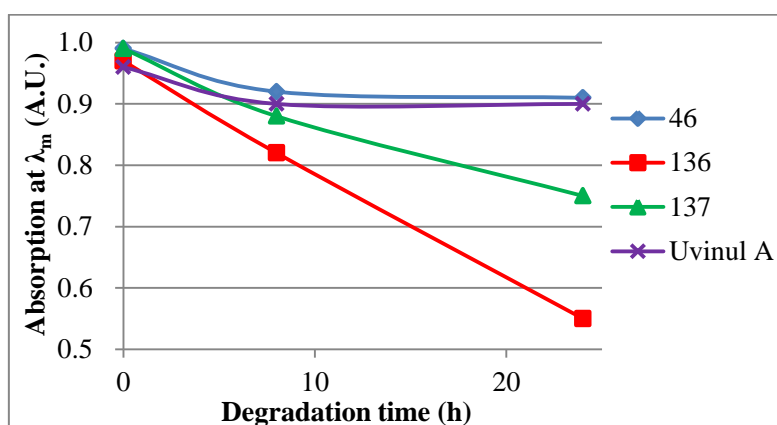


Figure 48. Comparison between new UV absorbers and Uvinul A in solution

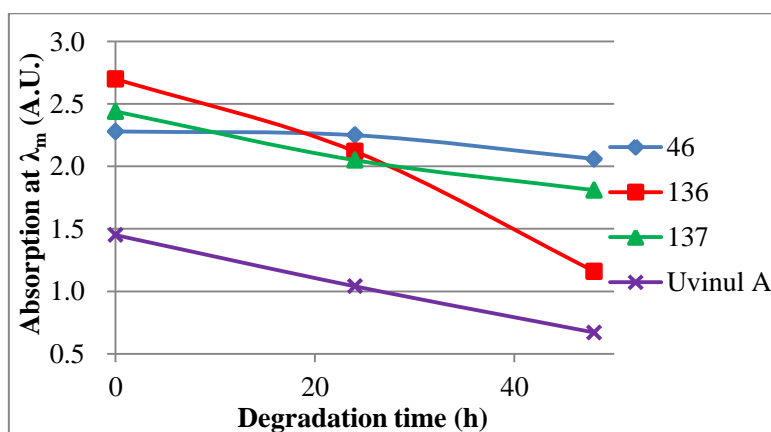


Figure 49. Comparison between new UV absorbers and Uvinul A in film

4.4 Conclusions

Phase transfer catalyst conditions followed by Fries rearrangement with 2 eq. $ZrCl_4$ in 1,2-DCE was confirmed to be a good method for synthesis of hydroxybenzophenones. Aromatic nucleophilic substitution of fluorine was still the easiest and best way to prepare amine substituted hydroxybenzophenones, and naphthalene based hydroxyketones.

Comparison of 3,5-difluorohydroxyketone **114** and its methoxy analogue **119**, and 2,4-difluorohydroxybenzophenone **116** with its cyclic analogue, xanthone **120**, showed the hydroxy substituted compounds have good photostability after irradiation for 8 hours. The methylated compound and the xanthone both showed significant degradation under UV radiation. The naphthalene derivatives (**82** and **85**) exhibited absorption around 333 nm, and phenol ring with a long alkyl chain groups showed higher stability than naphthalene derivatives. Fluorine and imidazole substituted hydroxybenzophenones provided strong absorption in the UV-C and UV-B region with good photostability.

Chimassorb 944 enhanced the stability for new hydroxybenzophenones in both the UV-A and UV-B region. Oxidative and reductive processes increased the degradation rate in the UV-A region, but reduced the increase in absorption occurring in the UV-B region in solution. An oxygen environment resulted in fast degradation of films in both the UV-A and UV-B region, but a nitrogen environment improved the stability of films, which confirms oxygen diffusion has a significant influence on film degradation.

Amine substituted **136** and **137** could be synthesised in three steps with high yield. They both afforded ideal absorption around 376 nm with good photostability under the Xenon arc lamp. Especially, the **137** films showed better UV absorption and photostability than Uvinul A films after 48 h irradiation. In this project, *N*-methylbutylamino hydroxybenzophenone **137** exhibited better UV absorption and photostability than the current UV absorber, Uvinul A Plus, and the UV absorption in the UV-A region of pyrrolidino hydroxybenzophenone **136** most closely matches the target.

Chapter 5. Overall conclusions

This thesis has demonstrated amino substituted hydroxybenzophenones exhibited excellent UV absorption and photostability properties for the desired application to selectively filter certain UV wavelengths. The compounds could be simply synthesised through three steps: ester formation (under phase transfer conditions), Fries rearrangement and aromatic nucleophilic substitution of fluorine. Reaction conditions with 2 eq. ZrCl₄ in 1,2-DCE was the best for the Fries rearrangement in this project. The numbers of fluorine and other substituents on the ring had a significant influence on rearrangement results. The fluorine at the *para*-position to carbonyl group was more conveniently replaced with amines, and the favoured substitution order of amines was pyrrolidine, *N*-methyl-1-butylamine and dihexylamine.

Fluorine substituted hydroxybenzophenones present maximum UV absorption in the UV-C region, but with a greatly improved light fastness, compared with amine substituted compounds which showed an ideal UV absorbance in the UV-A and UV-B regions. Hydroxybenzophenones substituted with two amino groups on different rings such as **68** and **70** showed a broad UV absorption in the range of 280-430 nm with the maximum UV absorbance around 385 nm. Two fluorine substituted amino-hydroxybenzophenones showed good photostability in ethyl acetate. Especially, compounds containing one fluorine on each ring such as **66**, **67** and **69** provided better stability than compounds **58**, **59** and **60** with two fluorines on the same ring.

The synthetic methods for Uvinul A Plus modification by starting with phthalic anhydride to react with 3,4-difluorophenol were not effective to provide the target product. Fries rearrangement was not successful with an ester group on the benzene ring (ring B, **Scheme 19**).

The methylated and xanthone compounds **119** and **120** confirmed the hydroxyl substituted compounds provided good photostability under Xenon arc lamp. The UV measurement on

the naphthalene derivatives (**82** and **85**) showed less stability compared with the phenol ring with a long alkyl chain group. Imidazole substituted hydroxybenzophenones demonstrated excellent photostability but with a maximum UV absorption in the UV-B region.

Hindered amine light stabiliser Chimassorb 944 (4 equivalent) enhanced stability in the UV-A region for all hydroxybenzophenones, and improved the stability in the UV-B region for some compounds. However, C944 could react with Uvitex OB in ethyl acetate under oxygen, which failed to enhance the photostability. But the films containing 0.2% Uvitex OB with 0.8% C944 degraded slower in first 100 h in QUV, which suggested C944 could help to stabilise in the films.

Uvitex OB degraded fast in oxygen presumably because of oxidation, and a nitrogen environment resulted in a slower degradation than air and oxygen, which is similar with hydroxybenzophenones. Pure nitrogen or oxygen environment significantly enhanced the photostability in ethyl acetate solution in both the UV-A and UV-B region, because an oxygen environment reduced reductive reaction, and a nitrogen saturated solution removed oxygen diffusion, which resulted in slower degradation than under air.

However, when UV absorbers (**46**, **136** and **137**) with 4 eq. Chimassorb 944 were added in films, an oxygen environment resulted in faster degradation than under air and nitrogen, which confirms oxygen diffusion has a significant influence on film degradation. After the measurement for UV absorption and testing for photostability under the Xenon arc lamp, these three lead UV absorbers produced better absorption and photostability than Uvitex OB and Uvinul A Plus in both solution and films.

Chapter 6. Future work

Due to the fast degradation of Uvitex OB in oxygen environment, future work will be aimed towards incorporating Uvitex OB into an oxygen impermeable material such as ethylene-vinyl alcohol copolymer (EVOH) to slow down oxidation. It has been shown that a high oxygen barrier can preserve and improve the quality of forage.^[177]

A different method for modification Uvinul A plus will be developed in order to add an ester group on the benzene ring to test the effects of the ester group on UV absorption and photostability. Diverse amines will be used to substitute fluorine on hydroxybenzophenone for UV absorbers formation to provide UV absorption below 400 nm wavelength with a maximum UV absorbance around 375 nm, and good photostability. The UV absorbers synthesised in this thesis were a light yellow colour, which led to a slightly yellow colouration of the films. Controlling the UV absorption of compounds in UV region, and not encroaching on the visible region will afford a clear colourless film.

Two or more different UV absorbers will be combined together for degradation in solution and films. For example, fluorine substituted hydroxybenzophenone could be combined with amino-hydroxybenzophenone which would provide a different UV absorption range. Fluorine substituted compounds with excellent light fastness are expected to stabilise other amino UV absorbers, which will extend the use of time of polytunnel films.

The three lead UV absorbers will be scaled up to kilogram quantities for field trials. Therefore, it is valuable to find a cheaper catalyst instead of zirconium(IV) chloride and a different solvent such as dichlorobenzene instead of 1,2-dichloroethane for Fries rearrangement. 4-Pentylphenol and dihexylamine are two expensive starting materials, thus phenol with a different long alkyl chains could be further investigated. Column chromatography was used for purification intermediates and final products in this project. It is worth to test how it affects the yield of target products without purifying intermediates. UV

absorption and photostability of crude UV absorbers should be measured to figure out whether impurities could improve or decrease UV absorption wavelength and stability.

The field trials experimental results will show how these three novel UV absorbers represent under the real environment in polytunnel film. With the results, further work will be focussed on modification of these three UV absorbers in order to provide good performance with regard to insect ingress and to improve the quality and quantity of crop and plants.

Chapter 7. Experimental

Chapter 2. Uvitex OB degradation and stabilisation

Materials

Uvitex OB, Chimassorb 944, Irganox 1010, Irgafos 168 and all the films were supplied by BPI. Tinogard Q was obtained from BASF. EVA COPO1003 contains 13.5% by weight vinyl acetate. Exxon FL00218 contains 18.0% by weight vinyl acetate.

UV absorption

The instrument used for UV absorption measurement was a Hewlett-Packard model 8453 diode-array UV/Vis spectrophotometer. The length of sample cell used was 1 cm. All the compounds were dissolved in ethyl acetate. A range of concentrations were measured with the absorptions between 0 and 1.

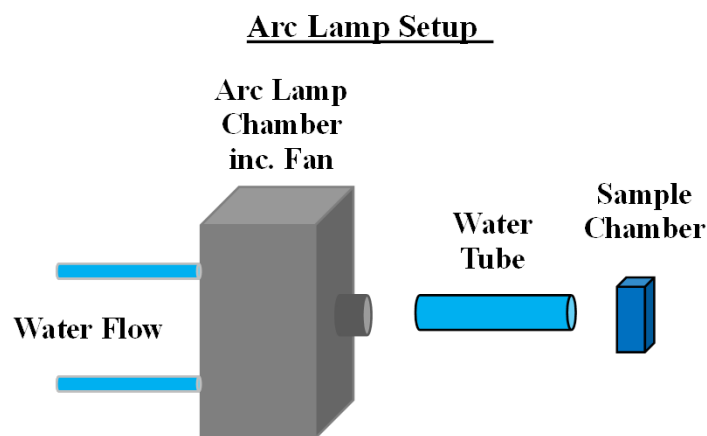
Degradation

The solutions of compounds were irradiated with a 300W Xenon arc lamp (Spectral distribution: 185 nm to 2000 nm). (Picture 5)



Picture 5. 300W Xenon arc lamp

A fan was set up in the arc lamp chamber and water was flowed through the chamber to protect against overheating. The Xenon arc lamp output was passed through 5 cm of water to reduce the infrared components and any consequent sample heating. (**Picture 6**)



Picture 6. Arc lamp set up

All the compounds were dissolved in ethyl acetate, and the concentration of the solution was selected by the solution can provide the absorption around 1 at the maximum absorption peak. Then solution was irradiated under arc lamp for the required number of hours and the absorption spectrum was measured every 1 or 2 h.

Oxidative and reductive reaction

Solution

Compounds were dissolved in ethyl acetate and placed in a sample cell. Then the sample cell was sealed by a septum stopper on the top. Nitrogen or oxygen was passed through the solution with a long needle. After 10 min, a nitrogen or oxygen balloon was set up on the top to provide a constant supply of nitrogen / oxygen during irradiation.

Film

The film was set in a sealed sample cuvette which was purged with nitrogen or oxygen for 10 mins. A nitrogen/oxygen balloon was set up on the top to provide a constant supply of nitrogen/oxygen. Then the film was kept in nitrogen/oxygen to allow exchange of any air in the film. After 2 days, the cuvette was flushed with fresh nitrogen/oxygen for 10 min to

remove the displaced air. A nitrogen/oxygen balloon was set up on the top and film was degraded under the arc lamp.

HPLC analysis

The instrument used for HPLC analysis was a GILSON system with autoinjector 234, 306 pump, 811C dynamic mixer and spectra SERIES UV 100. All the solvents used for HPLC were HPLC grade.

Method:

Column: silica, dynamax

Mobile phase: 98% hexane, 2% 2-propanol

Flow rate: 1 ml/min

Injection value: 0.115 ml.

Wavelength: 282 nm

Degradation and HPLC analysis of Uvitex OB

5 mg Uvitex OB was dissolved in 5 ml ethyl acetate ($C = 0.23 \times 10^{-2}$ mol/L) and oxygen was passed through the solution for 10 min. Then the solution was irradiated for 64 h with an oxygen balloon on the top provide a constant supply of oxygen. Solvent was evaporated and the residue was dissolved in 5 mL THF. Then a 0.5 mL aliquot was added into HPLC sample cell and diluted to 1 mL with hexane for HPLC analysis. The eluate from 4 min to 6 min and 16 min to 20 min were collected respectively. Then the solution from each part was concentrated. The residue was dissolved in ethyl acetate for UV-Vis measurement.

Degradation and preparative TLC analysis of Uvitex OB

10 mg Uvitex OB was dissolved in 5 ml ethyl acetate ($C = 0.47 \times 10^{-2}$ mol/L) and oxygen was passed through the solution for 10 min. Then the solution was irradiated for 137 h with an oxygen balloon on the top provide a constant supply of oxygen. Solvent was evaporated and the residue was dissolved in 1 mL DCM which was put on the blue line (base line) of the preparative TLC plate. After eluting 4 times with ethyl acetate: petroleum ether 1:20, three main fractions were collected and dissolved in ethyl acetate respectively for UV-Vis measurement.

Films degradation in QUV in company

The QUV accelerated weathering tester was used for irradiation in company. UVA-340 lamps were used, which provides sunlight in the critical short wavelength region from 365 nm down to the solar cut off of 295 nm, and the peak emission is at 340 nm.

Degradation and preparative TLC analysis of Uvitex OB combined with C944

10 mg Uvitex OB and 10 mg C944 was dissolved in 5 ml ethyl acetate ($C = 0.47 \times 10^{-2}$ mol/L). The solution was treated with oxygen for 10 min and with an oxygen balloon to provide a constant supply of O_2 and irradiated for 86 h. White solid precipitated out after 6 h and the white solid was filtered after irradiation. The solution was applied to the preparative TLC plate for separation. After eluting 4 times in ethyl acetate: petroleum ether 1:20, four main fractions were collected and dissolved in ethyl acetate respectively for UV-Vis measurement.

Fluorescence quantum yield and life time

The fluorescence spectra were recorded using fluorescence spectrophotometer (Edinburgh Instruments FLS900) at concentration of 1.86×10^{-6} M. The sample solution was contained in a quartz cell of 1 cm length. The fluorescence life time of UvitexOB was measured in ethyl acetate. The quantum yield was calculated from the following Eq.^[178]

$$\Phi_i = \Phi_s \times \frac{Int_i}{Int_s} \frac{1 - 10^{-A_s} n_i^2}{1 - 10^{-A_i} n_s^2}$$

where Φ_i and Φ_s represent the quantum yields of the sample and standard, respectively; Int_i and Int_s are the integrated intensities (areas) of sample and standard spectra, respectively (in units of photons); A_i and A_s represent the UV/vis absorbances of sample and standard, respectively; the refractive indices of the sample and reference solution are n_i and n_s , respectively. In principle, excitation wavelengths for sample and reference can be different, but this is generally not advisable because it introduces an additional uncertainty in the relative photon flux at the two wavelengths. The standard in this project was 1,4-bis(5-phenyloxazol-2-yl) benzene (POPOP) ($\Phi_s = \Phi_{popop} = 0.975$) in cyclohexane.^[178]

Chapter 3. Uvinul A plus modification

General

All the reagents used were obtained commercially and were not purified further. THF was distilled under a nitrogen atmosphere from sodium / benzophenone ketyl radical. Dichloromethane was distilled from calcium hydride. All other solvents were used as received. All anhydrous reactions were run under a nitrogen atmosphere in oven/flame dried glassware unless otherwise stated.

All chromatography column separations were monitored using Merck TLC silica gel 60 aluminium backed silica plates which were visualised by Ultra Violet light at 254 nm using a UVP chromate-vue cabinet model CC-60. Flash column chromatography was performed under pressure, using silica gel 60 from Davisil Fluorochem.

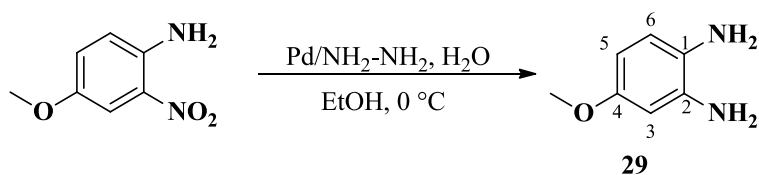
NMR spectra were recorded at 400 MHz (^1H), 100 MHz (^{13}C) and 376 MHz (^{19}F) on a Bruker Advance 400MHz instrument or Joel JNM-ECS400 MHz instrument. Samples were dissolved in CDCl_3 (unless otherwise stated) using TMS (tetramethylsilane) as the internal reference. ^{19}F NMR spectra are referenced to hexafluorobenzene as standard. Chemical shifts are given in parts per million (p.p.m) and coupling constants, J , in hertz (Hz).

Mass spectra were recorded using a Thermo Fisher Exactive with an ion max source and ESI probe fitted with an Advion Triversa Nanomate to obtain high resolution mass spectra. The solvent used for all samples was methanol.

IR spectra were recorded using FT-IR 8400S with GS10800-X Quest ATR diamond accessory and a Perkin-Elmer, spectrum 65 FT-IR spectrophotometer with sodium chloride plates were used to acquire thin film spectra using CH_2Cl_2 to apply the sample.

Melting points were recorded on a Stuart Scientific apparatus and are uncorrected. Organic extracts were dried over magnesium sulphate. Sodium hydride was dispersed in mineral oil as 60 %.

4-Methoxy-1,2-phenylenediamine (**29**) ^[148]

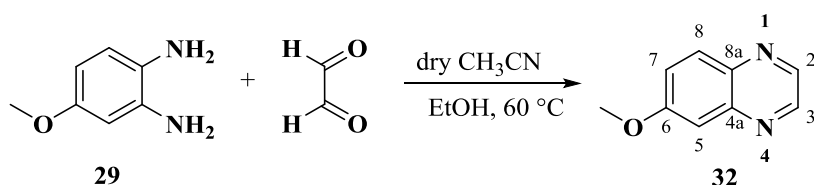


4-Methoxy-2-nitroaniline (0.84 g, 5.00 mmol) and 10% Pd/C (0.13 g) were added to ethanol (10 mL) and the mixture was cooled to 0 °C. Hydrazine monohydrate (65%, 1.25 mL) was added dropwise into the reaction. The reaction mixture was stirred for 5 min and then filtered to separate the catalyst, and the filtrate concentrated to give **29** (0.69 g, 100%) as a colourless oil (which darkened after a few minutes).

NMR δ_{H} (400 MHz, CDCl_3), 6.62 (1H, d, $J=8.0$ Hz, H-6), 6.30 (1H, d, $J=2.4$ Hz, H-3), 6.24 (1H, dd, $J=8.0, 2.4$ Hz, H-5), 3.78 (3H, s, CH_3), 3.28 (4H, bs, NH_2).

NMR δ_{C} (100 MHz, CDCl_3), 154.6 (C-4), 137.1 (C-1), 127.4 (C-2), 118.4 (C-6), 104.1 (C-5), 103.0 (C-3), 55.6 (CH_3).

6-Methoxyquinoxaline (**32**) ^[148]

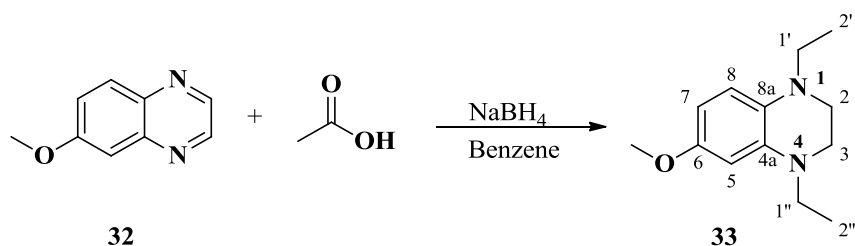


Following the procedure in the literature,^[148] reaction of **31** with glyoxal afforded **32** as a white solid in 64% yield with m.p. 59.5-61.2 °C. (Literature m.p. 58-60 °C)

NMR δ_{H} (400 MHz, CDCl_3), 8.75 (1H, d, $J=2.4$ Hz), 8.69 (1H, d, $J=2.4$ Hz), 7.97 (1H, d, $J=9.2$ Hz, H-8), 7.41 (1H, dd, $J=9.2, 2.8$ Hz, H-7), 7.36 (1H, d, $J=2.8$ Hz, H-5), 3.96 (3H, s, CH_3).

NMR δ_{C} (100 MHz, CDCl_3), 160.9 (C-6), 144.9, 144.7, 142.5, 139.3, 130.5 (C-8), 123.6 (C-7), 106.7 (C-5), 55.9 (CH_3).

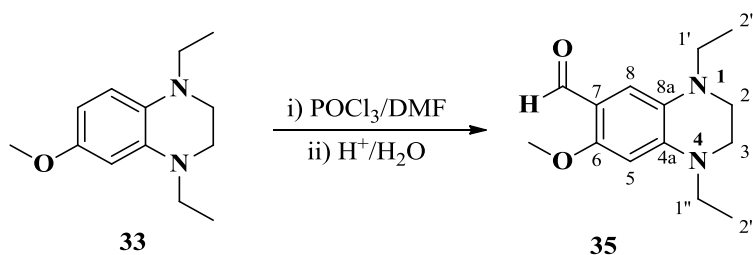
1,4-Diethyl-6-methoxy-1,2,3,4-tetrahydroquinoxaline (33) ^[148]



Following the procedure in the literature,^[148] reaction of **32** with acetic acid and sodium borohydride afforded **33** as a yellow oil in 58% yield after purification by chromatography on silica gel (elution with petrol ether/ ethyl acetate 10:1).

NMR δ_{H} (400 MHz, CDCl_3), 6.48 (1H, d, $J=8.4$ Hz, H-8), 6.17 (2H, m, H-5, H-7), 3.74 (3H, s, OCH_3), 3.32 (8H, m, CH_2), 1.32 (6H, t, $J=6.8$ Hz, CH_3).

1,4-Diethyl-6-methoxy-1,2,3,4-tetrahydroquinoxalin-7-carboxaldehyde (35)

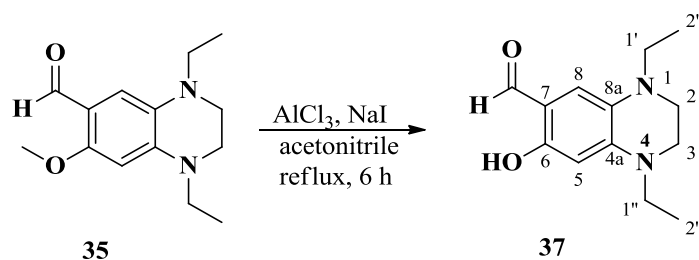


Following the procedure in the literature,^[148] Vilsmeier reaction of **33** afforded **35** as a yellow oil in 44% yield after purification by chromatography on silica gel (elution with petrol ether/ ethyl acetate 5:1).

NMR δ_{H} (400 MHz, CDCl_3), 10.12 (1H, s, CHO), 6.98 (1H, s, H-8), 6.01 (1H, s, H-5), 3.83 (3H, s, CH_3), 3.50 (2H, t, $J=4.8$ Hz), 3.40 (2H, q, $J=7.2$ Hz, CH_2), 3.29 (2H, q, $J=7.2$ Hz, CH_2), 3.14 (2H, t, $J=4.8$ Hz), 1.21 (3H, t, $J=6.8$ Hz, CH_3), 1.14 (3H, t, $J=6.8$ Hz, CH_3).

IR, $\nu_{\text{max}}/\text{cm}^{-1}$ 1645 (C=O).

1,4-Diethyl-6-hydroxy-1,2,3,4-tetrahydroquinoxalin-7-carboxaldehyde (**37**)^[150]



Under an anhydrous condition, NaI (1.47 g, 9.84 mmol) was added slowly into a solution of AlCl₃ (0.44 g, 3.28 mmol) in dry acetonitrile (1 mL). A solution of **35** (0.41 g, 1.64 mmol) in dry acetonitrile (2 mL) was added dropwise into the mixture. Then the reaction was gently refluxed for 6 h. After cooling to room temperature, 15 mL water was added. The mixture was extracted with ethyl acetate (3 x 15 mL), the extract was dried over anhydrous Mg₂SO₄ and concentrated to afford yellow oil which was purified by chromatography on silica gel (elution with petrol ether/ ethyl acetate 5:1) to afford **37** (0.27 g, 71%) as a yellow oil.

NMR δ_{H} (400 MHz, CDCl₃), 11.58 (1H, s, CHO), 9.47 (1H, s, H-8), 6.56 (1H, bs, OH), 6.06 (1H, s, H-5), 3.54 (2H, t, $J=4.0$ Hz), 3.40 (2H, q, $J=5.6$ Hz, CH₂), 3.28 (2H, q, $J=5.6$ Hz, CH₂), 3.17 (2H, t, $J=4.0$ Hz), 1.21 (6H, t, $J=5.6$ Hz, CH₃).

IR, ν_{max} /cm⁻¹ 3500-3047 (OH), 1631 (C=O).

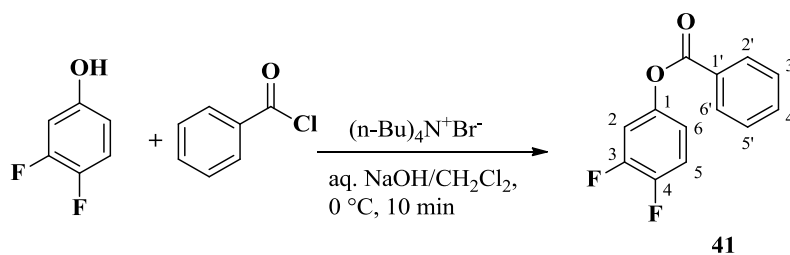
Phase-transfer condition procedure ^[151]

The substituted phenol (5 mmol) was dissolved in 10% NaOH (10 mL) and the resulting solution was cooled to 0 °C. The appropriate substituted benzoyl chloride (5 mmol) and tetra-*n*-butylammonium bromide (0.5 mmol) were dissolved in dichloromethane (10 mL) separately and cooled to 0 °C. After cooling all solutions to 0 °C, they were mixed at once and stirred at 0 °C for 10 min. The reaction mixture was then poured over 5 mL ice water. The organic layer was separated and the aqueous layer was extracted with ethyl acetate (3 x 10 mL). The combined organic extracts were washed with NaHCO₃ solution (2 x 10 mL) and brine (10 mL), dried over anhydrous Mg₂SO₄ and concentrated on a rotary evaporator to give the target compound.

Fries Rearrangement procedure

Under anhydrous conditions, ester (5 mmol) and zirconium chloride (10 mmol) were dissolved in 1,2-dichloroethane (25 mL). The mixture solution was stirred and heated under reflux. After cooling to room temperature, 10 mL water was added. The organic layer was separated and the aqueous layer was extracted with ethyl acetate (3 x 10 mL). The combined organic extracts were washed with brine (10 mL), dried over anhydrous Mg₂SO₄ and concentrated on a rotary evaporator to provide crude product which was purified by chromatography on silica gel to afford the target product.

3,4-Difluorophenyl benzoate (**41**)



Prepared using phase-transfer condition procedure from 3,4-difluorophenol (0.65 g, 5.00 mmol), benzoyl chloride (0.58 mL, 5.00 mmol) and tetra-*n*-butylammonium bromide (0.16 g, 0.50 mmol) yielding **41** as a white solid (1.15 g, 98%) with m.p. 73.4-74.4 °C.

NMR δ_{H} (400 MHz, CDCl_3), 8.17 (2H, dd, $J=8.0, 1.2$ Hz, H-2', H-6'), 7.65 (1H, t, $J=7.2$ Hz, H-4'), 7.52 (2H, t, $J=8.0$ Hz, H-3', H-5'), 7.21 (1H, m, H-2), 7.11 (1H, m, H-5), 6.97 (1H, m, H-6).

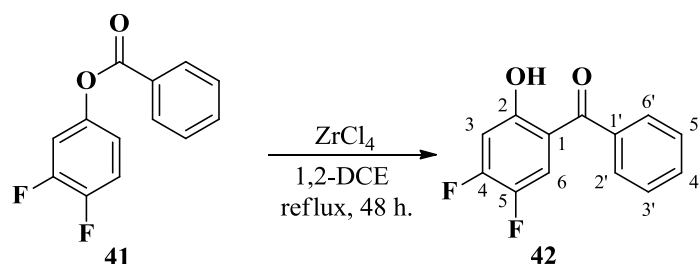
NMR δ_{C} (100 MHz, CDCl_3), 164.9 (C=O), 150.3 (1C, dd, $J=248.9, 13.3$ Hz, C-3), 148.5 (1C, dd, $J=245.1, 13.4$ Hz, C-4), 134.1 (C-4'), 130.3 (2C, C-2', C-6'), 129.0 (C-1'), 128.8 (2C, C-3', C-5'), 117.8 (1C, t, $J=5.7$ Hz, C-6), 117.4 (1C, d, $J=11.9$ Hz, C-2), 111.9 (1C, d, $J=20.0$ Hz, C-5).

NMR δ_{F} (376 MHz, CDCl_3), 27.4 (1F, m, F-3), 21.1 (1F, m, F-4).

MS, m/z found 235.0563 $\text{C}_{13}\text{H}_9\text{F}_2\text{O}_2$, ($\text{M}+\text{H}^+$) requires 235.0565; found 257.0382 $\text{C}_{13}\text{H}_8\text{F}_2\text{O}_2\text{Na}$, ($\text{M}+\text{Na}^+$) requires 257.0385; found 491.0872 $\text{C}_{26}\text{H}_{16}\text{F}_4\text{O}_4\text{Na}$, ($2\text{M}+\text{Na}^+$) requires 491.0877.

IR, $\nu_{\text{max}}/\text{cm}^{-1}$ 1728 (C=O).

4,5-Difluoro-2-hydroxybenzophenone (**42**)



The Fries rearrangement procedure was followed with **41** (1.15 g, 4.90 mmol) and ZrCl_4 (2.28 g, 9.80 mmol) under reflux for 48 h. The crude product was purified by chromatography on silica gel (elution with petrol ether/ ethyl acetate 100:1) to afford **42** (0.72 g, 62%) as a yellow solid with m.p. 77.8-78.4 °C.

NMR δ_{H} (400 MHz, CDCl_3), 12.17 (1H, d, $J=1.2$ Hz, OH), 7.63 (3H, m, H-2', H-4', H-6'), 7.53 (2H, t, $J=7.6$ Hz, H-3', H-5'), 7.42 (1H, dd, $J=10.8, 9.2$ Hz, H-6), 6.23 (1H, dd, $J=11.2, 6.4$ Hz, H-3),

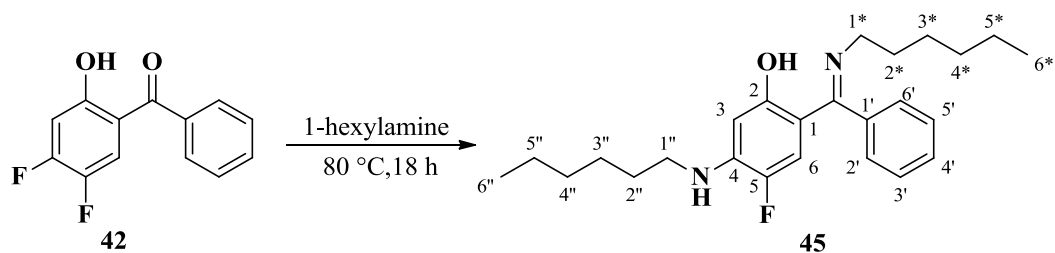
NMR δ_{C} (100 MHz, CDCl_3), 199.9 (C=O), 161.1 (d, $J=12.3$ Hz, COH), 155.7 (dd, $J=258.4, 14.3$ Hz, C-4), 143.2 (dd, $J=240.3, 13.4$ Hz, C-5), 137.3 (C-1'), 132.5 (C-4'), 128.9 (2C, C-2', C-6'), 128.7 (2C, C-3', C-5'), 120.7 (dd, $J=19.1, 3.8$ Hz, C-6), 114.8 (t, $J=3.8$ Hz, C-1), 107.1 (d, $J=19.1$ Hz, C-3).

NMR δ_{F} (376 MHz, CDCl_3), 39.0 (1F, m, F-4), 14.3 (1F, m, F-5).

MS, m/z found 235.0562 $\text{C}_{13}\text{H}_9\text{F}_2\text{O}_2$, ($\text{M}+\text{H}^+$) requires 235.0565; found 257.0382 $\text{C}_{13}\text{H}_8\text{F}_2\text{O}_2\text{Na}$, ($\text{M}+\text{Na}^+$) requires 257.0385.

IR, $\nu_{\text{max}}/\text{cm}^{-1}$ 3412 (OH), 1640 (C=O), 1151 (C-O).

5-Fluoro-4-(hexylamino)-2-((hexylimino)(phenyl)methyl)phenol (**45**)



42 (0.23 g, 1.00 mmol) was added to a 10 mL round bottom flask. 1-Hexylamine (1.00 mL) was added into the flask and the mixture was stirred and heated under reflux for 18 h and then cooled to room temperature. The reaction was quenched with 10 mL ice water and extracted with ethyl acetate (3 x 10 mL). The extract was dried over anhydrous Mg_2SO_4 and concentrated to afford a yellow oil which was purified by chromatography on silica gel (elution with petrol ether/ ethyl acetate 10:1) to afford **45** (0.39 g, 97%) as a yellow solid with m.p. 57.6-58.7 °C.

NMR δ_{H} (400 MHz, CDCl_3), 16.05 (1H, s, OH), 7.48 (3H, m, H-2', H-6', H-4'), 7.20 (2H, m, H-3', H-5'), 7.18 (1H, d, $J=13.2$ Hz, H-6), 6.00 (1H, d, $J=7.6$ Hz, H-3), 4.27 (1H, d, $J=2.8$ Hz, NH), 3.14 (4H, t, $J=7.6$ Hz, H-1'', H-1*), 1.58 (4H, m, H-2'', H-2*), 1.28 (12H, m, H-3'', H-3*, H-4'', H-4*, H-5'', H-5*), 0.85 (6H, m, H-6'', H-6*).

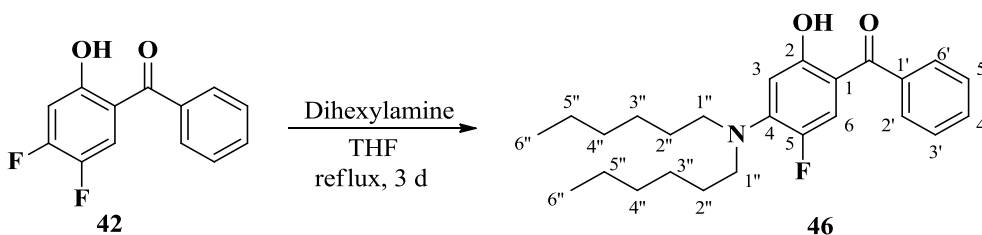
NMR δ_{C} (100 MHz, CDCl_3), 171.9 (C=N), 171.2 (C-2), 143.5 (d, $J=14.3$ Hz, C-4), 143.5 (d, $J=227.9$ Hz, C-5), 132.5 (C-1'), 129.4 (C-4'), 128.8 (2C, C-2', C-6'), 127.8 (2C, C-3', C-5'), 113.9 (d, $J=20.0$ Hz, C-6), 105.6 (d, $J=6.7$ Hz, C-1), 100.1 (d, $J=2.8$ Hz, C-3), 47.5, 42.9, 31.6, 31.5, 30.5, 29.1, 26.8, 26.7, 22.7, 22.6, 14.1 (2C, C-6*, C-6'').

NMR δ_{F} (376 MHz, CDCl_3), 10.9 (1F, s).

MS, m/z found 399.2799, $\text{C}_{25}\text{H}_{36}\text{FN}_2\text{O}$, ($\text{M}+\text{H}^+$) requires 399.2806; found 421.2618, $\text{C}_{25}\text{H}_{35}\text{FN}_2\text{ONa}$, ($\text{M}+\text{Na}^+$) requires 421.2626; found 819.5343, $\text{C}_{50}\text{H}_{70}\text{F}_2\text{N}_4\text{O}_2\text{Na}$, ($2\text{M}+\text{Na}^+$) requires 819.5359.

IR, ν_{max} / cm^{-1} 3500-3047 (OH, NH), 2927 (CH_2), 1722 (C=N), 1126 (C-N).

5-Fluoro-4-dihexylamino-2-hydroxybenzophenone (**46**)



42 (1.14 g, 4.87 mmol) and dihexylamine (2.83 mL, 12.18 mmol) were added in 10 mL THF in a 50 mL round bottom flask. The mixture solution was stirred under reflux for 3 days. After cooling to room temperature, the reaction was quenched with 10 mL ice water and extracted with ethyl acetate (3 x 20 mL). The extract was dried over anhydrous Mg_2SO_4 and concentrated to afford a yellow oil which was purified by chromatography on silica gel (elution with petrol ether) to afford **46** (1.80 g, 93%) as a yellow oil.

NMR δ_{H} (400 MHz, CDCl_3), 12.67 (1H, s, OH), 7.60 (2H, d, $J=7.2$ Hz, H-2', H-6'), 7.48 (3H, m, H-3', H-5', H-4'), 7.10 (1H, d, $J=16.0$ Hz, H-6), 6.19 (1H, d, $J=8.4$ Hz, H-3), 3.32 (4H, t, $J=8.0$ Hz, H-1''), 1.59 (4H, m, H-2''), 1.27 (12H, m, H-3'', H-4'', H-5''), 0.88 (6H, t, $J=6.8$ Hz, H-6'').

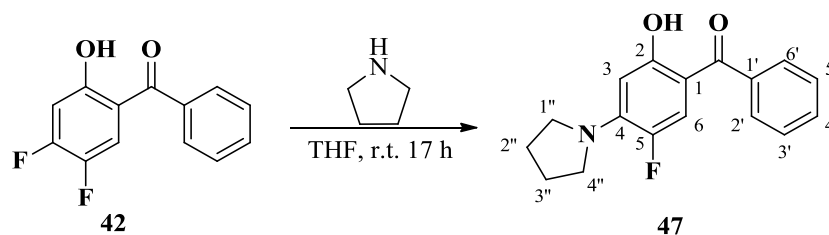
NMR δ_{C} (100 MHz, CDCl_3), 197.7 (C=O), 162.2 (COH), 145.2 (d, $J=9.5$ Hz, C-4), 144.7 (d, $J=233.6$ Hz, C-5), 138.5 (C-1'), 131.2 (C-4'), 128.6 (2C, C-2', C-6'), 128.4 (2C, C-3', C-5'), 119.7 (d, $J=25.8$ Hz, C-6), 108.0 (d, $J=6.7$ Hz, C-1), 102.2 (d, $J=3.8$ Hz, C-3), 52.9 (d, $J=6.7$ Hz, C-1''), 31.7 (C-2''), 28.0 (C-3''), 26.7 (C-4''), 22.7 (C-5''), 14.1 (C-6'').

NMR δ_{F} (376 MHz, CDCl_3), 26.8 (1F, dd, $J=15.8, 7.9$ Hz).

MS, m/z found 400.2642, $\text{C}_{25}\text{H}_{35}\text{NO}_2\text{F}$, ($\text{M}+\text{H}^+$) requires 400.2646; found 422.2460, $\text{C}_{25}\text{H}_{34}\text{NO}_2\text{FNa}$, ($\text{M}+\text{Na}^+$) requires 422.2466; found 821.5028, $\text{C}_{50}\text{H}_{68}\text{N}_2\text{O}_4\text{F}_2\text{Na}$, ($2\text{M}+\text{Na}^+$) requires 821.5039.

IR, $\nu_{\text{max}}/\text{cm}^{-1}$ 3500-3047 (OH), 2924 (CH_2), 1635 (C=O), 1111 (C-F).

5-Fluoro-4-(pyrrolidin-1-yl)-2-hydroxybenzophenone (47)



42 (0.47 g, 2.00 mmol) and pyrrolidine (0.66 mL, 8.00 mmol) were added in 15 mL THF to a 50 mL round bottom flask. The mixture solution was stirred at r.t. for 17 h. The reaction was quenched with 10 mL ice water and extracted with ethyl acetate (3 x 20 mL). The extract was dried over anhydrous Mg_2SO_4 and concentrated to afford crude product which was purified by chromatography on silica gel (elution with petrol ether/ ethyl acetate 50:1) to give **47** (0.51 g, 90%) as a yellow solid with m.p. 95.9-97.2 °C.

NMR δ_{H} (400 MHz, CDCl_3), 12.81 (1H, s, OH), 7.60 (2H, m, H-2', H-6'), 7.54-7.44 (3H, m, H-3', H-4', H-5'), 7.09 (1H, d, $J=15.2$ Hz, H-6), 6.08 (1H, d, $J=7.6$ Hz, H-3), 3.53 (4H, m, H-1'', H-4''), 1.96 (4H, m, H-2'', H-3'').

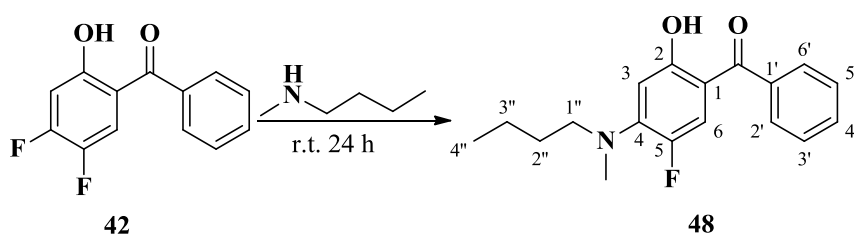
NMR δ_{C} (100 MHz, CDCl_3), 197.6 (C=O), 162.6 (COH), 144.1 (d, $J=11.4$ Hz, C-4), 143.9 (d, $J=233.6$ Hz, C-5), 138.6 (C-1'), 131.1 (C-4'), 128.6 (2C, C-2', C-6'), 128.4 (2C, C-3', C-5'), 118.8 (d, $J=23.8$ Hz, C-6), 107.2 (d, $J=6.6$ Hz, C-1), 100.8 (d, $J=4.8$ Hz, C-3), 50.0 (d, $J=5.8$ Hz, C-1'', C-4''), 25.5 (2C, C-2'', C-3'').

NMR δ_{F} (376 MHz, CDCl_3), 23.3 (1F, m, F-5).

MS, m/z found 286.1245, $\text{C}_{17}\text{H}_{17}\text{NO}_2\text{F}$, ($\text{M}+\text{H}^+$) requires 286.1238; found 308.1062, $\text{C}_{17}\text{H}_{16}\text{NO}_2\text{FNa}$, ($\text{M}+\text{Na}^+$) requires 308.1057.

IR, $\nu_{\text{max}}/\text{cm}^{-1}$ 3412 (OH), 2973 (CH_2), 1635 (C=O).

4-But-1-yl(methyl)amino-5-fluoro-2-hydroxybenzophenone (**48**)



42 (0.23 g, 1.00 mmol) and *N*-methyl-1-butylamine (0.5 mL) were added to a 5 mL round bottom flask. The mixture was stirred at r.t. for 24 h. Then the reaction was quenched with 10 mL water and extracted with ethyl acetate (3 x 10 mL). The extract was dried over anhydrous Mg_2SO_4 and concentrated to afford a yellow oil which was purified by chromatography on silica gel (elution with petrol ether/ ethyl acetate 100:1) to give **48** (0.25 g, 84%) as a yellow oil, and **48a** (5 mg, yellow oil) and **48b** (8 mg, yellow oil).

NMR δ_{H} (400 MHz, CDCl_3), 12.65 (1H, s, OH), 7.60 (2H, m, H-2', H-6'), 7.53 (1H, tt, $J=7.6, 2.8$ Hz, H-4'), 7.47 (2H, m, H-3', H-5'), 7.11 (1H, d, $J=15.6$ Hz, H-6), 6.23 (1H, d, $J=8.4$ Hz, H-3), 3.38 (2H, t, $J=7.6$ Hz, H-1''), 3.02 (3H, d, $J=2.0$ Hz, NCH_3), 1.60 (2H, m, H-2''), 1.30 (2H, m, H-3''), 0.92 (3H, t, $J=7.6$ Hz, H-4'').

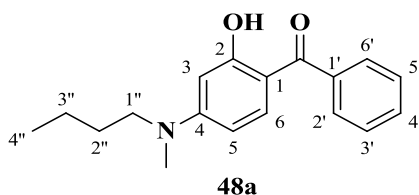
NMR δ_{C} (100 MHz, CDCl_3), 197.9 (C=O), 162.2 (C-2), 146.4 (d, $J=8.6$ Hz, C-4), 145.0 (d, $J=235.5$ Hz, C-5), 138.4 (C-1'), 131.3 (C-4'), 128.7 (2C, C-2', C-6'), 128.4 (2C, C-3', C-5'), 119.3 (d, $J=24.8$ Hz, C-6), 108.3 (d, $J=7.6$ Hz, C-1), 102.6 (d, $J=3.8$ Hz, C-3), 54.4 (d, $J=8.6$ Hz, C-1''), 40.0 (d, $J=3.9$ Hz, NCH_3), 30.0 (C-2''), 20.1 (C-3''), 14.0 (C-4'').

NMR δ_{F} (376 MHz, CDCl_3), 27.6 (1F, m).

MS, m/z found 302.1546, $\text{C}_{18}\text{H}_{21}\text{NO}_2\text{F}$, ($\text{M}+\text{H}^+$) requires 302.1551; found 324.1366, $\text{C}_{18}\text{H}_{20}\text{NO}_2\text{FNa}$, ($\text{M}+\text{Na}^+$) requires 324.1370; found 625.2841, $\text{C}_{36}\text{H}_{40}\text{N}_2\text{O}_4\text{F}_2\text{Na}$, ($2\text{M}+\text{Na}^+$) requires 625.2848.

IR, $\nu_{\text{max}}/\text{cm}^{-1}$ 3411 (OH), 2932 (CH_2), 1634 (C=O).

4-But-1-yl(methyl)amino-2-hydroxybenzophenone (48a)



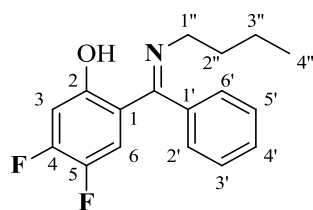
NMR δ_{H} (400 MHz, CDCl_3), 12.95 (1H, s, OH), 7.60 (2H, dd, $J=8, 1.6$ Hz, H-2', H-6'), 7.50-7.42 (3H, m, H-3', H-4', H-5'), 7.36 (1H, dd, $J=8, 1.2$ Hz, H-6), 6.14 (2H, H-3, H-5), 3.61 (2H, t, $J=7.6$ Hz, H-1''), 3.02 (3H, s, NCH_3), 1.60 (2H, m, H-2''), 1.33 (2H, m, H-3''), 0.94 (3H, t, $J=7.2$ Hz, H-4'').

NMR δ_{C} (100 MHz, CDCl_3), 198.2 (C=O), 166.1 (C-2), 155.1 (C-4), 139.0 (C-1'), 135.4 (C-6), 130.8 (C-4'), 128.8 (2C, C-2', C-6'), 128.2 (2C, C-3', C-5'), 109.3 (C-1), 103.7 (C-5), 97.8 (C-3), 52.3 (C-1''), 38.6 (NCH_3), 29.3 (C-2''), 20.3 (C-3''), 14.0 (C-4'').

MS, m/z found 282.1492, $\text{C}_{18}\text{H}_{20}\text{NO}_2$, ($\text{M}-\text{H}^+$) requires 282.1489; found 284.1657, $\text{C}_{18}\text{H}_{22}\text{NO}_2$, ($\text{M}+\text{H}^+$) requires 284.1645; found 306.1476, $\text{C}_{18}\text{H}_{21}\text{O}_2\text{NNa}$, ($\text{M}+\text{Na}^+$) requires 306.1465.

IR, $\nu_{\text{max}}/\text{cm}^{-1}$ 3500-3000 (OH), 2924 (CH_2), 1620 (C=O).

(E)-2-((Butylimino)(phenyl)methyl)-4,5-difluorophenol (48b)



48b

NMR δ_{H} (400 MHz, CDCl_3), 16.50 (1H, s, OH), 7.53 (3H, m, H-2', H-4', H-6'), 7.19 (2H, m, H-3', H-5'), 6.69 (1H, dd, $J=12.4, 6.8$ Hz, H-6), 6.51 (1H, dd, $J=11.6, 9.6$ Hz, H-3), 3.29 (2H, t, $J=6.8$ Hz, H-1''), 1.62 (2H, m, H-2''), 1.36 (2H, m, H-3''), 0.87 (3H, t, $J=7.2$ Hz, H-4'').

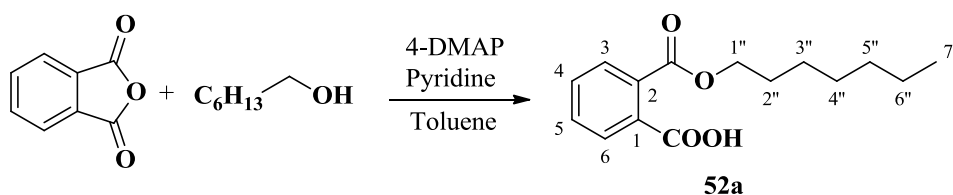
NMR δ_{C} (100 MHz, CDCl_3), 173.1 (C=N), 165.0 (d, $J=11.5$ Hz, C-2), 154.0 (dd, $J=255.7, 15.3$ Hz, C-4), 142.1 (dd, $J=235.5, 14.3$ Hz, C-5), 132.4 (C-1'), 129.8 (C-4'), 128.9 (2C, C-2', C-6'), 127.3 (2C, C-3', C-5'), 118.1 (dd, $J=19.1, 2.9$ Hz, C-6), 114.0 (C-1), 107.2 (d, $J=16.2$ Hz, C-3), 49.8 (C-1''), 32.6 (C-2''), 20.4 (C-3''), 13.8 (C-4'').

NMR δ_{F} (376 MHz, CDCl_3), 33.0 (1F, m, F-4), 9.9 (1F, m, F-5).

MS, m/z found 290.1351, $\text{C}_{17}\text{H}_{18}\text{NOF}_2$, ($\text{M}+\text{H}^+$) requires 190.1351; found 312.117, $\text{C}_{17}\text{H}_{17}\text{NOF}_2\text{Na}$, ($\text{M}+\text{Na}^+$) requires 312.1170; found 601.2449, $\text{C}_{34}\text{H}_{34}\text{N}_2\text{O}_2\text{F}_2\text{Na}$, ($2\text{M}+\text{Na}^+$) requires 601.2449.

IR, $\nu_{\text{max}}/\text{cm}^{-1}$ 3412 (OH), 2931 (CH_2), 1621 (C=N).

2-Heptyloxycarbonyl benzoic acid (**52a**) ^[144]

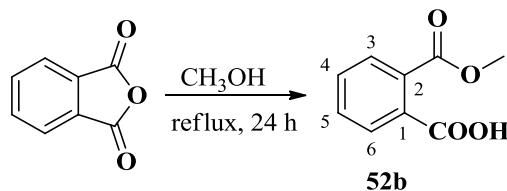


Following the procedure in the literature,^[144] reaction of phthalic anhydride with 1-heptanol afforded **52a** as a colourless oil in 85% yield.

NMR δ_H (400 MHz, $CDCl_3$), 11.35 (1H, s, COOH), 7.90 (1H, d, $J=7.2$ Hz, H-6), 7.68 (1H, d, $J=7.6$ Hz, H-3), 7.62-7.53 (2H, m, H-4, H-5), 4.31 (2H, t, $J=6.8$ Hz, H-1''), 1.72 (2H, m, H-2''), 1.42-1.23 (8H, m, H-3'', H-4'', H-5'', H-6''), 0.83 (3H, t, $J=6.8$ Hz, H-7'').

IR, ν_{max}/cm^{-1} 3500-3020 (COOH), 1728 (C=O), 1176 (C-O).

2-(Methoxycarbonyl)benzoic acid (**52b**) ^[153]

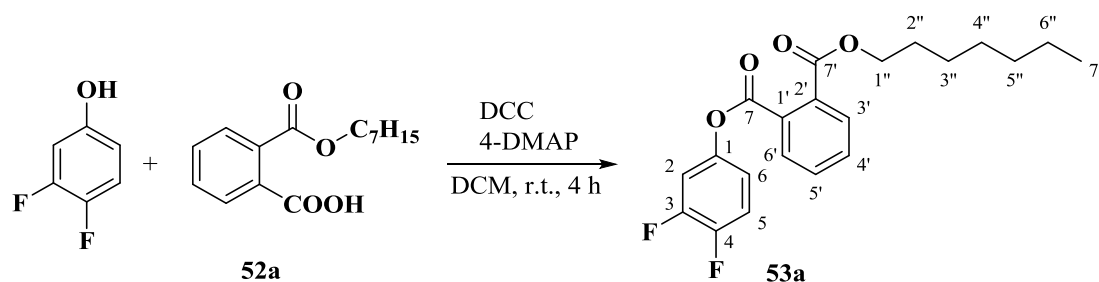


Following the procedure in the literature,^[153] reaction of phthalic anhydride with methanol afforded **52b** as a white solid in 100% yield. m.p. 81.5-83.1 °C.

NMR δ_H (400 MHz, $CDCl_3$), 9.00 (1H, s, COOH), 7.91 (1H, m, H-6), 7.64 (1H, s, H-3), 7.61-7.53 (2H, m, H-4, H-5), 3.91 (3H, s, CH_3).

IR, ν_{max}/cm^{-1} 3411 (OH), 1723 (C=O), 1049 (C-O).

3,4-Difluorophenyl heptyl phthalate (53a)



3,4-Difluorophenol (0.42 g, 3.20 mmol), **53a** (1.12 g, 4.30 mmol) and 4-dimethylaminopyridine (0.05 g, 0.40 mmol) were dissolved in dichloromethane (20 mL). To this mixture, *N,N*-dicyclohexylcarbodiimide (DCC) (0.72 g, 3.50 mmol) was slowly added and the reaction mixture was stirred at r.t. for 4 h. The solid formed was filtered off and the filtrate was concentrated. The residue was purified by chromatography on silica gel (elution with petrol ether / ethyl acetate 50:1) to afford **53a** (0.89 g, 74%) as a colourless oil.

NMR δ_{H} (400 MHz, CDCl_3), 7.85-7.80 (2H, m, H-3', H-6'), 7.61 (2H, m, H-4', H-5'), 7.25-7.16 (2H, m, H-2, H-5), 7.02 (1H, m, H-6), 4.31 (2H, t, $J=6.4$ Hz, H-1''), 1.71 (2H, m, H-2''), 1.41-1.24 (8H, m, H-3'', H-4'', H-5'', H-6''), 0.86 (3H, t, $J=6.8$ Hz, H-7'').

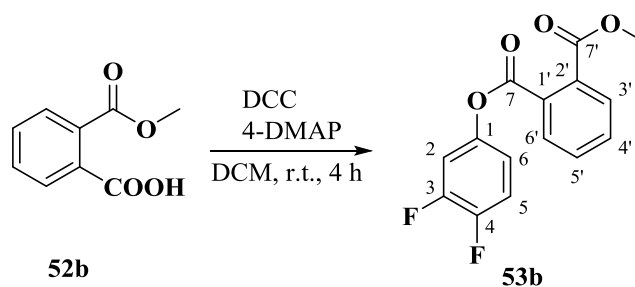
NMR δ_{C} (100 MHz, CDCl_3), 167.0 (C-7), 166.2 (C-7'), 150.3 (dd, $J=248.9, 14.3$ Hz, C-3), 148.5 (dd, $J=245.0, 12.4$ Hz, C-4), 146.5 (1C, dd, $J=8.6, 2.8$ Hz, C-1), 132.1 (C-2'), 131.7, 131.6 (C-1'), 131.5, 129.4, 129.1, 117.6 (m, C-6), 117.3 (d, $J=18.1$ Hz, C-5), 111.7 (d, $J=20$ Hz, C-2), 66.2 (C-1''), 31.8, 28.9, 28.7 (C-2''), 25.9, 22.6, 14.1 (C-7'').

NMR δ_{F} (376 MHz, CDCl_3), 27.4 (1F, m, F-3), 21.2 (1F, m, F-4).

MS, m/z found 377.1543 $\text{C}_{21}\text{H}_{23}\text{O}_4\text{F}_2$, ($\text{M}+\text{H}^+$) requires 377.1559; found 399.1362 $\text{C}_{21}\text{H}_{22}\text{O}_4\text{F}_2\text{Na}$, ($\text{M}+\text{Na}^+$) requires 399.1378; found 775.9547 $\text{C}_{42}\text{H}_{44}\text{O}_8\text{F}_4\text{Na}$, ($2\text{M}+\text{Na}^+$) requires 775.2865.

IR, $\nu_{\text{max}}/\text{cm}^{-1}$ 1759 (C7=O), 1721 (C7'=O).

3,4-Difluorophenyl methyl phthalate (53b)



Following the general method outlined for **54a**, 3,4-difluorophenol (0.59 g, 4.50 mmol), **53b** (0.90 g, 5.00 mmol) and 4-dimethylaminopyridine (0.06 g, 0.45 mmol) was dissolved in dichloromethane (15 mL). To this mixture, *N,N*-dicyclohexyl- carbodiimide (DCC) (1.39 g, 6.80 mmol) was added. Work-up as previously and purification by chromatography on silica gel (elution with petrol ether / ethyl acetate 10:1) afforded **53b** (1.29 g, 98%) as a white solid with m.p. 37.1-39.4 °C.

NMR δ_{H} (400 MHz, CDCl_3), 7.85-7.80 (2H, m, H-3', H-6'), 7.64-7.60 (2H, m, H-4', H-5'), 7.23-7.15 (2H, m, H-2, H-5), 7.02 (1H, m, H-6), 3.91 (3H, s, CH_3).

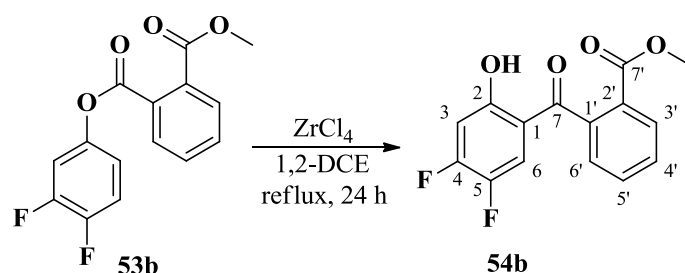
NMR δ_{C} (100 MHz, CDCl_3), 167.4 (C-7), 166.2 (C-7'), 150.3 (dd, $J=248.9, 13.4$ Hz, C-3), 148.6 (dd, $J=245.0, 12.4$ Hz, C-4), 146.5 (dd, $J=8.6, 2.8$ Hz, C-1), 131.7, 131.7, 131.6 (C-2'), 131.5, 129.4, 129.1, 117.6 (m, C-6), 117.4 (d, $J=19.1$ Hz, C-5), 111.7 (d, $J=20$ Hz, C-2), 52.9 (CH_3).

NMR δ_{F} (376 MHz, CDCl_3), 27.7 (1F, m, F-3), 21.6 (1F, m, F-4).

MS, m/z found 291.0479 $\text{C}_{15}\text{H}_9\text{O}_4\text{F}_2$, ($\text{M}-\text{H}^+$) requires 291.0463; found 315.0451 $\text{C}_{15}\text{H}_{10}\text{O}_4\text{F}_2\text{Na}$, ($\text{M}+\text{Na}^+$) requires 315.0439.

IR, $\nu_{\text{max}}/\text{cm}^{-1}$ 1757 (C7=O), 1727 (C7'=O).

Methyl 2-(4,5-difluoro-2-hydroxybenzoyl)benzoate (**54b**)



The Fries rearrangement procedure was followed with **54b** (0.44 g, 1.52 mmol) and ZrCl_4 (0.71 g, 3.03 mmol) under reflux for 60 h. The crude product was purified by chromatography on silica gel (elution with petrol ether/ ethyl acetate 50:1) to afford **54b** (6.00 mg, 2%) as a yellow oil.

NMR δ_{H} (400 MHz, CDCl_3), 12.01 (1H, d, $J=0.8$ Hz, OH), 8.11 (1H, dd, $J=8.0, 1.6$ Hz, H-3'), 7.68 (1H, td, $J=7.6, 1.2$ Hz, H-5'), 7.61 (1H, td, $J=8.0, 1.2$ Hz, H-4'), 7.34 (1H, dd, $J=7.6, 1.2$ Hz, H-6'), 6.84 (2H, m, H-3, H-6), 3.77 (3H, s, CH_3).

NMR δ_{C} (100 MHz, CDCl_3), 201.3 (C-7), 165.8 (C-7'), 160.1 (d, $J=11.5$ Hz, C-2), 155.6 (dd, $J=257.4, 14.3$ Hz, C-4), 143.3 (dd, $J=241.2, 13.4$ Hz, C-5), 139.6 (C-1'), 132.9 (C-5'), 130.7 (C-3'), 130.3 (C-4'), 128.4 (C-2'), 127.2 (C-6'), 119.5 (d, $J=22$ Hz, C-6), 116.0, 114.6, 106.9 (d, $J=19.1$ Hz, C-3), 52.7 (CH_3).

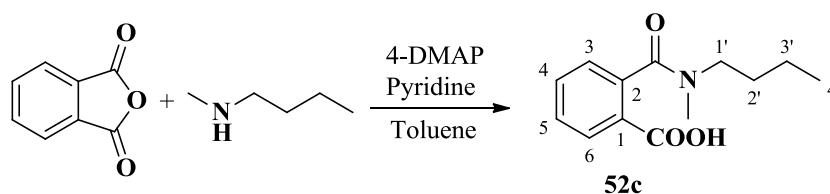
NMR δ_{F} (376 MHz, CDCl_3), 39.1 (1F, m, F-4), 14.6 (1F, ddd, $J=22.2, 10.2, 6.4$ Hz, F-5).

MS, m/z found 291.0468, $\text{C}_{15}\text{H}_9\text{O}_4\text{F}_2$, ($\text{M}-\text{H}^+$) requires 291.0463; found 315.0450 $\text{C}_{15}\text{H}_{10}\text{O}_4\text{F}_2\text{Na}$, ($\text{M}+\text{Na}^+$) requires 315.0439.

IR, $\nu_{\text{max}}/\text{cm}^{-1}$ 3428 (OH), 1722 (C7=O), 1644 (C7'=O).

2-(But-1-yl(methyl)carbamoyl)benzoic acid (**52c**)

(Mixture of rotamers formed in a 1:1 ratio)



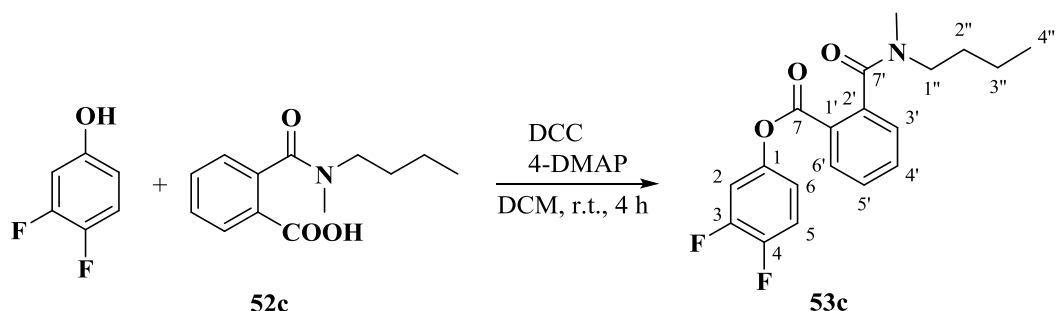
Following the procedure in the literature,^[144] reaction of phthalic anhydride (0.74 g, 5.00 mmol) and *N*-methyl-1-butylamine (0.64 mL, 5.50 mmol) afforded **52c** (0.87 g, 74%) as a colourless oil.

NMR δ_{H} (400 MHz, CDCl_3), 9.79 (1H, s, OH), 8.07 (1H, ddd, $J=8.0, 3.2, 0.8$ Hz, H-6), 7.90 (1H, m, H-4), 7.44 (1H, m, H-5), 7.33 (1H, ddd, $J=8.8, 3.6, 0.8$ Hz, H-3), 3.54 and 3.01 (2H, t, $J=7.6$ Hz, H-1'), 3.09 and 2.98 (3H, s, NCH_3), 1.63 and 1.43 (2H, m, H-2'), 1.33 and 1.12 (2H, m, H-3''), 0.96 and 0.74 (3H, t, $J=7.2$ Hz, H-4').

IR, $\nu_{\text{max}}/\text{cm}^{-1}$ 3418 (OH), 1773 and 1706 (C=O), 1106 (C-O).

3,4-Difluorophenyl 2-(butyl(methyl)carbamoyl)benzoate (**53c**)

(Mixture of rotamers formed in a 1:1 ratio)



Following the method outlined for **53a**, 3,4-difluorophenol (0.39 g, 3.00 mmol), **52c** (0.87 g, 3.70 mmol) and 4-DMAP (0.04 g, 0.30 mmol) were dissolved in DCM (10 mL) and DCC (0.93 g, 4.50 mmol) added. Work-up as previously and purification by chromatography on silica gel (elution with petrol ether / ethyl acetate 5:1) afforded **53c** (0.81 g, 77%) as a colourless oil.

NMR δ_{H} (400 MHz, CDCl_3), 8.14 (1H, td, $J=7.6, 1.2$ Hz, H-6'), 7.63 (H, tt, $J=7.6, 1.2$ Hz, H-4'), 7.50 (1H, m, H-5'), 7.33 (1H, td, $J=7.6, 1.2$ Hz, H-3'), 7.17 (1H, dd, $J=18.4, 8.8$ Hz, H-5), 7.08 (1H, m, H-2), 6.95 (1H, m, H-6), 3.49 and 3.05 (2H, t, $J=7.2$ Hz, H-1''), 3.05 and 2.79 (3H, s, NCH_3), 1.53 and 1.47 (2H, m, H-2''), 1.33 and 1.12 (2H, m, H-3''), 0.88 and 0.76 (3H, t, $J=7.6$ Hz, H-4'').

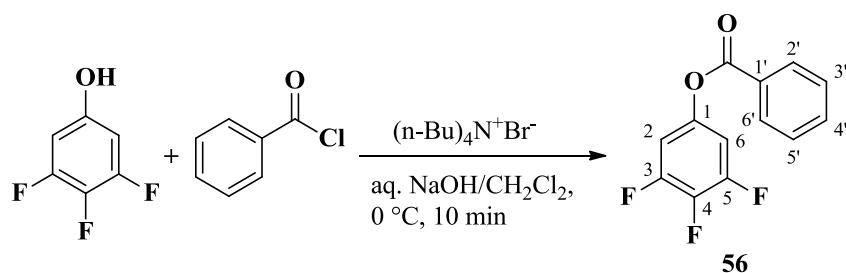
NMR δ_{C} (100 MHz, CDCl_3), 170.4 and 170.2 (C-7'), 164.1 and 164.0 (C-7), 150.2 (dd, $J=248.8, 13.3$ Hz, C-3), 148.5 (dd, $J=246.0, 12.4$ Hz, C-4), 146.2 (d, $J=7.6$ Hz, C-1), 140.2 and 139.9 (C-2'), 133.8 and 133.7 (C-4'), 131.2 (C-6'), 128.9 and 128.8 (C-5'), 127.4 and 127.2 (C-3'), 126.1 and 126.0 (C-1'), 117.8 (m, C-6), 117.4 (dd, $J=19.1, 4.8$ Hz, C-5), 111.8 (dd, $J=20, 6.6$ Hz, C-2), 50.7 and 46.9 (C-1''), 36.7 and 32.3 (NCH_3), 30.0 and 28.9 (C-2''), 20.2 and 19.8 (C-3''), 13.9 and 13.7 (C-4'').

NMR δ_{F} (376 MHz, CDCl_3), 27.5 and 27.4 (1F, m, F-3), 21.3 (1F, m, F-4).

MS, m/z found 346.1260 $\text{C}_{19}\text{H}_{18}\text{F}_2\text{NO}_3$, ($\text{M}-\text{H}^+$) requires 346.1249; found 348.1408 $\text{C}_{19}\text{H}_{20}\text{F}_2\text{NO}_3$, ($\text{M}+\text{H}^+$) requires 348.1406; found 370.1230 $\text{C}_{19}\text{H}_{19}\text{F}_2\text{NO}_3\text{Na}$, ($\text{M}+\text{Na}^+$) requires 370.1225; found 717.2569 $\text{C}_{38}\text{H}_{38}\text{F}_4\text{N}_2\text{O}_6$ Na, ($2\text{M}+\text{Na}^+$) requires 717.2558.

IR, $\nu_{\text{max}}/\text{cm}^{-1}$ 2931 (CH_2), 1743 (C7=O), 1635 (C7'=O), 1242 (C-O), 1141 (C-F).

3,4,5-Trifluorophenyl benzoate (**56**)



Prepared using the phase-transfer condition procedure from 3,4,5-trifluorophenol (0.30 g, 2.00 mmol), benzoyl chloride (0.28 g, 2.00 mmol) and tetra-*n*-butylammonium bromide (0.06 g, 0.20 mmol) yielding **56** as a white solid (0.48 g, 94%) with m.p. 76.3-77.0 °C.

NMR δ_{H} (400 MHz, CDCl_3), 8.19 (2H, m, H-2', H-6'), 7.56 (2H, m, H-3', H-5'), 7.70 (1H, tt, $J=6.8, 1.2$ Hz, H-4'), 7.01-6.93 (2H, m, H-2, H-6).

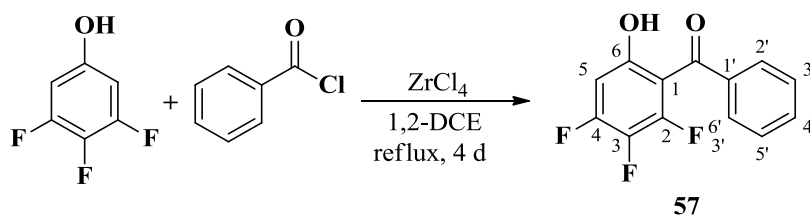
NMR δ_{C} (100 MHz, CDCl_3), 164.4 (C=O), 151.1 (2C, ddd, $J=249.0, 11.0, 5$ Hz, C-3, C-5), 145.5 (1C, td, $J=12.0, 5.0$ Hz, C-1), 138.2 (1C, dt, $J=248.5, 15.1$ Hz, C-4), 134.2 (C-4'), 130.3 (C-2', C-6'), 128.8 (C-3', C-5'), 128.5 (C-1'), 107.2 (2C, dd, $J=17.0, 6.0$ Hz, C-2, C-6).

NMR δ_{F} (376 MHz, CDCl_3), 29.4 (2F, m, F-3, F-5), -1.2 (1F, tt, $J=20.7, 6.0$ Hz, F-4).

MS, m/z found 251.0329, $\text{C}_{13}\text{H}_6\text{F}_3\text{O}_2$, ($\text{M}-\text{H}^+$) requires 251.0314.

IR, $\nu_{\text{max}}/\text{cm}^{-1}$ 1735 (C=O).

2,3,4-Trifluoro-6-hydroxybenzophenone (**57**)



Under anhydrous conditions, a mixture of 3,4,5-trifluorophenol (0.3 g, 2.00 mmol), benzoyl chloride (0.42 g, 3.00 mmol) and zirconium(IV) chloride (0.93, 4.00 mmol) in 1,2-dichloroethane was stirred under reflux for 4 days. After cooling to room temperature, the reaction was quenched with ice water (10 mL) and extracted with ethyl acetate (3 x 10 mL). The organic layer was washed with water (10 mL), dried over anhydrous Mg₂SO₄ and then evaporated. The residue was purified by chromatography on silica gel (elution with petrol ether / ethyl acetate 100:1) to afford **57** (0.170 g, 34%) as a yellow solid. m.p. 87.2-88.6 °C.

NMR δ_{H} (400 MHz, CDCl₃), 11.26 (1H, OH), 7.71 (2H, m, H-2', H-6'), 7.65 (1H, tt, $J=7.6$, 1.2 Hz, H-4'), 7.52 (2H, t, $J=7.6$ Hz, H-3', H-5'), 6.73 (1H, ddd, $J=11.6$, 6.0, 2.4 Hz, H-5).

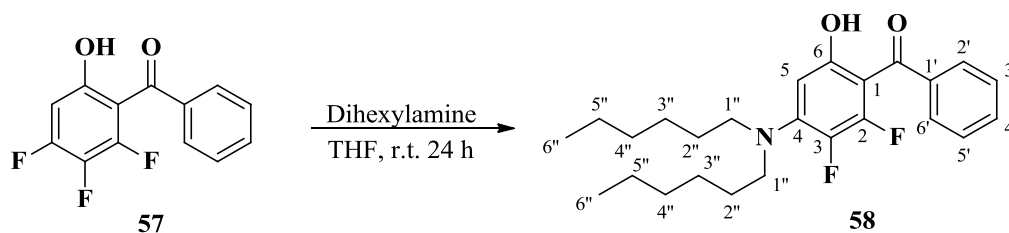
NMR δ_{C} (100 MHz, CDCl₃), 196.8 (C=O), 158.1 (ddd, $J=14.0$, 4.6, 2.3 Hz, C-6), 155.6 (ddd, $J=256.0$, 10.0, 5.0 Hz, C-4), 150.7 (ddd, $J=257.0$, 11.0, 7.0 Hz, C-2), 133.3 (dt, $J=244.0$, 16.0 Hz, C-3), 138.9 (d, $J=3.0$ Hz, C-1'), 133.2 (C-4'), 128.5 (2C, d, $J=4.0$ Hz, C-2', C-6'), 128.4 (2C, C-3', C-5'), 107.3 (1C, ddd, $J=11.7$, 7.6, 2.9 Hz, C-1), 101.2 (ddd, $J=20.0$, 3.0, 1.0 Hz, C-5).

NMR δ_{F} (376 MHz, CDCl₃), 39.9 (1F, m, F-2 or F-4), 39.0 (1F, m, F-2 or F-4), -8.2 (1F, td, $J=22.9$, 6.0 Hz, F-3).

MS, m/z found 251.0326, C₁₃H₆F₃O₂, (M-H⁺) requires 251.0314; found 253.0481 C₁₃H₈F₃O₂, (M+H⁺) requires 253.0471; found 275.0298 C₁₃H₇F₃O₂Na, (M+Na⁺) requires 275.0290.

IR, ν_{max} /cm⁻¹ 3412 (OH), 1650 (C=O), 1159 (C-O).

4-Dihexylamino-2, 3-difluoro-6-hydroxybenzophenone (58)



57 (0.20 g, 0.80 mmol) and dihexylamine (0.56 mL, 2.40 mmol) was dissolved in THF (5 mL). The mixture was stirred at r.t. for 24 h. Then the reaction was quenched with 10 mL water and extracted with ethyl acetate (3 x 10 mL). The extract was dried over anhydrous Mg_2SO_4 and concentrated to afford yellow oil which was purified by chromatography on silica gel (elution with petrol ether/ ethyl acetate 100:1) to give **58** (0.07 g, 22%) as a yellow oil.

NMR δ_{H} (400 MHz, CDCl_3), 12.30 (1H, s, OH), 7.60 (2H, m, H-2', H-6'), 7.51 (1H, tt, $J=7.2$, 2 Hz, H-4'), 7.42 (2H, t, $J=7.2$ Hz, H-3', H-5'), 5.99 (1H, dd, $J=7.6$, 2 Hz, H-5), 3.33 (4H, t, $J=3.2$ Hz, H-1''), 1.60 (4H, m, H-2''), 1.30 (12H, m, H-3'', H-4'', H-5''), 0.89 (6H, t, $J=6.8$ Hz, H-6'').

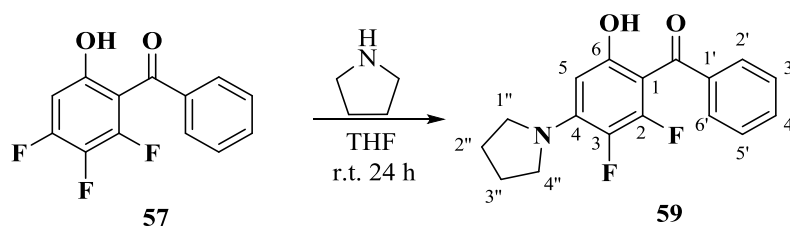
NMR δ_{C} (100 MHz, CDCl_3), 195.9 (C=O), 160.0 (d, $J=5.7$ Hz, C-6), 151.6 (dd, $J=251.8$, 14.3 Hz, C-2), 145.2 (t, $J=4.8$ Hz, C-4), 140.7 (d, $J=2.8$ Hz, C-1'), 134.6 (dd, $J=235.5$, 17.2 Hz, C-3), 131.5 (C-4'), 128.0 (C-2', C-6'), 128.0 (C-3', C-5'), 100.4 (d, $J=12.4$ Hz, C-1), 96.7 (C-5), 53.0 (2C, d, $J=5.8$ Hz, C-1''), 31.6 (2C, C-3''), 28.1 (2C, C-2''), 26.7 (2C, C-4''), 22.7 (2C, C-5''), 14.1 (2C, C-6'').

NMR δ_{F} (376 MHz, CDCl_3), 35.0 (1F, d, $J=19.2$ Hz, F-2), -1.3 (1F, dd, $J=19.2$, 7.1 Hz, F-3).

MS, m/z found 416.2395, $\text{C}_{25}\text{H}_{32}\text{F}_2\text{NO}_2$, ($\text{M}-\text{H}^+$) requires 416.2396; found 418.2571, $\text{C}_{25}\text{H}_{34}\text{F}_2\text{NO}_2$, ($\text{M}+\text{H}^+$) requires 418.2552; found 440.2390, $\text{C}_{25}\text{H}_{33}\text{F}_2\text{NO}_2\text{Na}$, ($\text{M}+\text{Na}^+$) requires 440.2372.

IR, $\nu_{\text{max}}/\text{cm}^{-1}$ 3500-3000 (OH), 2924 (CH_2), 1643 (C=O), 1296 (C-O), 1126 (C-F).

2,3-Difluoro-4-(pyrrolidin-1-yl)-6-hydroxybenzophenone (**59**)



Following the method outlined for **58**, a mixture of **57** (0.20 g, 0.78 mmol) and pyrrolidine (0.20 mL, 2.30 mmol) in THF (5 mL) was stirred at room temperature for 24 h. Work-up as previously and purification by chromatography on silica gel (elution with petrol ether / ethyl acetate 100:1) afforded **59** (0.24 g, 99%) as a yellow oil with m.p. 121.4-122.8 °C.

NMR δ_{H} (400 MHz, CDCl_3), 12.48 (1H, s, OH), 7.58 (2H, m, H-2', H-6'), 7.50 (1H, tt, $J=7.6$, 1.6 Hz, H-4'), 7.43 (2H, tt, $J=7.6$, 1.6 Hz, H-3', H-5'), 5.90 (1H, dd, $J=7.2$, 2 Hz, H-5), 3.54 (4H, m, H-1'', H-4''), 1.98 (4H, m, H-2'', H-3'').

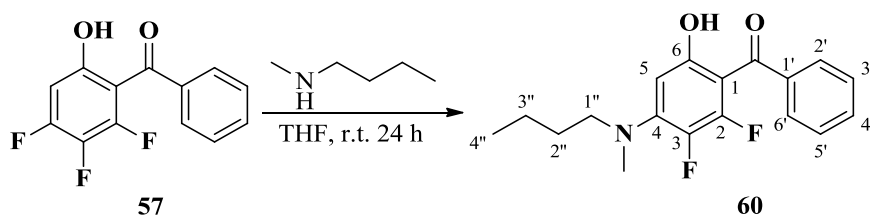
NMR δ_{C} (100 MHz, CDCl_3), 195.9 (C=O), 160.4 (d, $J=5.7$ Hz, C-6), 151.2 (dd, $J=252.7$, 13.3 Hz, C-2), 144.1 (t, $J=5.7$ Hz, C-4), 140.8 (d, $J=2.8$ Hz, C-1'), 133.8 (dd, $J=234.5$, 16.2 Hz, C-3), 131.4 (C-4'), 128.0 (2C, C-3', C-5'), 127.9 (2C, d, $J=2.8$ Hz, C-2', C-6'), 100.0 (d, $J=12.4$ Hz, C-1), 95.8 (C-5), 50.0 (2C, d, $J=5.7$ Hz, C-1'', C-4''), 25.4 (2C, d, $J=1.7$ Hz, C-2'', C-3'').

NMR δ_{F} (376 MHz, CDCl_3), 33.9 (1F, ddd, $J=19.6$, 5.3, 3.0 Hz, F-2), -4.3 (1F, m, F-3).

MS, m/z found 302.0990, $\text{C}_{17}\text{H}_{14}\text{F}_2\text{NO}_2$, ($\text{M}-\text{H}^+$) requires 302.0987; found 304.1158, $\text{C}_{17}\text{H}_{16}\text{F}_2\text{NO}_2$, ($\text{M}+\text{H}^+$) requires 304.1144; found 326.0978, $\text{C}_{17}\text{H}_{15}\text{F}_2\text{NO}_2\text{Na}$, ($\text{M}+\text{Na}^+$) requires 326.0963.

IR, $\nu_{\text{max}}/\text{cm}^{-1}$ 3500-3000 (OH), 2970 (CH_2), 1643 (C=O), 1211 (C-O), 1064 (C-F).

4-(But-1-yl(methyl)amino)-2,3-difluoro-6-hydroxybenzophenone (**60**)



Following the method outlined for **58**, a mixture of **57** (0.16 g, 0.64 mmol) and *N*-methyl-1-butylamine (0.19 mL, 1.60 mmol) in THF (5 mL) was stirred at room temperature for 24 h. Work-up as previously and purification by chromatography on silica gel (elution with petrol ether / ethyl acetate 100:1) afforded **60** (0.25 g, 99%) as a yellow oil.

NMR δ_{H} (400 MHz, CDCl_3), 12.30 (1H, s, OH), 7.60 (2H, m, H-2', H-6'), 7.51 (1H, tt, $J=7.6$, 2 Hz, H-4'), 7.43 (2H, t, $J=7.6$ Hz, H-3', H-5'), 6.02 (1H, dd, $J=7.6$, 2.0 Hz, H-5), 3.39 (2H, td, $J=8.0$, 1.2 Hz, H-1''), 3.04 (3H, d, $J=1.6$ Hz, CH_3), 1.62 (2H, m, H-2''), 1.33 (2H, m, H-3''), 0.94 (3H, t, $J=7.2$ Hz, H-4'').

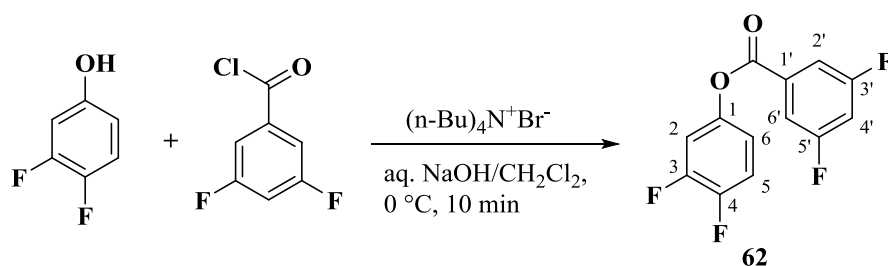
NMR δ_{C} (100 MHz, CDCl_3), 196.1 (C=O), 160.0 (d, $J=6.6$ Hz, C-6), 151.2 (dd, $J=251.7$, 13.3 Hz, C-2), 146.3 (t, $J=5.8$ Hz, C-4), 140.6 (d, $J=2.9$ Hz, C-1'), 134.9 (dd, $J=236.5$, 17.2 Hz, C-3), 131.6 (C-4'), 128.1 (C-2', C-6'), 128.0 (C-3', C-5'), 100.8 (d, $J=11.4$ Hz, C-1), 97.2 (C-5), 54.5 (d, $J=7.6$ Hz, C-1''), 40.1 (d, $J=4.7$ Hz, NCH_3), 30.1 (C-2''), 20.1 (C-3''), 14.0 (C-4'').

NMR δ_{F} (376 MHz, CDCl_3), 34.6 (1F, ddd, $J=19.2$, 4.9, 3.0 Hz, F-2), 17.7 (1F, dd, $J=19.2$, 6.8 Hz, F-3).

MS, m/z found 318.1302, $\text{C}_{18}\text{H}_{18}\text{F}_2\text{NO}_2$, ($\text{M}-\text{H}^+$) requires 318.1300; found 320.1472, $\text{C}_{18}\text{H}_{20}\text{F}_2\text{NO}_2$, ($\text{M}+\text{H}^+$) requires 320.1457, 342.1291; 342.1291, $\text{C}_{18}\text{H}_{19}\text{F}_2\text{NO}_2\text{Na}$, ($\text{M}+\text{Na}^+$) requires 342.1276.

IR, $\nu_{\text{max}}/\text{cm}^{-1}$ 3500-3000 (OH), 2931 (CH_2), 1643 (C=O), 1242 (C-O), 1118 (C-F).

3,4-Difluorophenyl 3',5'-difluorobenzoate (**62**)



Prepared using the phase-transfer condition procedure from 3,4-difluorophenol (0.39 g, 3.00 mmol), 3,5-difluorobenzoyl chloride (0.53 g, 3.00 mmol) and tetra-*n*-butylammonium bromide (0.10 g, 0.30 mmol) yielding **62** as a white solid (0.64 g, 79%) with m.p. 83.2-84.1 °C.

NMR δ_{H} (400 MHz, CDCl_3), 7.67 (2H, m, H-2', H-6'), 7.24-7.16 (1H, dd, $J=18.8, 9.2$ Hz, H-5), 7.11 (2H, m, H-2, H-4'), 6.96 (1H, m, H-6).

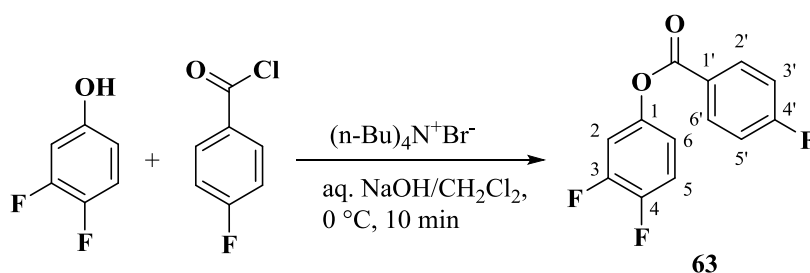
NMR δ_{C} (100 MHz, CDCl_3), 163.0 (2C, dd, $J=249.8, 11.4$ Hz, C-3', C-5'), 162.7 (C=O), 150.3 (dd, $J=248.9, 14.3$ Hz, C-3), 148.6 (dd, $J=246.0, 12.4$ Hz, C-4), 146.0 (dd, $J=8.6, 2.9$ Hz, C-1), 132.1 (t, $J=9.5$ Hz, C-1'), 117.6 (2C, m, C-5, C-6), 113.4 (2C, dd, $J=19.1, 7.7$ Hz, C-2', C-6'), 111.7 (d, $J=20.0$ Hz, C-2), 109.5 (t, $J=24.8$ Hz, C-4').

NMR δ_{F} (376 MHz, CDCl_3), 54.3 (2F, m, F-3', F-5'), 27.9 (1F, m, F-3), 21.9 (1F, m, F-4).

MS, m/z found 269.0236, $\text{C}_{13}\text{H}_5\text{F}_4\text{O}_2$, (M-H⁺) requires 269.0220.

IR, $\nu_{\text{max}}/\text{cm}^{-1}$ 1743 (C=O).

3,4-Difluorophenyl 4'-fluorobenzoate (**63**)



Prepared using the phase-transfer condition procedure from 3,4-difluorophenol (0.65 g, 5.00 mmol), 4-fluorobenzoyl chloride (0.59 mL, 5.00 mmol) and tetra-*n*-butylammonium bromide (0.16 g, 0.50 mmol) yielding **63** as a white solid (1.16 g, 92%) with m.p. 55.9-56.7 °C.

NMR δ_{H} (400 MHz, CDCl_3), 8.19 (2H, m, H-2', H-6'), 7.24-7.16 (3H, m, H-5, H-3', H-5'), 7.08 (1H, m, H-2), 6.96 (1H, m, H-6).

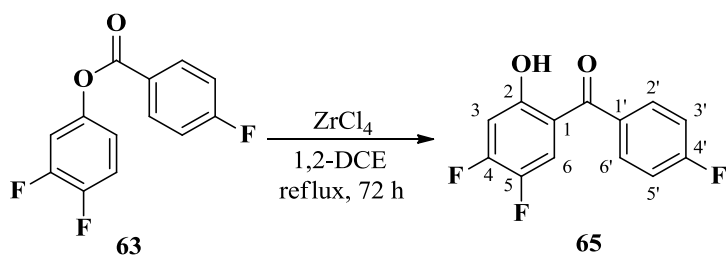
NMR δ_{C} (100 MHz, CDCl_3), 166.4 (1C, d, $J=254.6$ Hz, C-4'), 163.9 (C=O), 150.3 (1C, dd, $J=248.9, 14.3$ Hz, C-3), 148.6 (1C, dd, $J=246.0, 12.4$ Hz, C-4), 146.4 (1C, dd, $J=8.6, 3.8$ Hz, C-1), 133.0 (2C, d, $J=9.5$ Hz, C-2', C-6'), 125.2 (1C, d, $J=2.8$ Hz, C-1'), 117.7 (1C, m, C-6), 117.4 (1C, d, $J=19.1$ Hz, C-5), 116.0 (2C, d, $J=22$ Hz, C-3', C-5'), 111.8 (1C, d, $J=20.0$ Hz, C-2).

NMR δ_{F} (376 MHz, CDCl_3), 58.3 (1F, m, F-4'), 27.5 (1F, m, F-3), 21.2 (1F, m, F-4).

MS, m/z found 251.0328, $\text{C}_{13}\text{H}_6\text{F}_3\text{O}_2$, ($\text{M}-\text{H}^+$) requires 251.0314

IR, $\nu_{\text{max}}/\text{cm}^{-1}$ 1735 (C=O).

4,5-Difluoro-4'-fluoro-2-hydroxybenzophenone (**65**)



The Fries rearrangement procedure was followed with **63** (1.37 g, 5.45 mmol) and ZrCl₄ (2.54 g, 10.90 mmol) under reflux for 72 h. The crude product was purified by chromatography on silica gel (elution with petrol ether/ ethyl acetate 50:1) to afford **65** (0.94 mg, 68%) as a yellow oil.

NMR δ_{H} (400 MHz, CDCl₃), 12.03 (1H, d, $J=0.8$ Hz, OH), 7.69 (2H, m, H-2', H-6'), 7.39 (1H, dd, $J=10.4, 9.2$ Hz, H-6), 7.21 (2H, m, H-3', H-5'), 6.86 (1H, dd, $J=10.8, 6.4$ Hz, H-3).

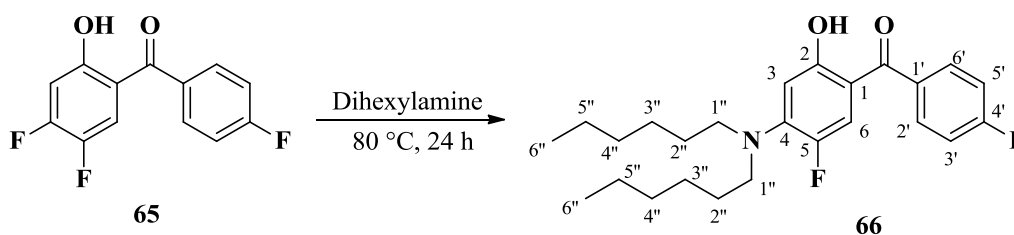
NMR δ_{C} (100 MHz, CDCl₃), 198.3 (C=O), 165.3 (d, $J=252.7$ Hz, C-4'), 161.1 (d, $J=11.5$ Hz, C-2), 155.7 (dd, $J=259.4, 14.3$ Hz, C-4), 143.3 (dd, $J=241.2, 14.3$ Hz, C-5), 133.4 (d, $J=3.0$ Hz, C-1'), 131.6 (2C, d, $J=9.6$ Hz, C-2', C-6'), 120.4 (dd, $J=19.0, 2.8$ Hz, C-6), 116.0 (2C, d, $J=22.0$ Hz, C-3', C-5'), 114.6 (C-1), 107.2 (d, $J=20.1$ Hz, C-3).

NMR δ_{F} (376 MHz, CDCl₃), 56.9 (1F, m, F-4'), 39.3 (1F, m, F-4), 14.6 (1F, m, F-5).

MS, m/z found 253.0468, C₁₃H₈F₃O₂, (M+H⁺) requires 253.0471.

IR, $\nu_{\text{max}}/\text{cm}^{-1}$ 3400-3020 (OH), 1597 (C=O), 1157 (C-O).

4-Dihexylamino-5-fluoro-4'-fluoro-2-hydroxybenzophenone (**66**)



A mixture of **65** (0.25 g, 1.00 mmol) and dihexylamine (1 mL) was stirred at 80 °C for 24 h. After cooling to room temperature, the reaction was quenched with ice water (10 mL) and extracted with ethyl acetate (3 x 10 mL). The organic layer was washed with water and then evaporated. The residue was purified by chromatography on silica gel (elution with petrol ether / ethyl acetate 100:1) to afford compound **66** (0.24 g, 58%) as a yellow oil.

NMR δ_{H} (400 MHz, CDCl_3), 12.57 (1H, s, OH), 7.63 (2H, m, H-2', H-6'), 7.15 (2H, tt, $J=8.4$, 2 Hz, H-3', H-5'), 7.06 (1H, d, $J=16$ Hz, H-6), 6.18 (1H, d, $J=8$ Hz, H-3), 3.32 (4H, t, $J=6.8$ Hz, H-1''), 1.59 (4H, m, H-2''), 1.27 (12H, m, H-3'', H-4'', H-5''), 0.88 (6H, t, $J=6.8$ Hz, H-6'').

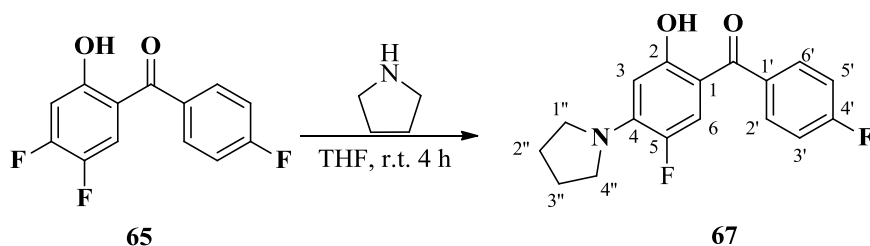
NMR δ_{C} (100 MHz, CDCl_3), 196.1 (C=O), 164.5 (d, $J=250.8$ Hz, C-4'), 162.2 (COH), 145.3 (d, $J=8.6$ Hz, C-4), 144.7 (d, $J=234.5$ Hz, C-5), 134.6 (d, $J=2.9$ Hz, C-1'), 131.1 (2C, d, $J=8.5$ Hz, C-2', C-6'), 119.3 (d, $J=25.8$ Hz, C-6), 115.5 (2C, d, $J=21.9$ Hz, C-3', C-5'), 107.7 (d, $J=6.7$ Hz, C-1), 102.1 (d, $J=3.8$ Hz, C-3), 52.9 (d, $J=6.7$ Hz, C-1''), 31.7 (C-3''), 28.0 (C-2''), 26.7 (C-4''), 22.7 (C-5''), 14.1 (C-6'').

NMR δ_{F} (376 MHz, CDCl_3), 53.9 (1F, m, F-4'), 27.0 (1F, dd, $J=15.8$, 7.9 Hz, F-5).

MS, m/z found 418.2559, $\text{C}_{25}\text{H}_{34}\text{F}_2\text{NO}_2$, ($\text{M}+\text{H}^+$) requires 418.2552; found 441.2413, $\text{C}_{25}\text{H}_{33}\text{F}_2\text{NO}_2\text{Na}$, ($\text{M}+\text{Na}^+$) requires 441.2450; found 857.4775, $\text{C}_{50}\text{H}_{66}\text{F}_4\text{N}_2\text{O}_4\text{Na}$, ($2\text{M}+\text{Na}^+$) requires 857.4851.

IR, $\nu_{\text{max}}/\text{cm}^{-1}$ 3500-3000 (OH), 2931 (CH_2), 1635 (C=O), 1111 (C-F).

5-Fluoro-4-(pyrrolidin-1-yl)-4'-fluoro-2-hydroxybenzophenone (**67**)



A mixture of **65** (0.25 g, 1.00 mmol) and pyrrolidine (1.0 mL) was stirred at r.t. for 4 h. The reaction was quenched with ice water (10 mL) and extracted with ethyl acetate (3 x 10 mL). The organic layer was washed with water and then evaporated. The residue was purified by chromatography on silica gel (elution with petrol ether/ ethyl acetate 20:1) to afford **67** (0.14 g, 56%) as yellow solid with m.p. 122.2-123.2 °C and **68** (0.13 g, 39%) as a yellow solid with m.p. 234.1-235.4 °C

NMR δ_{H} (400 MHz, CDCl_3), 12.71 (1H, s, OH), 7.62 (2H, m, H-2', H-6'), 7.15 (2H, tt, $J=8.4$, 2.0 Hz, H-3', H-5'), 7.05 (1H, d, $J=15.2$ Hz, H-6), 6.07 (1H, d, $J=8.0$ Hz, H-3), 3.53 (4H, m, H-1'', H-4''), 1.96 (4H, m, H-2'', H-3'').

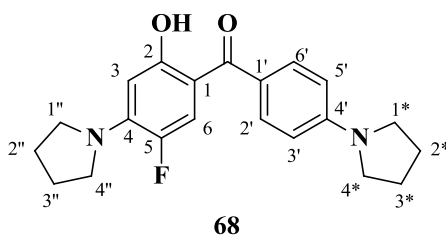
NMR δ_{C} (100 MHz, CDCl_3), 196.0 (C=O), 164.5 (d, $J=250.7$ Hz, C-4'), 162.6 (COH), 144.2 (d, $J=11.4$ Hz, C-4), 143.9 (d, $J=233.6$ Hz, C-5), 134.8 (d, $J=3.8$ Hz, C-1'), 131.0 (2C, d, $J=8.5$ Hz, C-2', C-6'), 118.6 (d, $J=23.8$ Hz, C-6), 115.5 (2C, d, $J=21.9$ Hz, C-3', C-5'), 107.7 (d, $J=6.7$ Hz, C-1), 100.9 (d, $J=4.7$ Hz, C-3), 50.0 (d, $J=5.7$ Hz, C-1'', C-4''), 25.4 (d, $J=1.9$ Hz, C-2'', C-3'').

NMR δ_{F} (376 MHz, CDCl_3), 53.6 (1F, m, F-4'), 23.5 (1F, m, F-5).

MS, m/z found 304.1149, $\text{C}_{17}\text{H}_{16}\text{F}_2\text{NO}_2$, ($\text{M}+\text{H}^+$) requires 304.1144; found 326.0968, $\text{C}_{17}\text{H}_{15}\text{F}_2\text{NO}_2\text{Na}$, ($\text{M}+\text{Na}^+$) requires 326.0963.

IR, $\nu_{\text{max}}/\text{cm}^{-1}$ 3500-3000 (OH, NH), 2954 (CH_2), 1635 (C=O), 1126 (C-O), 1095 (C-F).

5-Fluoro-4-(pyrrolidin-1-yl)-4'-(pyrrolidin-1-yl)-2-hydroxybenzophenone (68)



NMR δ_{H} (400 MHz, CDCl_3), 12.97 (1H, s, OH), 7.62 (2H, dt, $J=8.8, 2.0$ Hz, H-2', H-6'), 7.26 (1H, d, $J=15.6$ Hz, H-6), 6.55 (2H, dt, $J=8.8, 2.0$ Hz, H-3', H-5'), 6.09 (1H, d, $J=8.4$ Hz, H-3), 3.51 (4H, m, H-1'', H-4''), 3.36 (4H, m, H-1*, H-4*), 2.05 (4H, m, H-2*, H-3*), 1.96 (4H, m, H-2'', H-3'').

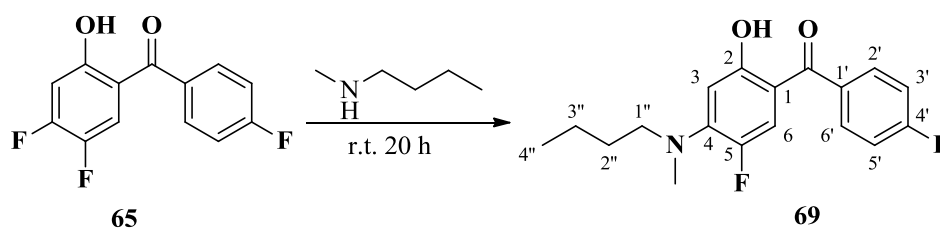
NMR δ_{C} (100 MHz, CDCl_3), 196.1 (C=O), 161.9 (COH), 150.2 (C-4'), 143.8 (d, $J=231.7$ Hz, C-5), 143.2 (d, $J=11.5$ Hz, C-4), 131.6 (2C, C-2', C-6'), 125.0 (C-1'), 118.9 (d, $J=23.8$ Hz, C-6), 115.5 (2C, d, $J=22.9$ Hz, C-6), 110.8 (2C, C-3', C-5'), 107.7 (d, $J=5.8$ Hz, C-1), 101.0 (d, $J=4.7$ Hz, C-3), 49.8 (2C, d, $J=5.7$ Hz, C-1'', C-4''), 47.6 (2C, C-1*, C-4*), 25.5 (4C, C-2'', C-3'', C-2*, C-3*).

NMR δ_{F} (376 MHz, CDCl_3), 22.5 (1F, m, F-5).

MS, m/z found 355.1825, $\text{C}_{21}\text{H}_{24}\text{FN}_2\text{O}_2$, ($\text{M}+\text{H}^+$) requires 355.1816; found 377.1643, $\text{C}_{21}\text{H}_{23}\text{FN}_2\text{O}_2\text{Na}$, ($\text{M}+\text{Na}^+$) requires 377.1636; found 731.3395, $\text{C}_{42}\text{H}_{46}\text{F}_2\text{N}_4\text{O}_4\text{Na}$, ($2\text{M}+\text{Na}^+$) requires 731.3379.

IR, $\nu_{\text{max}}/\text{cm}^{-1}$ 3500-3000 (OH, NH), 2962 (CH_2), 1604 (C=O), 1165 (C-O).

4-Butyl(methyl)amino-5-fluoro-4'-fluoro-2-hydroxybenzophenone (**69**)



A mixture of **65** (0.14 g, 0.54 mmol) and *N*-methyl-1-butylamine (0.5 mL) was stirred at r.t. for 20 h. The reaction was quenched with ice water (10 mL) and extracted with ethyl acetate (3 x 10 mL). The organic layer was washed with water and then evaporated. The residue was purified by chromatography on silica gel (elution with petrol ether/ ethyl acetate 100:1) to afford **69** (0.10 g, 58%) as a yellow oil.

NMR δ_{H} (400 MHz, CDCl_3), 12.55 (1H, s, OH), 7.63(2H, m, H-2', H-6'), 7.15(2H, d, $J=8.8$ Hz, H-3', H-5'), 7.07(1H, d, $J=15.6$ Hz, H-6), 6.21(1H, d, $J=8.4$ Hz, H-3), 3.38 (2H, t, $J=8.0$ Hz, H-1''), 3.02 (3H, d, $J=2.0$ Hz, NCH_3), 1.57 (2H, m, H-2''), 1.28 (2H, m, H-3''), 0.92(3H, t, $J=7.6$ Hz, H-4'').

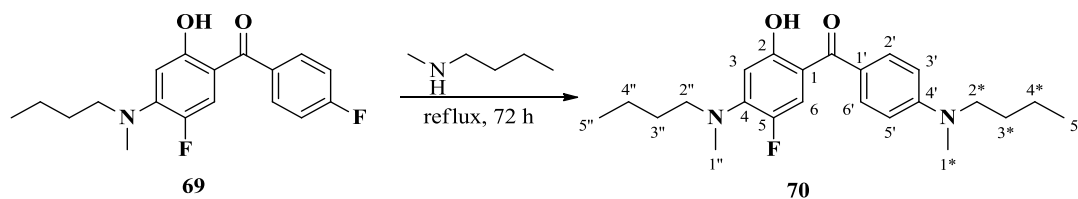
NMR δ_{C} (100 MHz, CDCl_3), 196.4 (C=O), 164.6 (d, $J=250.7$ Hz, C-4'), 162.2 (C-2), 146.3 (d, $J=21.9$ Hz, C-4), 145.2 (d, $J=266.0$ Hz, C-5), 134.6 (d, $J=3.8$ Hz, C-1'), 131.1 (2C, d, $J=8.6$ Hz, C-2', C-6'), 119.1 (d, $J=24.8$ Hz, C-6), 115.5 (2C, d, $J=21.0$ Hz, C-3', C-5'), 108.1 (d, $J=6.7$ Hz, C-1), 102.6 (d, $J=3.9$ Hz, C-3), 54.5 (d, $J=8.6$ Hz, C-1''), 40.0 (NCH_3), 30.0 (C-2''), 20.1 (C-3''), 14.0 (C-4'').

NMR δ_{F} (376 MHz, CDCl_3), 54.0 (1F, m, F-4'), 17.7 (1F, m, F-5).

MS, m/z found 320.1454, $\text{C}_{18}\text{H}_{20}\text{F}_2\text{NO}_2$, ($\text{M}+\text{H}^+$) requires 320.1457; found 342.1273, $\text{C}_{18}\text{H}_{19}\text{F}_2\text{NO}_2\text{Na}$, ($\text{M}+\text{Na}^+$) requires 342.1276; found 661.2656, $\text{C}_{36}\text{H}_{38}\text{F}_4\text{N}_2\text{O}_4\text{Na}$, ($2\text{M}+\text{Na}^+$) requires 661.2660.

IR, $\nu_{\text{max}}/\text{cm}^{-1}$ 3400-3000 (OH), 1635 (C=O), 1157 (C-O), 1111(C-F).

4-But-1-yl(methyl)amino-4'-(but-1-yl(methyl)amino-5-fluoro-2-hydroxybenzophenone
(70)



A mixture of **69** (0.26 g, 0.80 mmol) and *N*-methyl-1-butylamine (2 mL) was stirred under reflux for 72 h. After cooling to room temperature, the reaction was quenched with ice water (10 mL) and extracted with ethyl acetate (3 x 10 mL). The organic layer was washed with water and then evaporated. The residue was purified by chromatography on silica gel (elution with petrol ether/ ethyl acetate 20:1) to afford **70** (0.07 g, 23%) as a yellow oil.

NMR δ_{H} (400 MHz, CDCl_3), 12.80 (1H, s, OH), 7.66 (2H, dt, $J=8.8, 2.8$ Hz, H-2', H-6'), 7.32 (1H, d, $J=15.6$ Hz, H-6), 6.72 (2H, d, $J=8.8$ Hz, H-3', H-5'), 6.28 (1H, d, $J=8.0$ Hz, H-3), 3.41 (4H, m, H-2'', H-2*), 3.06 (3H, s, H-1*), 3.02 (3H, d, $J=1.6$ Hz, H-1''), 1.63 (4H, m, H-3'', H-3*), 1.28 (4H, m, H-4'', H-4*), 0.99 (3H, t, $J=7.6$ Hz, CH_3), 0.96 (3H, t, $J=7.6$ Hz, CH_3).

NMR δ_{C} (100 MHz, CDCl_3), 196.2 (C=O), 161.5 (C-2), 151.8 (C-4'), 145.5 (d, $J=9.5$ Hz, C-4), 145.2 (d, $J=233.6$ Hz, C-5), 131.1 (2C, C-2', C-6'), 125.0 (C-1'), 119.3 (d, $J=24.8$ Hz, C-6), 110.6 (2C, C-3', C-5'), 109.1 (d, $J=6.7$ Hz, C-1), 103.1 (d, $J=3.8$ Hz, C-3), 54.4 (d, $J=8.5$ Hz, C-2''), 52.3 (C-2*), 39.8 (d, $J=3.8$ Hz, C-1''), 38.5 (C-1*), 29.9 (C-3''), 29.1 (C-3*), 20.4 (C-4''), 20.2 (C-4*), 14.1 (C-5''), 14.0 (C-5*).

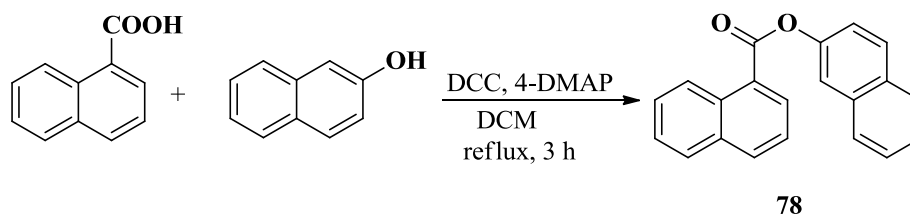
NMR δ_{F} (376 MHz, CDCl_3), 27.3 (1F, dd, $J=15.4, 7.9$ Hz, F-5).

MS, m/z found 387.2454, $\text{C}_{23}\text{H}_{32}\text{FN}_2\text{O}_2$, ($\text{M}+\text{H}^+$) requires 387.2442; found 409.2275, $\text{C}_{23}\text{H}_{31}\text{N}_2\text{FO}_2\text{Na}$, ($\text{M}+\text{Na}^+$) requires 409.2262; found 795.4658, $\text{C}_{46}\text{H}_{62}\text{F}_2\text{N}_4\text{O}_4\text{Na}$, ($2\text{M}+\text{Na}^+$) requires 795.4631.

IR, $\nu_{\text{max}}/\text{cm}^{-1}$ 3400 (OH), 1632 (C=O), 1187 (C-O).

Chapter 4. Synthesis and stabilisation new hydroxybenzophenones and related naphthalene analogues

Naphthalen-2-yl-1-naphthoate (**78**)^[179]



Following the procedure in the literature.^[161] 1-Napthoic acid (0.21 g, 1.20 mmol), 2-naphtol (0.14 g, 1.00 mmol), 4-dimethylaminopyridine (4-DMAP) (0.01 g, 0.10 mmol) and *N,N*-dicyclohexylcarbodiimide (DCC) (0.24 g, 1.20 mmol) were dissolved in DCM (10 mL). The crude product was purified by chromatography on silica gel (elution with petrol ether/ethyl acetate 50:1) to give **78** (0.17 g, 56%) as a white solid. m.p. 117.2-120.0 °C.

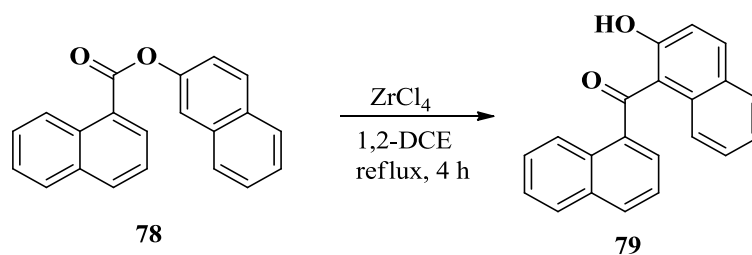
NMR δ_{H} (400 MHz, CDCl_3), 9.06 (1H, d, $J=8.4$ Hz), 8.54 (1H, d, $J=7.2$ Hz), 8.12 (1H, d, $J=8$ Hz), 7.94 (2H, d, $J=8.8$ Hz), 7.88 (2H, m), 7.75 (1H, s), 7.68-7.56 (3H, m), 7.51 (2H, m), 7.43 (1H, dd, $J=8.8, 2.4$ Hz).

NMR δ_{C} (100 MHz, CDCl_3), 166.1 (C=O), 148.7, 134.5, 134.0, 133.9, 131.8, 131.7, 131.4, 129.6, 128.8, 128.3, 127.9, 127.8, 126.7, 126.5, 126.0, 125.9, 124.6, 121.5, 118.9.

MS, m/z found 299.1066, $\text{C}_{21}\text{H}_{15}\text{O}_2$, ($\text{M}+\text{H}^+$) requires 299.1067; found 321.0084 $\text{C}_{21}\text{H}_{14}\text{O}_2\text{Na}$, ($\text{M}+\text{Na}^+$) requires 321.0886; found 619.1877, $\text{C}_{42}\text{H}_{28}\text{O}_4\text{Na}$, ($2\text{M}+\text{Na}^+$) requires 619.1880.

IR, $\nu_{\text{max}}/\text{cm}^{-1}$ 2924 (CH), 1720 (C=O).

(2-Hydroxynaphthalen-1-yl)(naphthalen-1-yl)methanone (79)



The Fries rearrangement procedure was followed with **78** (0.15 g, 0.50 mmol) and ZrCl_4 (0.23 g, 1.00 mmol) under reflux for 4 h. The crude product was purified by chromatography on silica gel (elution with petrol ether/ ethyl acetate 100:1) to afford **79** (0.04 g, 24%) as a yellow oil.

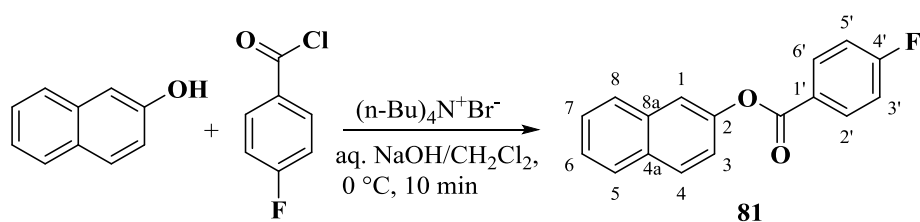
NMR δ_{H} (400 MHz, CDCl_3), 12.76 (1H, s, OH), 8.29 (1H, m), 8.04-7.97 (3H, m), 7.75 (1H, d, $J=8.0$ Hz), 7.58 (2H, m), 7.39 (2H, m), 7.31 (1H, d, $J=9.2$ Hz), 7.21 (1H, m), 7.11 (1H, d, $J=8.4$ Hz), 6.97 (1H, m).

NMR δ_{C} (100 MHz, CDCl_3), 202.0 (C=O), 138.6, 137.7, 134.1, 132.4, 131.7, 129.9, 128.8, 128.6, 128.5, 127.9, 127.7, 127.2, 126.7, 125.6, 125.4, 124.9, 123.7, 119.5, 114.8.

GC-MS, m/z found 298.4, 171.2, 155.2, 127.2.

IR, $\nu_{\text{max}}/\text{cm}^{-1}$ 3500-3300 (OH), 1621 (C=O).

Naphthalen-2-yl 4'-fluorobenzoate (**81**)



Prepared using phase-transfer condition procedure from 2-naphthol (0.29 g, 2.00 mmol), 4-fluorobenzoyl chloride (0.24 mL, 2.00 mmol) and tetra-*n*-butylammonium bromide (0.16 g, 0.50 mmol) yielding **81** as a white solid (0.53 g, 100%) with m.p. 156.1-158.2°C.

NMR δ_{H} (400 MHz, CDCl_3), 8.31 (2H, m, H-2', H-6'), 7.94 (1H, d, $J=8.8$ Hz, H-4), 7.90 (2H, m, H-5, H-8), 7.72 (1H, d, $J=2.0$ Hz, H-1), 7.54 (2H, m, H-6, H-7), 7.38 (1H, dd, $J=8.8, 2.0$ Hz, H-3), 7.24 (2H, td, $J=8.8, 2.0$ Hz, H-3', H-5').

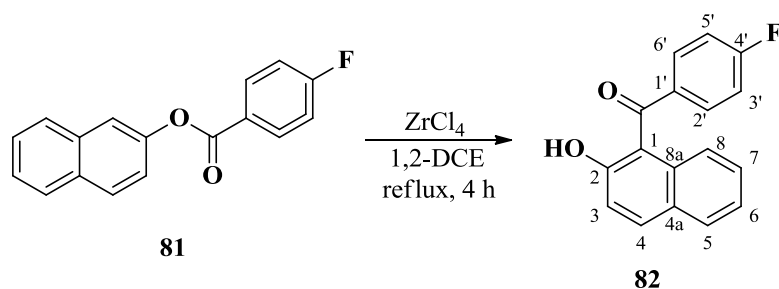
NMR δ_{C} (100 MHz, CDCl_3), 166.2 (d, $J=254.0$ Hz, C-4'), 164.4 (C=O), 148.5 (C-2), 133.8, 132.9 (d, $J=10.0$ Hz, C-2', C-6'), 131.6 (C-4a), 129.5, 127.8, 127.7, 126.7, 125.8, 121.1 (C-3), 118.7 (C-1), 115.9 (d, $J=22.0$ Hz, C-3', C-5').

NMR δ_{F} (376 MHz, CDCl_3), 57.7 (1F, m)

MS, m/z found 267.0815, $\text{C}_{17}\text{H}_{12}\text{FO}_2$, ($\text{M}+\text{H}^+$) requires 267.0816; found 289.0635 $\text{C}_{17}\text{H}_{11}\text{FO}_2\text{Na}$, ($\text{M}+\text{Na}^+$) requires 289.0635.

IR, $\nu_{\text{max}}/\text{cm}^{-1}$ 1732 (C=O).

1-(4'-Fluorobenzoyl)-2-naphthol (**81**)



The Fries rearrangement procedure was followed with **81** (0.53 g, 2.00 mmol) and ZrCl_4 (0.93 g, 4.00 mmol) under reflux for 20 h. The crude product was purified by chromatography on silica gel (elution with petrol ether/ ethyl acetate 20:1) to afford **82** (0.44 g, 82%) as a yellow solid. m.p. 136.9-137.6 °C.

NMR δ_{H} (400 MHz, CDCl_3), 10.96 (1H, s, OH), 7.96 (1H, d, $J=9.2$ Hz, H-4), 7.79 (1H, d, $J=8.4$ Hz, H-8), 7.69 (2H, m, H-2', H-6'), 7.35-7.22 (4H, m, H-3, H-5, H-6, H-7), 7.11 (2H, t, $J=8.8$ Hz, H-3', H-5').

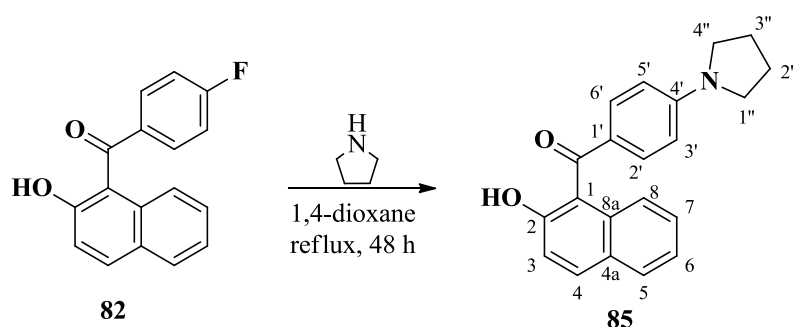
NMR δ_{C} (100 MHz, CDCl_3), 198.6 (C=O), 165.5 (d, $J=254.0$ Hz, C-4'), 161.0 (C-2), 136.4 (C-1'), 136.3 (C-8a), 136.2 (C-4), 132.2 (d, $J=9.0$ Hz, C-2', C-6'), 128.7 (C-8), 128.5 (C-4a), 126.9, 126.1, 123.8, 119.2, 115.7 (d, $J=22.0$ Hz, C-3', C-5'), 114.4 (C-1).

NMR δ_{F} (376 MHz, CDCl_3), 56.74 (1F, m)

MS, m/z found 265.0661, $\text{C}_{17}\text{H}_{10}\text{FO}_2$, ($\text{M}-\text{H}^+$) requires 265.0659; found 267.0825, $\text{C}_{17}\text{H}_{12}\text{FO}_2$, ($\text{M}+\text{H}^+$) requires 267.0816; found 289.0645 $\text{C}_{17}\text{H}_{11}\text{FO}_2\text{Na}$, ($\text{M}+\text{Na}^+$) requires 289.0635.

IR, $\nu_{\text{max}}/\text{cm}^{-1}$ 3336 (OH), 1596 (C=O), 1236 (C-O).

1-(4'-Pyrrolidinobenzoyl)-2-naphthol (**85**)



The mixture of **82** (0.27 g, 1.00 mmol) and pyrrolidine (0.34 mL, 4.00 mmol) in 1,4-dioxane (10 mL) was stirred and heated under reflux for 48 h. After cooling to room temperature, the reaction was quenched with 10 mL ice water and extracted with ethyl acetate (3 x 15 mL). The organic layer was washed with brine (2 x 10 mL), dried over anhydrous Mg_2SO_4 and concentrated to afford a yellow oil which was purified by chromatography on silica gel (elution with petrol ether/ ethyl acetate 10:1) to give **85** (0.14 g, 44%) as a yellow solid. m.p. 170.5-172.5 °C

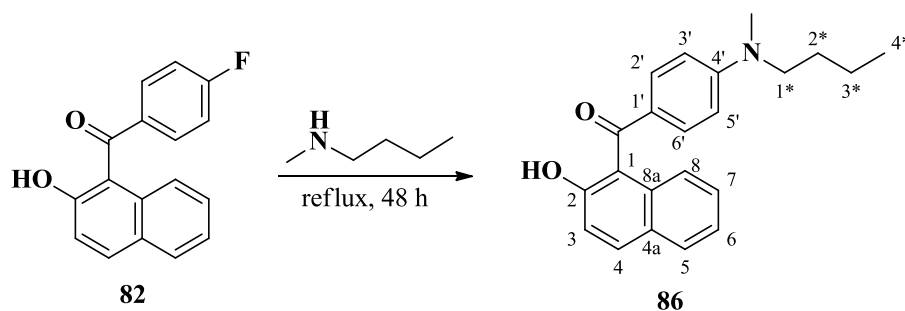
NMR δ_{H} (400 MHz, CDCl_3), 10.06 (1H, s, OH), 7.85 (1H, d, $J=8.4$ Hz, H-3), 7.74 (1H, d, $J=8.4$ Hz, H-8), 7.61 (2H, dt, $J=8.8, 2.8$ Hz, H-2', H-6'), 7.58 (1H, d, $J=8.0$ Hz, H-5), 7.24 (3H, m, H-4, H-6, H-7), 6.43 (2H, dt, $J=8.8, 2.8$ Hz, H-3', H-5'), 3.35 (4H, t, $J=6.8$ Hz, H-1'', H-4'') 2.03 (4H, m, H-2'', H-3'').

NMR δ_{C} (100 MHz, CDCl_3), 197.0 (C=O), 158.5 (C-2), 151.4 (C-1), 134.0 (C-3), 133.0 (C-2', C-6'), 132.7 (C-8a), 128.5 (C-1'), 128.3 (C-8), 126.5, 126.4 (C-5), 126.3 (C-4'), 123.4, 119.0, 110.8 (C-3', C-5'), 116.4 (C-4a), 47.7 (C-1'', C-4''), 25.5 (C-2'', C-3'').

MS, m/z found 318.1486, $\text{C}_{21}\text{H}_{20}\text{NO}_2$, ($\text{M}+\text{H}^+$) requires 318.1489; found 340.1306, $\text{C}_{21}\text{H}_{19}\text{NO}_2\text{Na}$, ($\text{M}+\text{Na}^+$) requires 340.1308; found 657.2719, $\text{C}_{42}\text{H}_{38}\text{N}_2\text{O}_4\text{Na}$, ($2\text{M}+\text{Na}^+$) requires 657.2724.

IR, $\nu_{\text{max}}/\text{cm}^{-1}$ 3238 (OH), 1574 (C=O), 1179 (C-O).

1-(4'-Butyl(methyl)aminobenzoyl)-2-naphthol (**86**)



The mixture of **82** (0.27 g, 1.00 mmol) and *N*-methyl-1-butylamine (1.5 mL) was stirred and heated under reflux for 24 h. After cooling to room temperature, the reaction mixture was poured into ice water (10 mL) and extracted with ethyl acetate (3 x 10 mL). The extract was dried over anhydrous Mg₂SO₄ and concentrated to afford a yellow oil which was purified by chromatography on silica gel (elution with petrol ether/ ethyl acetate 40:1) to give **86** as a yellow solid in a 60% yield with m.p. 143.8-145.2 °C.

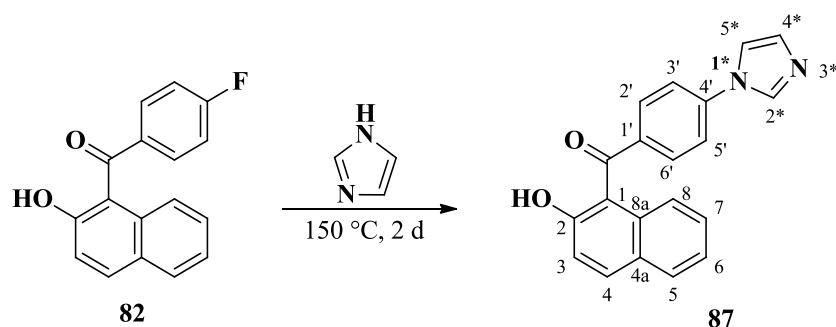
NMR δ_{H} (400 MHz, CDCl₃), 10.06 (1H, s, OH), 7.89 (1H, d, $J=8.8$ Hz, H-8), 7.79 (1H, d, $J=7.6$ Hz, H-4), 7.66-7.62 (3H, m, H-3, H-2', H-6'), 7.33-7.25 (3H, m, H-5, H-6, H-7), 6.58 (2H, dt, $J=9.2, 2.8$ Hz, H-3', H-5'), 3.41 (2H, t, $J=7.2$ Hz, H-1*) 3.05 (3H, s, NCH₃), 1.61 (2H, m, H-2*), 1.37 (2H, m, H-3*), 0.97 (3H, t, $J=7.2$ Hz, H-4*).

NMR δ_{C} (100 MHz, CDCl₃), 197.0 (C=O), 158.4 (C-2), 152.8 (C-4'), 134.0 (C-4), 132.9 (2C, C-2', C-6'), 132.6 (C-1'), 128.4 (C-8a), 128.2, 126.4, 126.3 (C-8), 126.2 (C-4a), 123.4, 118.9 (C-3), 116.3 (C-1), 110.3 (2C, C-3', C-5'), 52.2 (C-1*), 38.5 (NCH₃), 29.1 (C-2*), 20.3 (C-3*), 14.0 (C-4*).

MS, m/z found 334.1799, C₂₂H₂₄NO₂, (M+H⁺) requires 334.1802; found 356.1620, C₂₂H₂₃NO₂Na, (M+Na⁺) requires 356.1621; found 689.3346, C₄₄H₄₆N₂O₄Na, (2M+Na⁺) requires 689.3350.

IR, ν_{max} /cm⁻¹ 3242 (OH), 1578 (C=O), 1185 (C-N).

1-(4'-(1H-Imidazol-1-yl)benzoyl)-2-naphthol (**87**)



A mixture of **82** (0.57 g, 2.00 mmol) and imidazole (0.68 g, 10.00 mmol) was stirred at 150 °C for 2 days. After cooling to room temperature, the reaction was quenched with ice water (10 mL) and extracted with ethyl acetate (3 x 10 mL). The extract was dried over anhydrous Mg_2SO_4 and concentrated to afford a yellow oil which was purified by chromatography on silica gel (elution with petrol ether/ ethyl acetate 2:1) to give **87** (0.20 g, 32%) as a yellow solid with m.p. 153.2-155.6 °C.

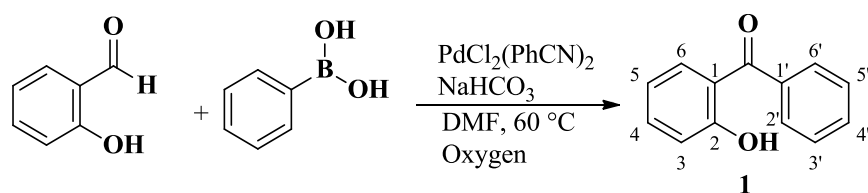
NMR δ_{H} (400 MHz, DMSO), 10.26 (1H, s, OH), 8.40 (1H, s, H-2*), 7.98 (1H, d, $J=8.8$ Hz, H-5*), 7.92 (1H, d, $J=8$ Hz, H-8), 7.88-7.81 (5H, m, H-4, H-2', H-6', H-3', H-5'), 7.43-7.33 (3H, m, H-5, H-6, H-7), 7.29 (1H, d, $J=8.8$ Hz, H-4*), 7.162 (1H, s, H-3).

NMR δ_{C} (100 MHz, DMSO), 195.5 (C=O), 151.9 (C-2), 140.0 (C-4'), 135.2 (C-2*), 135.0 (C-1'), 131.0 (C-8a), 130.6 (C-5*), 130.4 (C-2', C-6'), 129.9 (C-3), 127.8 (C-8), 127.0 (C-4a), 126.8, 122.7, 122.4, 119.6 (C-3', C-5'), 118.3 (C-1), 117.6 (C-4), 117.3 (C-4*).

MS, m/z found 315.1125, $\text{C}_{20}\text{H}_{15}\text{N}_2\text{O}_2$, ($\text{M}+\text{H}^+$) requires 315.1128; found 337.0945 $\text{C}_{20}\text{H}_{14}\text{N}_2\text{O}_2\text{Na}$, ($\text{M}+\text{Na}^+$) requires 337.0947; found 651.1999 $\text{C}_{40}\text{H}_{28}\text{N}_4\text{O}_4\text{Na}$, ($2\text{M}+\text{Na}^+$) requires 651.2003.

IR, (KBr) $\nu_{\text{max}}/\text{cm}^{-1}$ 3425 (OH), 1651 (C=O).

2-Hydroxybenzophenone (**1**) ^[158]

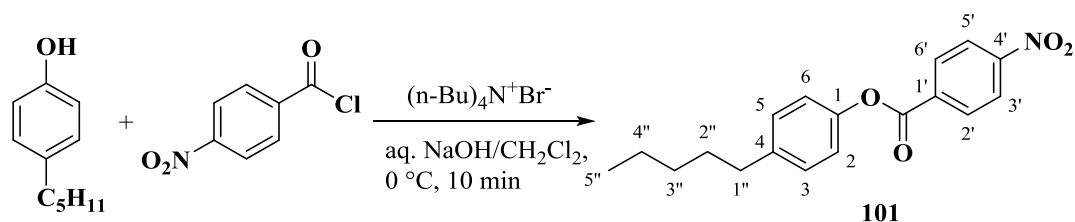


To a mixture of salicylaldehyde (0.11 mL, 1.00 mmol), phenylboronic acid (0.21 g, 1.70 mmol), PdCl₂(PhCN)₂ (0.02 g, 0.05 mmol) and NaHCO₃ (0.17 g, 2.00 mmol) was added DMF (4 mL). The resulting mixture was stirred at 60 °C under oxygen. After cooling to room temperature, the reaction mixture was quenched with HCl (1 M, 10 mL) and extracted with ethyl acetate (10 mL x 3). The extract was dried over anhydrous Mg₂SO₄ and concentrated. The residue was purified by silica gel (elution with petrol ether/ ethyl acetate 20:1) to afford **1** (0.15 g, 75%) as a yellow oil.

NMR δ_{H} (400 MHz, CDCl₃), 12.0 (1H, s, OH), 7.68 (2H, m, H-2', H-6'), 7.59 (2H, m, H-4', H-6), 7.51 (3H, m, H-4, H-3', H-5'), 7.08 (1H, dd, $J=8.4, 0.8$ Hz, H-3), 6.88 (1H, m, H-5).

IR, ν_{max} /cm⁻¹ 3500-3300 (OH), 1626 (C=O), 1243(C-O).

4-Pentylphenyl-4'-nitrobenzoate (**101**)



Prepared using phase-transfer condition procedure from 4-pentylphenol (0.34 mL, 2.00 mmol), 4-nitrobenzoyl chloride (0.37 g, 2.00 mmol) and tetra-*n*-butylammonium bromide (0.06 g, 0.20 mmol) yielding **101** as a white solid (0.52 g, 84%) with m.p. 63.5-65.1 °C.

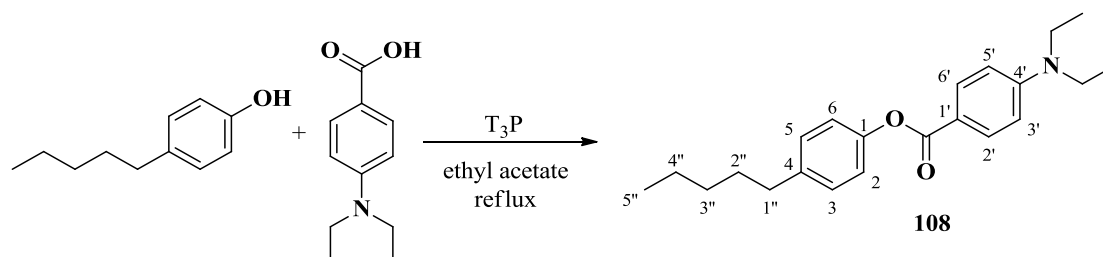
NMR δ_{H} (400 MHz, CDCl₃), 8.39 (4H, m, H-2', H-3', H-5', H-6'), 7.28 (2H, d, $J=8.4$ Hz, H-3, H-5), 7.15 (2H, d, $J=8.4$ Hz, H-2, H-6), 2.66 (2H, t, $J=7.6$ Hz, H-1''), 1.67 (2H, m, H-2''), 1.38 (4H, m, H-3'', H-4''), 0.83 (3H, t, $J=7.2$ Hz, H-5'').

NMR δ_{C} (100 MHz, CDCl₃), 163.5 (C=O), 150.9 (C-4'), 148.4 (C-1), 141.2 (C-5), 135.1 (C-1'), 131.3 (2C, C-2', C-6'), 129.5 (2C, C-3, C-5), 123.7 (2C, C-3', C-5'), 121.0 (2C, C-2, C-6), 35.4 (C-1''), 31.5 (C-3''), 31.2 (C-2''), 22.6 (C-4''), 14.1 (C-5'').

MS, m/z found 312.1256 C₁₈H₁₈NO₄, (M-H⁺) requires 312.1230; found 336.1206 C₁₈H₁₉NO₄Na, (M+Na⁺) requires 336.1206; found 649.2520 C₃₆H₃₈N₂O₈Na, (2M+Na⁺) requires 649.2520.

IR, ν_{max} /cm⁻¹ 1742 (C=O), 1525 (NO₂).

4-Pentylphenyl-4'-(diethylamino)benzoate (**108**)



Propylphosphonic anhydride solution (50% in ethyl acetate) (0.90 mL, 1.50 mmol) was added to the solution of 4-diethylaminobenzoic acid (0.19 g, 1.00 mmol) in ethyl acetate (5 mL). The mixture was stirred at room temperature for 10 min and then 4-pentylphenol (0.16 g, 1.00 mmol) added, and stirred under reflux for 16 h and then evaporated. The crude product was purified by silica gel column chromatography using petroleum ether to afford **108** as a yellow solid (0.27 g, 80%) with m.p. 44.3-46.1 °C.

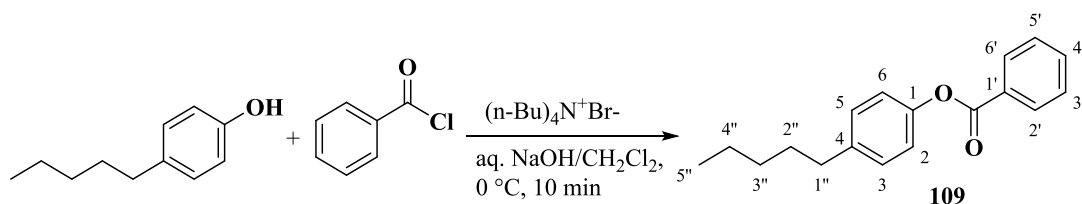
NMR δ_{H} (400 MHz, CDCl₃), 8.02 (2H, d, $J=9.2$ Hz, H-2', H-6'), 7.19 (2H, d, $J=8.8$ Hz, H-3, H-5), 7.08 (2H, d, $J=8.8$ Hz, H-2, H-6), 6.66 (2H, d, $J=9.2$ Hz, H-3', H-5'), 3.43 (4H, q, $J=7.2$ Hz, NCH₂CH₃), 2.61 (2H, t, $J=8$ Hz, H-1''), 1.62 (2H, m, H-2''), 1.33 (4H, m, H-3'', H-4''), 1.21 (6H, t, $J=8$ Hz, NCH₂CH₃), 0.89 (3H, t, $J=7.2$ Hz, H-5'').

NMR δ_{C} (100 MHz, CDCl₃), 165.7 (C=O), 151.4 (C-4'), 149.3 (C-1), 140.0 (C-4, 132.3 (2C, C-2', C-6'), 129.3 (2C, C-3, C-5), 121.7 (2C, C-2, C-6), 115.3 (C-1'), 110.3 (2C, C-3', C-5'), 44.7 (2C, NCH₂CH₃), 35.4 (C-1''), 31.6 (C-3''), 31.3 (C-2''), 22.6 (C-4''), 14.1 (C-5''), 12.6 (2C, NCH₂CH₃).

MS, m/z found 340.2282 C₂₂H₃₀NO₂, (M+H⁺) requires 340.2271; found 362.2100 C₂₂H₂₉NO₂Na, (M+Na⁺) requires 362.2091; found 701.4305 C₄₄H₅₈N₂O₄Na, (2M+Na⁺) requires 701.4289.

IR, ν_{max} /cm⁻¹ 1706 (C=O), 1176 (C-O).

4-Pentylphenyl benzoate (**109**)



Prepared using phase-transfer condition procedure from 4-pentylphenol (0.85 mL, 5.00 mmol), benzoyl chloride (0.58 mL, 5.00 mmol) and tetra-*n*-butylammonium bromide (0.16 g, 0.50 mmol) yielding **109** as a white solid (1.19 g, 90%) with m.p. 47.1-49.9 °C.

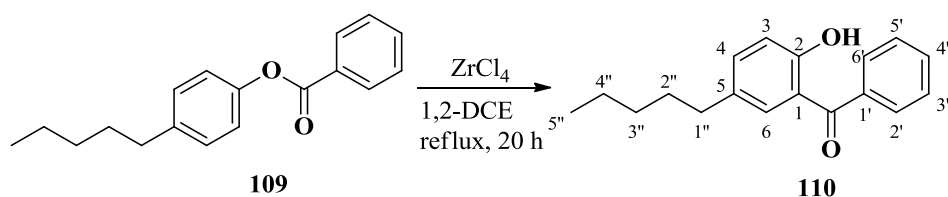
NMR δ_{H} (400 MHz, CDCl_3), 8.21 (2H, dt, $J=8.4, 1.6$ Hz, H-2', H-6'), 7.63 (1H, tt, $J=8.4, 1.6$ Hz, H-4'), 7.50 (2H, td, $J=8.4, 1.6$ Hz, H-3', H-5'), 7.23 (2H, dt, $J=8.4, 2.4$ Hz, H-3, H-5), 7.11 (2H, td, $J=8.4, 2.4$ Hz, H-2, H-6), 2.62 (2H, t, $J=7.2$ Hz, H-1''), 1.63 (2H, m, H-2''), 1.34 (4H, m, H-3'', H-4''), 0.91 (3H, t, $J=7.2$ Hz, H-5'').

NMR δ_{C} (100 MHz, CDCl_3), 165.5 (C=O), 148.9 (C-1), 140.7 (C-4), 133.6 (C-4'), 130.2 (2C, C-2', C-6'), 129.8 (C-1'), 129.4 (2C, C-3, C-5), 128.6 (2C, C-3', C-5'), 121.4 (2C, C-2, C-6), 35.5 (C-1''), 31.6 (C-3''), 31.3 (C-2''), 22.6 (C-4''), 14.2 (C-5'').

MS, m/z found 269.1540 $\text{C}_{18}\text{H}_{21}\text{O}_2$, ($\text{M}+\text{H}^+$) requires 269.1536.

IR, $\nu_{\text{max}}/\text{cm}^{-1}$ 1734 (C=O).

2-Hydroxy-5-pentylbenzophenone (**110**)^[180]



The Fries rearrangement procedure was followed with **109** (0.53 g, 1.98 mmol) and ZrCl_4 (1.07 g, 3.96 mmol) under reflux for 20 h. The crude product was purified by chromatography on silica gel (elution with petrol ether/ ethyl acetate 20:1) to afford **110** (0.51 g, 97%) as a yellow oil.

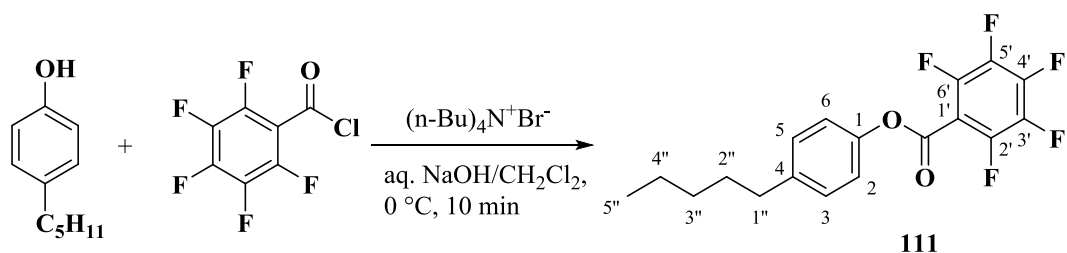
NMR δ_{H} (400 MHz, CDCl_3), 11.85 (1H, s, OH), 7.68 (2H, dt, $J=7.2$, 2 Hz, H-2', H-6'), 7.59 (1H, tt, $J=7.2$, 5 Hz, H-4'), 7.50 (2H, tt, $J=7.2$, 1.2 Hz, H-3', H-5'), 7.34 (2H, m, H-4, H-6), 7.00 (1H, d, $J=8.4$ Hz, H-3), 2.49 (2H, t, $J=7.6$ Hz, H-1''), 1.53 (2H, m, H-2''), 1.28 (4H, m, H-3'', H-4''), 0.87 (3H, t, $J=7.6$ Hz, H-5'').

NMR δ_{C} (100 MHz, CDCl_3), 201.6 (C=O), 161.3 (C-2), 138.1 (C-5), 136.8 (C-4), 133.1 (C-1'), 132.8 (C-6), 131.9 (C-4'), 129.3 (2C, C-2', C-6'), 128.4 (2C, C-3', C-5'), 118.9 (C-1), 118.2 (C-3), 34.9 (C-1''), 31.3 (C-3''), 31.2 (C-2''), 22.6 (C-4''), 14.1 (C-5'')

MS, m/z found 267.1382 $\text{C}_{18}\text{H}_{19}\text{O}_2$, ($\text{M}-\text{H}^+$) requires 267.1380; found 269.1546 $\text{C}_{18}\text{H}_{21}\text{O}_2$, ($\text{M}+\text{H}^+$) requires 269.1536; found 291.1365 $\text{C}_{18}\text{H}_{20}\text{O}_2\text{Na}$, ($\text{M}+\text{Na}^+$) requires 291.1356.

IR, $\nu_{\text{max}}/\text{cm}^{-1}$ 3500-3300 (OH), 1631 (C=O) and 1482 (benzene ring).

4-Pentylphenyl 2,3,4,5,6-pentafluorobenzoate (**111**)



Prepared using phase-transfer condition procedure from 4-pentylphenol (0.85 mL, 5.00 mmol), pentafluorobenzoyl chloride (0.72 mL, 5.00 mmol) and tetra-*n*-butylammonium bromide (0.16 g, 0.50 mmol) yielding **111** as a white solid (1.50 g, 84%) with m.p. 36.7-37.8 °C.

NMR δ_{H} (400 MHz, CDCl_3), 7.23 (2H, dt, $J=8.4, 2.0$ Hz, H-3, H-5), 7.13 (2H, dt, $J=8.4, 2.0$ Hz, H-2, H-6), 2.62 (2H, t, $J=7.6$ Hz, H-1''), 1.60 (2H, m, H-2''), 1.34 (4H, m, H-3'', H-4''), 0.89 (3H, t, $J=7.2$ Hz, H-5'').

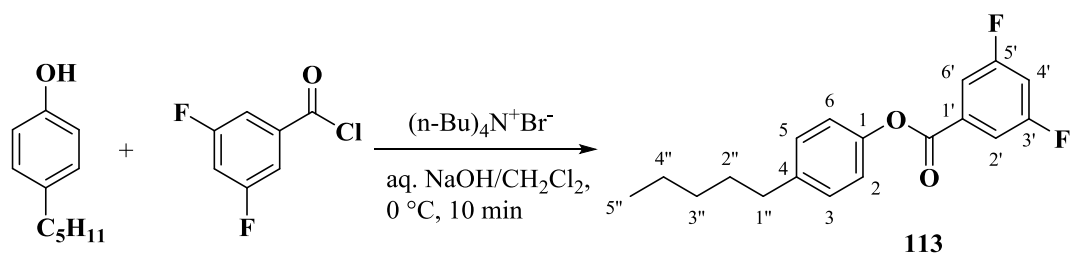
NMR δ_{C} (100 MHz, CDCl_3), 157.8 (C=O), 148.0 (C-1), 145.7 (2C, dm, $J=258.4$ Hz C-2', C-6'), 143.7 (dm, $J=258.4$ Hz C-4'), 141.7 (C-4), 137.6 (2C, dm, $J=255.6$ Hz C-3', C-5'), 129.6 (2C, C-3, C-5), 120.9 (2C, C-2, C-6), 108.0 (m, C-1'), 35.4 (C-1''), 31.5 (C-3''), 31.2 (C-2''), 22.6 (C-4''), 14.1 (C-5'')

NMR δ_{F} (376 MHz, CDCl_3), 24.8 (2F, m, F-2', F-6'), 14.7 (1F, tt, $J=20.7, 4.9$ Hz, F-4'), 2.24 (2F, m, F-3', F-5')

MS, m/z found 381.0870 $\text{C}_{18}\text{H}_{15}\text{F}_5\text{O}_2\text{Na}$, ($\text{M}+\text{Na}^+$) requires 381.0884.

IR, $\nu_{\text{max}}/\text{cm}^{-1}$ 2928 (CH_2), 1757 (C=O) and 1501 (benzene ring), 991 (C-F).

4-Pentylphenyl 3,5-difluorobenzoate (113)



Prepared using phase-transfer condition procedure from 4-pentylphenol (0.85 mL, 5.00 mmol), 3,5-difluorobenzoyl chloride (0.88 g, 5.00 mmol) and tetra-*n*-butylammonium bromide (0.16 g, 0.50 mmol) yielding **113** as a white solid (1.36 g, 89%) with m.p. 37.9-40.2 °C.

NMR δ_{H} (400 MHz, CDCl_3), 7.70 (2H, m, H-2', H-6'), 7.22 (2H, m, H-3, H-5), 7.11-7.05 (3H, m, H-2, H-6, H-4'), 2.62 (2H, t, $J=7.6$ Hz, H-1''), 1.62 (2H, m, H-2''), 1.34 (4H, m, H-3'', H-4''), 0.89 (3H, t, $J=7.2$ Hz, H-5'').

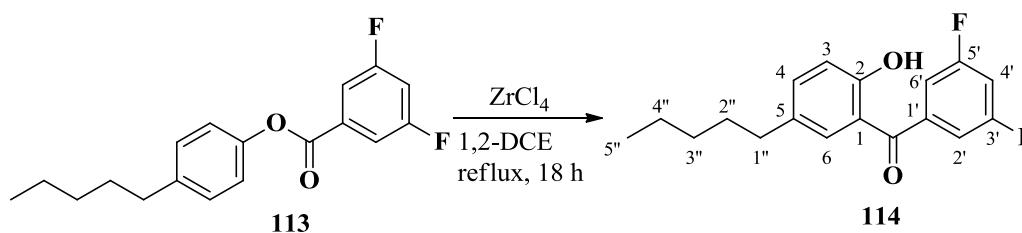
NMR δ_{C} (100 MHz, CDCl_3), 163.2 (C=O), 162.9 (2C, dd, $J=249.8, 12.3$ Hz, C-3', C-5'), 148.5 (C-1), 141.1 (C-4), 133.0 (t, $J=9.6$ Hz, C-1'), 129.5 (2C, C-3, C-5), 121.1 (2C, C-2, C-6), 113.2 (2C, dd, $J=19.1, 7.6$ Hz, C-2', C-6'), 109.0 (t, $J=24.8$ Hz, C-4'), 35.4 (C-1''), 31.5 (C-3''), 31.2 (C-2''), 22.6 (C-4''), 14.1 (C-5'').

NMR δ_{F} (376 MHz, CDCl_3), 54.1 (2F, m, F-3', F-5').

MS, m/z found 305.1342 $\text{C}_{18}\text{H}_{19}\text{F}_2\text{O}_2$, ($\text{M}+\text{H}^+$) requires 305.1348; found 327.1161 $\text{C}_{18}\text{H}_{18}\text{F}_2\text{O}_2\text{Na}$, ($\text{M}+\text{Na}^+$) requires 327.1167; found 631.2431 $\text{C}_{36}\text{H}_{36}\text{F}_4\text{O}_4\text{Na}$, ($2\text{M}+\text{Na}^+$) requires 631.2442.

IR, $\nu_{\text{max}}/\text{cm}^{-1}$ 2986 (CH_2), 1742 (C=O) and 1601, 1507 (benzene ring).

3',5'-Difluoro-2-hydroxy-5-pentylbenzophenone (**114**)



The Fries rearrangement procedure was followed with **113** (0.46 g, 1.52 mmol) and ZrCl_4 (0.71 g, 3.03 mmol) under reflux for 18 h. The crude product was purified by chromatography on silica gel (elution with petrol ether/ ethyl acetate 20:1) to afford **114** (0.44 g, 96%) as a yellow oil.

NMR δ_{H} (400 MHz, CDCl_3), 11.53 (1H, s, OH), 7.36 (1H, dd, $J=8.4, 2.4$ Hz, H-4), 7.26 (1H, d, $J=2.4$ Hz, H-6), 7.18 (2H, m, H-2', H-6'), 7.03 (1H, tt, $J=8.4, 2.0$ Hz, H-4'), 7.00 (1H, d, $J=8.4$ Hz, H-3), 2.51 (2H, t, $J=7.6$ Hz, H-1''), 1.53 (2H, m, H-2''), 1.29 (4H, m, H-3'', H-4''), 0.87 (3H, t, $J=7.2$ Hz, H-5'').

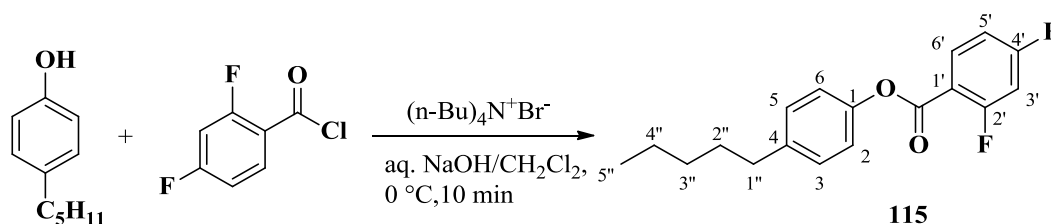
NMR δ_{C} (100 MHz, CDCl_3), 197.6 (C=O), 161.6 (2C, dd, $J=252.0, 12.0$ Hz, C-3', C-5'), 160.4 (C-2), 139.8 (t, $J=8.0$ Hz, C-1'), 136.6 (C-4), 132.4 (C-5), 131.0 (C-6), 117.5 (C-3), 117.0 (C-1), 111.1 (2C, dd, $J=19.0, 7.0$ Hz, C-2', C-6'), 106.1 (t, $J=25.0$ Hz, C-4'), 34.8 (C-1''), 31.1 (C-3''), 30.8 (C-2''), 22.5 (C-4''), 14.0 (C-5'').

NMR δ_{F} (376 MHz, CDCl_3), 54.2 (2F, m, F-3', F-5').

MS, m/z found 303.1191 $\text{C}_{18}\text{H}_{17}\text{F}_2\text{O}_2$, ($\text{M}-\text{H}^+$) requires 303.1191; found 305.1357 $\text{C}_{18}\text{H}_{19}\text{F}_2\text{O}_2$, ($\text{M}+\text{H}^+$) requires 305.1348; found 327.1176 $\text{C}_{18}\text{H}_{18}\text{F}_2\text{O}_2\text{Na}$, ($\text{M}+\text{Na}^+$) requires 327.1167.

IR, $\nu_{\text{max}}/\text{cm}^{-1}$ 3500-3088 (OH), 1633 (C=O), 1952, 1482 (benzene ring), 1123 (C-F).

4-Pentylphenyl 2,4-difluorobenzoate (**115**)



Prepared using phase-transfer condition procedure from 4-pentylphenol (0.85 mL, 5.00 mmol), 2,4-difluorobenzoyl chloride (0.60 mL, 5.00 mmol) and tetra-*n*-butylammonium bromide (0.16 g, 0.50 mmol) yielding **115** as a colourless oil (1.36 g, 90%).

NMR δ_{H} (400 MHz, CDCl₃), 8.13 (1H, m, H-6'), 7.21 (2H, dt, $J=8.8, 2.0$ Hz, H-3, H-5), 7.10 (2H, dt, $J=8.8, 2.0$ Hz, H-2, H-6), 7.02-6.98 (1H, m, H-5'), 6.94 (1H, m, H-3'), 2.61 (2H, t, $J=7.6$ Hz, H-1''), 1.60 (2H, m, H-2''), 1.33 (4H, m, H-3'', H-4''), 0.89 (3H, t, $J=7.2$ Hz, H-5'').

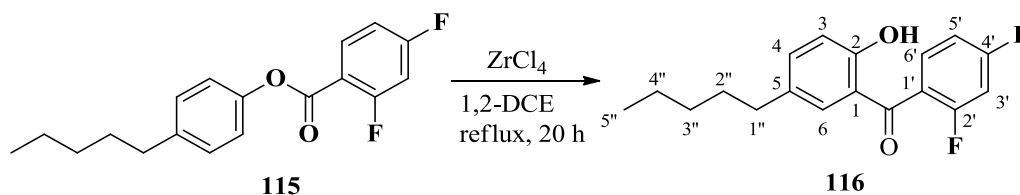
NMR δ_{C} (100 MHz, CDCl₃), 166.2 (dd, $J=255.6, 12.4$ Hz, C-4'), 163.3 (dd, $J=263.2, 12.4$ Hz, C-2'), 162.2 (d, $J=4.8$ Hz, C=O), 148.5 (C-1), 140.9 (C-4), 134.4 (d, $J=10.5$ Hz, C-6'), 129.5 (2C, C-3, C-5), 121.3 (2C, C-2, C-6), 114.8 (dd, $J=9.5, 3.8$ Hz, C-1'), 111.8 (dd, $J=21.0, 3.8$ Hz, C-5'), 105.6 (t, $J=25.7$ Hz, C-3'), 35.4 (C-1''), 31.5 (C-3''), 31.2 (C-2''), 22.6 (C-4''), 14.1 (C-5'').

NMR δ_{F} (376 MHz, CDCl₃), 61.2 (1F, m, F-2'), 59.3 (1F, m, F-4').

MS, m/z found 305.1341 C₁₈H₁₉F₂O₂, (M+H⁺) requires 305.1348; found 327.1159 C₁₈H₁₈F₂O₂Na, (M+Na⁺) requires 327.1167; found 631.2430 C₃₆H₃₆F₄O₄Na, (2M+Na⁺) requires 631.2442.

IR, ν_{max} /cm⁻¹ 2930 (CH₂), 1749 (C=O) and 1612, 1508 (benzene ring), 1195 (C-F).

2',4'-Difluoro-2-hydroxy-5-pentylbenzophenone (116)



The Fries rearrangement procedure was followed with **115** (0.53 g, 1.98 mmol) and ZrCl_4 (1.07 g, 3.96 mmol) under reflux for 20 h. The crude product was purified by chromatography on silica gel (elution with petrol ether/ ethyl acetate 20:1) to afford **116** (0.58 g, 97%) as a yellow oil.

NMR δ_{H} (400 MHz, CDCl_3), 11.73 (1H, s, OH), 7.50 (1H, m, H-6'), 7.35 (1H, dd, $J=8.4, 2.0$ Hz, H-4), 7.15 (1H, t, $J=2.4$ Hz, H-6), 7.03 (1H, ddd, $J=8.8, 2.4, 0.8$ Hz, H-5'), 6.97 (1H, d, $J=2.4$ Hz, H-3), 6.95 (1H, ddd, $J=8.8, 2.4, 0.8$ Hz, H-3'), 2.49 (2H, t, $J=3.2$ Hz, H-1''), 1.53 (2H, m, H-2''), 1.31 (4H, m, H-3'', H-4''), 0.88 (3H, t, $J=7.2$ Hz, H-5'').

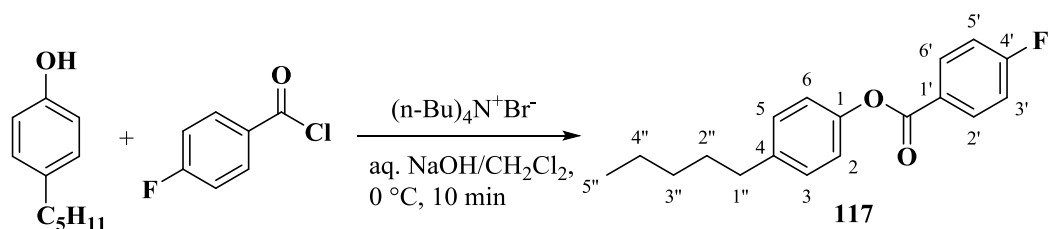
NMR δ_{C} (100 MHz, CDCl_3), 197.2 (C=O), 164.6 (dd, $J=253.0, 11.0$ Hz, C-4'), 161.2 (C-2), 159.4 (dd, $J=253.0, 11.0$ Hz, C-2'), 137.7 (C-4), 133.5 (C-5), 132.1 (C-6), 131.5 (dd, $J=10.0, 4.0$ Hz, C-6'), 122.9 (dd, $J=15.0, 4.0$ Hz, C-1'), 119.2 (C-1), 118.2 (C-3), 112.0 (dd, $J=22.0, 4.0$ Hz, C-5'), 104.8 (t, $J=25.0$ Hz, C-3'), 34.8 (C-1''), 31.2 (C-3''), 31.1 (C-2''), 22.5 (C-4''), 14.0 (C-5'').

NMR δ_{F} (376 MHz, CDCl_3), 57.7 (1F, m, F-4'), 54.6 (1F, m, F-2').

MS, m/z found 303.1206 $\text{C}_{18}\text{H}_{17}\text{F}_2\text{O}_2$, (M-H⁺) requires 303.1202.

IR, $\nu_{\text{max}}/\text{cm}^{-1}$ 3500-3032 (OH), 1633 (C=O) and 1593, 1482 (benzene ring), 1123 (C-F).

4-Pentylphenyl 4-fluorobenzoate (**117**)



Prepared using phase-transfer condition procedure from 4-pentylphenol (3.28 g, 20.00 mmol), 4-fluorobenzoyl chloride (3.17 g, 20.00 mmol) and tetra-*n*-butylammonium bromide (0.65 g, 2.00 mmol) yielding **117** as a white solid (5.63 g, 99%) with m.p. 116.3-117.7 °C.

NMR δ_{H} (400 MHz, CDCl₃), 8.21 (2H, m, H-2', H-6'), 7.21 (2H, m, H-3, H-5), 7.17 (2H, m, H-3', H-5'), 7.10 (2H, dt, $J=8.8, 2.4$ Hz, H-2, H-6), 2.62 (2H, t, $J=7.6$ Hz, H-1''), 1.61 (2H, m, H-2''), 1.32 (4H, m, H-3'', H-4''), 0.89 (3H, t, $J=7.2$ Hz, H-5'').

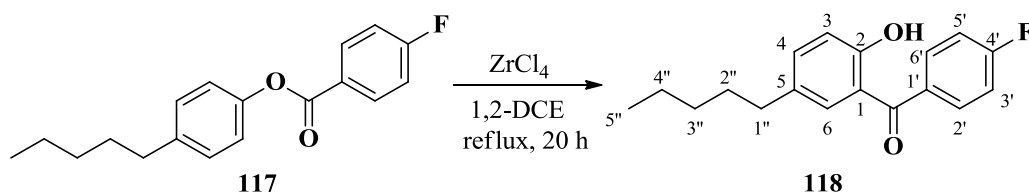
NMR δ_{C} (100 MHz, CDCl₃), 166.2 (d, $J=252.7$ Hz, C-4'), 164.5 (C=O), 148.8 (C-1), 140.8 (C-4), 132.8 (2C, d, $J=9.5$ Hz, C-2', C-6'), 129.5 (2C, C-3, C-5), 126.0 (d, $J=2.8$ Hz, C-1'), 121.3 (2C, C-2, C-6), 115.8 (2C, d, $J=21.9$ Hz, C-3', C-5'), 35.4 (C-1''), 31.6 (C-3''), 31.3 (C-2''), 22.6 (C-4''), 14.1 (C-5'').

NMR δ_{F} (376 MHz, CDCl₃), 57.3 (1F, m, F-4').

MS, m/z found 285.1292 C₁₈H₁₈FO₂, (M-H⁺) requires 285.1285; found 309.1272 C₁₈H₁₉FO₂Na, (M+Na⁺) requires 309.1261.

IR, ν_{max} /cm⁻¹ 2924 (CH₂), 1728 (C=O), 1504 (benzene ring), 1072 (C-F)

4'-Fluoro-2-hydroxy-5-pentylbenzophenone (**118**)



The Fries rearrangement procedure was followed with **117** (5.63 g, 20.00 mmol) and ZrCl_4 (9.32 g, 40.00 mmol) under reflux for 20 h. The crude product was purified by chromatography on silica gel (elution with petrol ether/ ethyl acetate 100:1) to afford **118** (5.41 g, 97%) as a yellow oil.

NMR δ_{H} (400 MHz, CDCl_3), 11.69 (1H, s, OH), 7.71 (2H, m, H-2', H-6'), 7.33 (1H, dd, $J=8.4, 2.0$ Hz, H-4), 7.31 (1H, d, $J=2.0$ Hz, H-6), 7.19 (2H, tt, $J=8.4, 2.8$ Hz, H-3', H-5'), 6.99 (1H, d, $J=8.4$ Hz, H-3), 2.50 (2H, t, $J=7.6$ Hz, H-1''), 1.56 (2H, m, H-2''), 1.28 (4H, m, H-3'', H-4''), 0.87 (3H, t, $J=7.2$ Hz, H-5'').

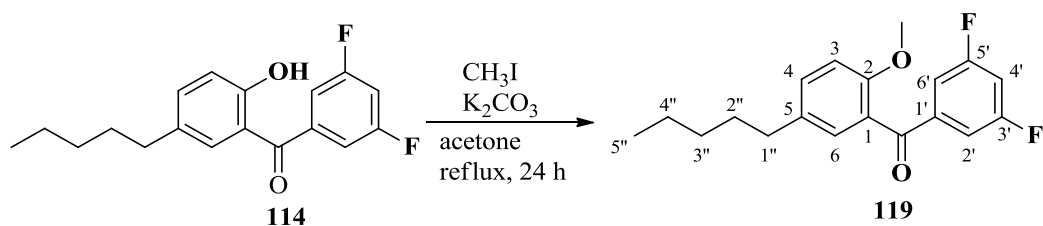
NMR δ_{C} (100 MHz, CDCl_3), 200.0 (C=O), 165.0 (d, $J=251.7$ Hz, C-4'), 161.3 (C-2), 136.9 (C-4), 134.3 (d, $J=2.9$ Hz, C-1'), 133.2 (C-5), 132.5 (C-6), 131.8 (2C, d, $J=9.6$ Hz, C-2', C-6'), 118.8 (C-1), 118.4 (C-3), 115.6 (2C, d, $J=21.9$ Hz, C-3', C-5'), 34.9 (C-1''), 31.4 (C-3''), 31.3 (C-2''), 22.6 (C-4''), 14.1 (C-5'').

NMR δ_{F} (376 MHz, CDCl_3), 57.3 (1F, m).

MS, m/z found 285.1302 $\text{C}_{18}\text{H}_{18}\text{FO}_2$, ($\text{M}-\text{H}^+$) requires 285.1285; found 287.1443 $\text{C}_{18}\text{H}_{20}\text{FO}_2$, ($\text{M}+\text{H}^+$) requires 287.1442; found 309.1262 $\text{C}_{18}\text{H}_{19}\text{FO}_2\text{Na}$, ($\text{M}+\text{Na}^+$) requires 309.1261; found 595.2637 $\text{C}_{36}\text{H}_{38}\text{F}_2\text{O}_4\text{Na}$, ($2\text{M}+\text{Na}^+$) requires 595.2630.

IR, $\nu_{\text{max}}/\text{cm}^{-1}$ 3500-3300 (OH), 1631 (C=O) and 1482 (benzene ring).

3', 5'-Difluoro-2-methoxy-5-pentylbenzophenone (**119**)



Methyl iodide (0.12 ml, 2.00 mmol) was added to a solution of **114** (0.22 g, 0.75 mmol) and anhydrous potassium carbonate (0.12 g, 0.90 mmol) in dry acetone (5 mL). The reaction mixture was stirred and heated under reflux for 24 h, and then evaporated to dryness. The residue was treated with ice water to dissolve potassium carbonate and extracted with ethyl acetate (3 x 10 mL). The organic layer was washed with 10% NaOH solution (3 x 10 mL) and water (3 x 10 mL), dried over Mg_2SO_4 and evaporated. The crude product was purified by chromatography on silica gel (elution with petrol ether / ethyl acetate 100:1) to afford **119** (0.19 g, 79%) as a yellow oil.

NMR δ_{H} (400 MHz, CDCl_3), 7.28 (3H, m, H-4, H-2', H-6'), 7.17 (2H, d, $J=2.4$ Hz, H-6), 7.00 (1H, tt, $J=8.8, 2.4$ Hz, H-4'), 6.89 (1H, d, $J=8.4$ Hz, H-3), 3.68 (3H, s, CH_3), 2.57 (2H, t, $J=7.6$ Hz, H-1''), 1.57 (2H, m, H-2''), 1.29 (4H, m, H-3'', H-4''), 0.87 (3H, t, $J=7.2$ Hz, H-5'').

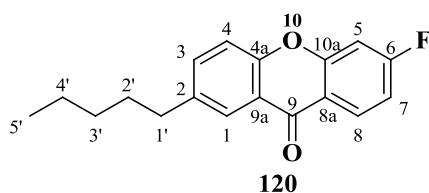
NMR δ_{C} (100 MHz, CDCl_3), 194.2 (C=O), 162.8 (2C, dd, $J=247.9, 11.4$ Hz, C-3', C-5'), 155.7 (C-2), 141.3 (t, $J=7.6$ Hz, C-1'), 135.4 (C-5), 132.7 (C-4), 129.6 (C-6), 127.3 (C-1), 112.4 (2C, dd, $J=19.0, 6.6$ Hz, C-2', C-6'), 111.6 (C-3), 107.9 (t, $J=25.7$ Hz, C-4'), 55.6 (OCH_3), 40.9 (C-1''), 31.9 (C-3''), 30.9 (C-2''), 22.5 (C-4''), 14.0 (C-5'').

NMR δ_{F} (376 MHz, CDCl_3), 51.3 (2F, m, F-3', F-5').

MS, m/z found 319.1492 $\text{C}_{19}\text{H}_{21}\text{F}_2\text{O}_2$, ($\text{M}+\text{H}^+$) requires 319.1504; found 341.1310 $\text{C}_{19}\text{H}_{20}\text{F}_2\text{O}_2\text{Na}$, ($\text{M}+\text{Na}^+$) requires 341.1324; found 659.2729 $\text{C}_{38}\text{H}_{40}\text{F}_4\text{O}_4\text{Na}$, ($2\text{M}+\text{Na}^+$) requires 659.2755.

IR, $\nu_{\text{max}}/\text{cm}^{-1}$ 1672 (C=O).

6-Fluoro-2-pentyl-9H-xanthen-9-one (120)



Following the method for **119**, methyl iodide (0.12 ml, 2.00 mmol) was added to a solution of **116** (0.27 g, 0.89 mmol) and anhydrous potassium carbonate (0.12 g, 0.90 mmol) in dry acetone (5 mL). Work-up as previously and the crude product was recrystallized from hexane to give **120** (0.12 g, 45%) with m.p. 81.8-82.7 °C.

NMR δ_{H} (400 MHz, CDCl_3), 8.34 (1H, dd, $J=8.8, 6.4$ Hz, H-8), 8.09 (1H, d, $J=2.4$ Hz, H-1), 7.53 (1H, dd, $J=8.4, 2.4$ Hz, H-3), 7.38 (1H, d, $J=8.4$ Hz, H-4), 7.13 (1H, dd, $J=9.2, 2.4$ Hz, H-5), 7.08 (1H, td, $J=8.8, 2.4$ Hz, H-7), 2.71 (2H, t, $J=7.6$ Hz, H-1'), 1.66 (2H, m, H-2'), 1.28 (4H, m, H-3', H-4'), 0.88 (3H, t, $J=7.2$ Hz, H-5').

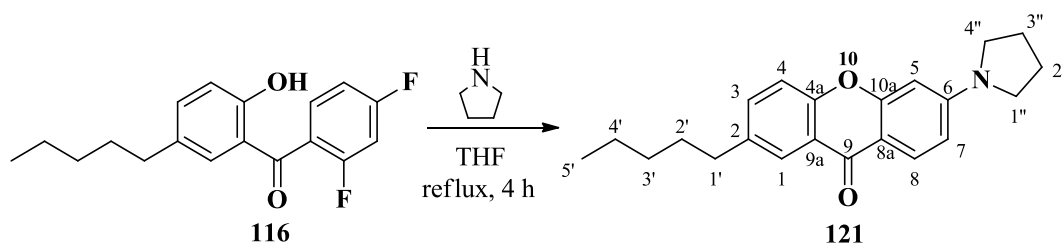
NMR δ_{C} (100 MHz, CDCl_3), 176.3 (C=O), 166.4 (d, $J=254.0$ Hz, C-6), 157.4 (d, $J=14.0$ Hz, C-10a), 154.6 (C-4a), 139.5 (C-2), 135.4 (C-3), 129.3 (d, $J=11.0$ Hz, C-8), 125.5 (C-1), 121.4 (C-9a), 118.7 (d, $J=3.0$ Hz, C-8a), 117.6 (C-4), 112.5 (d, $J=22.0$ Hz, C-7), 104.5 (d, $J=25.0$ Hz, C-5), 35.2 (C-1'), 31.3 (C-3'), 31.0 (C-2'), 22.5 (C-4'), 14.0 (C-5').

NMR δ_{F} (376 MHz, CDCl_3), 62.24 (1F, q, $J=7.5$ Hz)

MS, m/z found 283.1134 $\text{C}_{18}\text{H}_{16}\text{FO}_2$, ($\text{M}-\text{H}^+$) requires 283.1129; found 285.1299 $\text{C}_{18}\text{H}_{18}\text{FO}_2$, ($\text{M}+\text{H}^+$) requires 285.1285; found 307.1119 $\text{C}_{18}\text{H}_{17}\text{FO}_2\text{Na}$, ($\text{M}+\text{Na}^+$) requires 307.1105; found 591.2343 $\text{C}_{36}\text{H}_{34}\text{F}_2\text{O}_4\text{Na}$, ($2\text{M}+\text{Na}^+$) requires 591.2317.

IR, $\nu_{\text{max}}/\text{cm}^{-1}$ 1619 (C=O), 1482 (benzene ring).

2-Pentyl-6-(pyrrolidin-1-yl)-9H-xanthen-9-one (121)



2,4'-Difluoro-2-hydroxy-5-pentylbenzophenone (**116**) (0.31 g, 1.00 mmol) and pyrrolidine (0.34 mL, 4.00 mmol) were added in 6 mL THF. The reaction solution was stirred and heated under reflux for 4 h. After cooling to room temperature, the reaction mixture was quenched with ice water and extracted with ethyl acetate (3 x 20 mL). The organic layer was washed with water (10 mL) and then evaporated. The residue was purified by chromatography on silica gel (elution with petrol ether / ethyl acetate 5:1) to afford **121** (0.17 g, 56%) as a yellow solid. m.p. 116.3-117.9 °C.

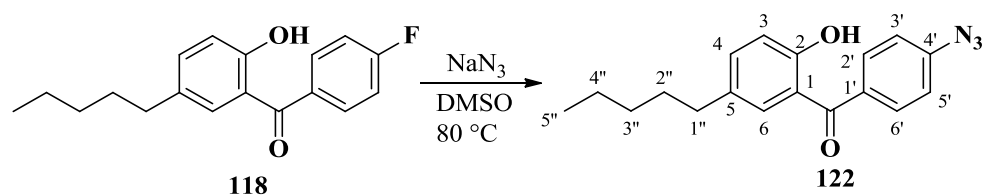
NMR δ_{H} (400 MHz, CDCl_3), 8.13 (1H, d, $J=8.8$ Hz, H-8), 8.09 (1H, d, $J=2.0$ Hz, H-1), 7.42 (1H, dd, $J=8.4, 2.0$ Hz, H-3), 7.28 (1H, d, $J=8.4$ Hz, H-4), 6.57 (1H, dd, $J=8.8, 2.4$ Hz, H-7), 6.34 (1H, d, $J=2.4$ Hz, H-5), 3.38 (4H, t, $J=6.4$ Hz, H-1'', H-4''), 2.68 (2H, t, $J=8.0$ Hz, H-1'), 2.05 (4H, m, H-2'', H-3''), 1.65 (2H, m, H-2'), 1.31 (4H, m, H-3', H-4'), 0.88 (3H, t, $J=6.8$ Hz, H-5').

NMR δ_{C} (100 MHz, CDCl_3), 176.3 (C=O), 158.4, 154.5, 152.4 (C-2), 138.1, 134.1 (C-3), 128.1 (C-8), 125.4 (C-1), 122.0, 117.2 (C-4), 111.6 (C-6), 110.0 (C-7), 96.5 (C-5), 47.8 (2C, C-1'', C-4''), 35.3 (C-1'), 31.5 (C-3'), 31.3 (C-2'), 25.5 (2C, C-2'', C-3''), 22.6 (C-4'), 14.1 (C-5').

MS, m/z found 334.1805 $\text{C}_{22}\text{H}_{24}\text{NO}_2$, ($\text{M}-\text{H}^+$) requires 334.1802; found 336.1973 $\text{C}_{22}\text{H}_{26}\text{NO}_2$, ($\text{M}+\text{H}^+$) requires 336.1958; found 358.1792 $\text{C}_{22}\text{H}_{25}\text{O}_2\text{NNa}$, ($\text{M}+\text{Na}^+$) requires 358.1778; found 693.3691 $\text{C}_{44}\text{H}_{50}\text{O}_4\text{N}_2\text{Na}$, ($2\text{M}+\text{Na}^+$) requires 693.3663.

IR, $\nu_{\text{max}}/\text{cm}^{-1}$ 1613 (C=O), 1484 (benzene ring), 1451(C-O).

4'-Azido-2-hydroxy-5-pentylbenzophenone (**122**)



Under anhydrous conditions, 4'-fluoro-2-hydroxy-5-pentylbenzophenone (**118**) (1.56 g, 5.50 mmol) was dissolved in DMSO (10 mL) in a round bottom flask. Sodium azide (0.72 g, 11.00 mmol) was added to the flask. After the mixture was stirred at 80 °C for 24 h, further sodium azide (0.13 g, 2.00 mmol) was added and stirred at 80 °C for another 24 h. After cooling to room temperature, the mixture was quenched with ice water (30 mL) and extracted with ethyl acetate (3 x 20 mL). The extract was dried over Mg₂SO₄ and concentrated to afford a yellow oil which was purified by chromatography on silica gel (elution with petrol ether/ethyl acetate 100:1) to give **122** (1.39 g, 83%) as a yellow oil.

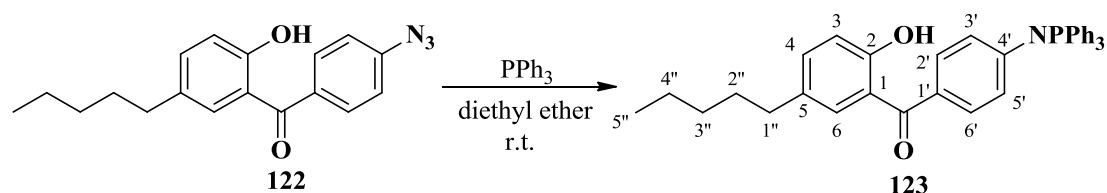
NMR δ_{H} (400 MHz, CDCl₃), 11.74 (1H, s, OH), 7.51 (2H, dt, $J=8.8$ Hz, 2.4 Hz, H-2', H-6'), 7.38 (2H, m, H-4, H-6), 7.17 (2H, dt, $J=8.8$ Hz, 2.4 Hz, H-3', H-5'), 7.01 (1H, d, $J=7.6$ Hz, H-3), 2.54 (2H, t, $J=8.0$ Hz, H-1''), 1.58 (2H, m, H-2''), 1.33 (4H, m, H-3'', H-4''), 0.91 (3H, $J=7.2$ Hz, H-5'').

NMR δ_{C} (100 MHz, CDCl₃), 199.9 (C=O), 161.2 (C-2), 144.0 (C-4'), 136.78 (C-4), 134.5 (C-5), 133.1 (C-1'), 132.3 (C-6), 131.4 (2C, C-2', C-6'), 118.9 (2C, C-3', C-5'), 118.8 (C-1), 118.3 (C-3), 34.9 (C-1''), 31.3 (C-3''), 31.2 (C-2''), 22.2 (C-4''), 14.1 (C-5'').

MS, m/z found 310.1551, C₁₈H₂₀N₃O₂, (M+H⁺) requires 310.1550; found 332.1370, C₁₈H₁₉N₃O₂Na, (M+Na⁺) requires 332.1369; found 641.2837 C₃₆H₃₈N₆O₄Na, (2M+Na⁺) requires 641.2847.

IR, ν_{max} /cm⁻¹ 3400-3060 (OH), 2126 (CN₃), 1630 (C=O), 1482 (benzene ring), 1179 (C-N).

4'-(Triphenylphosphoranylidene)amino-2-hydroxy-5-pentylbenzophenone (**123**)



To a stirring solution of **122** (0.44 g, 1.43 mmol) in diethyl ether (6 mL) was slowly added a solution of triphenylphosphine (0.38 g, 1.43 mmol) in diethyl ether (6 mL). The reaction mixture was stirred for 2 h at room temperature. The solid formed was filtered off and the filtrate was concentrated. The residue was purified by chromatography on silica gel (elution with DCM/ ethyl acetate 1:1) to afford **123** (0.71 g, 100%) as a yellow solid with m.p. 143.1-144.2 °C.

NMR δ_{H} (400 MHz, CDCl_3), 11.76 (1H, s, OH), 7.78-7.73 (6H, m, H-benzene ring), 7.59-7.55 (3H, m, H-benzene ring), 7.52-7.45 (8H, m, H-benzene ring), 7.23 (1H, dd, $J=8.4$, 2.4 Hz, H-4), 6.91 (1H, d, $J=8.4$ Hz, H-3), 6.81 (2H, d, $J=8.4$ Hz, H-3', H-5'), 2.53 (2H, t, $J=7.6$ Hz, H-1''), 1.56 (2H, m, H-2''), 1.31 (4H, m, H-3'', H-4''), 0.89 (3H, $J=6.8$ Hz, H-5'').

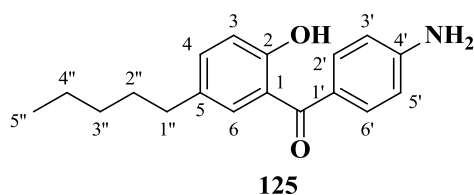
NMR δ_{C} (100 MHz, CDCl_3), 199.5 (C=O), 160.5 (C-2), 135.2 (C-4), 132.8-131.9 (C-benzene ring), 129.0 (2C, C-2', C-6'), 122.6 (2C, C-3', C-5'), 119.7 (C-1), 117.7 (C-3), 35.0 (C-1''), 31.4 (C-3''), 31.3 (C-2''), 22.6 (C-4''), 14.2 (C-5'').

NMR δ_{P} (161 MHz, CDCl_3), 29.79 (1P, s).

MS, m/z found 544.2397, $\text{C}_{36}\text{H}_{35}\text{NO}_2\text{P}$, ($\text{M}+\text{H}^+$) requires 544.2400; found 566.2220, $\text{C}_{36}\text{H}_{34}\text{NO}_2\text{PNa}$, ($\text{M}+\text{Na}^+$) requires 566.2219; found 1109.4547 $\text{C}_{72}\text{H}_{68}\text{N}_2\text{O}_4\text{P}_2\text{Na}$, ($2\text{M}+\text{Na}^+$) requires 1109.4547.

IR, $\nu_{\text{max}}/\text{cm}^{-1}$ 3400-3060 (OH), 1573 (C=O), 1482 (benzene ring), 1165 (C-N).

4'-Amino-2-hydroxy-5-pentylbenzophenone (**125**)



To a stirring solution of valeraldehyde (0.09 g, 1.00 mmol) in THF (5 mL) was added the solution of **123** (0.54 g, 1.00 mmol) in THF (5 mL) at 0 °C. Then the mixture was stirred and heated under reflux for 24 h. After cooling to room temperature, the reaction mixture was quenched with ice water (10 mL) and extracted with ethyl acetate (3 x 10 mL). The extract was dried and concentrated to afford a yellow oil which was purified by chromatography on silica gel (elution with petrol ether / DCM 1:1) to give side product **125** (0.18 g, 64%) as a yellow solid with m.p. 87.2-88.7 °C..

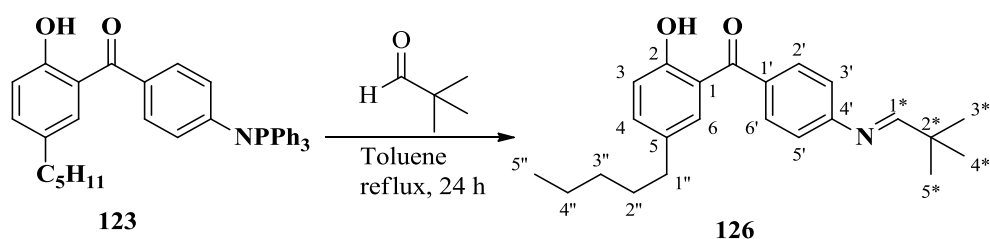
NMR δ_{H} (400 MHz, CDCl_3), 11.77 (1H, s, OH), 7.64 (2H, dt, $J=8.8$ Hz, 2.4 Hz, H-2', H-6'), 7.46 (1H, d, $J=2.0$ Hz, H-6), 7.31 (1H, dd, $J=8.4$ Hz, 2.0 Hz, H-4), 6.99 (1H, d, $J=8.4$ Hz, H-3), 6.74 (2H, dt, $J=8.8$ Hz, 2.0 Hz, H-3', H-5'), 4.20 (2H, s, NH_2), 2.55 (2H, t, $J=7.6$ Hz, H-1''), 1.60 (2H, m, H-2''), 1.33 (4H, m, H-3'', H-4''), 0.94 (3H, $J=7.2$ Hz, H-5'').

NMR δ_{C} (100 MHz, CDCl_3), 199.5 (C=O), 160.6 (C-2), 150.7 (C-4'), 135.7 (C-4), 132.7 (C-5), 132.5 (C-6), 132.4 (2C, C-2', C-6'), 127.7 (C-1'), 119.4 (C-1), 117.9 (2C, C-3', C-5'), 113.7 (C-3), 35.0 (C-1''), 31.3 (C-3''), 31.2 (C-2''), 22.15 (C-4''), 14.1 (C-5'').

MS, m/z found 284.1642, $\text{C}_{18}\text{H}_{22}\text{NO}_2$, ($\text{M}+\text{H}^+$) requires 284.1645; found 306.1461, $\text{C}_{18}\text{H}_{21}\text{NO}_2\text{Na}$, ($\text{M}+\text{Na}^+$) requires 306.1465; found 589.3031 $\text{C}_{36}\text{H}_{42}\text{N}_2\text{O}_4\text{Na}$, ($2\text{M}+\text{Na}^+$) requires 589.3037.

IR, $\nu_{\text{max}}/\text{cm}^{-1}$ 3435 (OH), 3375 (NH_2), 1627 (C=O), 1482 (benzene ring), 1174 (C-N).

(E)-4'-(2,2-Dimethylpropylidene)amino-2-hydroxy-5-pentylbenzophenone (126)



To a stirring solution of trimethylacetaldehyde (0.04 g, 0.50 mmol) in toluene (5 mL) was added the solution of **123** (0.27 g, 0.50 mmol) in toluene (5 mL). The reaction mixture was stirred under reflux for 24 h and then cooled to room temperature. Solvent was evaporated and afforded a black oil which was purified by chromatography on silica gel (elution with petrol ether/ ethyl acetate / DCM 10:1:0.2) to give **126** (0.04 g, 23%) as a yellow oil.

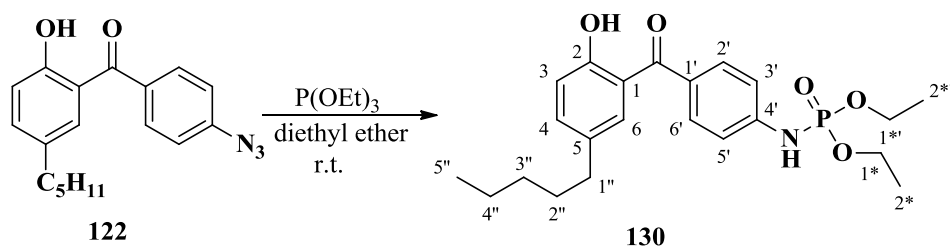
NMR δ_{H} (400 MHz, CDCl₃), 11.79 (1H, s, OH), 7.73 (4H, s, H-2', H-3', H-5', H-6'), 7.58 (1H, s, H-1*), 7.40 (1H, d, $J=2.4$ Hz, H-6), 7.35 (1H, dd, $J=8.4, 2.4$ Hz, H-4), 7.01 (1H, d, $J=8.4$ Hz, H-3), 2.52 (2H, t, $J=7.6$ Hz, H-1''), 1.56 (2H, m, H-2''), 1.38 (9H, s, H-3*, H-4*, H-5*), 1.31 (4H, m, H-3'', H-4''), 0.90 (3H, t, $J=7.2$ Hz, H-5'').

NMR δ_{C} (100 MHz, CDCl₃), 200.1 (C=O), 177.0 (C-2), 161.1 (C-4'), 141.6 (C-1*), 136.5 (C-4), 133.5 (C-5), 133.1 (C-1'), 132.5 (C-6), 130.8 (2C, C-2', C-6'), 119.1 (2C, C-3', C-5'), 118.9 (C-1), 118.1 (C-3), 39.9 (C-2*), 35.0 (C-1''), 31.3 (C-2'', C-3''), 27.6 (C-3*, C-4*, C-5*), 22.7 (C-4''), 14.2 (C-5'').

MS, m/z found 352.2285, C₂₃H₃₀NO₂, (M-H⁺) requires 352.2271.

IR, ν_{max} /cm⁻¹ 3352 (OH), 1669 (C=O) and 1177 (C-N).

Diethyl (4-(2-hydroxy-5-pentylbenzoyl)phenyl)phosphoramidate (**130**)



To a stirring solution of **122** (0.70 g, 2.27 mmol) in diethyl ether (10 mL) was slowly added a solution of triethyl phosphine (0.39 mL, 2.27 mmol) in diethyl ether (10 mL). The reaction mixture was stirred for 2 h at room temperature, and concentrated on a rotary evaporator. The residue was purified by chromatography on silica gel (elution with DCM/ ethyl acetate 1:1) to afford **130** (0.97 g, 100%) as yellow solid with m.p. 82.1-84.0 °C.

NMR δ_{H} (400 MHz, CDCl_3), 11.74 (1H, s, OH), 7.65 (2H, d, $J=8.8$ Hz, H-2', H-6'), 7.38 (1H, d, $J=2.0$ Hz, H-6), 7.31 (1H, dd, $J=8.8, 2.0$ Hz, H-4), 7.16 (2H, d, $J=8.8$ Hz, H-3', H-5'), 6.97 (1H, d, $J=8.8$ Hz, H-3), 6.78 (1H, d, $J=8.4$ Hz, NH), 4.27-4.06 (4H, m, H-1*', H-1*), 2.50 (2H, t, $J=8$ Hz, H-1''), 1.53 (2H, m, H-2''), 1.35 (6H, t, $J=7.2$ Hz, H-2*', H-2*), 1.27 (4H, m, H-3'', H-4''), 0.87 (3H, t, $J=7.2$ Hz, H-5'').

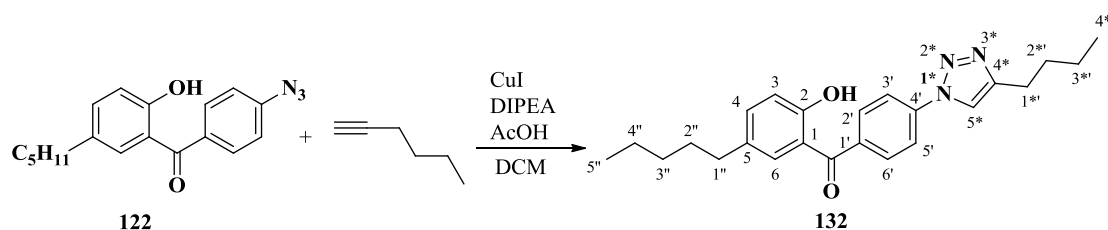
NMR δ_{C} (100 MHz, CDCl_3), 200.0 (C=O), 161.0 (C-2), 144.0 (C-4'), 136.4 (C-4), 132.9 (C-5), 132.5 (C-6), 131.6 (2C, C-2', C-6'), 131.2 (C-1'), 119.1 (C-1), 118.2 (C-3), 116.7 (2C, C-3', C-5'), 63.3 (2C, C-1*', C-1*), 35.0 (C-1''), 31.4 (C-3''), 31.3 (C-2''), 22.6 (C-4''), 16.2 (2C, C-2*', C-2*), 14.1 (C-5').

NMR δ_{P} (161 MHz, CDCl_3), 1.75 (1P, s).

MS, m/z found 420.1926 $\text{C}_{22}\text{H}_{31}\text{NO}_5\text{P}$, ($\text{M}+\text{H}^+$) requires 420.1934; found 442.1743 $\text{C}_{22}\text{H}_{30}\text{NO}_5\text{PNa}$, ($\text{M}+\text{Na}^+$) requires 442.1754; found 861.3596, $\text{C}_{44}\text{H}_{60}\text{N}_2\text{O}_{10}\text{P}_2\text{Na}$, ($2\text{M}+\text{Na}^+$) requires 861.3615.

IR, $\nu_{\text{max}}/\text{cm}^{-1}$ 3400-3060 (OH, NH), 1629 (C=O), 1265 (P=O), 1223 (C-N), 1025 (P-O ester).

4'-(4-Butyl-1H-1,2,3-triazol-1-yl)-2-hydroxy-5-pentylbenzophenone (132)



To a mixture of copper(I) iodide (0.004 g, 0.02 mmol), *N,N*-diisopropylethylamine (0.007 mL, 0.04 mmol) and acetic acid (0.002 mL, 0.04 mmol) in DCM (2 mL) was added a mixture of 1-hexyne (0.12 mL, 1.00 mmol) and **122** (0.31 g, 1.00 mmol). The reaction mixture was stirred at room temperature for 24 h. Then the mixture was concentrated and purified by chromatography on silica gel (elution with petrol ether/ ethyl acetate 10:1) to afford **132** (0.33 g, 83%) as a yellow solid with m.p. 93.1-94.6 °C.

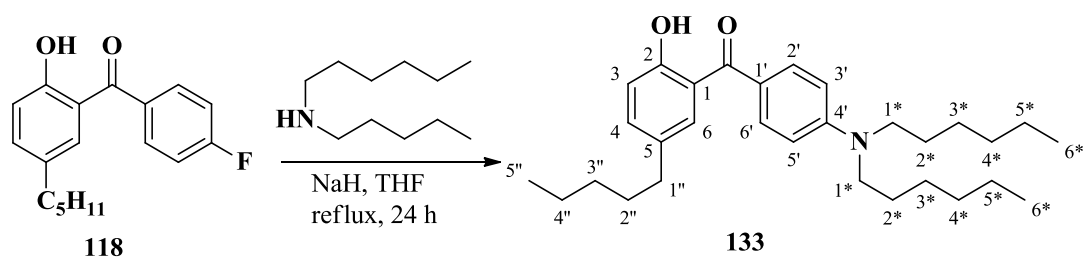
NMR δ_{H} (400 MHz, CDCl_3), 11.69 (1H, s, OH), 7.91-7.81 (5H, m, H-2', H-3', H-4', H-5', H-6', H-5*), 7.36 (1H, dd, $J=8.4, 2.4$ Hz, H-4), 7.32 (1H, d, $J=2.4$ Hz, H-6), 7.01 (1H, d, $J=8.4$ Hz, H-3), 2.82 (2H, t, $J=7.6$ Hz, H-1*'), 2.50 (2H, t, $J=7.6$ Hz, H-1''), 1.73 (2H, m, H-2*'), 1.52 (2H, m, H-2''), 1.43 (2H, m, H-3*'), 1.27 (4H, m, H-3'', H-4''), 0.96 (3H, t, $J=7.2$ Hz, H-4*'), 0.86 (3H, t, $J=7.8$ Hz, H-5'').

NMR δ_{C} (100 MHz, CDCl_3), 199.8 (C=O), 161.4 (C-2), 149.8 (C-4'), 139.6 (C-5), 139.6 (C-1'), 137.8 (C-4*), 137.3 (C-4), 133.4 (C-1), 132.4 (C-6), 131.0 (2C, C-2', C-6'), 119.9 (2C, C-3', C-5'), 118.7 (C-5*), 118.5 (C-3), 35.0 (C-1''), 31.5 (C-2*'), 31.3 (C-2'', C-3''), 25.4 (C-1*''), 22.6 (C-3*'), 22.4 (C-4''), 14.1 (H-5''), 13.9 (H-4*'').

MS, m/z found 392.2326 $\text{C}_{24}\text{H}_{30}\text{N}_3\text{O}_2$, ($\text{M}+\text{H}^+$) requires 392.2333; found 414.2145 $\text{C}_{24}\text{H}_{29}\text{N}_3\text{O}_2\text{Na}$, ($\text{M}+\text{Na}^+$) requires 414.2152; found 805.4396 $\text{C}_{48}\text{H}_{58}\text{N}_6\text{O}_4\text{Na}$, ($2\text{M}+\text{Na}^+$) requires 805.4412.

IR, $\nu_{\text{max}}/\text{cm}^{-1}$ 3435 (OH), 1631 (C=O), 1605, 1482 (benzene ring) and 1223 (C-N).

4'-Dihexylamino-2-hydroxy-5-pentylbenzophenone (133)



Under anhydrous conditions, sodium hydride (60% dispersion in mineral oil) (0.08 g, 2.00 mmol) and 3 mL anhydrous THF was added to a round bottom flask. Dihexylamine (0.46 mL, 2.00 mmol) was added to the flask and the mixture was stirred at room temperature for 10 min. A solution of **118** (0.286 g, 1 mmol) in anhydrous THF (3 mL) was added drop wise. The reaction mixture was stirred and heated under reflux for 24 h. After cooling to room temperature, the mixture was quenched with water (10 mL) and extracted with ethyl acetate (3 x 10 mL). The extract was dried and concentrated to afford a yellow oil which was purified by chromatography on silica gel (elution with petrol ether/ ethyl acetate 100:1) to give **133** (0.04 g, 8%) as a yellow oil.

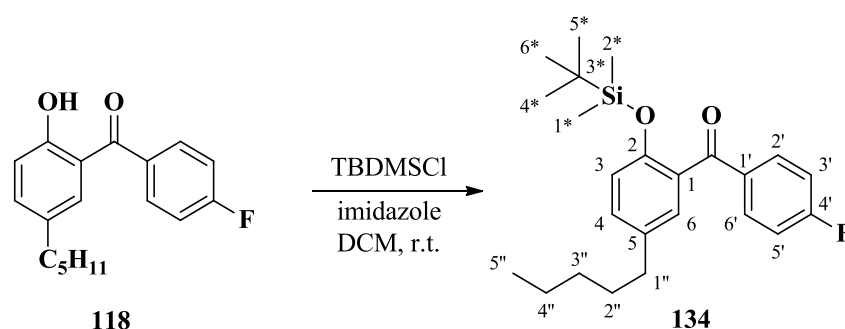
NMR δ_{H} (400 MHz, CDCl_3), 11.82 (1H, s, OH), 7.74 (2H, dt, $J=9.6, 2.4$ Hz, H-2', H-6'), 7.51 (1H, d, $J=2.4$ Hz, H-6), 7.30 (1H, dd, $J=8.4, 2.4$ Hz, H-4), 6.99 (1H, d, $J=8.4$ Hz, H-3), 6.68 (2H, dt, $J=9.6, 2.4$ Hz, H-3', H-5'), 3.38 (4H, t, $J=7.6$ Hz, H-1*) 2.56 (2H, t, $J=8.0$ Hz, H-1''), 1.63 (6H, m, H-2'', H-2*), 1.31 (14H, m, H-3'', H-4'', H-3*, H-4*, H-5*), 0.88 (9H, m, H-5'', H-6*).

NMR δ_{C} (100 MHz, CDCl_3), 197.5 (C=O), 159.4 (C-2), 150.3 (C-4'), 134.1 (C-4), 131.7 (2C, C-2', C-6'), 131.4 (C-5), 131.3 (C-6), 123.1 (C-1'), 118.7 (C-1), 117.0 (C-3), 109.2 (2C, C-3', C-5'), 50.1 (2C, C-1*), 33.9 (C-1''), 30.7 (2C, C-2*), 30.9 (C-3''), 30.7 (C-2''), 26.2 (2C, C-3*), 25.8 (2C, C-4*), 21.7 (C-4''), 21.5 (2C, C-5*), 13.1 (C-5''), 13.0 (2C, C-6*).

MS, m/z found 452.3518 $\text{C}_{30}\text{H}_{46}\text{NO}_2$, ($\text{M}+\text{H}^+$) requires 452.3523; found 474.3338 $\text{C}_{30}\text{H}_{45}\text{NO}_2\text{Na}$, ($\text{M}+\text{Na}^+$) requires 474.3343; found 925.6782, $\text{C}_{60}\text{H}_{90}\text{N}_2\text{O}_4\text{Na}$, ($2\text{M}+\text{Na}^+$) requires 925.6793.

IR, $\nu_{\text{max}}/\text{cm}^{-1}$ 3400-3060 (OH), 1626 (C=O), 1482 (benzene ring) and 1182 (C-N).

4'-Fluoro-2-((tert-butyldimethylsilyloxy)-5-pentylbenzophenone (**134**)



4'-Fluoro-2-hydroxy-5-pentylbenzophenone (**118**) (0.57 g, 2.00 mmol) and imidazole (0.41 g, 6.00 mmol) were dissolved in DCM (20 mL) in a round bottom flask. The mixture solution was cooled to 0 °C and *tert*-butyl(chloro)dimethylsilane (0.45 g, 3.00 mmol) was added to the flask. The reaction mixture was stirred at 0 °C for 10 min then warmed up to room temperature and stirred for 5 h. Solvent was evaporated and the residue was dissolved in ethyl acetate 20 mL which was washed with water (2 x 10 mL) and brine (5 mL). The organic layer was dried and concentrated to afford **134** (0.75 g, 94%) as a yellow oil.

NMR δ_{H} (400 MHz, CDCl_3), 7.88 (2H, m, H-2', H-6'), 7.21 (2H, m, H-4, H-6), 7.11 (2H, tt, $J=8.8, 2.0$ Hz, H-3', H-5'), 6.80 (1H, m, H-3), 2.59 (2H, t, $J=7.6$ Hz, H-1''), 1.63 (2H, m, H-2''), 1.34 (4H, m, H-3'', H-4''), 0.91 (3H, t, $J=7.6$ Hz, H-5''), 0.68 (9H, s, H-4*, H-5*, H-6*), 0.58 (6H, s, H-1*, H-2*).

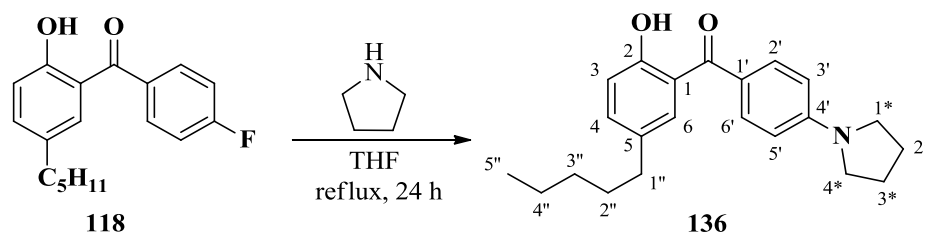
NMR δ_{C} (100 MHz, CDCl_3), 195.8 (C=O), 165.6 (d, $J=253.0$ Hz, C-4'), 150.9 (C-2), 136.0 (C-5), 134.3 (d, $J=2.0$ Hz, C-1'), 132.6 (2C, d, $J=9.0$ Hz, C-2', C-6'), 131.8 (C-4), 131.0 (C-1), 129.5 (C-6), 119.6 (C-3), 115.2 (2C, d, $J=21.0$ Hz, C-3', C-5'), 34.9 (C-1''), 31.5 (C-3''), 31.1 (C-2''), 25.2 (3C, C-4*, C-5*, C-6*), 22.5 (C-4''), 17.8 (C-3*), 14.2 (C-5''), -4.5 (C-1*, C-2*).

NMR δ_{F} (376 MHz, CDCl_3), 56.0 (1F, m, F-4').

MS, m/z found 401.2301 $\text{C}_{24}\text{H}_{34}\text{FO}_2\text{Si}$ ($\text{M}+\text{H}^+$) requires 401.2307; found 423.2118 $\text{C}_{24}\text{H}_{33}\text{FO}_2\text{SiNa}$, ($\text{M}+\text{Na}^+$) requires 423.2126.

IR, $\nu_{\text{max}}/\text{cm}^{-1}$ 1665 (C=O), 1250 (Si-CH₃).

4'-Pyrrolidin-1-yl-2-hydroxy-5-pentylbenzophenone (**136**)



A mixture of 4'-fluoro-2-hydroxy-5-pentylbenzophenone (**118**) (0.29 g, 1.00 mmol) and pyrrolidine (0.34 mL, 4.00 mmol) in THF was stirred and heated under reflux for 24 h. After cooling to room temperature, the mixture was quenched with water (10 mL) and extracted with ethyl acetate (3 x 10 mL). The extract was dried and concentrated to afford a yellow oil which was purified by chromatography on silica gel (elution with petrol ether/ethyl acetate 40:1) to give target product **136** (0.31 g, 92%) as a yellow solid with m.p. 87.9-89.2 °C.

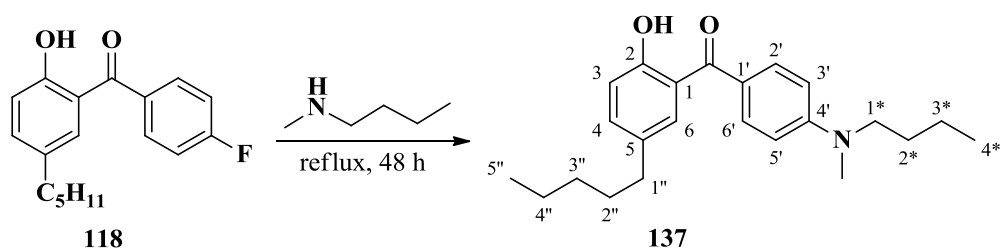
NMR δ_{H} (400 MHz, CDCl_3), 11.76 (1H, s, OH), 7.71 (2H, dt, $J=9.2, 2.8$ Hz, H-2', H-6'), 7.44 (1H, d, $J=2.0$ Hz, H-6), 7.25 (1H, dd, $J=8.8, 2.0$ Hz, H-4), 6.95 (1H, d, $J=8.8$ Hz, H-3), 6.57 (2H, dt, $J=9.2, 2.8$ Hz, H-3', H-5'), 3.39 (4H, t, $J=6.4$ Hz, H-1*, H-4*), 2.51 (2H, t, $J=7.2$ Hz, H-1''), 2.05 (4H, m, H-2*, H-3*), 1.54 (2H, m, H-2''), 1.30 (4H, m, H-3'', H-4''), 0.87 (3H, t, $J=7.2$ Hz, H-5'').

NMR δ_{C} (100 MHz, CDCl_3), 198.9 (C=O), 160.4 (C-2), 150.8 (C-4'), 135.2 (C-4), 132.6 (2C, C-2', C-6'), 132.5 (C-5), 132.4 (C-6), 124.6 (C-1'), 119.8 (C-1), 117.8 (C-3), 110.7 (2C, C-3', C-5'), 47.7 (2C, C-1*, C-4*), 35.1 (C-1''), 31.4 (2C, C-2'', C-3''), 25.6 (C-2*, C-3*), 22.6 (C-4''), 14.2 (C-5'').

MS, m/z found 338.2114, $\text{C}_{22}\text{H}_{28}\text{NO}_2$, ($\text{M}+\text{H}^+$) requires 338.2115; found 360.1932 $\text{C}_{22}\text{H}_{27}\text{NO}_2\text{Na}$, ($\text{M}+\text{Na}^+$) requires 360.1934; found 697.3974 $\text{C}_{44}\text{H}_{54}\text{N}_2\text{O}_4\text{Na}$, ($2\text{M}+\text{Na}^+$) requires 697.3976.

IR, $\nu_{\text{max}}/\text{cm}^{-1}$ 3500-3300 (OH), 1625 (C=O), 1483 (benzene ring), 1179 (C-O).

4'-Butyl (methyl)amino-2-hydroxy-5-pentylbenzophenone (137)



A mixture of 4'-fluoro-2-hydroxy-5-pentylbenzophenone (**118**) (0.29 g, 1.00 mmol) and *N*-methyl-1-butylamine (1.5 mL) was stirred and heated under reflux for 48 h. After cooling to room temperature, the mixture was quenched with water (10 mL) and extracted with ethyl acetate (3 x 10 mL). The extract was dried and concentrated to afford a yellow oil which was purified by chromatography on silica gel (elution with petrol ether/ ethyl acetate 40:1) to give **137** (0.21 g, 58%) as a yellow oil.

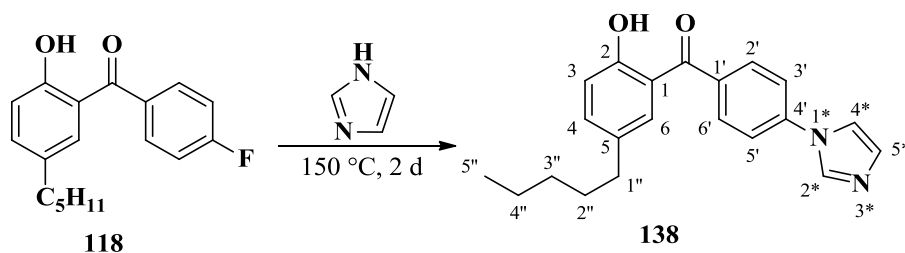
NMR δ_{H} (400 MHz, CDCl_3), 11.77 (1H, s, OH), 7.69 (2H, dt, $J=9.2, 2.8$ Hz, H-2', H-6'), 7.46 (1H, d, $J=2.4$ Hz, H-6), 7.26 (1H, dd, $J=8.4, 2.4$ Hz, H-4), 6.95 (1H, d, $J=8.4$ Hz, H-3), 6.71 (2H, dt, $J=9.2, 2.8$ Hz, H-3', H-5'), 3.41 (2H, t, $J=7.6$ Hz, H-1*), 3.03 (3H, s, NCH_3), 2.52 (2H, t, $J=7.6$ Hz, H-1''), 1.63-1.52 (4H, m, H-2'', H-2*), 1.43-1.24 (6H, m, H-3'', H-4'', H-3*), 0.96 (3H, t, $J=7.6$ Hz, H-4*), 0.88 (3H, t, $J=7.2$ Hz, H-5'').

NMR δ_{C} (100 MHz, CDCl_3), 198.8 (C=O), 160.5 (C-2), 152.3 (C-4'), 135.3 (C-4), 132.6 (3C, C-2', C-6', C-5), 132.4 (C-6), 124.7 (C-1'), 119.8 (C-1), 117.8 (C-3), 110.5 (2C, C-3', C-5'), 52.3 (C-1*), 38.6 (NCH_3), 35.1 (C-1''), 31.4 (2C, C-2'', C-3''), 29.1 (C-2*), 22.6 (C-4''), 20.4 (C-3*), 14.2 (C-5''), 14.0 (C-4*).

MS, m/z found 354.2421 $\text{C}_{23}\text{H}_{32}\text{NO}_2$, ($\text{M}+\text{H}^+$) requires 354.2428; found 376.2242 $\text{C}_{23}\text{H}_{31}\text{NO}_2\text{Na}$, ($\text{M}+\text{Na}^+$) requires 376.2247; found 729.4644, $\text{C}_{46}\text{H}_{62}\text{N}_2\text{O}_4\text{Na}$, ($2\text{M}+\text{Na}^+$) requires 729.4602.

IR, $\nu_{\text{max}}/\text{cm}^{-1}$ 3400-3060 (OH), 1626 (C=O), 1482 (benzene ring) and 1184 (C-N).

4'-(1H-Imidazol-1-yl)-2-hydroxy-5-pentylbenzophenone (**138**)



A mixture of 4'-fluoro-2-hydroxy-5-pentylbenzophenone (**118**) (0.57 g, 2.00 mmol) and imidazole (0.68 g, 10 mmol) was stirred at 150 °C for 48 h. After cooling to room temperature, the reaction mixture was quenched with water (15 mL) and extracted with ethyl acetate (3 x 15 mL). The extract was dried and then concentrated to afford a yellow oil which was purified by chromatography on silica gel (elution with petrol ether/ ethyl acetate 2:1) to give **138** (0.41 g, 72%) as a yellow solid with m.p. 90.5-92.2 °C.

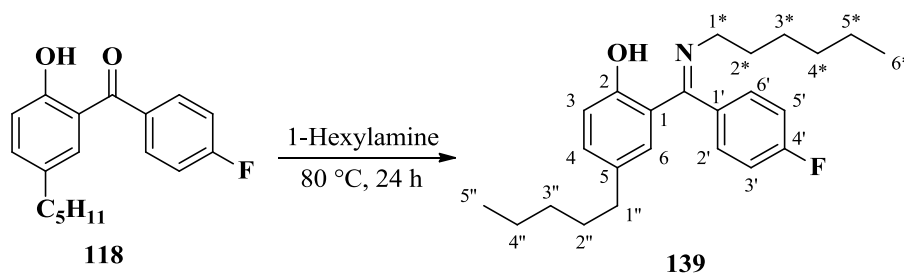
NMR δ_{H} (400 MHz, CDCl_3), 11.73 (1H, s OH), 8.06 (1H, s, H-2*), 7.86 (2H, dt, $J=8.8$, 2.0 Hz, H-2', H-6'), 7.59 (2H, dt, $J=8.8$, 2 Hz, H-3', H-5'), 7.43 (1H, s, H-5*), 7.39 (1H, dd, $J=8.4$, 2.4 Hz, H-4), 7.36 (1H, d, $J=2.4$ Hz, H-6), 7.32 (1H, s, H-4*), 7.04 (1H, d, $J=8.4$ Hz, H-3), 2.54 (2H, t, $J=8$ Hz, H-1''), 1.56 (2H, m, H-2''), 1.32 (4H, m, H-3'', H-4''), 0.93 (3H, t, $J=7.2$ Hz, H-5'').

NMR δ_{C} (100 MHz, CDCl_3), 199.8 (C=O), 161.3 (C-2), 139.9 (C-4'), 137.2 (C-4), 136.9 (C-1'), 135.5 (C-2*), 133.3 (C-5), 132.3 (C-6), 131.3 (2C, C-2', C-6'), 131.0 (C-4*), 120.8 (2C, C-3', C-5'), 118.6 (C-1), 118.4 (C-3), 117.9 (C-5*), 34.9 (C-1''), 31.3 (C-3''), 31.2 (C-2''), 22.5 (C-4''), 14.1 (C-5'').

MS, m/z found 335.1750 $\text{C}_{21}\text{H}_{23}\text{N}_2\text{O}_2$, ($\text{M}+\text{H}^+$) requires 335.1754; found 357.1569 $\text{C}_{21}\text{H}_{22}\text{N}_2\text{O}_2\text{Na}$, ($\text{M}+\text{Na}^+$) requires 357.1573.

IR, $\nu_{\text{max}}/\text{cm}^{-1}$ 3400-3060 (OH), 1629 (C=O), 1482 (benzene ring).

(E)-2-((4-fluorophenyl)(hexylimino)methyl)-5-pentylphenol (139)



A mixture of 4'-fluoro-2-hydroxy-5-pentylbenzophenone (**118**) (0.29 g, 1.00 mmol) and 1-hexylamine (2 mL) was stirred at 80 °C for 24 h. After cooling to room temperature, the mixture was quenched with water (10 mL) and extracted with ethyl acetate (3 x 10 mL). The extract was dried and concentrated to afford yellow oil which was purified by chromatography on silica gel (elution with petrol ether/ ethyl acetate 100:1) to give **139** (0.33 g, 89%) as a yellow oil.

NMR δ_{H} (400 MHz, CDCl_3), 15.69 (1H, s, OH), 7.27-7.19 (4H, m, H-2', H-3', H-5', H-6'), 7.13 (1H, dd, $J=8.4, 2.4$ Hz, H-4), 6.94 (1H, d, $J=8.4$ Hz, H-3), 6.55 (1H, d, $J=2.4$ Hz, H-6), 3.21 (2H, t, $J=7.2$ Hz, H-1*), 2.38 (2H, t, $J=8$ Hz, H-1''), 1.67 (2H, m, H-2*), 1.45 (2H, m, H-2''), 1.41-1.36 (2H, m, H-3*), 1.18 (8H, m, H-3'', H-4'', H-4*, H-5*), 0.91-0.84 (6H, m, H-5'', H-6*).

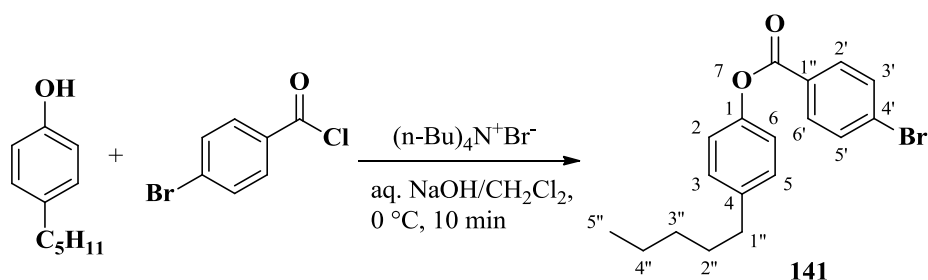
NMR δ_{C} (100 MHz, CDCl_3), 171.8 (C=O), 161.8 (d, $J=247$ Hz, C-4'), 160.6 (C-2), 131.7 (C-4), 130.4 (C-5), 129.5 (C-6), 129.0 (d, $J=4$ Hz, C-1'), 128.3 (d, $J=8$ Hz, C-2', C-6'), 118.2 (C-1), 116.9 (C-3), 114.8 (d, $J=22$ Hz, C-3', C-5'), 50.4 (C-1*), 33.9 (C-1''), 30.5 (C-3''), 30.3 (C-2''), 30.2 (C-4*), 29.8 (C-2*), 26.0 (C-3*), 21.5 (C-4''), 21.4 (C-5*), 13.1 (C-6*), 13.0 (C-5'').

NMR δ_{F} (376 MHz, CDCl_3), 50.2 (1F, m)

MS, m/z found 370.2526, $\text{C}_{24}\text{H}_{33}\text{FNO}$, ($\text{M}+\text{H}^+$) requires 370.2541; found 392.2344, $\text{C}_{24}\text{H}_{32}\text{FNONa}$, ($\text{M}+\text{Na}^+$) requires 392.2360; found 761.4800, $\text{C}_{48}\text{H}_{64}\text{F}_2\text{N}_2\text{O}_2\text{Na}$, ($2\text{M}+\text{Na}^+$) requires 761.4828.

IR, $\nu_{\text{max}}/\text{cm}^{-1}$ 3400-3060 (OH), 1608 (C=N) and 1158 (C-N).

4-Pentylphenyl 4-bromobenzoate (**141**)



Prepared using phase-transfer condition procedure from 4-pentylphenol (0.33 g, 2.00 mmol), 4-bromobenzoyl chloride (0.44 g, 2.00 mmol) and tetra-*n*-butylammonium bromide (0.06 g, 0.20 mmol) yielding **141** as a white solid (0.57 g, 82%) with m.p. 65.5-66.5 °C.

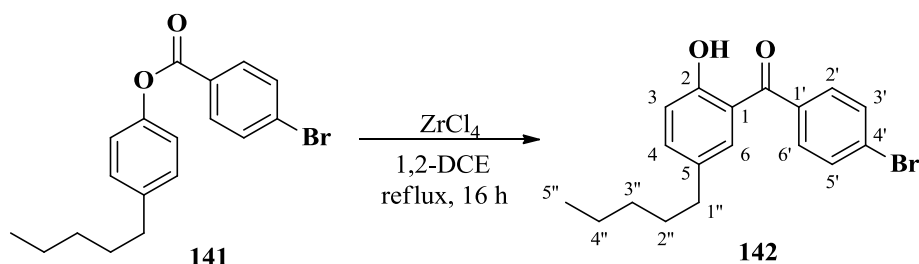
NMR δ_{H} (400 MHz, CDCl_3), 8.08 (2H, dt, $J=8.8$ Hz, 2.0 Hz, H-2', H-6'), 7.68 (2H, dt, $J=8.8$ Hz, 2.0 Hz, H-3, H-5), 7.25 (2H, dt, $J=8.8$ Hz, 2.0 Hz, H-3', H-5'), 7.13 (2H, dt, $J=8.8$ Hz, 2.0 Hz, H-2, H-6), 2.65 (2H, t, $J=8.0$ Hz, H-1''), 1.66 (2H, m, H-2''), 1.34 (4H, m, H-3'', H-4''), 0.92 (3H, t, $J=7.2$ Hz, H-5'').

NMR δ_{C} (100 MHz, CDCl_3), 163.7 (C=O), 147.6 (C-1), 139.8 (C-5), 130.9 (2C, C-2', C-6'), 130.6 (2C, C-3', C-5'), 128.4 (2C, C-3, C-5), 127.7 (C-4'), 127.6 (C-1'), 120.2 (2C, C-2, C-6), 34.4 (C-1''), 30.5 (C-3''), 30.2 (C-2''), 21.5 (C-4''), 13.1 (C-5'').

MS, m/z found 347.0645, $\text{C}_{18}\text{H}_{20}^{79}\text{BrO}_2$, ($\text{M}+\text{H}^+$) requires 347.0641; found 349.0624, $\text{C}_{18}\text{H}_{20}^{81}\text{BrO}_2$, ($\text{M}+\text{H}^+$) requires 349.0621; found 369.0466 $\text{C}_{18}\text{H}_{19}^{79}\text{BrO}_2\text{Na}$, ($\text{M}+\text{Na}^+$) requires 369.0461; found 371.0444 $\text{C}_{18}\text{H}_{19}^{81}\text{BrO}_2\text{Na}$, ($\text{M}+\text{Na}^+$) requires 371.0440; found 715.1034 $\text{C}_{36}\text{H}_{38}^{79}\text{Br}_2\text{O}_4\text{Na}$, ($2\text{M}+\text{Na}^+$) requires 715.1029; found 717.1011 $\text{C}_{36}\text{H}_{38}^{81}\text{Br}_2\text{O}_4\text{Na}$, ($2\text{M}+\text{Na}^+$) requires 717.1009.

IR, $\nu_{\text{max}}/\text{cm}^{-1}$ 1732 (C=O).

4'-Bromo-2-hydroxy-5-pentylbenzophenone (**142**)



The Fries rearrangement procedure was followed with **141** (0.57 g, 1.60 mmol) and ZrCl_4 (0.75 g, 3.20 mmol) under reflux for 16 h. The crude product was purified by chromatography on silica gel (elution with petrol ether/ ethyl acetate 20:1) to afford **142** (0.39 g, 70%) as a yellow oil.

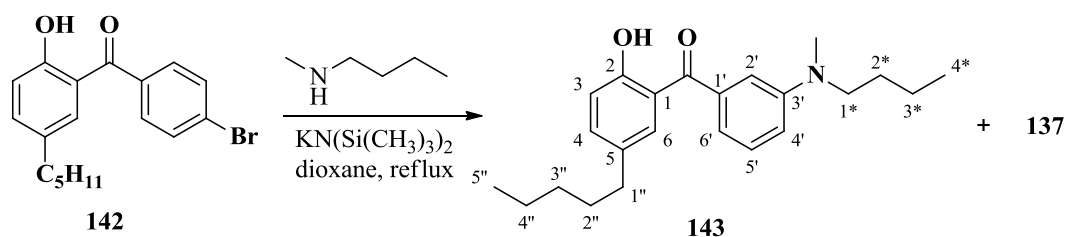
NMR δ_{H} (400 MHz, CDCl_3), 11.72 (1H, s, OH), 7.68 (2H, d, $J=8.8$ Hz, H-2', H-6'), 7.58 (2H, d, $J=8.8$ Hz, H-3', H-5'), 7.38 (1H, dd, $J=8.4$ Hz, 1.6 Hz, H-4), 7.32 (1H, s, H-6), 7.03 (1H, d, $J=8.4$ Hz, H-3), 2.53 (2H, t, $J=8.0$ Hz, H-1''), 1.56 (2H, m, H-2''), 1.32 (4H, m, H-3'', H-4''), 0.91 (3H, t, $J=7.2$ Hz, H-5'').

NMR δ_{C} (100 MHz, CDCl_3), 199.3 (C=O), 160.3 (C-2), 136.1 (C-4), 135.8 (C-5), 132.2 (C-1'), 131.3 (C-6), 130.6 (2C, C-2', C-6'), 129.8 (2C, C-3', C-5'), 125.8 (C-4'), 117.5 (C-1), 117.3 (C-3), 33.9 (C-1''), 30.3 (C-3''), 30.2 (C-2''), 21.5 (C-4''), 13.1 (C-5'').

MS, m/z found 347.0642, $\text{C}_{18}\text{H}_{20}^{79}\text{BrO}_2$, ($\text{M}+\text{H}^+$) requires 347.0641; found 349.0621 $\text{C}_{18}\text{H}_{20}^{81}\text{BrO}_2$, ($\text{M}+\text{H}^+$) requires 349.0621; found 369.0460 $\text{C}_{18}\text{H}_{19}^{79}\text{BrO}_2\text{Na}$, ($\text{M}+\text{Na}^+$) requires 369.0461; found 371.0439 $\text{C}_{18}\text{H}_{19}^{81}\text{BrO}_2\text{Na}$, ($\text{M}+\text{Na}^+$) requires 371.0440.

IR, $\nu_{\text{max}}/\text{cm}^{-1}$ 3400-3060 (OH), 1631 (C=O) and 1482 (benzene ring).

3'-Butyl (methyl)amino-2-hydroxy-5-pentylbenzophenone (143)



Under anhydrous conditions, **142** (0.32 g, 0.90 mmol), *N*-methyl-1-butylamine (0.13 mL, 1.01 mmol) and potassium bis(trimethylsilyl)amide (0.5 M in toluene) (4 mL, 1.80 mmol) were added to 1,4-dioxane (4 mL). The reaction mixture was stirred and heated under reflux for 16 h. After cooling to room temperature, the mixture was quenched with water (10 mL) and extracted with ethyl acetate (3 x 10 mL). The extract was dried over anhydrous Mg_2SO_4 and concentrated to afford a yellow oil which was purified by chromatography on silica gel (elution with petrol ether/ ethyl acetate 100:1) to give **143** (0.03 g, 18%) as a yellow oil, and elution with petrol ether/ ethyl acetate 40:1 gave **137** (0.04 g, 22%) as a yellow oil.

NMR δ_{H} (400 MHz, CDCl_3), 11.97 (1H, s, OH), 7.50 (1H, d, $J=2.4$ Hz, H-6), 7.40-7.33 (2H, m, H-4, H-5'), 7.01 (1H, d, $J=8.4$ Hz, H-3), 6.97-6.91 (3H, m, H-2', H-4', H-6'), 3.38 (2H, t, $J=7.2$ Hz, H-1*), 3.01 (3H, s, NCH_3), 2.52 (2H, t, $J=7.6$ Hz, H-1''), 1.65-1.52 (4H, m, H-2'', H-2*), 1.41-1.29 (6H, m, H-3'', H-4'', H-3*), 0.97 (3H, t, $J=7.6$ Hz, H-4*), 0.90 (3H, t, $J=6.8$ Hz, H-5'').

NMR δ_{C} (100 MHz, CDCl_3), 202.6 (C=O), 161.2 (C-2), 149.1 (C-3'), 138.9 (C-1'), 136.5 (C-5'), 133.0 (C-6), 132.8 (C-5), 128.9 (C-4), 119.0 (C-1), 118.0 (C-3), 116.7 (C-6'), 115.1 (C-4'), 112.1 (C-2'), 51.2 (C-1*), 37.5 (NCH_3), 33.9 (C-1''), 31.4 (C-3''), 31.3 (C-2''), 28.9 (C-2*), 22.5 (C-4''), 20.3 (C-3*), 14.1 (C-4*), 14.0 (C-5'').

MS, m/z found 352.2286 $\text{C}_{23}\text{H}_{30}\text{NO}_2$, ($\text{M}-\text{H}^+$) requires 352.2271.

IR, $\nu_{\text{max}}/\text{cm}^{-1}$ 3500-3060 (OH), 1630 (C=O), 1483 (benzene ring).

References

1. Paul, N. D. and Jones, D. G., Ecological roles of solar UV radiation: towards an integrated approach, *Trends Ecol. Evol.*, 2003, 18, 48-55.
2. UK climate,
<http://www.metoffice.gov.uk/public/weather/climate>, accessed 20/01/2016.
3. Balearics and North Africa climate,
<http://www.metoffice.gov.uk/weather/world-climate/africa/north-africa>, accessed 20/01/2016.
4. Radiation, <http://www.qdl.scs-inc.us/2ndParty/Pages/10522.html>, accessed 20/01/2016.
5. Paul, N. D., Jacobson, R. J., Taylor, A., Wargent, J. J. and Moore, J. P., The use of wavelength selective plastic cladding materials in horticulture: understanding of crop and fungal responses through the assessment of biological spectral weighting functions, *Photochem. Photobiol.*, **2005**, 81, 1052-1060.
6. Briggs, W. R. and Christie, J. M., Phototropins 1 and 2: versatile plant blue-light receptors, *Trends Plant Sci.*, **2002**, 7, 204-210.
7. McKenzie, R. L., Aucamp, P. J., Bais, A. F., Bjorn, L. O., Ilyasf, M. and Madronich, S., Ozone depletion and climate change: impacts on UV radiation, *Photochem. Photobiol. Sci.*, **2011**, 10, 182-198.
8. Lizana, X. C., Hess, S. and Calderini, D. F., Global increase in UV irradiance during the past 30 years (1979–2008) estimated from satellite data, *J. Geophys. Res.*, **2010**, 115.
9. Willams D.H. and Fleming, I., Spectroscopic methods in organic chemistry, *McGRAW-HILL Book company Europe*, 5th, edn, **1989**.
10. UV/Vis absorption spectroscopy,
<http://teaching.shu.ac.uk/hwb/chemistry/tutorials/molspec/uvvisab1.htm>, accessed 26/01/2016
11. Nielsen, E. S., On a complication in marine productivity work due to the influence of ultraviolet Light, *J. Cons. Perm. Int. Explor.*, **1964**, 29, 130–135.
12. Jitts, H.R., Morel, A. and Saijo, Y., The relation of oceanic primary production to available photosynthetic irradiance, *Aust. J. Mar. Freshw. Res.*, **1976**, 27, 441–454.
13. Day, T. A. and Neale, P. J., Effects of UV-B radiation on terrestrial and aquatic primary producers, *Annu. Rev. Ecol. Syst.*, **2002**, 33, 371– 396.
14. Caldwell, M. M. and Flint, S. D., Stratospheric ozone reduction, solar UV-B radiation and terrestrial ecosystems, *Clim. Change*, **1994**, 28, 375–394.
15. Flint, S. D., Ryel, R. J. and Caldwell, M. M., Ecosystem UV-B experiments in terrestrial communities: a review of recent findings and methodologies, *Agricultural and Forest Meteorology*, **2003**, 120, 177–189.
16. Norval, M., Cullen, A.P., Gruijl, F.R., Longstreth, J., Takizawa, Y., Lucas, R.M., Noonan, F. P. and Leun, J. C., The effects on human health from stratospheric ozone depletion and its inter-actions with climate change, *Photochem. Photobiol. Sci.*, **2007**, 3, 232-251.
17. Haeder, D.P., Williamson, C. E., Wangberg, S.A., Rautio, M., Rose, K.C., Gao,

- K.S., Helbling, E.W., Sinha, R.P. and Worrest, R., Effects of UV radiation on aquatic ecosystems and interactions with other environmental factors, *Photochem. Photobiol. Sci.*, **2015**, 1, 108-126.
18. Singh, R., Singh, S., Tripathi, R. and Agrawal, S. B., Supplemental UV-B radiation induced changes in growth, pigments and antioxidant pool of bean (*Dolichos lablab*) under field conditions. *J. Exp. Biol.*, **2011**, 2, 139-145.
 19. V.G. Kakani, K.R. Reddy, D. Zhao and A.R. Mohammed, Ultraviolet-B radiation effects on cotton (*Gossypium hirsutum* L.) morphology and anatomy, *Ann. Bot.*, **2003**, 817–826.
 20. Lidona, F.C. and Ramalho, Impact of UV-B irradiation on photosynthetic performance and chloroplast membrane components in *Oryza sativa* L, *Ann. Bot.* **2011**, 3, 457–466.
 21. Laposi, R., Veres, S., Lakatos, G., Olah, V., Fieldsend, A. and Meszaros, I., Responses of leaf traits of european beech (*Fagus sylvatica* L.) saplings to supplemental UV-B radiation and UV-B exclusion, *Agr. Forest. Meteorol.*, **2009**, 745–755.
 22. Takshak, S., and Agrawal, S.B., Defence strategies adopted by the medicinal plant *Coleus forskohlii* against supplemental ultraviolet-B radiation: Augmentation of secondary metabolites and antioxidants, *Plant Physiol. Biochem.*, **2015**, 97, 124-138.
 23. Yin, L.N., Zhang, M.C., Li, Z.H., Duan, L.S., and Wang, S.W., Enhanced UV-B Radiation Increases Glyphosate Resistance in Velvetleaf (*Abutilon theophrasti*), *Photochem. Photobiol.*, **2012**, 6, 1428-1432.
 24. Zhao, D., Reddy, K.R., Kakani, V.G., Read, J. and Sullivan, J., Growth and physiological responses of cotton (*Gossypium Hirsutum* L.) to elevated carbon dioxide and Ultraviolet-B radiation under controlled environment conditions, *Plant Cell Environ.*, **2003**, 26, 771–782.
 25. Scattino, C., Castagna, A., Neugart, S., Chan, H.M., Schreiner, M., Crisosto, C.H., Tonutti, P. and Ranieri, A., Post-harvest UV-B irradiation induces changes of phenol contents and corresponding biosynthetic gene expression in peaches and nectarines, *Food Chem.* **2014**, 163, 51–60.
 26. Correia, C. M., Coutinho, J. F., Björnc, L. O., and Torres-Pereira, J. M.G., Ultraviolet-B radiation and nitrogen effects on growth and yield of maize under mediterranean field conditions, *Eur. J. Agron.* **2000**, 12, 117–125.
 27. Reddy, K., Kakani, V.G., Zhao, D., Mohammed, A.R. and Gao, W., Cotton responses to ultraviolet-B radiation: experimentation, and algorithm development, *Agric. For. Meteorol.*, **2003**, 120, 249–265.
 28. Hakala, K., Jauhiainen, L., Koskela, T., KaËyhkoË, P. and Vorne, V., Sensitivity of crops to increased yltraviolet radiation in northern growing conditions, *J. Agronomy & Crop Science*, **2002**, 188, 8-18.
 29. Rodriguez, C., Torre, S. and Solhaug, K. A., Low levels of ultraviolet-B radiation from fluorescent tubes induce an efficient flavonoid synthesis in Lollo Rosso lettuce without negative impact on growth. *Acta Agric. Scand. Sect. B — Soil Plant Sci.*, **2014**, 64, 178–184.
 30. Paul, N. D., Moore, J. P., McPherson, M., Lambourne, C., Croft, P., Heaton J. C. and Wargent, J. J., Ecological responses to UV radiation: interactions between the biological effects of UV on plants and on associated organisms, *Physiol. Plant.*, **2012**, 145, 565–581.
 31. Raghuvanshi, R. and Sharma, R. K., Response of two cultivars of *Phaseolus*

- vulgaris L. (French beans) plants exposed to enhanced UV-B radiation under mountain ecosystem. *Environ. Sci. Pollut. Res. Int.* **2016**, 23, 831-842.
32. Liu, B., Liu, X., Li, Y. and Herbert, S. J. Field Crops Research Effects of enhanced UV-B radiation on seed growth characteristics and yield components in soybean. *Field Crop Res.* **2013**, 154, 158–163.
 33. Sakalauskaite, J., Viskelis, P., Duchovskis, P., Dambrauskiene, E., Sakalauskiene, S., Samuoliene, G. and Brazaityte, A., Supplementary UV-B irradiation effects on basil (*Ocimum basilicum* L.) growth and phytochemical properties, *J. Food, Agric. Environ.*, **2012**, 10, 342-346.
 34. Papaioannou, C., Katsoulas, N., Maletsika, P., Siomos, A. and Kittas, C., Effects of a UV-absorbing greenhouse covering film on tomato yield and quality, *Span. J. Agric. Res.*, **2012**, 10, 959-966.
 35. Sgherri, C., Scattino, C., Pinzino, C., Tonutti, P., and Ranieri, A.M., Ultraviolet-B radiation applied to detached peach fruit: A study of free radical generation by EPR spin trapping, *Plant Physiol. Biochem.*, **2015**, 96, 124-131.
 36. Shourie, A., Tomar, P., Srivastava, D. and Chauhan, R. Enhanced Biosynthesis of Quercetin Occurs as A Photoprotective Measure in *Lycopersicon esculentum* Mill. under Acute UV-B Exposure. *Braz. arch. biol. technol.* **2014**, 57, 317-325.
 37. Lavola, A., Aphalo, P.J., Lahti, M. and Julkunen-Tiitto, R., Nutrient availability and the effect of increasing UV-B radiation on secondary plant compounds in Scots pine. *Environ. Exp. Bot.* **2003**, 49, 49–60.
 38. Randriamanana, T. R., Nissinen, K., Moilanen, J. and Nybakken, L., Long-term UV-B and temperature enhancements suggest that females of *Salix myrsinifolia* plants are more tolerant to UV-B than males. *Environ Exp Bot.* **2015**, 109, 296-305
 39. Martínez-lüscher, J., Morales, F., Delrot, S., Sánchez-díaz, M. and Gomés, E., Short- and long-term physiological responses of grapevine leaves to UV-B radiation. *Plant Sci.* **2013**, 213, 114–122.
 40. Mazza, C.A., Giménez, P.I., Kantolic, A.G. and Ballaré, C.L., Beneficial effects of solar UV-B radiation on soybean yield mediated by reduced insect herbivory under field conditions. *Physiol. Plant.* **2013**, 147, 307-315.
 41. Braga, G. U. L., Rangel, D. E. N., Fernandes, E.K.K., Flint, S.D., and Roberts, D.W., Molecular and physiological effects of environmental UV radiation on fungal conidia, *Curr. Genet.*, **2015**, 3, 405-425.
 42. Mazza, C. A., Izaguirre, M. M., Zavala, J., Scopel, A.L. and Ballaré, C. L., Insect perception of ambient ultraviolet-B radiation, *Ecol. Lett.*, **2002**, 5, 722–726.
 43. Kuhlmann, F. and Müller, C., Independent responses to ultraviolet radiation and herbivore attack in broccoli, *J. Exp. Bot.*, **2009**, 60, 3467-3475.
 44. Caputo, C., M. Rutitzky and Ballaré, C. L., Solar ultraviolet-B radiation alters the attractiveness of *Arabidopsis* plants to diamondback moths (*Plutella xylostella* L.): impacts on oviposition and involvement of the jasmonic acid pathway, *Oecologia*, **2006**, 149, 81–90.
 45. Reitz, S., Yearby, E. L., Funderburk, J. E., Stavisky, J., Momol, M. T. and Olson, S. M., Integrated management tactics for frankliniella thrips (Thysanoptera: Thripidae) in field-grown pepper, *J. Econ. Entomol.* **2003**, 96, 1201-1214.
 46. Rousseaux, M. C., Tiitto, R. J., Searles, P. S., Scopel, A. L., Aphalo, P. J. and Ballaré, C. L., Solar UV-B radiation affects leaf quality and insect herbivory in the southern beech tree *Nothofagus Antarctica*, *Oecologia*, **2004**, 138, 505–512.

47. Bailaré, C., Scopel, A., Stapleton, A. and Yanovsky, M. J., Solar ultraviolet-B radiation affects seedling emergence, DNA integrity, plant morphology, growth rate, and attractiveness to herbivore insects in *datura ferox*, *Plant Physiol.* **1996**, 112, 161-170.
48. Rousseaux, M. C., Ballare, C. L., Scopel, A. L., Searles, P. S. and Caldwell, M. M., Solar ultraviolet-B radiation affects plant-insect interactions in a natural ecosystem of Tierra del Fuego (southern Argentina), *Oecologia*, **1998**, 116, 528-535.
49. Mazza, C. A., Zavala, J., Scopel, A.L. and Ballare, C.L., Perception of solar UVB radiation by phytophagous insects: Behavioral responses and ecosystem implications, *Proc. Natl. Acad. Sci. USA*, **1999**, 96, 980–985.
50. Zavala, J.A., Mazza, C.A., Dillon, F.M., Chludil, H.D., and Ballare, C.L., Soybean resistance to stink bugs (*Nezara viridula* and *Piezodorus guildinii*) increases with exposure to solar UV-B radiation and correlates with isoflavonoid content in pods under field conditions, *Plant Cell Environ.*, **2015**, 38, 920-928.
51. Aiamla-or, S., Yamauchi, N., Takino, S. and Shigyo, M., Effect of UV-A and UV-B irradiation on broccoli (*Brassica oleracea* L. Italica Group) floret yellowing during storage, *Postharvest Biol Technol.*, **2009**, 54, 177–179.
52. Nenadis, N., Llorens, L., Koufogianni, A., Diaz, L., Font, J., Gonzalez, J.A. and Verdaguier, D., Interactive effects of UV radiation and reduced precipitation on the seasonal leaf phenolic content/composition and the antioxidant activity of naturally growing *Arbutus unedo* plants, *J. Photochem. Photobiol. B, Biol.*, **2015**, 153, 435-444.
53. Kataria, S. and Guruprasad, K. N. Exclusion of solar UV components improves growth and performance of *Amaranthus tricolor* varieties. *Sci Hort.* **2014**, 174, 36–45.
54. Khoshimkhujayev, B., Kwon, JK., Park, KS., Choi, HG. and Lee, SY. Effect of monochromatic UV-A LED irradiation on the growth of tomato seedlings. *Hortic. Environ. Biotechnol.* **2014**, 55, 287-292.
55. Fujiwara, K., Yano, A. and Eijima, K., Design and development of a plant response experimental light-source system with LEDs of five peak wavelengths, *J Light Visual Environ*, **2011**, 35, 117–122.
56. Lee, M. J., Son, J.E. and Oh, M. M., Growth and phenolic compounds of *Lactuca sativa* L. grown in a closed-type plant production system with UV-A, -B, or -C lamp, *J. Sci. Food Agric.*, **2014**, 94, 197–204.
57. Krizek, D.T., Mirecki, R.M. and Britz, S.J., Inhibitory effects of ambient levels of solar UV-A and UV-B radiation on growth of cucumber, *Physiol.Plam.* **1997**, 100, 886-893.
58. Xu, J. and Gao, K., UV-A enhanced growth and UV-B induced positive effects in the recovery of photochemical yield in *Gracilaria lemaneiformis*(Rhodophyta), *J. Photochem. Photobiol. B: Biology*, **2010**, 100, 117–122.
59. Krizek, D.T., Britz, S.J. and Mirecki, R.M., Inhibitory effects of ambient levels of solar UV-A and UV-B radiation on growth of cv. New Red Fire lettuce, *Physiol. Plant.* **1998**, 103, 1-7.
60. Dáder, B., Gwynn-jones, D., Moreno, A., Winters, A. and Fereres, A. Biology Impact of UV-A radiation on the performance of aphids and whiteflies and on the leaf chemistry of their host plants, *J. Photochem. Photobiol.B.*, **2014**, 138, 307-316.
61. Guo, J. and Wang, M.H., Ultraviolet A-specific induction of anthocyanin biosynthesis and PAL expression in tomato (*Solanum lycopersicum* L.), *Plant Growth Regul.*, **2010**, 62, 1–8.

62. Honda, Y. and Yunoki, T., Control of Sclerotinia disease of greenhouse eggplant and cucumber by inhibition of development of apothecia, *Plant Dis. Rep.*, **1977**, 61, 1036-1040.
63. Raviv, M. and Antignus, Y., UV radiation effects on pathogens and insect pests of greenhouse-grown crops, *Photochem. Photobiol.*, **2004**, 79, 219-226.
64. Chyzik, R., Dorinin, S. and Antignus, Y., Effect of a UV-deficient environment on the biology and flight activity of *Myzus persicae* and its Hymenopterous parasite *Aphidius matricariae*, *Phytoparasitica*, **2003**, 31, 467-477.
65. Pálffy, K. and Vörös, L., Effects of UV-A radiation on *desmodesmus armatus*: changes in growth rate, pigment content and morphological appearance, *Internat. Rev. Hydrobiol.* **2006**, 91, 451-465.
66. Zhang, C., Meng, J., Wang, X., Zhu, F. and Lei, C., Effects of UV-A exposures on longevity and reproduction in *Helicoverpa armigera*, and on the development of its F1 generation, *Insect Sci.*, **2011**, 18, 697–702.
67. Mishra, M. and Meyer-Rochow, V. B., Eyes of male and female *Orgyia antiqua* (Lepidoptera; Lymantriidae) react differently to an exposure with UV-A, *Micron*, **2008**, 39, 471–480.
68. Meyer-Rochow, V. B. and Mishra, M., Structure and putative function of dark- and light-adapted as well as UV-exposed eyes of the food store pest *Psyllipsocus ramburi* Seelys-longchamps (Insecta: Psocoptera: Psyllipsocidae), *J. Insect Physiol.*, **2007**, 53, 157–169.
69. Coombe, P. E., Visual behaviour of the greenhouse whitefly, *Trialeurodes vaporariorum*, *Physiol. Entomol.*, **1982**, 7, 243-251.
70. Kigathi, R. and Poehling, H.M., UV-absorbing films and nets affect the dispersal of western flower thrips, *Frankliniella occidentalis* (Thysanoptera: Thripidae), *J. Appl. Entomol.* **2012**, 136, 761–771.
71. Kyrikou, I. and Briassoulis, D., Biodegradation of agricultural plastic films: a critical review, *J. Polym. Environ.*, **2007**, 15, 125–150.
72. Poly tunnels for the Garden, Farm or Nursery, <http://www.haygrove.co.uk/polytunnels/farm-polytunnels/telescopic-series/>, accessed 29/4/2014.
73. Briassoulis, D., Aristopoulou, A., Bonora, M. and Verlodt, I., Degradation characterisation of agricultural low-density polyethylene films, *Biosystems Engineering*, **2004**, 88, 131-143.
74. Production of plastics worldwide from 1950 to 2014 (in million metric tons), <http://www.statista.com/statistics/282732/global-production-of-plastics-since-1950/>, accessed 26/01/2016.
75. Plastics - the facts 2014/2015 An analysis of European plastics production, demand and waste data, http://issuu.com/plasticseuropeebook/docs/final_plastics_the_facts_2014_19122, accessed 26/01/2016.
76. Reingruber, E. and Buchberger, W., Analysis of polyolefin stabilisers and their degradation products, *J. Sep. Sci.* **2010**, 33, 3463–3475.
77. Ciba, Plastic Additives, Ciba Inc. Ciba Chimassorb 944, **1975**.
78. Ciba, Ciba Specialty Chemicals, Inc. Ciba Irganox 1010, **1998**.
79. Ciba, Ciba Inc. Ciba Irgafos 168, **1999**.

80. BASF, Plastic Additives, Technical Information, Tinuvin 770, **2010**.
81. Ciba, Ciba Specialty Chemicals, Inc. Ciba Irganox B215, **2001**.
82. Z. Liu, S. Chen and J. Zhang, Effect of UV Absorbers and Hindered Amine Light Stabilizers on the Photodegradation of Ethylene–Octene Copolymer, *Inc. J. Appl. Polym. Sci.* **2013**, 127, 1135–1147.
83. G. Balint, T. Kelen, F. Tudos and A. Rehak, Effect of hindered piperidine derivatives on polypropylene photooxidation, *Polym. Bull.* **1979**, 1, 647–652.
84. Allen, N.S., Gardette, J.L. and Lemaire, J., Stabilizer interactions with hindered piperidine compounds in polypropylene: influence of processing. *Polym. Degrad. Stabil.* **1981**, 3, 199–208.
85. BASF, Light stabilisers, Technical Information, Tinogard Q, **2012**.
86. N. S. Allen and A. Chirinis-Padron, The Photo-stabilisation of Polypropylene: A review, *Polym. Degrad. Stabil.*, **1985**, 13, 31-76.
87. George, G. A., The mechanism of photoprotection of polystyrene film by some Ultraviolet absorbers, *J. Appl. Polym. Sci.*, **1974**, 18, 117-124.
88. Ciba, plastic additives, Ciba Specialty Chemicals, Inc. Ciba Chimassorb 81, **1978**.
89. Ciba, plastic additives, Ciba Specialty Chemicals, Inc. Ciba Tinuvin 326, **1966**.
90. Gu, X. and Peng, G, study on the synthesis method of UV 531, *Jiangsu Chemical Industry*, **2008**, 36, 27-38. (Chinese)
91. Ding, Z., Production and application of ultraviolet absorber UV-326 for polymer, *suliao zhuj*, **2004**, 4, 17-20. (Chinese)
92. Zakrzewski, J. and Szymanowski, J., 2-Hydroxybenzophenone UV-absorber containing 4,4,5,5,-tetramethylimidazolidine fragment, *Polym. Degrad. Stabil.*, **2001**, 72, 109-113.
93. Cui, Z., Li, X., Wang, X., Pei, K. and Chen, W., Structure and properties of N-heterocycle-containing benzotriazoles as UV absorbers, *J. Mol. Struct.*, **2013**, 1054-1055, 94–99.
94. Pei, K., Cui, Z. and Chen, W., An adduct of Cl-substituted benzotriazole and hydroxy benzophenone as a novel UVA/UVB absorber: Theory-guided design, synthesis, and calculations, *J. Mol. Struct.*, **2013**, 1032, 100–104.
95. Liu, M.O., Lin, H.F, Yang, M.C, Lai, M.J, Chang, C.C, Liu, H.C., Shiao, P.L., Chen, I.M. and Chen J.Y., Thermal and fluorescent properties of optical brighteners and their whitening effect for pelletization of cycloolefin copolymers. *Mater. Lett.* **2006**, 60, 2132-2137.
96. Zhang, H., Lei, M., Du, F., Li, H. and Wang, J., Using an optical brightening agent to boost peroxide bleaching of a spruce thermomechanical pulp. *Ind. Eng. Chem. Res.* **2013**, 52, 13192–13197
97. Saeed, A., Shabir, G. and Batool, I. Novel stilbene-triazine symmetrical optical brighteners: synthesis and applications. *J. Fluoresc.* **2014**, 24, 1119-27.
98. Plastics Additives & Compounding, Elsevier Science Ltd, Optical brighteners: improving the colour of plastics, **2003**.
99. Mayzo, Mayzo Inc, Benetex OB-1, **2010**.
100. BASF, Formulation Additives, Tinopal NFW Liquid, **2010**.
101. Liu, M. O., Lin, H., Yang, M., Lai, M., Chang, C., Liu, H., Shiao, P., Chen, I. and Chen, J., Thermal and fluorescent properties of optical brighteners and their whitening effect for pelletization of cycloolefin copolymers. *Mater. Lett.*, **2006**, 2132–2137.

102. Mayzo, Mayzo Inc, Benetex OB, **2010**
103. Optical brighteners: improving the colour of plastics, *Plastics Additives & Compounding*, **2003**.
104. Optical brighteners for: Synthetic Plastics, Washing powder, Printing, Artificial Fibres, Nylon, Cotton, Paper, Polyester Fibre, AB Chemitrans.
105. Dougherty, E., Guthrie, K. and Shapiro, M., Optical brighteners provide baculovirus activity enhancement and UV radiation protection. *Biol. Control*. **1996**, 7, 71–74
106. Jayashankar, B., Lokanath, R. K., Baskaran, N. and Sathish H., Synthesis and pharmacological evaluation of 1,3,4-oxadiazole bearing bis (heterocycle) derivatives as anti-inflammatory and analgesic agents. *Eur. J. Med. Chem.* **2009**, 44, 3898–3902.
107. Zhu, Y., Lu, H., He, D., and Yang, Z., Synthesis, fluorescence properties and applications of two novel oxadiazole-based stilbene optical brighteners as UV protectants for insect baculovirus, *J. Photochem. Photobiol. B. Biology.*, **2013**, 125, 8-12.
108. Sambandan, D.R. and Ratner, D., Sunscreens: an overview and update. *J Am Acad Dermatol*, **2011**, 748-758.
109. Moyal, DD. and Fourtanier, AM. Broad-spectrum sunscreens provide better protection from solar ultraviolet-simulated radiation and natural sunlight-induced immunosuppression in human beings. *J. Am. Acad. Dermatol.* **2008**, 58, 149-154.
110. Sayre, R.M., Dowdy, J.C., Gerwig, A.J., Shields, W.J. and Lloyd, R.V., Unexpected photolysis of the sunscreen octinoxate in the presence of the sunscreen avobenzone. *Photochem. Photobiol.* **2005**, 81, 452-456.
111. Palm, M.D. and O'Donoghue M.N., Update on photoprotection. *Dermatol. Ther.* **2007**, 20, 360-76.
112. Fourtanier, A., Moyal, D. and Seite, S., Sunscreens containing the broad-spectrum UVA absorber, Mexoryl SX, prevent the cutaneous detrimental effects of UV exposure: a review of clinical study results. *Photodermatol. Photoimmunol. Photomed.*, **2008**, 164-174.
113. Fourtanier, A., Moyal, D. and Seite, S.. UVA filters in sun-protection products: regulatory and biological aspects. *Photochem. Photobiol. Sci.* **2012**, 1, 81-89.
114. Girigoswami, K., Viswanathan, M., Murugesan, R. and Girigoswami. A., Studies on polymer-coated zinc oxide nanoparticles: UV-blocking efficacy and in vivo toxicity. *Mater. Sci. Eng.C*, **2015**, 501–510.
115. Lademann, J., Schanzer, S., Jacobi, U., Schaefer, H., Pflucker, F., Driller, H., Beck, J., Meinke, M., Roggan, A. and Sterry, W. Synergy effects between organic and inorganic UV filters in sunscreens. *J Biomed Opt.* **2005**, 10, 14008.
116. Giampieri, F., Alvarez-Suarez, J.M., Tulipani, S., Gonzales-Paramas, A.M., Santos-Buelga, C., Bompadre, S., Quiles, J.L., Mezzetti, B. and Battino, M., Photoprotective potential of strawberry (*Fragaria ananassa*) extract against UV-A irradiation damage on human fibroblasts, *J. Agric. Food Chem.* **2012**, 60 2322–2327.
117. Pietta, P.G., Flavonoids as Antioxidants, *J. Nat. Prod.* **2000**, 63, 1035–1042.
118. Veberic, R., Jakopic, J., Stampar, F. and Schmitzer, V., European elderberry (*Sambucus nigra* L.) rich in sugars, organic acids, anthocyanins and selected polyphenols, *Food Chem.* **2009**, 114, 511–515.
119. Gancarz, R., Wilk, K.A., Jarzycka, A. and Lewin, A., Assessment of extracts of

- Helichrysum arenarium , Crataegus monogyna , Sambucus nigra in photoprotective UVA and UVB ; photostability in cosmetic emulsions. *J. Photochem. Photobiol. B, Biol.* **2013**, 128, 50-57.
120. Burchard, P., Bilger, W. and Weissenböck, G., Contribution of hydroxycinnamates and flavonoids to epidermal shielding of UV-A and UV-B radiation in developing rye primary leaves as assessed by ultraviolet-induced chlorophyll fluorescence measurements. *Plant Cell Env.* **2000**, 23, 1373–1380.
 121. Rock, R. S. and Stowell, M. H. B., Photoresponsive sunscreen compositions, US6280711 B1, **2001**.
 122. Martin, R., Uses of the Fries rearrangement for the preparation of hydroxyarylketones. a review, *Org. Prep. Proced. Int.*, **1992**, 24, 369-435.
 123. Mahendra, M., Doreswamy, B. H., Sridhar, M. A., Prasad, J. S., Khanum, S. A., Shashikanth, S. and Venu, T. D., Synthesis and crystal structure of 2-benzoyl-4- methyl phenyl benzoate, *J. Chem. Crystallogr.*, **2005**, 35, 463-467.
 124. Giesbrecht, G. R., Boller, T. M., Voskoboynikov, A. Z., Asachenko, A. F., Nikulin, M. V. and Tsarev, A. A., Catalyst compounds and use thereof, U.S. patent 05334, **2010**.
 125. Moghaddam, F. M., Ghaffarzadeha, M. and Abdi-Oskoui, S. H., Tandem Fries reaction-conjugate addition under microwave irradiation in dry media; one-pot synthesis of flavanones, *J. Chem. Research (S)*, **1999**, 574-575.
 126. Kobayashi, S., Moriwaki, M. and Hachiya, L., The catalytic Fries Rearrangement of acyloxy naphthalenes using scandium trifluoromethanesulfonate as a catalyst, *J. Chem. Soc., Chem. Commun.*, **1995**, 1527-1528.
 127. Kobayashi, S.L., Moriwaki, M. and Hachiya, L., Hafnium trifluoromethanesulfonate (Hf(OTf)₄) as an efficient catalyst in the fries rearrangement and direct acylation of phenol and naphthol derivatives, *Tetrahedron Lett.*, **1996**, 37, 2053-2056.
 128. Harrowven, D. C. and Dainty, R. F., Zirconium tetrachloride as a mediator for ambient temperature ortho-Fries rearrangements, *Tetrahedron Lett.*, **1996**, Vol. 37, 42, 7659-7660.
 129. Naeimi, H. and Moradi, L., Facile, convenient and regioselective direct ortho-acylation of phenols and naphthols catalyzed by Lewis acids under free solvent and microwave conditions, *J. Mol. Catal. A: Chem.*, **2006**, 256, 242–246.
 130. Murashige, R., Hayashi, Y., Ohmori, S., Torii, A., Aizu, Y., Muto, Y., Murai, Y., Oda, Y. and Hashimoto, M., Comparisons of o-acylation and Friedele Crafts acylation of phenols and acyl chlorides and Fries rearrangement of phenyl esters in trifluoromethanesulfonic acid: effective synthesis of optically active homotyrosines, *Tetrahedron*, **2011**, 67, 641-649.
 131. Olah, G. A.; Prahash, G. K. S.; Sommer, Superacids, *J. Science*, **1979**, 206, 13-20.
 132. Daley, R.F., Daley, Chapter 18 Aromatic nucleophilic substitution, in *Organic chemistry: A preliminary first edition*, McGraw-Hill education, **1996**, 914-977.
 133. Aroskar, E.V., Brown, P. J. N., Plevy, P. G. and Stephens, R., Aromatic polyfluoro-compounds. Part XLI. Some reactions of pentafluorobenzaldehyde, *J. Chem. Soc. C.*, **1968**, 1569-1575.
 134. Pazitny, A., Solcan, T. and Vegh, D., Pentafluorobenzaldehyde and its utilizing in organic synthesis, *J. Fluorine Chem.*, **2009**, 267–294.
 135. Kirsch, P, Introduction, in *Modern Fluoroorganic Chemistry Synthesis, Reactivity, Applications*, 1st edn, WILEY-VCH Verlag GmbH & Co., Weinheim, **2004**, pp 1-24.

136. Chambers, R.D. Chapter 9 Polyfluoroaromatic compounds in *Fluorine in Organic Chemistry*, 1st edn, John Wiley & Sons, Inc., Canada, **1973**, pp 261-334.
137. Uneyama, K. Chapter 2 Unique Reactions induced by fluorine in *Organofluorine Chemistry*, 1st edn, Blackwell Publishing Ltd, UK, **2006**, pp 101-138.
138. Joule, J.A. and Mills, K. Chapter 3 substitutions of aromatic heterocycles in *Heterocyclic Chemistry*, 5th edition, Blackwell Publishing Ltd, UK, **2010**, pp 19-33.
139. Gryko, D.T., Wyrostek, D., Nowak-Król, A., Abramczyk, K. and Rogacki, M. K., Straightforward transformation of pentafluorobenzaldehyde into 4-aryloxy-2,3,5,6-tetrafluorobenzaldehydes from pentafluorobenzaldehyde, *Synthesis*, **2008**, 24, 4028–4032.
140. Brooke, G. M., The preparation and properties of polyfluoro aromatic and heteroaromatic compounds, *J. Fluorine Chem.*, **1997**, 1, 1–76.
141. Arnoud, O., Moroni, M. and Roux, S., Halogenated styrene compounds and very low-loss polymers made therefrom, US 20040077874 A1, **2004**.
142. Eliu V. P. and Hauser J., Production of bis-benzazolyl fluorescent brighteners, PCT Int. patent 32886, **2002**.
143. BASF introduces Uvinul A Plus to the North American cosmetics market, http://www.cosmeticsonline.com.br/materia_prima/MP102_Daltomare_Uvinul_APlus.pdf, accessed 3/2/2016.
144. Sallares, R.J., Nonell, S., Marquillas, O.F., Miralles, R. and Gallardo S.A., 3-Dialkylaminophenyl 2-alkoxycarbonylbenzoic compounds, Int. patent 125092, **2010**.
145. Uvinul® A Plus Granular, <http://www.personal-care.basf.com/ProductDetails?PRD=30338477>, accessed 3/2/2016.
146. Tian, Z., Tian, B. and Zhang, J., Synthesis and characterization of new rhodamine dyes with large Stokes shift, *Dyes Pigm.*, **2013**, 1132-1136.
147. Bolliger, J. L. and Frech, C. M., Transition metal-free amination of aryl halides- A simple and reliable method for the efficient and high-yielding synthesis of *N*-arylated amines, *Tetrahedron*, **2009**, 1180-1187.
148. Satam, V., Rajule, R., Bendre, S., Bineesh, P. and Kanetkar, V., Synthesis and application of novel styryl dyes derived from 1,4-diethyl-1,2,3,4-tetrahydro-6-methoxyquinoxaline, *J.Heterocyclic Chem.*, **2009**, 46, 221-225.
149. Weng, F., Wang, C. and Xu, B., Direct C-H Bond arylation of 2-hydroxybenzaldehydes with arylboronic acid via ligand-free palladium catalysis, *Tetrahedron Lett.* **2010**, 51, 2593-2596.
150. Ghiacia, M. and Asghari, J., Dealkylation of alkyl and aryl ethers with AlCl₃ – NaI in the absence of solvent, *Synth. Commun.*, **1999**, 29, 973-979.
151. Simion, A.M., Hashimoto, I., Mitoma, Y., Egashira, N. and Simion, C., *O*-acylation *o*-substituted phenols with various alkanoyl chlorides under phase-transfer catalyst conditions, *Synth. Commun.*, **2012**, 42, 921-931.
152. Wu, W.B., Li, M. L. and Huang, J. M., Electrochemical hydrodefluorination of fluoroaromatic compounds, *Tetrahedron Lett.*, **2015**, 12, 1520–1523.
153. Chen, L., Dai, J., Zhang, Y. and Shen, K., Preparation of quinazoline derivatives as anticoagulants, China patent 101654441 A, 24/02/**2010**.
154. Kobayashi, S., Moriwaki, M. and Hachiya, I., The catalytic Fries Rearrangement of acyloxy naphthalenes using scandium trifluoromethanesulfonate as a catalyst, *J. Chem. Soc., Chem. Commun.*, **1995**, 1527-1528.
155. DuPont Packaging and Industrial Polymers, DuPont™ Elvax® 460, **2014**.

156. Goswami, P., Chinnadayala, S.S., Chakraborty, M., Kumar, A.K. and Kakoti, A., An overview on alcohol oxidases and their potential applications, *Appl Microbiol Biotechnol.* **2013**, 10, 4259-4275.
157. Diepensa, M. and Gijsman, P., Photostabilizing of bisphenol A polycarbonate by using UV-absorbers and self protective block copolymers based on resorcinol polyarylate blocks, *Polym. Degrad. Stab.*, **2009**, 94, 1808–1813.
158. Weng, F., Wang, C. and Xu, B., Direct C-H Bond arylation of 2-hydroxybenzaldehydes with arylboronic acid via ligand-free palladium catalysis, *Tetrahedron Lett.* **2010**, 51, 2593-2596.
159. Wang, D. and Cui, S., Rh(III)-catalyzed aldehyde C-H bond functionalization of salicylaldehydes with arylboronic acids, *Tetrahedron*, **2015**, 8511-8516.
160. Rao, H. and Li, C. J., Rearrangement of 2-aryloxybenzaldehydes to 2-hydroxybenzophenones by Rhodium-Catalyzed cleavage of aryloxy C-O bonds, *Angew. Chem. Int. Ed.* **2011**, 50, 8936–8939.
161. Negi, A., S., Darokar, M., P., Chattopadhyay, S., K., Garg, A., Bhattacharya, A., K., Srivastava, V. and Khanuja, S., P., S, Synthesis of a novel plant growth promoter from gallic acid, *Bioorg. Med. Chem. Lett.*, **2005**, 1243-1247.
162. Aziz, N., Kelly, S. M., Duffy, W. and Goulding, M., Rod-shaped dopants or flexoelectric nematic mixtures, *Liq. Cryst.*, **2009**, 36, 503-520.
163. Hou, Y., Huck, L., A., and Wan, P., Long-range intramolecular photoredox reaction via coupled charge and proton transfer of triplet excited anthraquinones mediated by water, *Photochem. Photobiol. Sci.*, **2009**, 8, 1408–1415
164. Liu, L., Zhang, H., Li, A., Xie, J. and Jiang, Y., Intramolecular charge transfer dual fluorescent sensors from 4-(dialkylamino)benzanilides with metal binding site within electron acceptor, *Tetrahedron*, **2006**, 62, 10441–10449.
165. Ghosh, K. and Saha, I., Triphenylamine-based simple chemosensor for selective fluorometric detection of fluoride, acetate and dihydrogenphosphate ions in different solvents, *J. Incl Phenom Macrocycl Chem.*, **2011**, 70, 97–107.
166. Naeimi, H. and Moradi, L., Facile, convenient and regioselective direct ortho-acylation of phenols and naphthols catalyzed by Lewis acids under free solvent and microwave conditions, *J. Mol. Catal. A: Chem.*, **2006**, 256, 242–246.
167. Sharghi, H., Sarvari, M., H. and Eskandari, R., Direct acylation of phenol and naphthol derivatives in a mixture of graphite and methanesulfonic acid, *Synthesis*, **2006**, 12, 2047-2052.
168. Kumar, A., Ahmad, P., Maurya, R. A., Singh, A. B. and Srivastava, A. K., Novel 2-aryl-naphtho[1,2-*d*]oxazole derivatives as potential PTP-1B inhibitors showing antihyperglycemic activities, *Eur. J. Med. Chem.*, **2009**, 109-116.
169. Murashige, R., Hayashi, Y., Ohmori, S., Torii, A., Aizu, Y., Muto, Y., Mura, Y., Oda, Y. and Hashimoto, M., Comparisons of o-acylation and Friedel-Crafts acylation of phenols and acyl chlorides and Fries Rearrangement of phenyl esters in trifluoromethane sulfonic acid: effective synthesis of optically active homotyrosines, *Tetrahedron*, **2011**, 641-649.
170. Kankanala, K., Reddy, V. R., Mukkanti, K., and Pal, S., A TFAA-H₃PO₄- mediated direct, metal-free and high-speed synthesis of aryl carboxylate esters from phenols, *J. Fluorine Chem.*, **2009**, 505-508.
171. Venu, T. D., Sudha, B. S., Satish, S., Shashikanth, S., and Raveesha, K. A.,

- Synthesis and antibacterial activity of a series of novel dihydrobenzo-furanols, *Bulg. Chem. Commun.*, **2009**, 409–413.
172. Leyva, E., Leyva, S., Moctezuma, E., Gonza'lez-Balderas, R. M. and Loera, D. Microwave-assisted synthesis of substituted fluorophenyl mono- and diazides by S_NAr. A fast methodology to prepare photoaffinity labeling and crosslinking reagents, *J. Fluorine Chem.*, **2013**, 164–169.
173. Enders, D., Henseler, A. and Lowins, S., N-Heterocyclic carbene catalyzed nucleophilic acylation of trifluoromethyl ketimines, *Synthesis*, **2009**, 4125–4128.
174. Shao, C., Wang, X., Zhang, Q., Luo, S., Zhao, J. and Hu, Y., Acid-base jointly promoted copper (I) –catalyzed azide-alkyne cycloaddition, *J. Org. Chem.*, **2011**, 76, 6832–6836.
175. Huang, L., Lu, C., Sun, Y., Mao, F., Luo, Z., Su, T., Jiang, H., Shan, W. and Li, X., Multitarget-directed benzylideneindanone derivatives: anti-β-amyloid (Aβ) aggregation, antioxidant, metal chelation, and monoamine oxidase B (MAO-B) inhibition properties against Alzheimer's disease, *J Med Chem.*, **2012**, 19, 8483–8492.
176. Bolliger, J. L. and Frech, C. M. Transition metal-free amination of aryl halides—A simple and reliable method for the efficient and high-yielding synthesis of N-arylated amines, *Tetrahedron*, **2009**, 65, 1180–1187.
177. SoarnoL™ (EVOH), <http://www.nippon-gohsei.com/soarno>, accessed 23/2/2016.
178. Brouwer, A.M., Standards for photoluminescence quantum yield measurements in solution (IUPAC Technical Report), *Pure Appl. Chem.*, **2011**, 12, 2213–2228.
179. Chakraborti, A.K. and Gulhane, R., Indium(III) chloride as a new, highly efficient, and versatile catalyst for acylation of phenols, thiols, alcohols, and amines, *Tetrahedron Lett.*, **2003**, 35, 6749–6753.
180. Mamat, C., Büttner, S., Trabhardt, T., Fischer, C. and Langer, P., Regioselective synthesis of 5-alkylsalicylates, 5-alkyl-2-hydroxy-acetophenones, and 5-alkyl-2-hydroxy-benzophenones by [3 + 3] cyclization of 1,3-bis(silyl enol ethers) with 2-alkyl-1,1,3,3-tetraethoxypropanes, *J. Org. Chem.*, **2007**, 16, 6273–6275.